Distributed Coding for Wireless Cooperative Networks.

Atoosa Hatefi

N° d'ordre : 2012-15-TH

THÈSE DE DOCTORAT

DOMAINE : STIC

SPECIALITE : Télécommunications

Ecole Doctorale « Sciences et Technologies de l'Information des Télécommunications et des Systèmes »

Présentée par :

Atoosa HATEFI

Sujet :

Codage Distribué pour les Réseaux Coopératifs sans fil

Distributed Coding for Wireless Cooperative Networks

Soutenue le 25 octobre 2012 devant les membres du jury :

M. Antoine BERTHET	Supélec	Directeur de Thèse
M. Jean-Pierre CANCES	ENSIL de Limoges	Examinateur
M. Pierre DUHAMEL	L2S CNRS/Supélec/ Univ. Paris-Sud 11	Président
M. Marc MOENECLAEY	Ghent University	Rapporteur
M. Ramesh PYNDIAH	Telecom Bretagne	Rapporteur
M. Hikmet SARI	Supélec	Examinateur
M. Mikael SKOGLUND	KTH Royal Institute of Technology	Examinateur
M. Raphaël VISOZ	Orange Labs	Encadrant

To my lovely family

Acknowledgment

I would like to take advantage of this opportunity to acknowledge all the people who have supported me during this work.

First and foremost, I would express my gratitude to my Ph.D. advisors, Professor Antoine Berthet and Doctor Raphaël Visoz for providing me the chance to do a Ph.D. under their guidance on an interesting and challenging research topic, and for their permanent support till my defense day.

I would also thank the jury members for their interest in my work. I thank Professor Pierre Duhamel for acting as the chairman. I was honored that Professor Marc Moeneclaey and Professor Ramesh Pyndiah accepted to review and evaluate my thesis. Additionally, I thank Professor Mikael Skoglund, Professor Jean-Pierre Cances, and Professor Hikmet Sari for their participation in the jury as examiners.

This thesis is the result of three years of work spent mainly at Orange Labs and partly at Supelec. I address my gratitude to Orange Labs for the financial support to my thesis. Many thanks go to all the members of the RIDE team at Orange labs, especially my successive office mates Michel, Baozhu, Daniel and Yohan, who contributed to a good atmosphere, and also for our valuable technical and non-technical discussions. Special thanks to Pierre, Arturo, Ahmed and Alexandre who have kindly forwarded me several job opportunities. Many thanks to Hajer, Sarah, and Sofia for their continuous support, and who are now very good friends of mine. I also thank all my colleagues and friends at Supelec for their hospitality during my short stay there. Special thanks to Catherine for her kindness and guidance in administrative matters.

A thought goes also to all my friends outside Orange labs and Supelec.

Many thanks to Sina for his continuous presence from the onset of this work, and for the cultural melting pot and discussions of any kind during all these time.

I specially mention my best friend Azin. When I first met her in Sharif University eleven years ago, I did not think that our friendship would last so long. I thank her for her kindness and unconditional support.

The years spent during my Ph.D., would not be the same, without the patience and endless support of Michael. I have always been overwhelmed with his optimism and positive energy. Thank you for being the source of re-motivation, and for your appreciable help, all the more during the most difficult moments of this thesis and during the preparation of my new journey.

Last but not least, I want to express my deep gratitude to my parents and my brothers, for their unconditional love, their advices and unlimited support. I owe them the success of my studies, and this thesis is also theirs.

Abstract

With the rapid growth of wireless technologies, devices and mobile applications, the quest of high throughput and ubiquitous connectivity in wireless communications increases rapidly as well. Relaying is undoubtedly a key concept to provide coverage extension and capacity increase in wireless networks. Network coding, which allows the intermediate nodes to share their computation capabilities in addition to their resource and their power, has grabbed a significant research attention since its inception in information theory. It has become an attractive candidate to bring promising performance improvement, especially in terms of throughput, in relay-based cellular networks. Substantial research efforts are currently focused on theoretical analysis, implementation and evaluation of network coding from a physical layer perspective. The question is, what is the most efficient and practical way to use network coding in wireless relay-based networks, and whether it is beneficial to exploit the broadcast and multiple-access properties of the wireless medium to perform network coding. It is in such a context, that this thesis proceeds.

In the first part of the thesis, the problem of Joint Network-Channel Coding (JNCC) for a Multiple Access Relay Channel (MARC) is investigated in the presence of multiple access interferences and for both of the relay operating modes, namely, half-duplex and full-duplex. To this end, three new classes of MARC, referred to as Half-Duplex Semi-Orthogonal MARC (HD-SOMARC), Half-Duplex Non-Orthogonal MARC (HD-NOMARC), and Full-Duplex Non-Orthogonal MARC (FD-NOMARC) have been introduced and studied. The relaying function in all of the classes is based on a Selective Decode-and-Forward (SDF) strategy, which is individually implemented for each source, i.e, the relay forwards only a deterministic function of the error-free decoded messages. For each class, an information-theoretic analysis is conducted, and practical coding and decoding techniques are proposed. The proposed coding schemes, perform very close to the outage limit for both cases of HD-SOMARC and HD-NOMARC. Besides, in the case of HD-NOMARC, the optimal allocation of the transmission time to the relay is considered. It is also verified that exploiting multiple access interferences, either partially or totally, results in considerable gains for MARC compared to the existing interference-avoiding structures, even in the case of single receive antenna.

In the second part of the thesis, the network model is extended by considering multiple relays which help multiple sources to communicate with a destination. A new class of Multiple Access Multiple Relay Channel (MAMRC), referred to as Half-Duplex Semi-Orthogonal MAMRC (HD-SOMAMRC) is then proposed and analyzed from both information theo-

retic and code design perspective. New practical JNCC schemes are proposed, in which binary channel coding and non binary network coding are combined, and they are shown to perform very close to the outage limit. Moreover, the optimal allocation of the transmission time to the sources and relays is considered.

Finally, in the third part of the thesis, different ways of implementing cooperation, including practical relaying protocols are investigated for the half-duplex MARC with semi-orthogonal transmission protocol and in the case of JNCC. The hard SDF approach is compared with two Soft Decode and Forward (SoDF) relaying functions: one based on log a posterior probability ratios (LAPPRs) and the other based on Mean Square Error (MSE) estimate. It is then shown that SDF works well in most of the configurations and just in some extreme cases, soft relaying functions (based on LAPPR or MSE estimate) can slightly outperform the hard selective one.

List of Publications

Journal papers

1. A. Hatefi, R. Visoz, A.O. Berthet, *Joint Network-Channel Coding for the Semi-Orthogonal MARC: Theoretical Bounds and Practical Design,* submitted to the IEEE Trans. on Wireless Communication, 2012.

2. A. Hatefi, R. Visoz, A.O. Berthet, *Joint Network-Channel Coding for the Non-Orthogonal MARC: Theoretical Bounds and Practical Design,* submitted to the IEEE Trans. on Wireless Communication, 2012.

3. A. Hatefi, R. Visoz, A.O. Berthet, *Joint Network-Channel Coding for the Semi-Orthogonal MAMRC: Theoretical Bounds and Practical Design,* to be submitted to the IEEE Trans. on Wireless Communication, 2012.

Conference papers

1. A. Hatefi, R. Visoz, A.O. Berthet, *Near Outage Limit Joint Network Coding and Decoding for the Non-Orthogonal Multiple-Access Relay Channel,* Proc. IEEE PIMRC'12, Sydney, Australia, Sep. 2012.

2. A. Hatefi, R. Visoz, A.O. Berthet, *Near Outage Limit Joint Network Coding and Decoding for the Semi-Orthogonal Multiple-Access Relay Channel,* Proc. International Symposium on Network Coding (NETCOD'12), Boston, MA, USA, Jul. 2012.

3. A. Hatefi, R. Visoz, A.O. Berthet, *Full diversity distributed coding for the multiple access half-duplex relay channel,* Proc. International Symposium on Network Coding (NETCOD'11), Beijing, China, Jul. 2011.

4. A. Hatefi, R. Visoz, A.O. Berthet, *Joint network-channel distributed coding for the multiple access full-duplex relay channel,* Proc. IEEE ICUMT'10, Moscow, Russia, Oct. 2010.

5. A. Hatefi, R. Visoz, A.O. Berthet, *Joint channel-network turbo-coding for the non-orthogonal multiple access relay channel,* Proc. IEEE PIMRC'10, Istanbul, Turkey, Sep. 2010.

6. A. Hatefi, R. Visoz, A.O. Berthet, *Relaying functions for the multiple access relay channel,* Proc. 6th International Symposium on Turbo Codes, Brest, France, Sep. 2010.

7. A. Hatefi, R. Visoz, A.O. Berthet, *Joint channel-network coding for the semi-orthogonal multiple access relay channel,* Proc. IEEE VTC'10 Fall, Ottawa, Canada, Sep. 2010.

Patent Filings

1. M. Benammar, A. Hatefi, R. Visoz, *Method for transmitting a digital signal in a multi-source, multi-relay network with a semi-orthogonal transmission protocol and a half-duplex relay,* Filed as a European patent application by France Telecom.

2. M. Benammar, A. Hatefi, R. Visoz, *Method for transmitting a digital signal in a multi-source, multi-relay network with a half-duplex relay,* Filed as a European patent application by France Telecom.

3. A. Hatefi, R. Visoz, A.O. Berthet, *Method for transmitting a digital signal in a MARC system ensuring full diversity, and corresponding program product and relay device,* World Patent Application, Publication Number: WO 2011/051893, Issue Date: 09-08-2011, Filed on 19-08-2010 by France Telecom.

4. A. Hatefi, R. Visoz, A.O. Berthet, *Method for transmitting a digital signal in a MARC system with a full-duplex relay, and corresponding program product and relay device,* World Patent Application, Publication Number: WO 2011/033237, Issue Date: 24-03-2011, Filed on 17-09-2010 by France Telecom.

5. A. Hatefi, R. Visoz, A.O. Berthet, *Method for transmitting a digital signal in a MARC system with a half-duplex relay, and corresponding program product and relay device,* World Patent Application, Publication Number: WO 2011/033239, Issue Date: 24-03-2011, Filed on 17-09-2010 by France Telecom.

6. A. Hatefi, R. Visoz, A.O. Berthet, *Method for transmitting a digital signal in a semi-orthogonal frame system having a half-duplex relay, and corresponding program product and relay device,* World Patent Application, Publication Number: WO 2011/067534, Issue Date: 09-06-2011, Filed on 01-12-2010 by France Telecom.

Contents

List of Figures

List of Acronyms

AEP	Asymptotic Equipartition Property
AF	Amplify-and-Forward
AWGN	Additive White Gaussian Noise
BC	Broadcast Channel
BEC	Block Erasure Channel
BICM	Bit-Interleaved Coded Modulation
BLER	Block Error Rate
CC	Convolutional Code
CDF	Cumulative Distribution Function
CF	Compress-and-Forward
CoF	Compute-and-Forward
CRC	Cyclic Redundancy Check
DNF	DeNoise-and-Forward
DF	Decode-and-Forward
FD	Full-Duplex
GA	Genie-Aided
HD	Half-Duplex
ISI	Inter-Symbol Interference
JNCC	Joint Network Channel Coding
JNCD	Separate Network Channel Decoding
LAPPR	Log A Posterior Probability Ratios
LAPR	Log A Priori probability Ratio
LAR	Link-Adaptive Regenerative
LDPC	Low Density Parity Check
MAC	Multiple Access Channel
MAMRC	Multiple Access Multiple Relay Channel
MAP	Maximum A Posteriori
MARC	Multiple Access Relay Channel
MCS	Modulation Coding Scheme
MIMO	Multiple-Input, Multiple-Output
MSE	Mean Square Error
NOMARC	Non-Orthogonal Multiple Access Relay Channel
OMARC	Orthogonal Multiple Access Relay Channel
PAPR	Peak-to-Average Power Ratio

PD	Partial Decoding
PDF	Probability Density Function
PNC	Physical Layer Network Coding
PSK	Phase Shift Keying
QAM	Quadratic Amplitude Modulation
RBC	Relay Broadcast Channel
RSC	Recursive Systematic Convolutional
SDF	Selective Decode and Forward
SINR	Signal to Interference Ratio
SISO	Soft-In Soft-Out
SNCC	Separate Network Channel Coding
SNCD	Separate Network Channel Decoding
SNR	Signal-to-Noise Ratio
SOMAMRC	Semi-Orthogonal Multiple Access Multiple Relay Channel
SoDF	Soft Decode-and-Forward
SOMARC	Semi-Orthogonal Multiple Access Relay Channel
TC	Turbo Code
TWRC	Two-Way Relay Channel
WEF	Weight Enumerator Function

Notations

$\mathbb{R}$	Set of reals
$\mathbb{C}$	Set of complex numbers
$\mathbb{F}_q$	Finite field with q elements
$\lvert x \rvert$	Absolute value of a scalar x
$\lceil x \rceil$	Smallest integer greater than or equal to x
$\lfloor x \rfloor$	Greatest integer less than or equal to x
$\mathbf{x}$	A vector
$\lVert \mathbf{x} \rVert$	Euclidean norm of the vector $\mathbf{x}$
$\mathbf{X}$	A matrix
$x_{i;j,\ell}$ or $[\mathbf{X}_i]_{j,\ell}$	The entry (j, ℓ) of the matrix $\mathbf{X}_i$ with i designating a user.
$\det(\mathbf{X})$	Determinant of the matrix $\mathbf{X}$
$\mathrm{diag}(\mathbf{X})$	Diagonal operator on the square matrix $\mathbf{X}$. $\mathrm{diag}(p_1, p_2, \cdots, p_n)$ is a diagonal matrix with the diagonal entries equal to $p_1, p_2, \cdots, p_n$.
$\mathbf{I}_n$	The n-square identity matrix
$\mathbf{0}_n$	n-tuples of zeros
$\mathbf{1}_n$	n-tuples of ones
$\lvert \mathscr{X} \rvert$	Cardinality of the set $\mathscr{X}$
$\mathbf{x} \sim p(\mathbf{x})$	The random vector $\mathbf{x}$ follows the probability distribution function $p(\mathbf{x})$.
$\mathcal{CN}(\boldsymbol{\mu}, \boldsymbol{\Sigma})$	The circularly-symmetric complex Gaussian distribution with mean $\boldsymbol{\mu}$ and covariance matrix $\boldsymbol{\Sigma}$.
$[P]$	The Iverson bracket [1]: the $\{0, 1\}$-valued function indicating the truth of P, where P is a predicate (Boolean proposition) involving some set of variables. Thus, $[P] = 1$ if P is true and $[P] = 0$ otherwise.
$(\cdot)^\top$	Transpose operator
$(\cdot)^\dagger$	Complex conjugate transpose / Hermitian operator
$(\cdot)^{-1}$	Inverse operator
$\exp(\cdot)$	Exponential function
$\log(\cdot)$	Logarithmic function
$\mathbb{E}\{\cdot\}$	Operator of expected value

Résumé Détaillé de la Thèse

Communications coopératives et codage réseau

Les communications au sein d'un réseau gagnent en fiabilité et en efficacité quand les utilisateurs (ou noeuds) partagent leurs ressources et leur budget de puissance pour transmettre des données. Une telle coopération conduit dans de nombreux cas à des économies de ressources et d'énergie dans l'ensemble du réseau. On conçoit aisément que la coopération n'intervient qu'à partir de trois noeuds. Ainsi, le modèle du réseau à trois terminaux initialement introduit et étudié par Van der Meulen [2], en constitue certainement la brique fondamentale. Depuis, la littérature sur le sujet a connu une croissance régulière, notamment dans le domaine de la théorie de l'information, où l'idée de coopération a été formalisée au travers du modèle de canal à relais et de ses multiples variantes (canal à relais multiples, canal à relais bi-directionnel, etc.). En marge de ses travaux, Sendonaris et al. ont imaginé une forme de coopération entre utilisateurs, où chaque utilisateur joue le rôle de relais pour les autres [3] [4].

Le modèle de canal à relais :

L'étude du canal à relais remonte à [5], où les auteurs ont présenté de nombreux schémas de codage aléatoires et comparé les rendements atteignables correspondants avec la borne supérieure sur la région de capacité donnée par le théorème du flot-maximal/coupe-minimale (min-cut max-flow). Dans le schéma de coopération [5, Théorème 1], le relais décode le message de la source et coopère avec elle pour aider la destination à décoder. Cette stratégie de coopération, appelée stratégie de coopération par "décodage-et-retransmission" (Decode-and-Forward ou DF), permet d'atteindre la capacité d'un canal à relais dégradé. Dans le schéma d'observation [5, Théorème 6], le relais transmet à la destination une estimation (ou une version quantifiée) de ses observations du message source en utilisant les outils du codage de source avec information adjacente [6, 7]. Cette stratégie de coopération stratégie est appelée stratégie de coopération par compression-et-retransmission (Compress-and-Forward ou CF) [8]. Un théorème a aussi été présenté dans [5, Théorème 7] pour le canal à relais général, qui combine coopération et observation. D'autres stratégies de coopération, comme le décodage partiel (Partial Decoding ou PD) ou l'amplification-et-retransmission (Amplify-and-Forward ou AF) ont aidé à élargir les analyses [9–13]. Plusieurs contributions

incluant de nouvelles bornes, des stratégies de contrôle d'énergie, et plusieurs résultats valables pour les relais en mode half-duplex, ont été proposés dans [14].

Les canaux à relais multiples, qui consistent en une seule source, une seule destination et plus d'un relais, ont été étudié dans différents travaux [15–17], et leurs taux atteints avec DF, PD et CF ont été présentés dans [17]. Le relayage a été traité avec une attention particulière dans les environnements sans fil. Parmi les contributions importantes, nous pouvons citer celles de Laneman et Wornell étudiant les performances des protocoles de relayage importants dans les environnements sans fil [18–20]. Un certain nombre de protocoles de relayage intéressants ont été proposés et analysés dans [21–23] incluant le codage à répétition et la coopération via le codage espace-temps (space-time coded cooperation) [24]. D'autres contributions complémentaires viennent de résultats novateurs en théorie de l'information, ainsi que de nouvelles idées en codage aléatoire pour les relais par Kramer et al. [25] et Chong et al. [26].

Extension du modèle à plusieurs sources ou destinataires :

L'extension des résultats précédents aux schémas multi-accès et diffusion avec plusieurs sources ou destinataires, ont été traités dans plusieurs travaux :

- Premièrement, un canal à accès multiples avec relais (MARC) a été présenté dans [8, 27, 28], et les régions des taux atteints correspondantes avec AF, DF, et PD ont été déduites. Les bornes de capacité pour le MARC avec un relais half-duplex et les taux atteints correspondants avec AF, DF, et PD ont été étudiés dans [29]. En outre, un protocole de relayage linéaire appelé AF multi-accès est analysé dans [30] pour le MARC, et montre qu'il est optimal dans le régime à fort gain de multiplexage.

- D'autre part, le canal à diffusion avec relais (broadcast relay channel ou BRC) a tout d'abord été étudié dans [31, 32]. Les auteurs ont considéré un réseau avec une seule source et deux destinataires, et ont introduit deux modèles de canaux, nommés BRC partiellement coopératif (un seul destinataire agit comme un relais pour les autres) et BRC pleinement coopératif (chaque destinataire agit comme un relais pour l'autre). Ils ont ainsi extrait et comparé les régions des taux atteints correspondantes en considérant DF. Le BRC partiellement coopératif fut davantage étudié dans [33] pour le cas de plus d'une destination. Un troisième modèle BRC fut introduit et étudié dans [8, 34], où un relais additionnel a été inséré dans le canal de diffusion avec pour seule fonction le relayage. Les régions des taux atteints et les bornes supérieures de la capacité pour RBC ont été davantage développées dans [35, 36]. En parallèle, AF pour le canal à accès multiples (MAC) multi sauts (multihop MAC) et pour le canal à diffusion (sans liens directs entre les sources et les destinataires) ont été étudiés dans [37], où l'allocation optimale de puissance au niveau des relais a été présentée, tout comme la dualité MAC-BC pour le relais AF.

- Finalement, l'idée principale du canal à relais bidirectionnel (two-way relay channel ou TWRC) a été d'abord présentée dans [38] pour les canaux non-bruités. Dans

TWRC, deux noeuds échangent leurs informations via un relais. La transmission par diffusion et à accès multiple simultané peuvent tous deux être considérés dans ce modèle de canal, et ont été l'objet de plusieurs travaux de recherche. Dans [39–41], les auteurs extraient les taux atteints en considérant les noeuds full-duplex, la transmission par diffusion à chaque noeud et l'accès multiple simultané de tous les noeuds. Dans [39, 40], les taux atteints ont été calculé pour AF, DF, et CF, alors que dans [41], la région des taux atteints pour la stratégie de relayage calcul-et-retransmission (compute-and-forward ou CoF) a été extraite. Dans la stratégie CoF [42, 43], le relais calcule (ou décode) une combinaison linéaire des messages transmis du MAC noeuds-vers-relais. Davantage de contributions sont basées sur les prémices des noeuds half-duplex, pour lesquelles nous distinguons deux catégories principales : (i) le canal à relais bidirectionnel à deux phases avec le protocole de diffusion multi-accès dans lequel les deux noeuds communicants transmettent simultanément au relais pendant la première phase, et le relais diffuse aux deux pendant la seconde phase. Dans ce modèle, il n'y a pas de lien direct entre les noeuds communicants ; (ii) le canal à relais bidirectionnel à trois phases avec transmission par diffusion à tous les noeuds et sans accès multiples. Le premier modèle de canal a été considéré dans [44–48] où les auteurs ont extrait les taux atteints en considérant différents schémas de relayage (AF, DF, PD, CF, et CoF). De plus, la région de capacité du canal à diffusion (broadcast channel capacity region) a été extraite dans [49], où chaque destinataire connait parfaitement le message adressé à l'autre noeud. La conception de code et les taux atteints pour le second modèle ont été étudiés dans [50, 51]. Plusieurs stratégies de relayage et leurs taux atteints correspondants ont également été présentés dans [52] pour les deux catégories.

Codage réseau pour canal à accès multiple avec relais :

Dans un réseau multi-terminaux général avec plusieurs paires source-destination, les noeuds intermédiaires n'ont pas besoin de traiter séparément et indépendamment chaque flux de données entrant. Il existe plusieurs façons d'effectuer des opérations algébriques sur l'ensemble des flux entrants. C'est le concept fondamental de codage réseau, qui a été initialement proposé par Ahlswede, Cai, Li, et Yeung in [53], et a suscité une intense activité de recherche. Il est important de souligner que de nombreux schémas coopératifs qui ont déjà été mentionnés, notamment pour MARC et TWRC, peuvent être placés dans le cadre du codage réseau. Ahlswede et al. ont démontré dans [53] que pour les configurations "multicast", seule une stratégie de codage réseau pouvait atteindre la région de capacité du flot-maximal-coupe minimale (min-cut max-flow capacity region). Cette publication majeure a très vite suscité une intense activité de recherche tant sur le plan théorique que pratique, afin d'étendre ce concept aux communications sans fil, qui, bien qu'ayant des pertes de transmission, facilite largement son application. Par exemple, la diffusion est garantie sans frais. L'application du concept de codage réseau aux réseaux sans fil à

paquets a donné lieu à de nombreuses études. Le codage réseau déterministe a été introduit dans [54], ce qui nécessite une connaissance complète de l'ensemble du réseau. Les auteurs de [54] ont démontré que le codage réseau linéaire d'un alphabet de taille finie peut atteindre la région de capacité min-cut max-flow. Cet aspect a été davantage analysé dans [55, 56]. Cependant, une connaissance complète des réseaux de paquets de grandes tailles ne sont en général pas disponibles, ce qui explique l'intérêt particulier d'effectuer le codage réseau aléatoire [57, 58]. Dans ce cas, les opérations du codage réseau sont choisies de manière aléatoire et indépendante à chaque noeud. Comme il est démontré dans [58], les codes linéaires et aléatoires de grands longueurs peuvent asymptotiquement atteindre la région de capacité min-cut max-flow. Ces contributions, conjointement avec [59, 60], ont également démontré l'efficacité du codage réseau aléatoire distribué sur un réseau constitué des sources corrélées (par exemple, réseaux de capteurs), où une compression distribuée est nécessaire. Le caractère asymptotiquement optimal du codage réseau aléatoire (distribué) a été établi en l'absence et en présence de paquets de données effacés dans [61–63]. Parmi les autres contributions, [38, 64, 65] se focalisent sur les canaux sans erreurs, et [66] considère les canaux d'effacement avec erreurs dans les réseaux de capteurs. Finalement, la nécessité de codage bout en bout dans les réseaux multi-terminaux a été étudiée dans [67], où les auteurs ont démontré que seule une approche unifiée qui traite conjointement le codage source, codage canal et codage réseau, peut atteindre la région capacité min-cut max-flow.

Du point de vue de la couche physique, le codage réseau sans fil peut être utilisé dans une variété de contextes, en combinaison avec le codage canal et le codage source. Dans les réseaux multi-terminaux densément déployés (par exemple, réseaux de capteurs), où il existe une corrélation entre les sources, les noeuds doivent combiner le codage source, le codage canal, et le codage réseau. Plusieurs idées et contributions ont été proposées à ce sujet dans le but d'introduire certaines conceptions de code dans un cadre unifié [68–70]. Toutefois, dans le cas des sources indépendantes et incompressibles, la combinaison du codage réseau et du codage canal a suscité une intense activité de recherche, et diverses contributions dans le cadre de MARC [71, 72], de TWRC [73–75], de la coopération entre utilisateurs [76–79] ou du codage entre paquets pour les systèmes ARQ hybrides (crosspacket channel coding for hybrid ARQ systems) [80], ont été proposés au cours des dernières années. Ici, l'objectif principal du codage réseau est de fournir une transmission fiable et spectralement efficace sur le réseau. D'un point de vue purement codage, le défi est de parvenir à la diversité pleine et de maximiser le gain de codage. Il est important de souligner que la diversité pleine ne peut être atteinte qu'avec des limitations sur le débit de transmission. De plus, assurer la diversité pleine (en espace) n'est pas nécessairement le critère de conception le plus important dans les environnements sans fil réalistes, car de nombreuses autres sources de diversité existent (diversité fréquentielle, diversité spatiale par les antennes de réception, etc.). Il existe deux approches radicalement différentes pour combiner le codage canal et le codage réseau : le codage canal réseau séparé (separate network coding coding ou SNCC) et le codage conjoint canal réseau (joint network channel coding ou JNCC). Dans le SNCC, le codage de canal est effectué localement et séparément pour chaque transmission afin de convertir les canaux bruités en liens à effacements. Le codage réseau est effectué sur les canaux à effacements fournis par les couches inférieures [81]. Le décodage canal réseau procède également par étapes successives (separate network channel

decoding ou SNCD) : le décodage canal préalablement effectué au niveau de chaque lien physique fournit une estimation des messages au décodeur réseau. L'approche JNCC, quant à elle, utilise la redondance du codage réseau pour renforcer le codage canal afin d'améliorer le gain de codage du système. Elle fait appel à un décodage conjoint canal et réseau (joint network channel decoding ou JNCD) à la destination, dans lequel les informations souples sont échangées entre le décodeur réseau et les décodeurs canaux.

Aspects pratiques du codage réseau dans les environnements sans fil

Cette partie donne un aperçu de l'état de l'art des conceptions pratiques de codage réseau pour la communication sans fil avec codage canal. Les contributions sont divisées en deux catégories : (i) codage réseau basé sur le protocole DF dans lequel nous revenons à l'espace des messages à tous les noeuds intermédiaires pour construire le message réseau codé, ou (ii) codage réseau dans lequel le message réseau codé est construit sans revenir à l'espace des messages, i.e., serait une fonction arbitraire d'une estimation des combinaisons des mots de code transmis par les sources.

1) Stratégie de coopération DF

Hausl et al. semblent avoir été les premiers à proposer des mises en oeuvre pratiques de codage canal réseau à base de codes LDPC [71] ou de turbo codes [72]. Les hypothèses adoptées par ces travaux précurseurs sont en général : (i) le mode half-duplex pour le fonctionnement du relais ; (ii) pas d'interférence grâce à l'orthogonalité des liens ; (iii) une stratégie de relayage de type décodage conjoint et retransmission conditionnelle (joint selective DF), c.-à-d., le relais coopère si et seulement si il parvient à décoder sans erreurs l'ensemble des messages des sources. Concernant la première hypothèse, nous savons de la théorie de l'information que le mode half-duplex est fondamentalement sous-optimal par rapport au mode full-duplex, mais souvent retenu pour des raisons pratiques. Les contraintes physiques (une très forte atténuation sur le canal sans fil, une isolation électrique insuffisante entre les circuits de transmission et de réception, etc.), la complexité et le coût, expliquent très probablement l'intérêt modéré pour le mode de fonctionnement full-duplex. Concernant la seconde hypothèse, comme nous l'avons déjà souligné, le canal radio offre une diffusion naturelle des signaux. Toutefois, cette diffusion naturelle a un prix : la superposition des signaux ou interférence au niveau de tous les noeuds intermédiaires et aussi à la destination. Pour lutter contre cette interférence, un accès orthogonal (en temps, en fréquence, en codes, etc.) est très souvent supposé dans les systèmes de communications avec coopération. Si l'orthogonalité simplifie la conception du codage conjoint canal réseau, son analyse et le décodage associé, elle a aussi pour conséquence de réduire significativement l'efficacité spectrale des systèmes, surtout en présence d'antennes de réceptions multiples. En effet,

on peut montrer théoriquement que l'accès orthogonal n'est pas optimal pour les canaux MACs à évanouissements lents (slow fading MAC), bien qu'il puisse conduire à des performances proches de l'optimal dans les régions de rapports signal-à-bruit (signal-to-noise ratio ou SNR) très faibles. De plus, les auteurs de [71] prennent pour hypothèse des liens sources vers relais sans erreurs. Pour justifier cette hypothèse, on pourrait imaginer des scénarii de communications où les sources sont très proches du relais et en vue directe. Cependant même dans ce cas, des erreurs de décodage seront possibles car, en pratique, il n'existe pas de schéma de modulation et de codage parfait (au sens de la théorie de l'information). D'autre part, les codes des références précitées ne garantissent pas structurellement une diversité pleine. Plus récemment, dans le même contexte, Duyck et al. ont proposé un JNCC à base de codes LDPC, prenant comme hypothèses les liens orthogonaux et les liens sources-relais sans erreurs [82]. Leur but est de construire un JNCC garantissant la diversité pleine, ce qui, en effet, conduit à un raisonnement analytique asymptotique (valable à SNR infini) et le durcissement des canaux à évanouissements lents aux canaux à effacement par bloc. Dans cette perspective, la diversité atteintes par le JNCC proposé ne dépend pas de la qualité des liens source-relais, et pour des raisons de simplicité, les auteurs ont supposé des liens source-relais sans erreur. Malheureusement, la conception proposée n'est pas générique en terme de choix de codage et de nombre de sources. De plus, les performances s'écroulent dès que les liens sources-relais deviennent imparfaits, même si la propriété de diversité pleine est préservée. L'application du JNCC en présence d'erreurs de décodage au niveau du relais a été traité dans [83]. Les auteurs supposent que les signaux transmis du relais vers la destination sont de nature analogique, et le JNCC qu'ils emploient est extrêmement simpliste comparé à [71, 72, 82]. De plus, pour transmettre efficacement les signaux analogiques du relais de façon efficace dans une bande passante donnée, il est nécessaire de recourir à des opérations de quantification/compression [84, 85] nécessitant une connaissance à priori au relais de l'état du canal relais-destination. En outre, dans toutes ces contributions, les sources et le relais n'interfèrent pas. Des conceptions JNCC similaires ont également été proposées dans le cas d'un TWRC avec un accès multiple orthogonal par répartition en temps (time division multiple access ou TDMA) [73, 74].

Dans l'ensemble, les schémas mentionnés ci-dessus sont conçus pour les réseaux sans fil de petite taille, avec des topologies spécifiques, qui ne peuvent être facilement appliquées aux grands réseaux multi-terminaux sans fil. Pour le MARC avec M sources, $M > 2$, plusieurs schémas de codage ont été récemment proposés, parmi lesquelles se trouvent [86] qui est basé sur les codes linéaires des produits, et [87] qui est basé sur les codes LDPC multi-arête (multi edge type LDPC). Plusieurs conceptions de code ont également été proposées dans le cas où M sources, $M > 2$, communiquent avec une destination commune et chaque source peut relayer l'information pour les autres [88–90]. Dans [88], un cadre pour la coopération réseau adaptative a été proposée dans lequel l'adaptation en temps réel des codes réseau à la qualité variable des liens a été principalement abordée. Ce schéma a été davantage étudié dans [89] en prenant en compte les défaillances des liens de communications. En parallèle, un certain nombre de contributions étudient l'application de codage réseau dans un canal à accès multiples avec des relais multiples (multiple access multiple relay channel ou MAMRC) constitué de M sources, L relais et une destination ($M, L \geq 2$), ce qui est une extension naturelle du MARC. Parmi les premières contributions

se trouvent [81, 91] avec ces hypothèses communes : (i) l'orthogonalité entre tous les liens radio ; (ii) des liens sources-relais sans erreur ; (iii) le schéma SNCC ; (iv) les schémas de codage réseau binaire. Le codage réseau binaire basé sur l'addition modulo 2 (XOR) n'est pas optimal pour les réseaux avec des relais multiples en terme de gain de diversité. Cet aspect a été initialement adressé dans [92] pour le cas de MAMRC, et dans [93] pour le cas d'un réseau coopératif avec deux utilisateurs. Les auteurs ont démontré, grâce à des calculs de probabilité de coupure, que la diversité pleine ne peut être atteinte qu'en utilisant les codes réseau algébriques ou non binaires. Ils ont également examiné les différentes situations possibles des canaux source-relais (en coupure ou non) et ils ont prouvé qu'il existe des schémas de codage réseau dans les alphabets d'ordres suffisamment élevés pouvant atteindre la diversité pleine. Leur travail dans [93] a ensuite été généralisé dans [94] pour le cas d'un réseau coopératif avec M utilisateurs, où les auteurs ont proposé une conception équivalente, mais en tenant compte des codes en blocs linéaires sur un corps fini non binaire. Ils ont ensuite démontré que le schéma proposé est optimal en terme de métrique de Hamming et peut augmenter l'ordre de diversité sans sacrifier le débit du système. Cependant, dans l'ensemble des contributions susmentionnées, les sources et les relais n'interfèrent pas, et les bénéfices d'un JNCC efficace n'ont pas été explorés. Récemment, une conception JNCC/JNCD basée sur les codes LDPC a été proposée dans [95] pour le MAMRC, où les auteurs ont considéré des liens orthogonaux et des codes canal/réseau non binaire. Ils ont montré que leur schéma a de meilleures performances par rapport au JNCC/JNCD binaire dans lequel toutes les opérations de codage sont basées sur XOR. Toutefois, celui-ci est déjà connu pour être sous-optimal lorsque le nombre de relais est supérieure à un. L'efficacité de leur approche par rapport à une conception JNCC/JNCD dans laquelle les codes canal binaires et les codes réseau non binaires sont employés, n'a pas été étudiée.

Un codage réseau opérant sur le corps des nombres complexes a été proposé dans [96], différent du codage réseau dans le corps Galois qui était la base de tous les schémas ci-dessus. Celui-ci est basé sur l'utilisation de vecteurs de précodage linéaire tirés du corps des nombres complexes, et une fonction de relayage particulière consistant à pondérer en puissance les estimées des symboles transmis par les sources en fonction de la qualité (en moyenne) des liens sources-relais et relais-destination. Les auteurs ont considéré des liens non parfaits et ont démontré que leur schéma garantie la diversité pleine dans les cas de MARC et de MAMRC. Le gain de codage d'une telle approche reste cependant à clarifier par rapport à une approche basée sur le corps de Galois.

2) Autres stratégies de coopération

Lorsque le relais ne peut pas décoder correctement les messages des sources, la stratégie de coopération DF conduit à la propagation d'erreurs vers la destination, tandis que la stratégie de coopération DF adaptative (par exemple DF sélectif conjoint) contraint le relais à rester silencieux. La stratégie de coopération DF souple (Soft DF ou SoDF) fondée sur le décodage souple des messages des sources et sur un JNCC souple, est une approche alternative à la stratégie de coopération DF adaptative. Elle pourrait donner de meilleures

performances par rapport à la stratégie de coopération DF adaptative. Notons que le relais peut faciliter le décodage à la destination en transmettant une fonction arbitraire des combinaisons linéaires et bruitées des mots de code transmis par les sources sans recourir au décodage dur ou souple de chaque message des sources. Cet aspect a été abordé dans plusieurs contributions et différents schémas de relayage ont été proposés.

Dans [97], les auteurs ont considéré un MARC avec des liens orthogonaux, et ont proposé de conjointement quantifier les signaux reçus au niveau du relais, opération suivie par un codage source et canal. Cela nécessite également la connaissance de l'état du canal relais-destination au relais.

L'avantage potentiel du codage réseau basé sur l'estimation-et-transmission et tenant compte des caractéristiques du MAC remonte à [42–44, 52, 75, 98–101]. Dans [44, 98], la stratégie AF a été introduite pour le TWRC à deux phases, où le relais diffuse le signal superposé qu'il a reçu après l'amplification. Cette stratégie a été mise en oeuvre dans [99] sous le nom de codage réseau analogique. Exploiter la fonction naturelle d'un MAC pour calculer la fonction de codage réseau, en utilisant des signaux transmis simultanément, semble être proposé indépendamment par plusieurs groupes de recherche en 2006 [75, 100, 101]. Dans [100], les auteurs ont démontré les avantages d'exploiter des interférences en utilisant les codes structurés pour le réseau papillon. Ceci a été davantage étudié dans [42], et une nouvelle stratégie de coopération a été introduite, basée sur l'utilisation de réseaux de points et de codes en treillis. Plusieurs autres schémas ont ensuite été suggérés dans [43,48,102] en utilisant le codage basé sur le treillis et de différentes techniques de décodage. Dans [52,101], les auteurs ont proposé le protocole de relayage débruitage-et-retransmission (denoise-and-forward ou DNF) pour le TWRC à deux phases, qui a été davantage étudié dans [103], en mettant l'accent sur la conception des constellations, représentant la fonction de codage réseau. La même idée a également été proposée dans [75] sous le nom de codage réseau au niveau physique (physical layer network coding ou PNC). Les auteurs de [75] ont considéré un TWRC à deux phases, dans lequel le relais transforme directement les paquets superposés qu'il a reçus au paquet XOR par un mapping adapté (mapping PNC). DNF et PNC peuvent être considérés comme des cas particuliers de la stratégie CoF. La PNC a été davantage développée dans plusieurs contributions en utilisant des schémas de codage canal différents. Parmi les contributions importantes sont [104] avec les codes a répétition-accumulation (repeat accumulate codes) [105] avec les codes LDPC, et [106] avec les codes convolutifs. Différentes façons d'intégrer le décodage canal et le mapping PNC au relais (une conception séparée ou conjointe) ont également été discutées et comparées dans [104, 107]. Toutefois, comme illustré dans [48, 52, 108, 109], l'utilisation de DNF, PNC ou CoF, ne peut s'approcher de la borne supérieure de la capacité du TWRC que dans le régime à fort SNR.

Récemment, différentes stratégies de décodage au relais, afin d'obtenir la séquence du message réseau codé, ont été comparées dans [110], en considérant PNC pour le TWRC à deux-phases. Les auteurs ont démontré qu'une détection et décodage conjointe de la paire des mots de code transmise, a des performances similaires au schéma de décodage en liste sur un canal sélectif en fréquence. L'algorithme de décodage en liste est une mise en oeuvre approximative de la stratégie de décodage optimal pour trouver la séquence réseau codée la plus probable à partir des signaux reçus superposés, et a été discuté dans [110]. Des

résultats similaires ont également été déduits dans [111] dans le cas du canal AWGN sans interférence entre symboles.

Dans l'ensemble, une étude plus approfondie devrait être menée pour étendre l'approche PNC, qui a été principalement étudiée dans le cas du TWRC, aux autres topologies de réseau, et afin de circonscrire les configurations dans lesquelles le PNC donne de meilleures performances par rapport aux autres solutions.

Hypothèses et scénarii retenus dans la thèse

Cette thèse étudie les performances de plusieurs réseaux multi-terminaux coopératifs, et vise à concevoir des schémas de codage appropriés et à trouver un moyen efficace de mettre en oeuvre la coopération dans un environnement sans fil. La conception comprend également le codage réseau à tous les noeuds intermédiaires. Nous considérons les deux réseaux multi-terminaux qui sont représentés dans la Fig. 1.1.

1. Un MARC avec M sources indépendantes ($M \geq 2$), un relais et une destination.
2. Un MAMRC qui est une extension naturelle du MARC avec M sources indépendantes, L relais et une destination ($M, L \geq 2$).

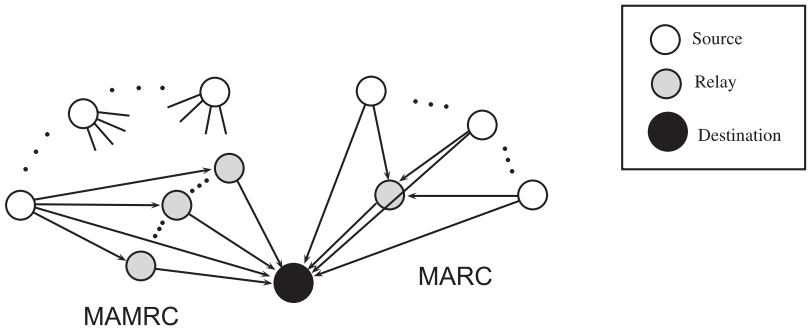

FIGURE 1 – Un canal à accès multiple avec relais (MARC) et un canal à accès multiples avec relais multiples (MAMRC)

Tout au long de la thèse, nous supposons que tous les liens du réseau sont bruités et sujets à des évanouissements lents. Les deux modes de fonctionnement du relais, à savoir, half-duplex et full-duplex sont considérés. L'hypothèse d'orthogonalité entre les liens radio est partiellement ou totalement enlevée. Cela signifie que les noeuds dans le réseau sont autorisés à transmettre simultanément en même temps ou dans la même bande de fréquence. Les sources et le(s) relais sont en mouvement et ne sont pas en vue directe. Tous les noeuds sont parfaitement synchronisés. La destination sait toujours si le(s) relais coopèrent ou non, mais les sources peuvent être ou ne pas être informées de la coopération. Ni les sources ni le relais, lorsqu'il transmettent, n'ont d'information sur l'état des canaux, par exemple au

moyen d'une voie de retour. La connaissance du canal en réception est supposée parfaite au niveau du relais et de la destination. Finalement, la métrique de performance utilisée dans la thèse est soit la probabilité de coupure conjointe, soit la probabilité de coupure individuelle.

Principales contributions

Les principales contributions de cette thèse peuvent être divisées en cinq chapitres :

Chapitre 2 : JNCC pour le MARC half-duplex semi-orthogonal

Dans ce chapitre, on propose une nouvelle classe de MARC (dans la suite : HD-SOMARC ou SOMARC) définie comme suit :

- les sources indépendantes communiquent avec la destination aidées par un relais ;
- le relais travaille en mode half-duplex et applique une stratégie de coopération de type décodage-et-retransmission sélective (selective decode and forward ou SDF) dans laquelle il transmet une fonction déterministe des messages qu'il a pu décoder sans erreurs ;
- les sources peuvent transmettre simultanément pendant la phase d'écoute du relais (phase 1) mais restent silencieuses pendant sa phase de transmission (phase 2).

Le fait de permettre des collisions au niveau du relais et de la destination exploite au mieux le caractère de diffusion du canal radio. De plus, la fonction de relayage SDF du SOMARC évite la propagation d'erreurs du relais vers la destination tout en diminuant le taux d'erreurs par bloc (BLER) et par utilisateur.

Puisque le SOMARC se décompose en deux MAC au relais et à la destination (phase 1) et un canal mono-utilisateur du relais vers la destination (phase 2), sa région de coupure est parfaitement connue pour un état du canal donné. On exprime la probabilité de coupure (outage probability) ou les rendements atteignables pour un taux de coupure ϵ (ϵ-outage achievable rates) du SOMARC par utilisateur pour le JNCC et le SNCC. Les probabilités de coupure sont détaillées sous l'hypothèse d'entrées indépendantes, gaussiennes ou discrètes, et sont comparées à celles obtenues pour un protocole d'accès orthogonal (OMARC). On propose ensuite un JNCC basé sur l'emploi de codes convolutifs et de turbo codes qui garantit la propriété de diversité pleine, dans le sens où il atteint la même diversité que le cas d'un seul utilisateur (sans interférence). En effet, dans l'annexe A, nous prouvons que la probabilité de coupure d'un canal MAC à évanouissements lents de M utilisateurs est la même que celle d'un canal MAC orthogonal, pour le cas d'une antenne de réception et des canaux indépendants de Rayleigh pour tous les liens. Suite à l'argument de [82], nous voyons qu'à fort SNR γ, les MAC au relais et à la destination ainsi que le canal mono-utilisateur du relais vers la destination deviennent $2M + 1$ canaux à effacement par bloc

(block erasure channel ou BEC) indépendants. Nous affirmons que notre design JNCC garantit la propriété de diversité pleine, quand la probabilité d'erreur par source se comporte en ϵ^2, où ϵ est la probabilité d'effacement de chaque lien. Par ailleurs, les implémentations pratiques proposées de codage canal et réseau ainsi que leurs décodages itératifs associés pour le SOMARC donnent des performances très proches de la probabilité de coupure (notamment d'environ 1 dB pour l'efficacité spectrale $\eta = 4/3$ b./c.u.) dans les cas d'une seule antenne et d'antennes multiples en réception. On montre également que pour les efficacités spectrales $\eta = 4/3$ b./c.u. et $\eta = 8/3$ b./c.u., nos schémas proposés sont plus efficaces que (1) les schémas JNCC distribués pour OMARC ; (2) les schémas SNCC. Finalement, on vérifie que SOMARC est toujours plus performant que OMARC tant sur le plan théorique que pratique. Ceci montre qu'au détriment des architectures de réception plus complexes, l'application de la non-orthogonalité est plutôt un avantage.

Chapitre 3 : JNCC pour le MARC half-duplex non-orthogonal

Dans HD-SOMARC, les sources doivent rester silencieuses pendant la durée de transmission du relais. Ceci nécessite des signalisations supplémentaires pour informer les sources de la coopération. Cependant, si nous permettons aux sources de transmettre, seule la destination doit être informée de la coopération, ce qui réduit considérablement la surcharge de signalisation de contrôle. En même temps, les sources peuvent utiliser de meilleurs codes (bits de parité supplémentaires), mais étant donné que les signaux des sources interfèrent avec le signal du relais pendant la deuxième phase, un décodage conjoint plus complexe est nécessaire à la destination. Ce que nous gagnons d'un point de vue codage pur pourrait être perdu en raison de la sous-optimalité du décodage itératif. L'autre problème intéressant est de concevoir des codes qui ont de bonnes performances dans leurs versions partielles sur les liens source-relais, et aussi dans leur versions complètes à la destination (c.à.d, compte tenu des bits de parité supplémentaires des sources au cours de la deuxième phase et ceux du relais en cas de coopération).

Motivé par les points mentionnés ci-dessus, nous proposons dans ce chapitre une nouvelle classe de MARC (dans la suite : HD-NOMARC ou NOMARC) définie comme suit :

- les sources indépendantes communiquent avec la destination aidées par un relais ;
- le relais travaille en mode half-duplex et applique la stratégie SDF dans laquelle il transmet une fonction déterministe des messages qu'il a pu décoder sans erreurs ;
- les sources peuvent transmettre simultanément pendant les deux phases d'écoute et de transmission du relais.

Au cours de la première phase de transmission, les sources diffusent simultanément la première partie de leurs messages, interférant au relais et à la destination. Pendant la deuxième phase, ils continuent à transmettre la deuxième partie de leurs messages, et donc interfèrent avec le relais en cas de transmission, mais, en même temps, la destination bénéficie des codes plus puissants pour effectuer la détection et le décodage conjoint. C'est en effet la forme la plus générale de relayage half-duplex où l'accès n'est pas orthogonal [112, 113]. Concernant le protocole SDF, ses intérêts théoriques et pratiques ont

été confirmés dans le chapitre 2 pour HD-SOMARC. Cependant, de nombreuses questions doivent encore être abordées, y compris l'impact de l'interférence d'accès multiples au cours des deux phases de transmission sur la probabilité de coupure. En se basant sur une analyse minutieuse des événements de coupure, on exprime la probabilité de coupure ou les rendements atteignables pour un taux de coupure ϵ du HD-NOMARC par utilisateur pour le JNCC et le SNCC. Les probabilités de coupure sont détaillées sous l'hypothèse d'entrées indépendantes, gaussiennes ou discrètes. Elle sont également utilisées pour optimiser de façon numérique la fraction des utilisations de canal disponible au cours desquelles le relais écoute et celles pendant lesquelles les sources et le relais transmettent, pour une efficacité spectrale fixe. Cette allocation optimale est ensuite appliquée à nos conceptions pratiques. Les probabilités de coupure sont également comparées à celles obtenues pour un protocole d'accès orthogonal (OMARC), en considérant un budget énergétique fixe par source (par les dimensions disponibles). On propose ensuite un JNCC basé sur l'emploi de turbo codes qui garantit la propriété de diversité pleine, et est flexible en terme de nombre de sources et de schémas de codage et modulation (modulation coding scheme ou MCS). La justification de notre construction de code a été déjà discutée dans le chapitre 2. Par ailleurs, les implémentations pratiques proposées de codage canal et réseau ainsi que leurs décodages itératifs associés pour le HD-NOMARC donnent des performances très proches de la probabilité de coupure, dans les cas d'une seule antenne et antennes multiples en réception, et pour l'efficacité spectrale $\eta = 4/3$ b./c.u.. On montre également que pour les efficacités spectrales $\eta = 4/3$ b./c.u. et $\eta = 8/3$ b./c.u., nos schémas proposés sont plus efficaces que (1) les schémas JNCC distribués pour OMARC ; (2) les schémas SNCC. Finalement, l'avantage d'utiliser la nature de diffusion de l'environnement sans fil est confirmé par des simulations.

Chapitre 4 : JNCC pour le MARC full-duplex non-orthogonal

Dans les chapitres précédents, nous avons introduit et analysé deux classes différentes de MARC avec un relais half-duplex. Comme déjà mentionné, un relais full-duplex peut atteindre une capacité supérieure à celle d'un relais half-duplex, d'un point de vue théorique. En outre, l'application des relais full-duplex est de plus en plus faisable en pratique. Cela inspire une analyse théorique plus approfondie et la conception des schémas JNCC pratiques pour le MARC avec un relais full-duplex.

Dans ce chapitre, nous prenons un pas de plus et nous enlevons la contrainte half-duplex du MARC. Nous proposons une nouvelle classe de MARC (dans la suite : FD-NOMARC) définie comme suit :

- les sources indépendantes communiquent avec la destination aidées par un relais ;
- le relais travaille en mode half-duplex et applique la stratégie SDF dans laquelle il transmet une fonction déterministe des messages qu'il a pu décoder sans erreurs ;
- les sources et le relais peuvent transmettre simultanément.

Un nouveau protocole de transmission adapté à cette classe de MARC est proposé, qui combine plusieurs idées trouvées dans [5] [114] [112] [71]. Suivant [5], nous considérons un

codage de type block Markov superposition coding. Pendant la transmission du premier bloc (bloc initial), les sources diffusent simultanément leurs messages, interférant au niveau des relais et de la destination. La destination stocke simplement les signaux reçus. Le relais décode conjointement les messages des sources, et combine linéairement les messages correctement décodés pour produire son propre message à transmettre au cours de la transmission de bloc suivant. Notez que le délai de traitement au niveau du relais est généralement négligé dans notre modèle du système. En cas d'échec de décodage de tous les messages, il ne fait rien et reste silencieux lors de la transmission de bloc suivant. Au cours de la transmission du deuxième bloc, les sources diffusent des nouveaux messages à la fois au relais et à la destination. Le relais décode conjointement les messages des sources et applique la même procédure que précédemment. En même temps, si le décodage sélectif au cours de la transmission du bloc précédent a réussi, le relais transmet le message produit à la destination. La destination continue de stocker tous les signaux reçus qui interfèrent. Le processus est répété pour les blocs suivants. Une fois que tous les blocs ont été reçus, la destination commence à décoder. Ce type de décodage peut introduire des retards importants, mais offre les meilleures performances. Il est important de souligner que la destination sait toujours si le relais coopère ou non, mais en fonction de la stratégie de codage, les sources peuvent être ou ne pas être informées de la coopération. Concernant le protocole SDF, ses intérêts théoriques et pratiques ont été confirmés dans le chapitre 2 pour HD-SOMARC et dans le chapitre 3 pour HD-NOMARC. Bien que ces analyses théoriques du protocole SDF a permis de mieux comprendre le comportement du système, en particulier en présence d'interférences d'accès multiples, de nombreuses questions doivent encore être abordées, y compris l'impact d'un relais full-duplex. En se basant sur les taux atteints par un MARC utilisant un relais full-duplex et le protocole DF dans [8, 27, 115], on exprime la probabilité de coupure conjointe ou les rendements atteignables pour un taux de coupure conjointe ϵ du FD-NOMARC avec JNCC, block Markov superposition coding, et au décodage bloc par bloc à la destination. Les probabilités de coupure sont détaillées sous l'hypothèse d'entrées indépendantes, gaussiennes ou discrètes, et comparées à celles obtenues pour un protocole d'accès orthogonal (OMARC), en considérant un budget énergétique fixe par source (par les dimensions disponibles). Nous proposons ensuite un JNCC basé sur l'emploi de turbo codes qui garantit la propriété de diversité pleine, et est flexible en terme de nombre de sources et de MCS. La justification de notre construction de code a été déjà discutée dans le chapitre 2. En outre, contrairement au décodage bloc par bloc, notre approche proposée pour le décodage fonctionne sur tous les blocs transmis. Les performances des schémas proposés sont ensuite comparés avec les probabilités de coupure extraites, qui peuvent être considérées comme des bornes inférieures sur les performances théoriques de nos conceptions. On montre également que pour les efficacités spectrales $\eta = 4/3$ b./c.u. et $\eta = 8/3$ b./c.u., nos schémas proposés sont plus efficaces que les schémas JNCC existants pour OMARC.

Chapitre 5 : JNCC pour le MAMRC half-duplex semi-orthogonal

Dans ce chapitre, nous étendons le modèle de réseau en tenant compte de plusieurs relais qui aident les sources pour communiquer avec une destination. Les relais fonctionnent en

mode half-duplex. Tous les noeuds du réseau sont informés qu'ils coopèrent. Nous proposons une nouvelle classe de MAMRC (dans la suite : HD-SOMAMRC ou SOMAMRC) définie comme suit :

- les sources indépendantes communiquent avec la destination aidées par de multiples relais ;
- les relais travaillent en mode half-duplex et appliquent la stratégie SDF dans laquelle ils transmettent une fonction déterministe des messages qu'ils ont pu décoder sans erreurs ;
- les sources peuvent transmettre simultanément pendant la phase d'écoute des relais (phase 1) mais restent silencieuses pendant leur phase de transmission (phase 2). Les relais peuvent transmettre simultanément pendant la phase 2.

Autoriser les collisions au niveau du relais et la destination restitue la réalité des environnements sans fil et exploite mieux l'aspect diffusion du canal radio que le MAMRC orthogonal (OMAMRC). Concernant le protocole SDF, ses intérêts théoriques et pratiques ont été confirmés dans le chapitre 2 pour HD-SOMARC, dans le chapitre 3 pour HD-NOMARC, et dans le chapitre 4 pour FD-NOMARC. Bien que ces analyses théoriques du protocole SDF ont fourni un aperçu du comportement du système, de nombreuses questions doivent encore être abordées dans le cas du MAMRC, y compris l'impact du JNCC et des interférences d'accès multiple.

En se basant sur une analyse minutieuse des événements de coupure, on exprime la probabilité de coupure ou rendements atteignables pour un taux de coupure ϵ du HD-SOMAMRC par utilisateur pour le JNCC et le SNCC. Les probabilités de coupure sont détaillées sous l'hypothèse d'entrées indépendantes, gaussiennes ou discrètes. Elle sont également utilisées pour optimiser de façon numérique la fraction des utilisations de canal disponible au cours desquelles les relais écoutent et ceux pendant lesquelles les relais transmettent, pour une efficacité spectrale fixe. Cette allocation optimale est ensuite appliquée à nos conceptions pratiques. Les probabilités de coupure sont également comparées à celles obtenues pour un protocole d'accès orthogonal (OMAMRC), en considérant un budget énergétique fixe par source (par les dimensions disponibles). Pour exploiter efficacement la diversité maximale disponible, le codage XOR est généralisé aux alphabets d'ordre supérieur. On propose ensuite des schémas pratiques de JNCC, dans lesquels le codage canal binaire et le codage réseau non binaire sont combinés. Notre schéma garantit également la propriété de diversité pleine. Comme nous avons déjà vu dans le chapitre 2, à fort SNR, les MAC aux relais et à la destination deviennent $ML+M+L$ BEC indépendants (correspondant aux ML liens source-relais et $M+L$ liens source-destination et relais-destination). Nous affirmons que notre design JNCC garantit la propriété de diversité pleine, quand la probabilité d'erreur par source se comporte en ϵ^{L+1}, où ϵ est la probabilité d'effacement de chaque lien. Finalement, les analyses théoriques et les simulations ont démontré que le HD-SOMAMRC/JNCC proposé peut pleinement exploiter la diversité spatiale, et a des bénéfices significatifs comparés aux schémas existants. De plus, il donne des performances très proches de la limite de coupure pour les cas d'une seule ou de multiples antennes de réception à la destination, et pour l'efficacité spectrale $\eta = 4/3$ b./c.u..

Chapitre 6 : Stratégies de coopération pour le MARC half-duplex semi-orthogonal

Dans HD-SOMARC, comme l'interférence générée par le relais à la destination n'impacte pas les performances globales (contrairement à HD-NOMARC, FD-NOMARC, ou HD-SOMAMRC), le choix de la fonction de relayage est un degré de liberté intéressant qui reste à être exploité et optimisé. Dans ce chapitre, nous étudions l'approche JNCC et nous comparons le relayage SDF avec deux fonctions de relayage s'appuyant sur le décodage-et-retransmission souple (SoDF) : l'une basée sur les rapports logarithmiques de probabilité à posteriori (log a posteriori probability ratios ou LAPPRs) [116], et l'autre basée sur l'estimation d'erreur quadratique moyenne (mean square error ou MSE) [117]. En effet, SoDF peut être considérée comme une approche alternative à SDF. Le JNCC que nous proposons est générique et peut être facilement étendu à des constellations arbitraires, permettant ainsi d'améliorer l'efficacité spectrale du système. Les résultats de simulation montrent que SDF fonctionne bien dans la plupart des configurations ; et seulement dans certains cas extrêmes, SoDF (basées sur LAPPR ou sur estimation MSE) peut légèrement surpasser SDF en terme de performance. Les résultats de simulation confirment également que l'estimation MSE est une fonction de compression des LAPPRs efficace pour les modulations d'ordre élevé.

Perspectives

Comme perspectives pour les travaux futurs, nous proposons les directions suivantes :

- Nous avons montré que nos conceptions proposées pour les HD-SOMARC, HD-NOMARC et HD-SOMAMRC ont des performances qui sont très proches de la probabilité de coupure pour l'efficacité spectrale $\eta = 4/3$ b./c.u.. Cependant, l'optimisation de gain de codage devrait encore être faite pour les constellations d'ordres plus élevés. Dans le cas du FD-NOMARC, les probabilités de coupures individuelles doivent être dérivées dans un première temps, conditionnées au décodage conjoint de tous les blocs transmis. Cela nous permet de mesurer l'écart entre nos schémas proposés et les limites exactes de coupure, et ainsi nous pousse à atteindre les limites théoriques par l'optimisation de gain de codage.

  Afin d'optimiser le gain de codage, il est également important de calculer les bornes supérieures sur les performances d'erreurs en utilisant des codes spécifiques, qui pourraient ensuite servir de base pour trouver le code optimal. Ces bornes sont connues pour être serrées dans le régime des SNRs moyens à grands. À cette fin, des outils et des techniques de [118–120] doivent être utilisées conjointement avec les connaissances sur les fonctions énumératrices des poids complètes (weight enumerating function ou WEF) des codes convolutifs et sur les fonctions énumératrices des poids entrées-sorties moyennes (average input-output weight enumerating functions ou IOWEF) des turbo codes [121, 122]. Une telle analyse est effectuée pour OMARC avec BPSK

et pour un canal AWGN dans [123]. Cependant, l'analyse des performances pour le cas de la transmission non-orthogonale et pour des canaux à évanouissements lents restent une question ouverte pour les travaux futurs. Les limites extraites seraient également utilisées pour prédire les performances du système à très faible taux d'erreur binaire ou taux d'erreur par bloc, et pourraient également servir de référence pour les algorithmes de décodage itératif sous-optimaux.

- En ce qui concerne le MAMRC, le codage canal non binaire au niveau des sources et des relais pourrait être étudié, notamment en cas de JNCC. Dans ce cas, comme les schémas du codage et de la modulation aux sources et aux relais sont définis dans le corps non-binaire, où les coefficients du codage réseau sont choisis, il n'y a plus besoin d'utiliser la conversion "bit à symbole" ou "symbole à bit". Cela peut améliorer les performances, mais en même temps, il pourrait être restrictif en terme d'efficacité spectrale. Une conception possible basée sur les codes LDPC a été traitée dans [95] pour OMAMRC. D'autres conceptions basées sur les turbo codes non-binaires pourraient être étudiées dans le futur.

- Dans cette thèse, nous n'avons considéré que le HD-SOMAMRC. Toutefois, il serait utile d'examiner des conceptions pratiques et des limites théoriques de schémas plus complexes comme MAMRC non-orthogonale avec un relais half-dupelx (HD-NOMAMRC) ou Full-Duplex (FD-NOMAMRC). Dans HD-NOMAMRC, la contrainte que les sources restent silencieuses durant la phase d'émission des relais est enlevée, et dans FD-NOMAMRC, la contrainte half-duplex des relais est aussi supprimée. Ce travail ne sera pas une simple généralisation des résultats actuels.

- Il n'est pas clair qu'il existe une meilleure fonction de relayage pratique que SDF dans le cadre du HD-NOMARC, FD-NOMARC et HD-SOMAMRC. Toutefois, d'autres fonctions de relayage pouvant donner de meilleures performances que le SDF ou l'estimation MSE, pourraient être explorées dans le cadre du MARC half-duplex avec un protocole de transmission semi-orthogonal. Une perspective possible est de considérer l'approche PNC. Comme déjà mentionné, le PNC a surtout été étudié dans le cas du TWRC à deux-phases, où les deux sources agissent également en tant que destination, et une destination distincte est absente. Ainsi, l'un des messages réseaux codés est parfaitement connu à chaque source. De plus, puisqu'il n'y a pas de lien direct entre les sources, elles ne reçoivent que les informations diffusées de la part du relais pendant la deuxième phase, ce qui conduit à une diversité d'ordre un (comme dans le cas des réseaux multi-sauts). Par conséquent, l'étude du PNC dans des situations où la diversité coopérative peut être exploitée, tel que MARC, reste un sujet d'intérêt. En utilisant l'approche PNC, le relais décode l'addition modulo 2 des messages des sources à partir du signal reçu superposé. Pour réduire encore la propagation d'erreur du relais vers la destination, nous pouvons considérer le PNC avec DF conjoint ; ici, le relais transmet s'il peut décoder avec succès le XOR des messages. La probabilité de celui-ci est toujours plus grande que la probabilité de succès de décodage des messages de tous les sources. Par conséquent, le relais est plus souvent actif, ce qui peut améliorer les performances globales par rapport au DF conjoint classique. Les

avantages par rapport à SDF restent discutables. Cependant, cette approche semble difficile à mettre en oeuvre du point de vue pratique. La raison réside dans le fait que le relais ne décode pas individuellement chaque message des sources, et il ne peut pas utiliser les codes CRC (cyclic redundancy check) utilisés en détection d'erreurs inclus dans les messages des sources, pour effectuer le PNC sélectif conjoint. Le relayage souple peut résoudre ce problème : le relais peut calculer directement les informations souples sur le message réseau codé pour construire l'estimation MSE. Ce dernier, s'il est combiné avec le décodage ML à la destination tenant compte l'estimation MSE [124], semble être une solution prometteuse. Toutefois, dans les travaux futurs, nous pouvons tenter d'identifier les configurations où le PNC souple peut donner de meilleurs performances que l'approche SDF dans le cadre du MARC half-duplex avec le protocole de transmission semi-orthogonal. Finalement, il est intéressant de mettre au point une stratégie de coopération et une conception de code appropriée, qui superpose les deux approches du SDF et du PNC souple, ou plus généralement, du SDF et du CoF.

- Nous avons montré par des analyses théoriques et des schémas de codage pratiques qu'exploiter partiellement ou totalement la structure de l'interférence, est presque toujours bénéfique par rapport au protocole de transmission orthogonal. Cependant, le choix entre le protocole de transmission semi-orthogonal et non-orthogonal dans les cas de MARC ou MAMRC dépend de la configuration et reste une question ouverte. L'objectif serait d'identifier en fonction du scénario le protocole réalisant le meilleur compromis performance/complexité et d'adapter d'une façon dynamique le codage et le décodage.

Chapter 1

Introduction

Cooperative communications and network coding

Communications in multi-terminal networks become more reliable and efficient when nodes share their resource and power to transmit data with the hope that such a cooperative approach leads to savings for the overall network resources and power consumption. Obviously, user cooperation in networks can potentially take place whenever the number of communicating nodes exceeds two. Therefore, the three-terminal network, first introduced by Van der Meulen in 1968 [2], certainly constitutes a fundamental unit in user cooperation. A vast portion of the literature, especially in the realm of information theory, has already been devoted to the relay channel and its multiple variants such as multiple relay channels or two-way relay channels, which can be seen as special cases. Moreover, Sendonaris et al. have proposed user cooperation as a form of diversity in a cellular uplink scenario and show its benefit under various metrics [3] [4].

The study of relay channels dates back to [5], where the authors presented several structurally different random coding schemes and compared their achievable rates with the min-cut max-flow capacity upper bounds. In the cooperation scheme [5, Theorem 1], the relay decodes the source message and cooperates with the source to help the destination in decoding. This has given rise to Decode-and-Forward (DF) relaying protocol. In the observation scheme [5, Theorem 6], the relay transmits an estimate (or quantized version) of its observation of the source message to the destination, using ideas from source coding with side information [6, 7]. This scheme has more often been referred to as Compress-and-Forward (CF) strategy [8]. A general theorem was also presented in [5, Theorem 7] that combines cooperation and observation in a single coding scheme in order to maximize the achievable rates. Other relaying strategies such as Partial Decoding (PD) and Amplify-and-Forward (AF) helped to widen the analysis [9–13]. Furthermore, a variety of contributions

including new bounds, power control strategies and some results on half-duplex relaying were proposed in [14].

Multiple relay channels, consisting of single-source, single-destination, and more than one relay, were studied in different contributions [15–17], and their achievable rates with DF, PD and CF were presented in [17]. Relaying have also grabbed particular attention in wireless environments. Among the important contributions are those of Laneman and Wornell addressing the performance of important relaying protocols in wireless environments [18–20]. A number of interesting relaying protocols are also proposed and analyzed in [21–23] including repetition coding, and in [24] including space time coded cooperation. Other complementary contributions come in the form of novel information-theoretic results and new insights into information theoretic (random) coding for relays by Kramer et al. [25] and Chong et al. [26].

The extension of the previous results to multiple-access and broadcast schemes, where multiple sources or multiple receivers are present, has been considered in a variety of contributions:

First, a Multiple Access Relay Channel (MARC) was presented in [8, 27, 28], and the corresponding rate regions with AF, DF and CF were derived. Capacity bounds for the MARC with a half-duplex relay and the corresponding achievable rates with AF, DF, and PD were also investigated in [29]. Additionally, a linear relaying protocol called multi-access AF is analyzed in [30] for the MARC, and shown to be optimal at the high multiplexing gain regime.

On the other hand, a cooperative Relay Broadcast Channel (RBC) has first been studied in [31, 32]. The authors considered a network with a single source and two receivers, and introduced two channel models, namely, partially cooperative RBC (only one receiver act as a relay for the other) and fully cooperative RBC (both receivers act as relay nodes for each other). They then derived and compared the corresponding achievable rate regions considering DF. The partially cooperative RBC was further studied in [33] for the case of more than one destination. A third RBC model, called dedicated RBC was introduced and studied in [8, 34], where an additional relay node was inserted into the broadcast channel with the sole function of relaying. Rate regions and upper bounds for the cooperative RBC were further developed in [35, 36]. In parallel, AF for the multi-hop Multiple Access Channel (MAC) and Broadcast Channel (BC) (i.e., no direct links between the sources and the receivers) has been studied in [37], where the optimal power allocation on the relays were presented, as well as the AF relay MAC-BC duality.

Finally, the basic idea of the bidirectional or Two-Way Relay Channel (TWRC) was first presented in [38] for noiseless channels. In TWRC, two nodes exchange their information

with the help of a relay. Both broadcast transmission and simultaneous multiple access can be considered in this channel model which have been the subject of several research efforts. In [39–41], the authors derived the achievable rates considering full-duplex nodes, broadcast transmission at all nodes and simultaneous multiple-access of all nodes. In [39, 40] the achievable rates were derived for AF, DF, and CF, while in [41], an achievable rate region for Compute-and-Forward (CoF) relaying strategy was derived. In the CoF strategy [42, 43], the relay computes (or decodes) a linear combination of the transmitted messages from the nodes-to-relay MAC. Further contributions are based on the premise of half-duplex nodes, for which we distinguish two main categories: (i) two phase bidirectional relay channel with Multiple Access Broadcast protocol in which the two communicating nodes transmit simultaneously to the relay node during the first phase, and the relay broadcasts to both of them during the second phase. In this model there is no direct link between the two communicating nodes; (ii) three phase bidirectional relay channel with broadcast transmission at all nodes and without multiple access. The first channel model has been considered in [44–48] where the authors derived achievable rates considering different relaying schemes (AF, DF, PD, CF, and CoF). Moreover, the broadcast capacity region was derived in [49], where each receiver node knows perfectly the message intended for the other node. Code design and achievable rates for the second model have been considered in [50, 51]. Several relaying strategies and their corresponding achievable rates were also discussed in [52] for both categories.

In a general multiterminal network with multiple source-destination pairs, the intermediate nodes do not need to process separately and independently each incoming data flow, and there exist several ways to perform algebraic operations on all the incoming flows. This is the fundamental concept of network coding, which was initially proposed by Ahlswede, Cai, Li, and Yeung in [53], and has motivated intensive research. We note that many of the cooperative schemes that have already been mentioned, especially for MARC and TWRC, can be cast into the framework of network coding. By applying network coding in multicast transmission with a single source and lossless links, the authors of [53] have proved that the network throughput could achieve the min-cut max-flow capacity between the source and the sinks. This remarkable result has motivated further theoretical and practical research to extend network coding to wireless media, which, albeit lossy, greatly facilitate its application, for broadcast is guaranteed at no cost. The application of network coding to wireless packet networks has been investigated from a network perspective in a variety of contributions. Deterministic network coding was introduced in [54], which necessitates a complete knowledge of the whole network. The authors of [54] showed that the linear network coding with finite alphabet size can achieve the min-cut max-flow capacity. This issue

was further analyzed in [55, 56]. However, a complete knowledge of the large packet networks are in general not available, which explains the particular interest to perform random network coding [57, 58]. In this case, the network coding operations are chosen randomly and independently at each node. As shown in [58], random linear codes can asymptotically achieve the min-cut max-flow capacity for large code lengths. These contributions together with [59,60] also demonstrated the effectiveness of distributed random network coding over a network with correlated sources (e.g. sensor network) where distributed compression is required. The asymptotic optimality of random distributed network coding for wireless networks with or without packet erasures has also been demonstrated in [61–63]. Among the other contributions are [38,64,65] which focus on lossless channels, and [66] which considers lossy erasure channels in sensor networks. Finally, the need for end-to-end coding in multiterminal networks has been investigated in [67], where the authors showed that only a unified approach which jointly treats source coding, channel coding, and network coding can achieve the capacity.

From a physical layer perspective, wireless network coding can be used in a variety of contexts, in conjunction with channel coding and source coding. In densely deployed multiterminal networks (e.g. sensor networks) where correlation exists between the sources, the nodes need to combine source coding, channel coding, and network coding. Several ideas and contributions have been proposed in this matter with the aim of introducing some code designs in a unified framework [68–70]. However, in the case of independent incompressible sources, the combination of network coding and channel coding has received particular research attention, and various contributions in the context of MARC [71,72], TWRC [73–75], user cooperation [76–79] or cross-packet coding for hybrid ARQ systems [80], have been proposed over the last few years. Here, the primary goal of network coding is to provide reliable and spectrally-efficient transmission over the network. From a pure coding perspective, the challenge is to achieve full diversity and to maximize the coding gain. It is worth stressing that full diversity cannot be achieved without limitations on the transmission rate. Moreover, ensuring full (space) diversity is not necessarily the most critical design criterion in realistic wireless environments since many other sources of diversity exist (multipath diversity, receive antenna diversity, etc.). There are essentially two ways to combine network coding and channel coding: Separate Network Channel Coding (SNCC) and Joint Network Channel Coding (JNCC). In SNCC, channel coding is performed locally and separately for each transmission to transform the noisy channels into erasure-based links. On the network layer, network coding is performed for the erasure-based networks which are provided by the lower layers [81]. SNCC requires Separate Network Channel Decoding (SNCD) at the destination, in which channel decoding is first performed at the physical layer and outputs

the estimates to the network decoder. However, in JNCC, we exploit the redundancy of the network code to support the channel code, which can finally improve the coding gain of the system. A Joint Network Channel Decoding (JNCD) is then performed at the destination, in which soft information between the network decoder and the channel decoders is exchanged.

Practical network coding in wireless environments

This part gives an overview of the state of the art of practical network coding designs for wireless communication together with channel coding. The contributions are divided into two main categories, namely, DF based network coding in which we come back to the message space at all intermediate nodes to construct the network coded message, and estimate-and-forward based network coding in which the network coded message is constructed without returning to the message space, i.e., it would be an arbitrary function of the noisy linear combinations of the codewords transmitted by the sources.

1) DF based network coding

Hausl et al. were amongst the first to describe efficient JNCC for MARC based on Low-Density Parity Check (LDPC) codes [71] or turbo codes [72]. Common to this set of contributions are the hypotheses of (i) time-division half-duplex mode for relaying operation; (ii) orthogonality between all the radio links; (iii) joint selective DF strategy, i.e., the relay cooperates if and only if all the decoded messages are error-free. Concerning the first hypothesis, we know from information theory that half-duplex relaying is basically sub-optimal with respect to full-duplex one, but often retained for practical reasons. Physical constraints (severe attenuation over the wireless channel, insufficient electrical isolation between the transmit and receive circuitry, etc.), complexity and cost considerations, most likely explain the moderate interest for the full-duplex relaying schemes. Concerning the second hypothesis, we have already pointed out that wireless media naturally offer broadcast without an additional cost. This intrinsic property comes at the price of signal superposition (i.e. interference) at all intermediate nodes and at the destination. In order to fight back this impediment, orthogonal medium access (in time, frequency or code space) is often assumed in cooperative communications. If orthogonality greatly simplifies the design of JNCC/JNCD and the performance analysis, it also substantially reduces the spectral efficiency of the proposed systems. Indeed, from an information-theoretic point

of view, orthogonal multiple-access is, in general, not optimal for the slow fading (quasi-static) channel, although it may be close to optimal at a very low Signal-to-Noise Ratio (SNR). In [71], the authors also assumed error-free source-to-relay links. To justify this hypothesis, we could imagine a restrictive communication scenario where the relay is very close to, and in line of sight with, the two sources. But even in this case, some decoding errors would occur at the relay, since, in practice, constituent codes used on point-to-point links are never perfect. Furthermore, neither of the above code designs guarantee full diversity. More recently, JNCC based on LDPC codes were presented in [82] where the authors also elaborate on orthogonal links and error-free source-to-relay links. Their purpose is to construct JNCC guaranteeing full diversity, which, in essence, leads on an asymptotical analytical reasoning (with respect to the SNR) and the hardening of slow-fading channels into block erasure channels. In this perspective, the achieved diversity of the proposed JNCC does not depend on the quality of the source-to-relay links and, for the sake of simplicity, the authors assumed error free source-to-relay links. However, their proposed JNCC is not generic in terms of coding choice and the number of sources. Moreover, its coding gain decreases enormously for the case of error-prone source-to-relay links, even if its full diversity structure is maintained. The benefit of JNCC in situations where the relay is not able to decode reliably, has also been addressed in [83]. But the authors assume that the signals transmitted from the relay to the destination are analog, and the coding scheme that they employ is oversimplistic compared to [71, 72, 82]. To forward the analog information at the relay in a bandwidth efficient manner, the quantization (or compression) of the log a posteriori ratios of the relay parity bits, has been investigated in [84, 85], which requires the knowledge of the relay-to-destination channel state at the relay. Besides, in all these contributions, the sources and the relay do not interfere. Similar JNCC designs were also proposed in the case of TWRC with time division multiple-access [73, 74].

Overall, the aforementioned schemes are designed for small wireless networks with specific topologies, which cannot be easily applied to large multi-terminal wireless networks. For the MARC with M sources, $M > 2$, several coding schemes have been recently proposed, among which are [86] which is based on linear product codes, and [87] which is based on multi-edge type LDPC codes. Several code designs have also been presented in the case where M sources, $M > 2$, communicate with a common destination and each source can relay information for the others [88–90]. In [88], a framework for adaptive network coded cooperation was proposed in which the real-time adaptation of network codes to variant link qualities was mainly addressed. This scheme was further investigated in [89] by taking into account the communication link failures. In parallel, a number of contributions study the application of network coding in Multiple Access Multiple Relay Channel (MAMRC) with M sources, L relays and one destination ($M, L \geq 2$), which is a natural extension

of a MARC. Among the first contributions are [81, 91] with the common hypotheses of (i) orthogonality between all the radio links; (ii) error-free source-to-relay links; (iii) separate network channel coding and decoding; (iv) binary network coding schemes. Binary network coding, based on the addition modulo 2 (XOR), is not optimal for networks with multiple relays in terms of diversity gain. This issue has initially been addressed in [92] in the case of MAMRC, and in [93] in the case of two-user cooperative network. The authors demonstrated, through outage probability calculations, that the full diversity can only be achieved by using the algebraic or non-binary network codes. They also considered different possible source-to-relay channel situations (outage or not) and they proved the existence of the full diversity achieving network coding schemes in sufficiently high order alphabets. Their work in [93] has then been generalized in [94] for the case of M-user cooperative network, where the authors proposed an equivalent design, but by considering linear block codes over a non binary finite field. They then demonstrated that their proposed scheme is optimal in terms of the Hamming metric and can increase the diversity order without sacrifice in the system rate. However, in all of the above contributions, the sources and the relays do not interfere and the benefit of efficient JNCC has not been explored. Recently, a JNCC/JNCD design based on LDPC code has been proposed in [95] for MAMRC where the authors considered orthogonal links and non-binary channel and network codes. Their proposed scheme was shown to outperform binary JNCC/JNCD in which all network coding operations are binary XOR. However, the latter is already known to be suboptimal when the number of relays exceeds one. The efficiency of their approach compared to a JNCC/JNCD design in which binary channel codes and non binary network codes are employed, has not been investigated.

Different from Galois-field network coding which was the basis of all the above schemes, a complex-filed network coding has been proposed in [96]. The latter is based on the use of linear constellation precoding vectors drawn from complex-field, and Link-Adaptive Regenerative (LAR) relaying scheme in which the detected symbols at the relay are scaled in power according to the SNR of the source-to-relay and the intended relay-to-destination channels. The authors assumed error-prone links and showed that their proposed scheme guarantee the full diversity in the case of MARC and MAMRC. However, the benefit of their proposed complex-field network coding compared to Galois-field network coding in terms of coding gain remains unclear.

2) Estimate-and-forward based network coding

When the relay cannot decode successfully the source messages, DF strategy leads to error propagation towards the destination, while adaptive DF (such as joint selective DF),

constrain the relay to remain silent. Soft DF (SoDF), conditional on soft-in soft-out channel decoding of the source signals and soft-in soft-out JNCC, is an alternative approach to adaptive DF, which may perform better than the latter, if it does not negatively impact the decoding at the destination when the source-to-relay link is error-prone. However, the relay can facilitate the decoding at the destination by transmitting an arbitrary function of the noisy linear combinations of the codewords transmitted by the sources, without invoking the hard or soft decoding of each source message. This issue was addressed in a variety of contributions and different relaying schemes were proposed.

In [97], the authors considered a MARC with orthogonal links, and proposed to jointly quantize the received signals at the relay, which was then followed by source and channel coding. This also requires the knowledge of the relay-to-destination channel state at the relay.

The potential benefit of estimate-and-forward based network coding taking into account the characteristics of the MAC dates back to [42–44,52,75,98–101]. In [44,98], the AF strategy was introduced for the two-phase TWRC, where the relay broadcasts the superimposed received signal after amplification. This strategy has been implemented in [99] under the name of analog network coding. Exploiting the natural function of a MAC to compute the desired network coded function from simultaneously transmitted signals appears to be proposed independently by several research groups in 2006 [75, 100, 101]. In [100], the authors demonstrated the benefits of exploiting interference using structured codes for butterfly network. This was further studied in [42], and a new relaying strategy called CoF was introduced based on the use of lattice codes. Several other schemes have then been suggested in [43, 48, 102] using lattice based coding and different decoding techniques. In [52, 101], the authors proposed DeNoise-and-Forward (DNF) relaying protocol for a two phase TWRC, which was further studied in [103] with the focus on the design of constellations and maps, representing the network coding function. The same idea was also proposed in [75] under the name of Physical Layer Network Coding (PNC). The authors of [75] considered a two phase TWRC in which the relay directly transforms the superimposed received packets to the XOR (network-coded) packet by a suitable mapping (PNC mapping). DNF and PNC can be seen as special cases of CoF strategy. PNC was further developed in a variety of contributions using different channel coding schemes. Among the important contributions are [104] with repeat accumulate codes, [105] with low density parity check codes, and [106] with convolutional codes. Different ways of integrating channel-decoding and PNC mapping at the relay (separate or joint design) were also discussed and compared in [104, 107]. However, as demonstrated in [48, 52, 108, 109], the use of the DNF, PNC or CoF, could only approach the upper bound on the capacity of the TWRC at the high SNR regime.

Recently, different decoding strategies at the relay, in order to obtain the network coded

message sequence, have been compared in [110] considering PNC for a two-phase TWRC. The authors showed that jointly detecting and decoding the pair of the transmitted codewords, has a performance similar to the list decoding scheme over a frequency selective channel. The list decoding algorithm is an approximate implementation of the optimal decoding strategy to find the most likely network coded sequence from the superimposed received signals, and is discussed in [110]. Similar results have also been deduced in [111] in case of an Additive White Gaussian Noise (AWGN) channel with no Inter-Symbol Interference (ISI).

Overall, further investigation should be conducted to extend the PNC approach, which has been mainly studied in the case of TWRC, to other network topologies and to circumscribe the configurations in which PNC outperforms other solutions.

Assumptions and Considered Scenarios

This thesis studies the performance of multiterminal cooperative networks and aims to design appropriate coding scheme and to find an efficient way to implement cooperation in a realistic wireless environment. The design also includes network coding at all intermediate nodes. We consider the following two multiterminal networks which are depicted in Fig. 1.1.

1. A MARC with M independent sources ($M \geq 2$), one relay and one destination.

2. A MAMRC which is a natural extension of a MARC with M independent sources, L relays and one destination ($M, L \geq 2$).

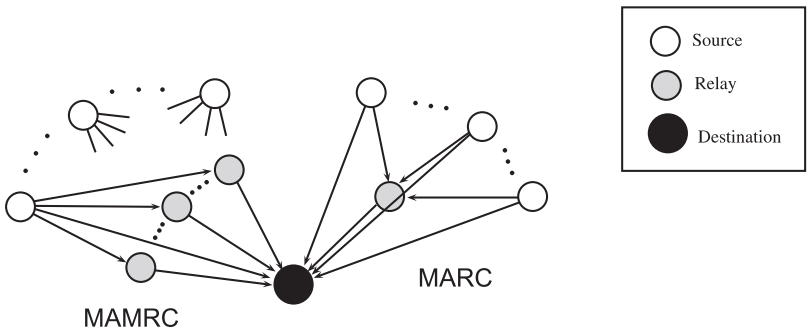

Figure 1.1: A multiple access relay channel (MARC) and a multiple access multiple relay channel (MAMRC)

Throughout the thesis, we assume that all links of the network are subject to slow fading and additive white Gaussian noise. Both operation modes of the relay, namely, half-duplex and full-duplex are considered. The hypothesis of orthogonality between the radio links is partially or totally relaxed. This means that the nodes in the network are allowed to transmit simultaneously during the same time in the same frequency band. The sources and the relays move and are not in line of sight. All nodes in the network are perfectly synchronized. The destination always knows whether the relay(s) cooperate or not, but the sources may or may not be informed of the cooperation. Neither the sources nor the relays when they transmit have channel state information, e.g., by means of feedback channels. The relays, when they listen and decode, and the destination have perfect channel state information. Finally, the performance metric used in the thesis is either the joint or individual information outage probability.

Thesis Contributions and Outline

The main contributions of this thesis can be divided in five chapters:

In **Chapter 2**, a new class of MARC, called Half-Duplex Semi-Orthogonal MARC (HD-SOMARC or SOMARC) is proposed. In HD-SOMARC, (1) the relay operates in half-duplex mode; (2) the signals of the sources interfere at the relay and destination during the listening phase of the relay, while during the transmission phase of the relay, it transmits alone; (3) a Selective Decode and Forward (SDF) relaying approach is applied which depends on the number of correctly decoded messages. We derive the HD-SOMARC individual information outage probability, conditional on JNCC and SNCC, and we present different full diversity JNCC schemes which are flexible in terms of number of sources, encoders and modulations. These new JNCC schemes are shown to perform close to the outage limit in a variety of simulation scenarios. We also demonstrate, theoretically and in practice, that at the expense of more complex reception architectures, the applied non-orthogonality is rather an advantage.

This chapter has led to the following publications:

- A. Hatefi, R. Visoz, A.O. Berthet, *Joint Network-Channel Coding for the Semi-Orthogonal MARC: Theoretical Bounds and Practical Design,* submitted to the IEEE Trans. on Wireless Communication, 2012.

- A. Hatefi, R. Visoz, A.O. Berthet, *Near Outage Limit Joint Network Coding and Decoding for the Semi-Orthogonal Multiple-Access Relay Channel,* Proc. International Symposium on Network Coding (NETCOD'12), Boston, MA, USA, Jul. 2012.

- A. Hatefi, R. Visoz, A.O. Berthet, *Full diversity distributed coding for the multiple access half-duplex relay channel,* Proc. International Symposium on Network Coding (NETCOD'11), Beijing, China, Jul. 2011.

- A. Hatefi, R. Visoz, A.O. Berthet, *Joint channel-network coding for the semi-orthogonal multiple access relay channel,* Proc. IEEE VTC'10 Fall, Ottawa, Canada, Sep. 2010.

two patent filings:

- A. Hatefi, R. Visoz, A.O. Berthet, *Method for transmitting a digital signal in a MARC system ensuring full diversity, and corresponding program product and relay device,* World Patent Application, Publication Number: WO 2011/051893, Issue Date: 09-08-2011, Filed on 19-08-2010 by France Telecom.

- A. Hatefi, R. Visoz, A.O. Berthet, *Method for transmitting a digital signal in a semi-orthogonal frame system having a half-duplex relay, and corresponding program product and relay device,* World Patent Application, Publication Number: WO 2011/067534, Issue Date: 09-06-2011, Filed on 01-12-2010 by France Telecom.

and a book chapter:

- A. Hatefi, R. Visoz, A.O. Berthet, *Joint Network-Channel Coding for the Semi-Orthogonal MARC: Theoretical Bounds and Practical Design,* chapter 7 in "Network Coding," Ed. Wiley-ISTE, ISBN: 978-1-84821-353-1, April, 2012.

In **Chapter 3**, the constraint that the sources remain silent during the transmission phase of the relay is removed, and a new class of MARC, called Half-Duplex Non-orthogonal MARC (HD-NOMARC or NOMARC) is proposed. In this class of MARC, only the destination node should be informed of the cooperation, which reduces significantly the number of control signaling. At the same time, HD-NOMARC would be interesting in the context of a dynamic random access environment, since the sources are not required to be aware of the existence of a potential relay. Furthermore,, it allows the sources to use additional parity bits, but since the source signals interfere with the relay signal, a more complex processing is required at the destination. Individual information outage probability are derived for HD-NOMARC, conditional on JNCC and SNCC. Using the outage analysis, the optimization of the fraction of available channel uses during which the relay listens and those during which the sources and the relay transmit, is performed numerically for a fixed spectral efficiency. Practical JNCC schemes are proposed and are shown to perform close to the outage limit. Finally, the advantage of using the broadcast nature of wireless media is reconfirmed through a variety of simulations.

This chapter has led to the following publications:

- A. Hatefi, R. Visoz, A.O. Berthet, *Joint Network-Channel Coding for the Non-Orthogonal MARC: Theoretical Bounds and Practical Design,* submitted to the IEEE Trans. on Wireless Communication, 2012.

- A. Hatefi, R. Visoz, A.O. Berthet, *Near Outage Limit Joint Network Coding and Decoding for the Non-Orthogonal Multiple-Access Relay Channel,* Proc. IEEE PIMRC'12, Sydney, Australia, Sep. 2012.

- A. Hatefi, R. Visoz, A.O. Berthet, *Joint channel-network turbo-coding for the non-orthogonal multiple access relay channel,* Proc. IEEE PIMRC'10, Istanbul, Turkey, Sep. 2010.

and a patent filing:

- A. Hatefi, R. Visoz, A.O. Berthet, *Method for transmitting a digital signal in a MARC system with a half-duplex relay, and corresponding program product and relay device,* World Patent Application, Publication Number: WO 2011/033239, Issue Date: 24-03-2011, Filed on 17-09-2010 by France Telecom.

In **Chapter 4**, the half duplex constraint of the relay is also relaxed, and a new class of MARC, called Full-Duplex Non-orthogonal MARC (FD-NOMARC) is proposed. Joint information outage probability are derived for FD-NOMARC, conditional on JNCC, superposition block Markov encoding and block by block decoding. Then, practical JNCC designs are presented together with advanced receiver architectures at the destination, which, contrary to block by block decoding, operate over all the transmitted blocks. The performance of the proposed designs are then compared with the derived information outage probabilities, which can be considered as lower bounds on the theoretical performance of our designs.

This chapter has led to the following publication:

- A. Hatefi, R. Visoz, A.O. Berthet, *Joint network-channel distributed coding for the multiple access full-duplex relay channel,* Proc. IEEE ICUMT'10, Moscow, Russia, Oct. 2010.

and a patent filing:

- A. Hatefi, R. Visoz, A.O. Berthet, *Method for transmitting a digital signal in a MARC system with a full-duplex relay, and corresponding program product and relay device,* World Patent Application, Publication Number: WO 2011/033237, Issue Date: 24-03-2011, Filed on 17-09-2010 by France Telecom.

Chapter 5 extends the network model by considering multiple relays which help multiple sources to communicate with a destination. A new class of MAMRC, called Half-Duplex Semi-Orthogonal MAMRC (HD-SOMAMRC or SOMAMRC) is proposed, in which (1) the relays operate in half-duplex mode; (2) During the listening phase of the relays, the sources transmit simultaneously, but they remain silent during their transmission phases. The relays are also allowed to transmit simultaneously all together; (3) an SDF relaying approach is applied which depends on the number of correctly decoded messages. Individual information outage probability are derived for HD-SOMAMRC, conditional on JNCC and SNCC. Using the outage analysis, the optimization of the fraction of available channel uses during which the relays listen and those during which the relays transmit, is performed numerically for a fixed spectral efficiency. To efficiently exploit the maximum available diversity, the XOR-coded concept is generalized to higher order alphabets. Practical JNCC schemes are proposed and are shown to perform close to the outage limit. Finally, the advantage of the proposed scheme is explored through a variety of simulations.

This chapter has led to the following publication:

- A. Hatefi, R. Visoz, A.O. Berthet, *Joint Network-Channel Coding for the Semi-Orthogonal MAMRC: Theoretical Bounds and Practical Design,* to be submitted to the IEEE Trans. on Wireless Communication, 2012.

and a patent filing:

- M. Benammar, A. Hatefi, R. Visoz, *Method for transmitting a digital signal in a multi-source, multi-relay network with a semi-orthogonal transmission protocol and a half-duplex relay,* Filed as a European patent application by France Telecom.

In HD-SOMARC, since the interference generated by the relay at the destination does not impact the overall performance (contrary to HD-NOMARC, FD-NOMARC, or HD-SOMAMRC), the choice of the relaying function is an interesting degree of freedom that remains to be exploited and optimized. Accordingly, **Chapter 6** studies different (digital or analog) relaying functions. The SDF function proposed in preceding chapters are compared with two analog relaying functions: one based on log a posterior probability ratios (LAPPR) and the other based on Mean Square Error (MSE) estimate. The proposed JNCC scheme based on MSE estimate is generic and can be easily extended to arbitrary signal constellations. It can also be considered as an efficient LAPPR compression function for high order modulation.

This chapter has led to the following publication:

- A. Hatefi, R. Visoz, A.O. Berthet, *Relaying functions for the multiple access relay channel,* Proc. 6th International Symposium on Turbo Codes, Brest, France, Sep. 2010.

Finally, conclusions and some perspectives for future works are given in **Chapter 7**.

Chapter 2

Joint Network-Channel Coding for the Half-Duplex Semi-Orthogonal MARC

In this chapter, we revisit the field of JNCC for the MARC with a half-duplex relay. To implement the half-duplex constraint, we split the duration of transmitted codewords into two orthogonal transmission phases, the processing delay at the relay being typically neglected. The sources and the relay move and are not in line of sight. All nodes in the network are informed that they cooperate and are perfectly synchronized. All links of the network are subject to slow fading and additive white Gaussian noise. Neither the sources nor the relay when it transmits has channel state information, e.g., by means of feedback channels. The relay, when it listens and decodes, and the destination have perfect channel state information.

As a first contribution, we propose a new class of MARC that we call Half-Duplex Semi-Orthogonal MARC (HD-SOMARC or SOMARC) and is defined as follows: (1) Independent sources communicate with a single destination in the presence of a relay; (2) The relay is half-duplex and applies a Selective Decode and Forward (SDF) relaying strategy, i.e, it forwards only a deterministic function of the messages that it can decode without errors; (3) The sources are allowed to transmit simultaneously during the listening phase of the relay, but are constrained to remain silent during its transmission phase. Allowing collisions at the relay and the destination renders the reality of wireless environments and leverages better the broadcast nature of the radio channel than the Orthogonal MARC (OMARC). The proposed SDF in SOMARC is a modification of the relaying protocol presented in [125]

The work presented in this chapter is submitted to IEEE Transaction on Wireless Communication. It was presented in part at IEEE VTC Fall 2010, in part at IEEE NETCOD 2011, and in part at IEEE NETCOD 2012. It has also been published as a chapter of the book "Network Coding," Ed. Wiley-ISTE, ISBN: 978-1-84821-353-1, April, 2012.

so as to allow partial cooperation if some of the sources are successfully decoded at the relay and the others are not. Thus, it not only prevents the error propagation from the relay to the destination, but also decreases the individual Block Error Rate (BLER), i.e., the BLER for each source. This SDF approach is theoretically analyzed in [126] for the OMARC/SNCC, and is shown to have a good information outage probability, when the quality of source-to-relay links is poor. For the case of JNCC, the information outage probability of OMARC is analyzed in [82] conditional on the error-free source-to-relay links, and can be easily generalized to the case of selective relaying. While information-theoretic analysis of OMARC with selective relaying has provided insight into the behavior of the system, many issues need to be addressed, including the impact of the non-orthogonality and the multiple access interference. Based on a careful outage analysis, the SOMARC individual information outage probability (e.g., for S_1) is derived for both JNCC or SNCC. The individual information outage probability and the individual ϵ-outage achievable rate (e.g., for S_1) are then numerically evaluated assuming independent Gaussian inputs or discrete independent identically and uniformly distributed inputs and compared with the ones of a OMARC at fixed energy budget per source (per available dimensions). As a second contribution, we propose practical JNCC designs for SOMARC that are flexible in terms of number of sources and Modulation Coding Scheme (MCS). Our designs are built on convolutional codes and turbo codes, and rely on advanced (iterative) joint detection and decoding receiver architectures. We further demonstrate that they also guarantee the full diversity in the sense that they achieve the same diversity gain as the single-user case, even in the case of one receive antenna. The rationale behind our code construction is the following: In the large SNR regime and for the special case of one receive antenna, the outage probability of an M-user slow fading MAC behaves as the one of an orthogonal MAC. Besides, a necessary condition for JNCC to achieve full diversity in the critical case of just one receive antenna, is that it achieves full diversity over the Block Erasure Channel (BEC) defined as an abstraction of the original channel in which the fading gains belong to the set $\{0, \infty\}$. This corresponds to the large SNR regime (see [82] and the references therein). As a result, in the large SNR regime, the MACs at the relay and at the destination and the point-to-point channel from relay to destination turn into $2M + 1$ independent BECs. We claim that our proposed JNCC schemes are full diversity since the BLER of each source decays as ϵ^2 where ϵ is the probability of each link to be in erasure.

2.1 System Model

The M statistically independent sources $S_1, \ldots, S_M$ want to communicate with the destination D in the presence of a relay R. In order to create virtual uplink Multiple-Input,

Multiple-Output (MIMO) channels and to benefit from spatial multiplexing gains, we assume that the relay R and the destination D are equipped with N_R and N_D receive antennas. We consider that the baud rate of the sources and relay is $D = 1/T_s$ and the overall transmission time is fixed to T, thus the number of available channel uses to be shared between the sources and the relay is $N = DT$. We consider the case of Nyquist rate and cardinal sine transmission pulse shape, i.e., $N = DT$ is the total number of available complex dimensions and D is the total bandwidth of the system. Our channel models are inspired by the following assumptions: (1) The delay spreads of the radio channels from the sources to the relay and the destination as well as from the relay to the destination are much lower than T_s ensuring no frequency selectivity; (2) the coherence time of all the aforementioned radio channels are supposed to be much larger than T. The Semi-orthogonal transmission protocol is considered. The N available channel uses are divided into two successive time slots corresponding to the listening phase of the relay, say $N_1 = \alpha N$ channel uses, and to the transmission phase of the relay, say $N_2 = \bar{\alpha} N$ channel uses, with $\alpha \in [0, 1]$ and $\bar{\alpha} = 1 - \alpha$. Each source i broadcasts its messages $\mathbf{u}_i \in \mathbb{F}_2^K$ of K information bits under the form of a modulated sequence during the first transmission phase. Without loss of generality, the modulated sequences are chosen from the complex codebooks ζ_i of rate $K/(\alpha N)$ and take the form of sequences $\mathbf{x}_i \in \zeta_i \subset \mathscr{X}_i^{\alpha N}$, $i \in \{1, \ldots, M\}$, where $\mathscr{X}_i \subset \mathbb{C}$ denote a complex signal set of cardinality $|\mathscr{X}_i| = 2^{q_i}$, with energy normalized to unity. The corresponding received signals at the relay and destination are expressed as

$$\mathbf{y}_{R,k}^{(1)} = \sum_{i=1}^{M} \sqrt{P_{iR}} \mathbf{h}_{iR} x_{i,k} + \mathbf{n}_{R,k}^{(1)} \tag{2.1}$$

$$\mathbf{y}_{D,k}^{(1)} = \sum_{i=1}^{M} \sqrt{P_{iD}} \mathbf{h}_{iD} x_{i,k} + \mathbf{n}_{D,k}^{(1)} \tag{2.2}$$

for $k = 1, \ldots, \alpha N$. In (2.1) and (2.2), the channel fading vectors $\mathbf{h}_{iR} \in \mathbb{C}^{N_R}$, and $\mathbf{h}_{iD} \in \mathbb{C}^{N_D}$, $i \in \{1, \ldots, M\}$ are mutually independent, constant over the transmission of $\mathbf{x}_1$, …, $\mathbf{x}_M$ and change independently from one transmission of the sources to the next. The channel fading vectors $\mathbf{h}_{iR}$, $i \in \{1, \ldots, M\}$, are identically distributed (i.d.) following the probability density function (pdf) $\mathcal{CN}(\mathbf{0}_{N_R}, \mathbf{I}_{N_R})$. The channel fading vectors $\mathbf{h}_{iD}$, $i \in \{1, \ldots, M\}$, are i.d. following the pdf $\mathcal{CN}(\mathbf{0}_{N_D}, \mathbf{I}_{N_D})$. The additive noise vectors $\mathbf{n}_{R,k}^{(1)}$ and $\mathbf{n}_{D,k}^{(1)}$ are independent and follow the pdf $\mathcal{CN}(\mathbf{0}_{N_R}, N_0 \mathbf{I}_{N_R})$ and $\mathcal{CN}(\mathbf{0}_{N_D}, N_0 \mathbf{I}_{N_D})$, respectively. $P_{ij} \propto (d_{ij}/d_0)^{-\kappa} P_i$, $i \in \{1, \ldots, M\}$, $j \in \{R, D\}$ is the average received energy per dimension and per antenna (in Joules/symbol), where d_{ij} is the distance between the transmitter and receiver, d_0 is a reference distance, κ is the path loss coefficient, with values

typically in the range $[2, 6]$, and P_i is the transmit power (or energy per symbol) of S_i. Note that the shadowing could be included within P_{ij}. To fairly compare the performance with respect to α, we fix the total energy per available dimensions $NP_{0,i}$ (recall that N is the number of available dimensions or channel uses) spent by S_i, i.e., $P_i = P_{0,i}/\alpha$. During the second phase, the sources are silent. The relay uses a SDF approach, which depends on the number of correctly decoded messages. Let $J = \{j_1, j_2, \ldots, j_{|J|}\}$, $|J| \leq M$ denote the set of message indices with cardinality $|J|$ that have been successfully decoded. If $J = \emptyset$, the relay remains silent. Otherwise, according to the number of correctly decoded messages and the chosen network coding scheme, it transmits a modulated sequence of the form $\mathbf{x}_R \in \mathscr{X}_R^{\bar{\alpha}N}$, where $\mathscr{X}_R \subset \mathbb{C}$ is a complex constellation of order $|\mathscr{X}_R| = 2^{q_R}$ with energy normalized to unity. The modulated sequence $\mathbf{x}_R$ is chosen such that $(\mathbf{x}_{j_1}, \ldots, \mathbf{x}_{j_{|J|}}, \mathbf{x}_R)$ is a codeword on message $(\mathbf{u}_{j_1}, \ldots, \mathbf{u}_{j_{|J|}})$ belonging to a codebook $\zeta_{J,R}$ of rate $|J|K/N$. The received signal at the destination is expressed as

$$\mathbf{y}_{D,k}^{(2)} = \theta\sqrt{P_{RD}}\mathbf{h}_{RD}x_{R,k} + \mathbf{n}_{D,k}^{(2)} \tag{2.3}$$

for $k = 1, \ldots, \bar{\alpha}N$. In (2.3), the channel fading vector $\mathbf{h}_{RD} \in \mathbb{C}^{N_D}$ follows the pdf $\mathcal{CN}(\mathbf{0}_{N_D}, \mathbf{I}_{N_D})$, is independent of $\mathbf{h}_{iD}$, $i \in \{1, \ldots, M\}$, constant over the transmission of $\mathbf{x}_R$ and changes independently from one transmission of the relay to another. The additive noise vector $\mathbf{n}_{D,k}^{(2)}$ is independent of $\mathbf{n}_{R,k}^{(1)}$ and $\mathbf{n}_{D,k}^{(1)}$, and follows the pdf $\mathcal{CN}(\mathbf{0}_{N_D}, N_0\mathbf{I}_{N_D})$. $P_{RD} \propto (d_{RD}/d_0)^{-\kappa}P_R$, with P_R the transmit power of the relay, is the average received power per dimension and per antenna at the destination. Here again, we fix the total energy per available dimensions $NP_{0,R}$ spent by the relay, i.e., $P_R = P_{0,R}/\bar{\alpha}$. The parameter θ is a discrete Bernoulli distributed random variable: $\theta = 1$ if the relay successfully decodes at least one source message, and $\theta = 0$ otherwise.

Concerning the relay functionality, we distinguish the two cases of JNCC and SNCC:

- JNCC: The relay interleaves each message $\mathbf{u}_j$, $j \in J$, by π and applies a function $\Theta_{R,|J|}$

$$\Theta_{R,|J|} : \underbrace{\mathbb{F}_2^K \times \mathbb{F}_2^K \times \ldots \times \mathbb{F}_2^K}_{|J|} \to \mathbb{C}^{\bar{\alpha}N} \tag{2.4}$$

  to obtain the modulated sequence $\mathbf{x}_R$. In general, the function $\Theta_{R,|J|}$ is not a bijection on the interleaved correctly decoded messages. In practice, the relay would add some in-band signaling to make the destination aware of the set J. Finally, the relay signal, together with the source signals, forms a distributed joint network-channel codebook. The block diagram of the system model is depicted in Fig. 2.1 for the case of $M = 2$.

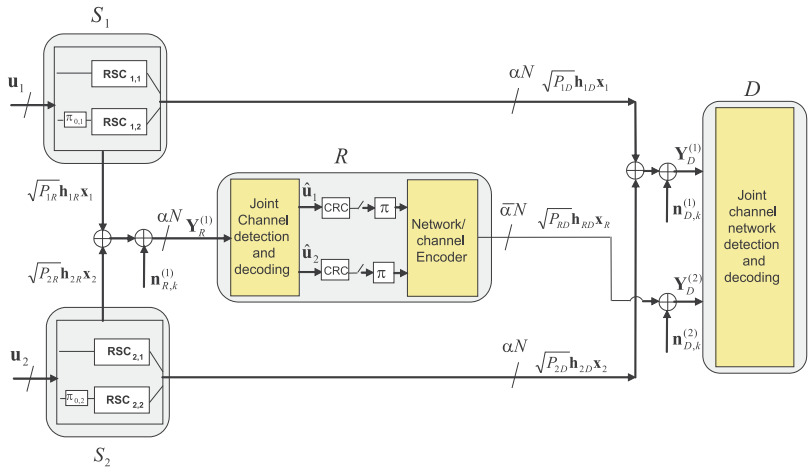

Figure 2.1: System model (relay cooperates)

- SNCC: the relay sums the correctly decoded messages using XOR (or the addition in $\mathbb{F}_2$). The resulting vector $\mathbf{u}_R \in \mathbb{F}_2^K$ is then mapped to $\mathbf{x}_R$ using the codebook ζ_R of rate $K/\bar{\alpha}N$.

In the rest of the chapter, for the sake of notational simplicity, we consider $M = 2$ sources that transmit with an overall spectral efficiency $r = K/N$. For the specific case of SNCC, we can associate the same spectral efficiency r to the relay transmission. The generalization to the cases of $M > 2$ sources is straightforward.

2.2 Information-theoretic Analysis

The SOMARC breaks down into two MACs at the relay and destination, and one classical single user channel from the relay to the destination thanks to the SDF relaying function. Thus, its outage region is perfectly known conditional on a given channel state $\mathbf{H} = \begin{bmatrix} \mathbf{h}_{1R} & \mathbf{h}_{2R} & \mathbf{h}_{1D} & \mathbf{h}_{2D} & \mathbf{h}_{RD} \end{bmatrix}$. Let us define the independent input random variables $x_1 \sim p(x_1)$, $x_2 \sim p(x_2)$ and $x_R \sim p(x_R)$ and the associated independent output random vectors $\mathbf{y}_D^{(1)}$, $\mathbf{y}_D^{(2)}$ and $\mathbf{y}_R^{(1)}$ whose channel transition conditional pdfs are $p\left(\mathbf{y}_D^{(1)} \mid x_1, x_2, \mathbf{H}\right) = \mathcal{CN}\left(\sqrt{P_{1D}}\mathbf{h}_{1D}x_1 + \sqrt{P_{2D}}\mathbf{h}_{2D}x_2, N_0\mathbf{I}_{N_D}\right)$, $p\left(\mathbf{y}_D^{(2)} \mid x_R, \mathbf{H}\right) = \mathcal{CN}\left(\theta\sqrt{P_{RD}}\mathbf{h}_{RD}x_R, N_0\mathbf{I}_{N_D}\right)$ and $p\left(\mathbf{y}_R^{(1)} \mid x_1, x_2, \mathbf{H}\right) = \mathcal{CN}\left(\sqrt{P_{1R}}\mathbf{h}_{1R}x_1 + \sqrt{P_{2R}}\mathbf{h}_{2R}x_2, N_0\mathbf{I}_{N_R}\right)$. It follows that the mutual informations $I(x_1, x_2; \mathbf{y}_D^{(1)})$, $I(x_R; \mathbf{y}_D^{(2)})$ and $I(x_1, x_2; \mathbf{y}_R^{(1)})$ are perfectly defined by the pdfs $p(x_1)$, $p(x_2)$, $p(x_R)$ and the aforementioned channel transition probabilities. It is clear from our context that the mutual information conditional on any given channel state is

maximized for the pdfs $p(x_1)$, $p(x_2)$, $p(x_R)$ being circularly symmetric complex Gaussian pdfs. As a result, the latter pdfs minimize the information outage probabilities. However, in practice, $p(x_1)$, $p(x_2)$, $p(x_R)$ are uniformly distributed pmfs (dirac comb pdfs) over the chosen constellation alphabets. That is why both cases are investigated in the following. We recall that in our analysis:

1. The theoretical bounds are derived conditional on both JNCC and SNCC.

2. The SDF relaying function is used under the hypothesis that all the links are prone to errors.

3. The sequences $\mathbf{x}_1$, $\mathbf{x}_2$ and $\mathbf{x}_R$ are the outcomes of independent discrete time i.i.d. processes whose associated pdfs are $p(x_1)$, $p(x_2)$ and $p(x_R)$ and their respective length is infinite ($N \to \infty$) such that the Asymptotic Equipartition Property (AEP) holds.

4. The outage limit is either the individual information outage probability or the individual ϵ-outage achievable rate (e.g., for S_1). The efficiency of our proposed JNCC/JNCD is evaluated in terms of gap to the information outage probability, keeping in mind that the information outage probability remains a relevant measure of the best possible BLER even for finite code lengths [119].

2.2.1 Outage analysis of SOMARC/JNCC

As the relay uses a SDF approach, an evaluation of the source-to-relay channel quality has first to be processed. Let $\mathcal{E}_R(\mathbf{H})$ denote the outage event of the source-to-relay MAC conditional on $\mathbf{H}$. It corresponds to the case where the relay cannot decode both messages correctly, and can be expressed as

$$\mathcal{E}_R(\mathbf{H}) = \mathcal{E}_{R,1|2}(\mathbf{H}) \cup \mathcal{E}_{R,2|1}(\mathbf{H}) \cup \mathcal{E}_{R,1,2}(\mathbf{H}) \tag{2.5}$$

where $\mathcal{E}_{R,i|j}(\mathbf{H})$, $i, j \in \{1, 2\}$, $j \neq i$ is the outage event of S_i if the information of S_j is known, and $\mathcal{E}_{R,1,2}(\mathbf{H})$ is the outage event of both sources at the relay. The three possible outage events are then given by

$$\mathcal{E}_{R,i|j}(\mathbf{H}) = \left\{ \alpha I(x_i; \mathbf{y}_R^{(1)} \mid x_j) < r \right\} \tag{2.6}$$

$$\mathcal{E}_{R,1,2}(\mathbf{H}) = \left\{ \alpha I(x_1, x_2; \mathbf{y}_R^{(1)}) < 2r \right\} \tag{2.7}$$

When the outage event $\mathcal{E}_R(\mathbf{H})$ holds, in order to verify whether only one of the messages $\mathbf{x}_i$ can be successfully decoded or not, we define the following outage event

$$\mathcal{E}_{R,i}(\mathbf{H}) = \left\{ \alpha I(x_i; \mathbf{y}_R^{(1)}) < r \right\} \tag{2.8}$$

in which the relay treats the signal $\mathbf{x}_j$ as interference. Thus, the relay outage events for the SDF approach can be summarized as follows: (1) In case of $\mathcal{Q}_R^{(1)}(\mathbf{H}) = \bar{\mathcal{E}}_R(\mathbf{H})$, which indicates the complement of the outage event $\mathcal{E}_R(\mathbf{H})$, the relay cooperates with both sources; (2) In case of $\mathcal{Q}_R^{(2)}(\mathbf{H}) = \mathcal{E}_R(\mathbf{H}) \cap \bar{\mathcal{E}}_{R,1}(\mathbf{H})$ the relay cooperates only with S_1; (3) In case of $\mathcal{Q}_R^{(3)}(\mathbf{H}) = \mathcal{E}_R(\mathbf{H}) \cap \bar{\mathcal{E}}_{R,2}(\mathbf{H})$ the relay cooperates only with S_2; (4) Otherwise, in case of $\mathcal{Q}_R^{(4)}(\mathbf{H}) = \mathcal{E}_R(\mathbf{H}) \cap \mathcal{E}_{R,1}(\mathbf{H}) \cap \mathcal{E}_{R,2}(\mathbf{H})$ the relay does not cooperate. Now, depending on the relay transmission, we distinguish four outage events at the destination:

Case 1: The relay cooperates with both sources. The destination always receives the cooperative information from the relay during the second phase. Since the relay transmits over orthogonal parallel channel with respect to the source-to-destination MAC, the outage at the destination occurs if the target rate exceeds the sum of the mutual informations of the two parallel channels. Let $\mathcal{E}_D^{(1)}(\mathbf{H})$ denote the outage event at the destination conditional on $\mathbf{H}$. It can be expressed as

$$\mathcal{E}_D^{(1)}(\mathbf{H}) = \mathcal{E}_{D,1|2}^{(1)}(\mathbf{H}) \cup \mathcal{E}_{D,2|1}^{(1)}(\mathbf{H}) \cup \mathcal{E}_{D,1,2}^{(1)}(\mathbf{H}). \tag{2.9}$$

where

$$\mathcal{E}_{D,i|j}^{(1)}(\mathbf{H}) = \left\{ \alpha I(x_i; \mathbf{y}_D^{(1)} \mid x_j) + \bar{\alpha} I(x_R; \mathbf{y}_D^{(2)}) < r \right\} \tag{2.10}$$

for $i, j \in \{1, 2\}$ and $j \neq i$, and

$$\mathcal{E}_{D,1,2}^{(1)}(\mathbf{H}) = \left\{ \alpha I(x_1, x_2; \mathbf{y}_D^{(1)}) + \bar{\alpha} I(x_R; \mathbf{y}_D^{(2)}) < 2r \right\}. \tag{2.11}$$

In (2.10), $\mathcal{E}_{D,i|j}^{(1)}(\mathbf{H})$, $i \in \{1, 2\}$ is the outage event of S_i if the information of S_j, $j \neq i$, is known. In this case, $\mathbf{x}_R$ can be considered as a part of the codeword of S_i. Typically, this is the case when $\mathbf{x}_R$ is a codeword representing the XOR of the two source messages. The outage event in (2.11) corresponds to the constraint that the total throughput cannot exceed the sum of the mutual informations of (1) a point-to-point channel with the aggregate received signals of the two sources, and (2) the relay-to-destination channel. When $\mathcal{E}_D^{(1)}(\mathbf{H})$ holds, the destination cannot decode both source messages correctly. As we are interested

in calculating the outage event of S_1, we define the following event

$$\mathcal{E}_{D,1}^{(1)}(\mathbf{H}) = \left\{\alpha I(x_1; \mathbf{y}_D^{(1)}) < r\right\} \tag{2.12}$$

in which the destination treats the signal $\mathbf{x}_2$ as interference. It is worth noting that the relay transmission in this case cannot help S_1 as it contains the interference from S_2. Thus, it is considered as interference as well. Finally, the outage event of S_1 is calculated as $\mathcal{O}_{D,1}^{(1)}(\mathbf{H}) = \mathcal{E}_D^{(1)}(\mathbf{H}) \cap \mathcal{E}_{D,1}^{(1)}(\mathbf{H})$.

Case 2: The relay cooperates with S_1. The outage event at the destination $\mathcal{E}_D^{(2)}(\mathbf{H})$ is calculated as

$$\mathcal{E}_D^{(2)}(\mathbf{H}) = \mathcal{E}_{D,1|2}^{(2)}(\mathbf{H}) \cup \mathcal{E}_{D,2|1}^{(2)}(\mathbf{H}) \cup \mathcal{E}_{D,1,2}^{(2)}(\mathbf{H}). \tag{2.13}$$

where

$$\mathcal{E}_{D,1|2}^{(2)}(\mathbf{H}) = \left\{\alpha I(x_1; \mathbf{y}_D^{(1)} \mid x_2) + \bar{\alpha} I(x_R; \mathbf{y}_D^{(2)}) < r\right\} \tag{2.14}$$

$$\mathcal{E}_{D,2|1}^{(2)}(\mathbf{H}) = \left\{\alpha I(x_2; \mathbf{y}_D^{(1)} \mid x_1) < r\right\} \tag{2.15}$$

$$\mathcal{E}_{D,1,2}^{(2)}(\mathbf{H}) = \left\{\alpha I(x_1, x_2; \mathbf{y}_D^{(1)}) + \bar{\alpha} I(x_R; \mathbf{y}_D^{(2)}) < 2r\right\} \tag{2.16}$$

In order to calculate the outage event of S_1, we define the following event

$$\mathcal{E}_{D,1}^{(2)}(\mathbf{H}) = \left\{\alpha I(x_1; \mathbf{y}_D^{(1)}) + \bar{\alpha} I(x_R; \mathbf{y}_D^{(2)}) < r\right\} \tag{2.17}$$

in which the destination treats the signal $\mathbf{x}_2$ as interference during the first transmission phase. Finally, the outage event of S_1 is calculated as $\mathcal{O}_{D,1}^{(2)}(\mathbf{H}) = \mathcal{E}_D^{(2)}(\mathbf{H}) \cap \mathcal{E}_{D,1}^{(2)}(\mathbf{H})$.

Case 3: The relay cooperates with S_2. Swapping the roles of S_1 and S_2, the outage event at the destination $\mathcal{E}_D^{(3)}(\mathbf{H})$ is identical to the previous case. In order to calculate the outage event of the source S_1, we define the event $\mathcal{E}_{D,1}^{(3)}(\mathbf{H})$ as in (2.12). Thus, the outage event of S_1 is calculated as $\mathcal{O}_{D,1}^{(3)}(\mathbf{H}) = \mathcal{E}_D^{(3)}(\mathbf{H}) \cap \mathcal{E}_{D,1}^{(3)}(\mathbf{H})$.

Case 4: The relay does not cooperate. The outage at the destination $\mathcal{E}_D^{(4)}(\mathbf{H})$ occurs if the source-to-destination MAC is in outage which is calculated similar to (2.5). The outage event of S_1 can also be derived as $\mathcal{O}_{D,1}^{(4)}(\mathbf{H}) = \mathcal{E}_D^{(4)}(\mathbf{H}) \cap \mathcal{E}_{D,1}^{(4)}(\mathbf{H})$, with $\mathcal{E}_{D,1}^{(4)}(\mathbf{H})$ calculated as in (2.12).

Finally, the outage event of S_1 in the error-prone SOMARC/JNCC, can be expressed as

$$\mathcal{O}_{D,1}(\mathbf{H}) = \bigcup_{i=1}^{4} \left(\mathcal{Q}_R^{(i)}(\mathbf{H}) \cap \mathcal{O}_{D,1}^{(i)}(\mathbf{H})\right). \tag{2.18}$$

The above outage event is conditional on the channel state $\mathbf{H}$. The information outage probability for S_1 is then obtained as

$$P_{out,1} = \int_{\mathbf{H}} [\mathcal{O}_{D,1}(\mathbf{H})] \;\; p(\mathbf{H}) d(\mathbf{H}) \tag{2.19}$$

where $p(\mathbf{H})$ is the pdf of $\mathbf{H}$. The ϵ-outage achievable rate of S_1 is defined as the largest rate of S_1 such that its corresponding information outage probability for a given transmission protocol, is smaller than or equal to ϵ.

2.2.2 Outage analysis of SOMARC/SNCC

In the case of SNCC/SNCD, we still have two MACs at the relay and destination corresponding to the first time slot, and a point-to-point channel corresponding to the second time slot. The outage event analysis at the relay remains the same as in (2.2.1). However, the received signals at the destination from the sources and the relay are now decoded separately. Therefore, the outage event analysis at the destination related to the first time slot exactly follows the one of the relay. More specifically, the outage events $\mathcal{E}_D(\mathbf{H})$, $\mathcal{E}_{D,1}(\mathbf{H})$, $\mathcal{E}_{D,2}(\mathbf{H})$ are defined similarly to $\mathcal{E}_R(\mathbf{H})$, $\mathcal{E}_{R,1}(\mathbf{H})$, $\mathcal{E}_{R,2}(\mathbf{H})$ (by replacing the subscript R by D). Let also $\mathcal{E}_{RD}(\mathbf{H})$ denote the outage event of the relay-to-destination channel:

$$\mathcal{E}_{RD}(\mathbf{H}) = \left\{ \bar{\alpha} I(x_R; \mathbf{y}_D^{(2)}) < r \right\} \tag{2.20}$$

where r bits per channel use is recalled to be the spectral efficiency of the relay transmission. Depending on the relay transmitted signal, we distinguish four different cases at the destination:

Case 1: The relay cooperates with both sources. If the message of S_1 cannot be correctly decoded from the MAC, it can be recovered, provided that the destination can decode successfully the message of S_2 during the first time slot, and the relay message during the second time slot. Thus, the outage event of S_1 is calculated as

$$\mathcal{O}_{D,1}^{(1)}(\mathbf{H}) = \left(\mathcal{E}_D(\mathbf{H}) \cap \mathcal{E}_{D,1}(\mathbf{H}) \cap \mathcal{E}_{RD}(\mathbf{H})\right) \cup \left(\mathcal{E}_D(\mathbf{H}) \cap \mathcal{E}_{D,1}(\mathbf{H}) \cap \bar{\mathcal{E}}_{RD}(\mathbf{H}) \cap \mathcal{E}_{D,2}(\mathbf{H})\right). \tag{2.21}$$

Case 2: The relay cooperates with S_1. The outage event of S_1 is expressed as

$$\mathcal{O}_{D,1}^{(2)}(\mathbf{H}) = \left(\mathcal{E}_D(\mathbf{H}) \cap \mathcal{E}_{D,1}(\mathbf{H}) \cap \mathcal{E}_{RD}(\mathbf{H})\right). \tag{2.22}$$

Case 3: The relay cooperates with S_2. If the message of S_2 is decoded successfully from the relay transmission, the interference of it could be removed from the source-to-destination MAC, which becomes then a point-to-point channel. Let denote by $\mathcal{E}_{D,1|2}(\mathbf{H})$ the outage event corresponding to S_1 if the message of S_2 is known, i.e. $\mathbf{x}_2$ and $\mathbf{x}_R$ are both known. The outage event of S_1 can be expressed as

$$\mathcal{O}_{D,1}^{(3)}(\mathbf{H}) = \left(\mathcal{E}_{RD}(\mathbf{H}) \cap \mathcal{E}_D(\mathbf{H}) \cap \mathcal{E}_{D,1}(\mathbf{H})\right) \cup \left(\bar{\mathcal{E}}_{RD}(\mathbf{H}) \cap \mathcal{E}_{D,1|2}(\mathbf{H})\right). \tag{2.23}$$

Case 4: The relay does not cooperate. The outage event of S_1 is calculated as

$$\mathcal{O}_{D,1}^{(4)}(\mathbf{H}) = \left(\mathcal{E}_D(\mathbf{H}) \cap \mathcal{E}_{D,1}(\mathbf{H})\right). \tag{2.24}$$

Finally, the outage event of S_1 in the error-prone SOMARC/SNCC can be expressed as

$$\mathcal{O}_{D,1}(\mathbf{H}) = \bigcup_{i=1}^{4} \left(\mathcal{Q}_R^{(i)}(\mathbf{H}) \cap \mathcal{O}_{D,1}^{(i)}(\mathbf{H})\right). \tag{2.25}$$

Here again, the outage event $\mathcal{O}_{D,1}(\mathbf{H})$ is conditional on the channel state $\mathbf{H}$, and the information outage probability for S_1 is derived as

$$P_{out,1} = \int_{\mathbf{H}} \left[\mathcal{O}_{D,1}(\mathbf{H})\right] \; p(\mathbf{H}) d(\mathbf{H}). \tag{2.26}$$

2.2.3 Types of input distributions

Gaussian i.i.d. inputs maximize the mutual information. In this case, all the mutual information can be calculated using the expressions given in Appendix B. However, the assumption of Gaussian inputs can only be justified in the case of large signal constellations. In practical systems, the channel inputs are selected from a finite and discrete alphabet (typically QPSK or 16QAM). Thus, to make fair outage comparisons, discrete i.i.d. channel inputs should be chosen from the constellations $\mathscr{X}_i$ of order 2^{q_i}, $i \in \{1, 2, R\}$. In this case, we compute numerically the mutual information assuming uniform input distributions. The expressions are given in Appendix B.

2.2.4 Information outage probability achieving codebooks

To achieve the information outage probability bounds, the codebooks ζ_1, ζ_2, ζ_{1R}, ζ_{2R} and ζ_{12R} should be universal codebooks. As defined in [127], a universal codebook of a given rate is a codebook that simultaneously achieves reliable communication over every channel that is not in outage for the chosen rate. Finally, it is worth stressing that, in practice, there exist codebooks with finite lengths whose performance are very close to the ones of universal codebooks. The simulation Section 2.5 exemplifies such codebook constructions based on convolutional or turbo codes.

2.3 Joint Network Channel Coding and Decoding

In this section, we make explicit our proposed JNCC/JNCD approach. We explain the structure of the encoders, when and how JNCC is performed, and the structure of the corresponding multiuser receivers.

2.3.1 Coding at the sources

The messages of the two sources are binary vectors $\mathbf{u}_1 \in \mathbb{F}_2^K$ and $\mathbf{u}_2 \in \mathbb{F}_2^K$ of length K. Each source employs a Bit-Interleaved Coded Modulation (BICM) [128]. Binary vectors are first encoded with linear systematic binary encoders $C_i : \mathbb{F}_2^K \to \mathbb{F}_2^{n_i}$, $i = \{1, 2\}$ into binary codewords $\mathbf{c}_i \in \mathbb{F}_2^{n_i}$ of respective lengths n_i. The codes ζ_i are in general punctured turbo codes, consisting of two Recursive Systematic Convolutional (RSC) encoders, denoted by $\text{RSC}_{i,1}$ and $\text{RSC}_{i,2}$, concatenated in parallel using optimized semi-random interleavers $\pi_{0,i}$. The coded bits are then interleaved using interleavers Π_i and reshaped as two binary matrices $\mathbf{V}_i \in \mathbb{F}_2^{\alpha N \times q_i}$. Memoryless modulators based on one-to-one binary labeling maps $\phi_i : \mathbb{F}_2^{q_i} \to \mathscr{X}_i$ transform the binary arrays $\mathbf{V}_i$ into the complex vectors $\mathbf{x}_i \in \mathscr{X}_i^{\alpha N}$. For ϕ_i, we choose Gray labeling. In the sequel, we denote by $v_{i,k,\ell} = \phi_{i,\ell}^{-1}(x_{i,k})$ the ℓ-th bit of the binary labeling of each symbol $x_{i,k}$ for $i \in \{1, 2\}$ and $k = 1, \cdots, \alpha N$.

2.3.2 Relaying Function

Relay processing is divided in two steps, as shown in Fig. 2.2. During the first time slot, based on (2.1), the relay performs a joint detection and decoding procedure to obtain the hard binary estimation of the information bits, $\hat{\mathbf{u}}_i \in \mathbb{F}_2^K$. Based on this estimation, the relay chooses a SDF approach for cooperation. Different cases can then be distinguished, depending on the number of successfully decoded messages. In the sequel, first, we briefly

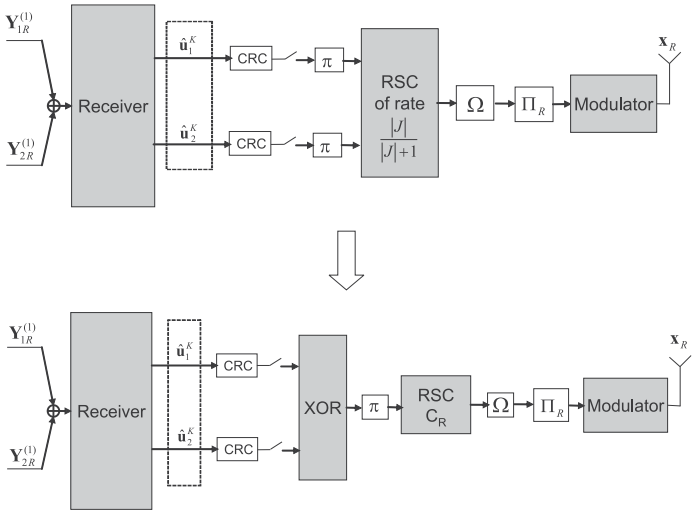

Figure 2.2: Block diagram of the sequential processing at relay

describe the relay detection and decoding algorithm, and then, we detail our proposed JNCC scheme.

2.3.2.1 Relay detection and decoding

The joint detection and decoding is performed in a suboptimal iterative way [129]. An inner Soft-In Soft-Out (SISO) Maximum A Posteriori (MAP) detector generates extrinsic information on coded bits using the received signal (2.1) and a priori information coming from the outer SISO decoders SISO_1 and SISO_2 (referring to the decoding of ζ_1 and ζ_2). For the general case of turbo codes at the sources, the outer SISO decoder of S_i generates extrinsic information on both systematic and coded bits of S_i by activating the SISO decoder $\text{SISO}_{i,1}$ corresponding to $\text{RSC}_{i,1}$, and then $\text{SISO}_{i,2}$ corresponding to $\text{RSC}_{i,2}$. It is important to remember that each SISO decoding stage takes into account all the available a priori information on systematic bits [130] (and Algorithm 1 of Section 2.3.3.2). The extrinsic information on both source codewords is then interleaved and fed back to the detector, which in turn employs it as a priori information for the next iteration. It is worth noting that the proper (de)multiplexing and (de)puncturing are also performed if needed. The process is repeated until convergence. For the representation of the input/output soft information, we use log ratios of probabilities. The Log A Posterior Probability Ratio

(LAPPR) on bit $v_{i,k,\ell} = \phi_{i,\ell}^{-1}(x_{i,k})$ delivered by the SISO MAP detector is defined as

$$\Lambda(v_{i,k,\ell}) = \log \frac{P(v_{i,k,\ell} = 1|\mathbf{y}_{R,k}^{(1)})}{P(v_{i,k,\ell} = 0|\mathbf{y}_{R,k}^{(1)})} \tag{2.27}$$

and, in practice, evaluated as

$$\Lambda(v_{i,k,\ell}) \simeq \log \frac{\sum_{a \in \mathscr{X}_i : \phi_{i,\ell}^{-1}(a)=1, b \in \mathscr{X}_j} P(\mathbf{y}_{R,k}^{(1)}|x_{i,k} = a, x_{j,k} = b) e^{\xi(a)+\xi(b)}}{\sum_{a \in \mathscr{X}_i : \phi_{i,\ell}^{-1}(a)=0, b \in \mathscr{X}_j} P(\mathbf{y}_{R,k}^{(1)}|x_{i,k} = a, x_{j,k} = b) e^{\xi(a)+\xi(b)}} \tag{2.28}$$

for $i, j \in \{1, 2\}, i \neq j$, with,

$$\xi(a) = \sum_{\ell'=1}^{\log_2|\mathscr{X}_i|} \phi_{i,\ell'}^{-1}(a) E(v_{i,k,\ell'}) \tag{2.29}$$

$$\xi(b) = \sum_{\ell'=1}^{\log_2|\mathscr{X}_j|} \phi_{j,\ell'}^{-1}(b) E(v_{j,k,\ell'}) \tag{2.30}$$

where $\{E(v_{i,k,\ell})\}$ and $\{E(v_{j,k,\ell})\}$ are Log A Priori probability Ratios (LAPRs) on bits $v_{i,k,\ell}$ and $v_{j,k,\ell}$ provided by the SISO decoders SISO_1 and SISO_2. The extrinsic information on bit $v_{i,k,\ell}$ is given by $L(v_{i,k,\ell}) = \Lambda(v_{i,k,\ell}) - E(v_{i,k,\ell})$, and after de-interleaving, feeds the corresponding outer SISO decoder.

2.3.2.2 JNCC

As previously mentioned, the relay chooses a SDF approach for cooperation, which is based on the number of successfully decoded messages, the knowledge of which being ensured by using Cyclic Redundancy Check (CRC) codes for each source message. Let $J = \{j_1, \ldots, j_{|J|}\}$, $|J| \leq 2$ denote the set of message indices that have been successfully decoded. For the case where $J = \emptyset$, the relay does not cooperate. Otherwise, it interleaves each message $\mathbf{u}_j$, $j \in J$ by π. The interleaved binary streams are then linearly combined over $\mathbb{F}_2$ using binary linear encoders

$$\begin{cases} C_{R,1} : \mathbb{F}_2^K \to \mathbb{F}_2^{2K} \\ C_{R,2} : \mathbb{F}_2^K \times \mathbb{F}_2^K \to \mathbb{F}_2^{3K} \end{cases} \tag{2.31}$$

for $J \neq \emptyset$. For $C_{R,|J|}$, we choose an RSC encoder of rate $\frac{|J|}{|J|+1}$ defined by the generator matrix

$$G_{R,|J|}(D) = \left[\begin{array}{c|c} & \frac{p_1(D)}{q(D)} \\ I_{|J|} & \vdots \\ & \frac{p_{|J|}(D)}{q(D)} \end{array}\right] \tag{2.32}$$

where $p_i(D)$, $i \in \{1, ..., |J|\}$, and $q(D)$ are the generator polynomials of the encoder $C_{R,|J|}$. This yields the binary vector $\mathbf{c}_R \in \mathbb{F}_2^{K(|J|+1)}$. A linear transformation $\Omega : \mathbb{F}_2^{K(|J|+1)} \to \mathbb{F}_2^K$ is then applied which selects only the parity bits of $\mathbf{c}_R$ to obtain the new vector $\mathbf{c}'_R \in \mathbb{F}_2^K$. As all the systematic bits are removed, this structure maximizes the spectral efficiency. The vector $\mathbf{c}'_R$ is bit interleaved using the interleaver Π_R and reshaped as a binary matrix $\mathbf{V}_R \in \mathbb{F}_2^{\bar{\alpha}N \times q_R}$. Finally, a memoryless modulator based on a one-to-one binary labeling map $\phi_R : \mathbb{F}_2^{q_R} \to \mathscr{X}_R$ transforms the binary array $\mathbf{V}_R$ into the complex vector $\mathbf{x}_R \in \mathscr{X}_R^{\bar{\alpha}N}$. $\mathscr{X}_R \subset \mathbb{C}$ is a complex constellation of order $|\mathscr{X}_R| = 2^{q_R}$ with energy normalized to unity. For ϕ_R, we choose Gray labeling. In the sequel, we denote by $v_{R,k,\ell} = \phi_{R,\ell}^{-1}(x_{R,k})$ the ℓ-th bit of the binary labeling of each symbol $x_{R,k}$ for $k = 1, \cdots, \bar{\alpha}N$. Finally, to let the destination detect which of the messages are included in the relay signal, the relay transmits side information (additional bits) to indicate its state to the receiver.

The proposed coding scheme entails the need of a decoder corresponding to the code of rate $\frac{|J|}{|J|+1}$, which increases the complexity while $|J|$ becomes larger. Furthermore, it does not guarantee the full diversity for low memory orders, as shown in [131]. But if we assume that all the feedforward generators of $G_{R,|J|}(D)$ are the same, i.e., $p_i(D) = p(D)$, we obtain an equivalent model, as depicted in Fig. 2.2, which ensures full diversity and simplifies the decoder structure. In this model, the relay combines all the correctly decoded messages by XOR, i.e., $\mathbf{u}_R = \mathbf{u}_{j_1} \oplus \ldots \oplus \mathbf{u}_{j_{|J|}}$, and interleaves the resulting vector by π. Interestingly, the interleaver commutes with the XOR. The interleaved vector is then encoded to $\mathbf{c}_R$ using a binary linear encoder $C_R : \mathbb{F}_2^K \to \mathbb{F}_2^{2K}$. For C_R, we choose the RSC encoder defined by the generator matrix $G_R(D) = \left[\begin{array}{cc} 1 & \frac{p(D)}{q(D)} \end{array}\right]$. The selection function Ω then removes the systematic bits. The rest of the operations remains the same. The XOR operation ensures full diversity for the OMARC using SNCC [126] or JNCC [82]. As shown in Appendix A, the high SNR slope of the outage probability of MAC versus SNR (in dB scale), for the critical case of just one receive antenna, is the same as the one of the orthogonal MAC. Thus, the full diversity design for OMARC remains valid when we have collisions at the relay and destination.

2.3.3 JNCD at the Destination

The JNCD at the destination depends on the side information received from the relay: In case 1, where the relay has successfully decoded both source messages, two distributed turbo codes are formed at the destination. In case 2 (case 3), where the relay has successfully decoded the information of S_1 (S_2), one distributed turbo code is formed at the destination corresponding to S_1 (S_2), and a separate decoder corresponding to C_2 (C_1) is used to decode the information of the other source. In these cases, at the end of the second transmission time slot, the destination starts to detect and decode the original data, processing the received signals (2.2) and (2.3). Finally, in case 4, where the relay does not cooperate, the destination applies iterative detection and decoding, processing the received signal (2.2), and using the two separate decoders corresponding to C_1 and C_2. Here again, we resort to a suboptimal iterative procedure. Extrinsic information on coded bits circulates between SISO MAP detector and demapper corresponding to two transmission time slots and the outer decoders, while, at the same time, extrinsic information on systematic bits circulates between the SISO decoders of each code.

2.3.3.1 SISO MAP Detector and Demapper

The SISO MAP detector computes the LAPPR $\Lambda(v_{i,k,\ell})$ with $v_{i,k,\ell} = \phi_{i,\ell}^{-1}(x_{i,k})$, $i \in \{1,2\}$, using the received signal (2.2) and a priori information coming from the outer SISO decoders. Expression is similar to (2.28) substituting $\mathbf{y}_{D,k}^{(1)}$ for $\mathbf{y}_{R,k}^{(1)}$. We now turn to the SISO MAP demapper which delivers soft information on the additional relay parity bits in case of relay cooperation (successful selective relaying). The LAPPR on bit $v_{R,k,\ell} = \phi_{R,\ell}^{-1}(x_{R,k})$ is defined as

$$\Lambda(v_{R,k,\ell}) = \log \frac{P(v_{R,k,\ell} = 1 | \mathbf{y}_{D,k}^{(2)})}{P(v_{R,k,\ell} = 0 | \mathbf{y}_{D,k}^{(2)})}. \tag{2.33}$$

and evaluated as

$$\Lambda(v_{R,k,\ell}) \simeq \log \frac{\sum_{c \in \mathscr{X}_R : \phi_{R,\ell}^{-1}(c)=1} P(\mathbf{y}_{D,k}^{(2)} | x_{R,k} = c) e^{\xi(c)}}{\sum_{c \in \mathscr{X}_R : \phi_{R,\ell}^{-1}(c)=0} P(\mathbf{y}_{D,k}^{(2)} | x_{R,k} = c) e^{\xi(c)}} \tag{2.34}$$

with

$$\xi(c) = \sum_{\ell'=1}^{\log_2 |\mathscr{X}_R|} \phi_{R,\ell'}^{-1}(c) E(v_{R,k,\ell'}) \tag{2.35}$$

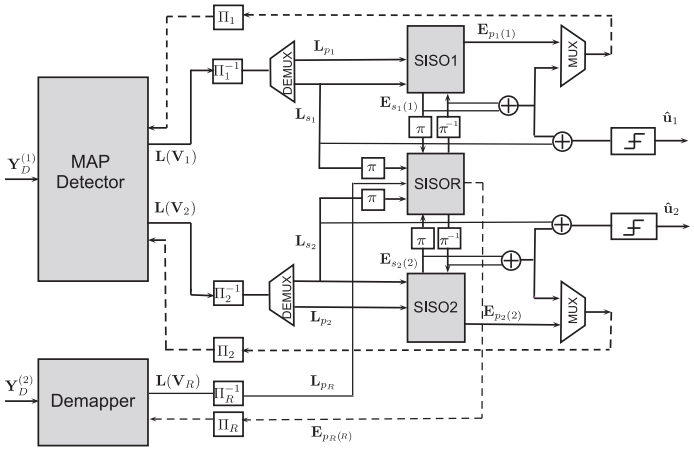

Figure 2.3: JNCD at the destination (relay cooperates with both sources)

where $\{E(v_{R,k,\ell})\}$ is the LAPR on bit $v_{R,k,\ell}$ provided by the SISO decoder SISO_R corresponding to the relay joint network-channel encoder ($C_{R,|J|}$ or XOR followed by C_R). Finally, the extrinsic information on $v_{R,k,\ell}$ is given by $L(v_{R,k,\ell}) = \Lambda(v_{R,k,\ell}) - E(v_{R,k,\ell})$ and, after de-interleaving, feeds SISO_R.

2.3.3.2 Message-Passing Schedule

A recapitulative block diagram of the JNCD is depicted in Fig. 2.3. In this paragraph, we detail the message-passing for the case where the relay cooperates with both sources using a XOR followed by a linear encoding. We also consider the case of turbo codes at the sources, i.e., each C_i, $i \in \{1,2\}$ consists of two RSC encoders separated by $\pi_{0,i}$. The generalization to other cases is straightforward. The SISO decoder SISO_i corresponds to C_i, $i \in \{1,2\}$, and SISO_R corresponds to the relay encoder (XOR followed by C_R). Each SISO_i, $i \in \{1,2\}$, is made up of the two SISO decoders $\text{SISO}_{i,1}$ and $\text{SISO}_{i,2}$. Let $\mathbf{L}_{s_i}$, $\mathbf{L}_{p_i}$, and $\mathbf{L}_{p_R}$, $i \in \{1,2\}$, denote respectively the soft information of the systematic and parity bits of the two sources and the relay, obtained from the channel MAP detector and demapper. It is worth noting that the proper (de)multiplexing and (de)puncturing are also performed if needed. In Fig. 2.3, the (de)puncturing is included in the blocks corresponding to (de)multiplexing. Let also denote by $\mathbf{E}_{s_i(j)}$, $\mathbf{E}_{p_i(j)}$, and $\mathbf{E}_{p_R(j)}$ the extrinsic information generated by SISO_j, $j \in \{1,2,R\}$. Similarly, let $\mathbf{L}_{p_{i,1}}$ and $\mathbf{L}_{p_{i,2}}$ denote respectively the soft information of the parity bits corresponding to $\text{SISO}_{i,1}$ and $\text{SISO}_{i,2}$ obtained from the MAP detector, $\mathbf{E}_{s_i(i,1)}$ and $\mathbf{E}_{s_i(i,2)}$ denote respectively the extrinsic information on systematic bits generated by $\text{SISO}_{i,1}$ and $\text{SISO}_{i,2}$, and $\mathbf{E}_{p_i(i,1)}$ and $\mathbf{E}_{p_i(i,2)}$ denote respectively the extrinsic information on parity bits generated by $\text{SISO}_{i,1}$ and $\text{SISO}_{i,2}$.

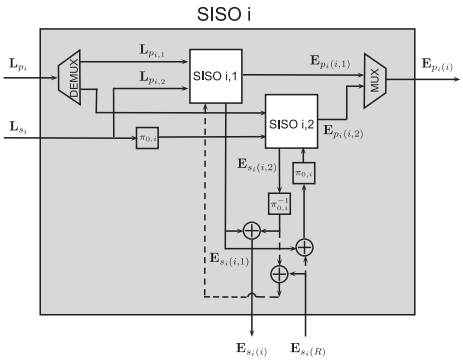

Figure 2.4: SISO decoder SISO_i in case of compound codes at sources

The SISO MAP detector generates the LAPPRs for the systematic and parity bits in $\mathbf{V}_1$ using $\mathbf{E}_{s_1(1)} + \pi^{-1}(\mathbf{E}_{s_1(R)})$ and $\mathbf{E}_{p_1(1)}$, respectively (after proper multiplexing interleaving). It also generates the LAPPRs for the systematic and parity bits in $\mathbf{V}_2$ using $\mathbf{E}_{s_2(2)} + \pi^{-1}(\mathbf{E}_{s_2(R)})$ and $\mathbf{E}_{p_2(2)}$, respectively. It is worth stressing that $\mathbf{E}_{s_1(1)} = \mathbf{E}_{s_1(1,1)} + \pi_{0,1}^{-1}(\mathbf{E}_{s_1(1,2)})$, and $\mathbf{E}_{s_2(2)} = \mathbf{E}_{s_2(2,1)} + \pi_{0,2}^{-1}(\mathbf{E}_{s_2(2,2)})$, as depicted in Fig. 2.4. The MAP demapper generates the LAPPRs for the parity bits in $\mathbf{V}_R$ using $\mathbf{E}_{p_R(R)}$. Then, the two distributed decoders are activated and calculate the extrinsic information for both the systematic and parity bits which are fed back to the SISO MAP detector and demapper.

In the case of an XOR encoding scheme (full diversity by construction), we detail in Fig. 2.5 and hereafter, the low complexity implementation of SISO_R. As depicted in Fig. 2.5, the SISO decoder corresponding to C_R (DEC_R) should collect all the a priori information $\mathbf{L}_{u_R}$ on $\mathbf{u}_R$. Denoting $\mathbf{L}_1 = \pi(\mathbf{L}_{s_1} + \mathbf{E}_{s_1(1)})$ and $\mathbf{L}_2 = \pi(\mathbf{L}_{s_2} + \mathbf{E}_{s_2(2)})$, it yields, taking into account the XOR constraint node (see, e.g., [132]),

$$L_{u_R,k} = L_{1,k} \boxplus L_{2,k} = \log \frac{e^{L_{1,k}} + e^{L_{2,k}}}{1 + e^{(L_{1,k}+L_{2,k})}}. \tag{2.36}$$

Note, that independency between messages should hold in order to apply (2.36). Finally, SISO_R computes at its output, the extrinsic information $\mathbf{E}_{s_i(R)}$ from $\mathbf{L}_j$ and $\mathbf{E}_{u_R(R)}$, $i, j \in \{1, 2\}$, $i \neq j$, where $\mathbf{E}_{u_R(R)}$ is the extrinsic information on $\mathbf{u}_R$ computed by the decoder corresponding to C_R. The message-passing schedule for the JNCD at each iteration, and the final hard decisions are recapitulated in the Algorithm 1.

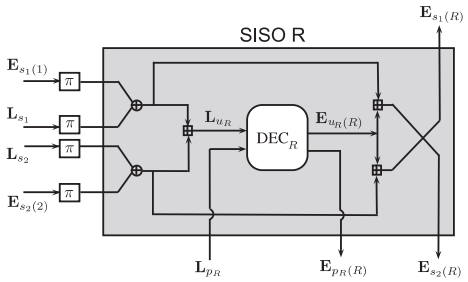

Figure 2.5: XOR decoder

Algorithm 1 : JNCD at the destination

(Initialization)
Set all the a priori information to zero.

(Iterations)
Iterate until convergence:

1. Activate the SISO MAP detector using the received signal $\mathbf{Y}_D^{(1)}$, and the messages $\mathbf{E}_{s_1(1)}+\pi^{-1}(\mathbf{E}_{s_1(R)})$, $\mathbf{E}_{p_1(1)}$ and $\mathbf{E}_{s_2(2)}+\pi^{-1}(\mathbf{E}_{s_2(R)})$, $\mathbf{E}_{p_2(2)}$, where $\mathbf{E}_{s_i(i)} = \mathbf{E}_{s_i(i,1)}+\pi_{0,i}^{-1}(\mathbf{E}_{s_i(i,2)})$.

2. Activate the SISO MAP demapper using the received signal $\mathbf{Y}_D^{(2)}$, and the message $\mathbf{E}_{p_R(R)}$.

3. Activate simultaneously the SISO decoders SISO_1 and SISO_2

   (a) Activate simultaneously $\mathrm{SISO}_{1,1}$ and $\mathrm{SISO}_{2,1}$ with the messages $\mathbf{L}_{s_1}$, $\mathbf{L}_{p_{1,1}}$ and $\mathbf{L}_{s_2}$, $\mathbf{L}_{p_{2,1}}$ provided by the MAP detector, and $\pi_{0,1}^{-1}(\mathbf{E}_{s_1(1,2)})+\pi^{-1}(\mathbf{E}_{s_1(R)})$ and $\pi_{0,2}^{-1}(\mathbf{E}_{s_2(2,2)})+\pi^{-1}(\mathbf{E}_{s_2(R)})$, which are derived from the previous iteration.

   (b) Activate simultaneously the $\mathrm{SISO}_{1,2}$ and $\mathrm{SISO}_{2,2}$ with, respectively, the messages $\pi_{0,1}(\mathbf{L}_{s_1})$, $\mathbf{L}_{p_{1,2}}$ and $\pi_{0,2}(\mathbf{L}_{s_2})$, $\mathbf{L}_{p_{2,2}}$ provided by the MAP detector, and $\pi_{0,1}(\mathbf{E}_{s_1(1,1)})+\pi_{0,1}\circ\pi^{-1}(\mathbf{E}_{s_1(R)})$ and $\pi_{0,2}(\mathbf{E}_{s_2(2,1)})+\pi_{0,2}\circ\pi^{-1}(\mathbf{E}_{s_2(R)})$.

4. Activate the SISO decoder SISO_R with the messages $\mathbf{L}_{p_R}$ provided by the MAP demapper, and $\mathbf{L}_1 = \pi(\mathbf{L}_{s_1}+\mathbf{E}_{s_1(1)})$ and $\mathbf{L}_2 = \pi(\mathbf{L}_{s_2}+\mathbf{E}_{s_2(2)})$.

(Hard decisions)
Combine all the available information on the systematic bits $\mathbf{u}_1$ and $\mathbf{u}_2$:

$$\mathbf{L}_{s_1}+\mathbf{E}_{s_1(1,1)}+\pi_{0,1}^{-1}(\mathbf{E}_{s_1(1,2)})+\pi^{-1}(\mathbf{E}_{s_1(R)})\rightarrow\hat{\mathbf{u}}_1$$
$$\mathbf{L}_{s_2}+\mathbf{E}_{s_2(2,1)}+\pi_{0,2}^{-1}(\mathbf{E}_{s_2(2,2)})+\pi^{-1}(\mathbf{E}_{s_2(R)})\rightarrow\hat{\mathbf{u}}_2$$

2.4 Separate Network Channel Coding and Decoding

As previously mentioned, the SNCC scheme is based on the XOR operation at the relay, and the network-coded signal is separately decoded at the destination. Thus, in case of SOMARC/SNCC, a joint detection and decoding procedure similar to section (2.3.2.1) is performed at the destination on the signal received during the first transmission phase, and a separate decoding is performed on the relay signal received during the second phase. The channel decoders make hard decisions and output the estimates to the network decoder. When the relay cooperates with both sources, if at least two out of three channel output estimates are error-free, the network decoder can retrieve both source messages.

2.5 Numerical Results

In this section, we provide some numerical results to evaluate the effectiveness of our approach. In our comparisons, we consider both SOMARC and OMARC using JNCC or SNCC. We also consider the MAC reference system in which both sources transmit simultaneously to the destination during the available number of channel uses N. We start by detailing the topology of the network. For the sake of simplicity, we consider a symmetric MARC and MAC, i.e., $d_{1R} = d_{2R}$ and $d_{1D} = d_{2D}$. The average energy per available dimension allocated to the two sources is the same, i.e., $P_{0,1} = P_{0,2} = P_0$. We fix the same path loss factor, i.e., $\kappa = 3$, free distance, i.e., $d_0 = 1$ and noise power spectral density, i.e., $N_0 = 1$, for all links. In the case of relay assisted communication schemes, due to the half-duplex nature of the relay, the transmission time slot of the sources and the relay are separated in time. We fix $\alpha = 2/3$ for SOMARC, which yields $P_1 = P_2 = 3/2P_0$. In OMARC, the two sources transmit in consecutive, equal duration, time slots. Thus, the first two time slots are dedicated to the sources, and the third to the relay. It comes that $P_1 = P_2 = 3P_0$ for OMARC. The relay, in case of cooperation, transmits always at $P_R = 3P_{0,R}$ for both OMARC and SOMARC. For MAC, since the sources are active during both transmission phases, we have $P_1 = P_2 = P_0$. For simulation purposes, two different configurations are considered: In the first configuration, we fix the number of receive antennas to one both at the relay and destination, i.e., $N_R = N_D = 1$. The geometry is chosen such that $d_{ij} = d_{RD} = d$ which yields $P_{i,j} = P_{RD} = \gamma$ for SOMARC, $P_{i,j} = 2\gamma$, $P_{RD} = \gamma$ for OMARC, and $P_{iD} = 2/3\gamma$ for MAC, $i \in \{1, 2\}$, $j \in \{R, D\}$ where γ is the received SNR per symbol or dimension. In the second configuration, we increase the number of receive antennas at the destination to 4, i.e. , $N_R = 1$ and $N_D = 4$. The geometry is chosen such that $d_{iR} = d_1$ and $d_{iD} = d_{RD} = d$ with $(d_1/d)^{-3} = 100$, $i \in \{1, 2\}$. It yields $P_{iR} = 100\gamma$ (or $\gamma + 20$ in dB) and $P_{iD} = P_{RD} = \gamma$ for SOMARC which

translates into $P_{iR} = 200\gamma$, $P_{iD} = 2\gamma$ and $P_{RD} = \gamma$ for OMARC, $i \in \{1, 2\}$. P_{iD} in case of MAC remains unchanged. Each message of the sources has length $K = 1024$ information bits. In our proposed JNCC, the complex signal sets $\mathscr{X}_1$, $\mathscr{X}_2$, and $\mathscr{X}_R$ used in BICM are either QPSK or 16QAM constellation (Gray labeling) and their corresponding sum rates are $\eta = 4/3$ bits per channel use (b./c.u.) and $\eta = 8/3$ b./c.u., respectively.

2.5.1 Information-theoretic comparison of the protocols

2.5.1.1 Individual ϵ-outage achievable rate with Gaussian inputs

In the first set of simulations, we consider the ϵ-outage achievable rate of S_1, and we compare the individual ϵ-outage achievable rate $C_\epsilon(\gamma)$ of JNCC and SNCC for the SOMARC and the OMARC. We also compare the individual ϵ-outage achievable rate of the aforementioned schemes with that of the MAC. In our analysis, we fix $\epsilon = 10^{-2}$. The number of receive antennas at the destination is either $N_D = 1$ or $N_D = 4$. The corresponding results are depicted in Fig. 2.6. As we can see, the ϵ-outage achievable rate for the SOMARC is always higher than the ϵ-outage achievable rate for the OMARC regardless of the network channel coding strategy (i.e., JNCC or SNCC); Especially, in the case of $N_D = 4$, JNCC with orthogonal multiple access (OMARC/JNCC) is strictly suboptimal and the ϵ-outage achievable rate gain of SOMARC/JNCC versus OMARC/JNCC for individual rates above 2b./c.u. is more than 5 dB. This results from the fact that, in the presence of multiple receive antennas, a non-orthogonal MAC can better exploit the available degrees of freedom. Moreover, even in the case of $N_D = 1$ which is not a priori favorable for a MAC, we see that SOMARC/JNCC can provide an ϵ-outage achievable rate gain of approximately 4 dB for data rates above 2 b./c.u.. In Fig. 2.6, we also see that the JNCC schemes outperform the SNCC ones for both transmission protocols. For the data rate of 2 b./c.u., the ϵ-outage achievable rate gains are about 5 dB in case of SOMARC for both $N_D = 1$ and $N_D = 4$, 3 dB and 4 dB in case of OMARC with respectively $N_D = 1$ and $N_D = 4$. Finally, it is interesting to see that, beyond a certain threshold for γ, the individual ϵ-outage achievable rate of MAC becomes higher than that of SOMARC or OMARC using either JNCC or SNCC. This is certainly due to the non-usage of all the available number of channel uses by the sources in SOMARC and OMARC.

2.5.1.2 Individual information outage probability with discrete inputs

In the second set of simulations, our purpose is first to compare the individual outage probability of SOMARC/JNCC and OMARC/JNCC, and for the fixed sum rates of $\eta = 4/3$ and $\eta = 8/3$ b./c.u.. In order to achieve the same spectral efficiency as the SOMARC, we

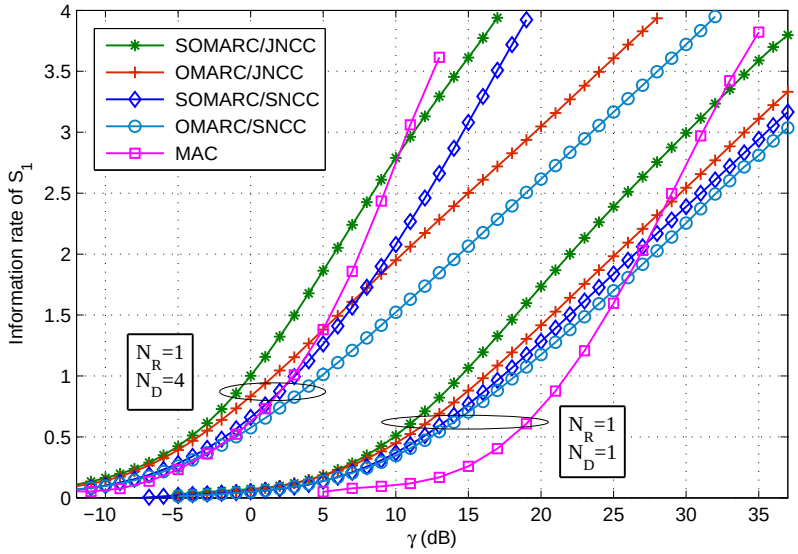

Figure 2.6: Individual ϵ-outage achievable rate - $\epsilon = 10^{-2}$ - SOMARC vs. OMARC - JNCC vs. SNCC

consider two approaches for OMARC: (1) We impose on the transmitters to use the same input alphabet as in the case of SOMARC, which makes sense if we want to preserve the same level of peak-to-average power ratio (PAPR); (2) We employ constellation expansion for the sources in OMARC. In the first approach, the two sources have no other choice but to transmit their information symbols without any coding, and thus, from a theoretical perspective ($N \to \infty$), the system is always in outage. In the second approach, the sources increase the cardinality of their modulation while preserving the same spectral efficiency, which makes room for coding. Thus, the information outage probability of SOMARC with QPSK is compared with the information outage probability of OMARC with 16QAM at the sources and QPSK at the relay. Similarly, the information outage probability of SOMARC with 16QAM is compared with the information outage probability of OMARC with 64QAM at the sources and 16QAM at the relay. The corresponding results are depicted in Fig. 2.7 for the sum rate of $\eta = 4/3$ b./c.u. and in Fig. 2.8 for the sum rate of $\eta = 8/3$ b./c.u., for both $N_D = 1$ and $N_D = 4$. As we can see, in all cases, the information outage probability of SOMARC is smaller than the one of OMARC. Considering the second approach, for $\eta = 8/3$ b./c.u., and at the BLER of 10^{-2}, the power gain is approximately equal to 2.5 dB for $N_D = 1$ and becomes even larger for $N_D = 4$, attaining 3.5 dB at the BLER of 10^{-2}, which reconfirms the sub-optimality of the orthogonal multiple access in case of multiple receive antennas.

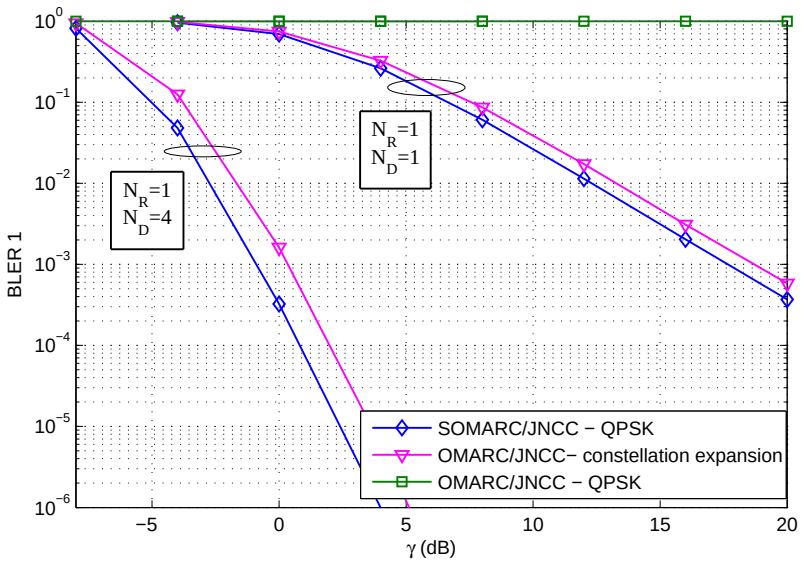

Figure 2.7: Individual outage probability (e.g., for S_1) - SOMARC/JNCC vs. OMARC/JNCC - $\eta = 4/3$ b./c.u.

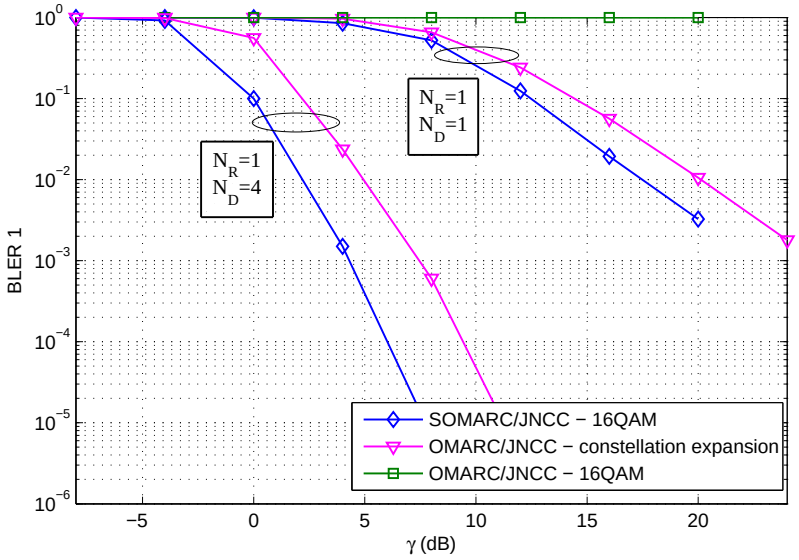

Figure 2.8: Individual outage probability (e.g., for S_1) - SOMARC/JNCC vs. OMARC/JNCC - $\eta = 8/3$ b./c.u.

To pursue our analysis, we compare the individual information outage probabilities of SOMARC/JNCC and SOMARC/SNCC. Here again, to keep the same spectral efficiency for the SNCC case, we have the aforementioned two approaches. Using the first approach, the relay-to-destination channel is always in outage in the case of SOMARC/SNCC, and thus it leads to the performance of a MAC corresponding to the first transmission time slot. This explains the difference of slopes between the two curves in the corresponding figures. In the second approach, constellation expansion is employed for the relay-to-destination channel. Thus, in SOMARC/SNCC, the relay uses 16QAM for $\eta = 4/3$ b./c.u., and 64QAM for $\eta = 8/3$ b./c.u.. The corresponding results are depicted in Fig. 2.9 and Fig. 2.10 for both $N_D = 1$ and $N_D = 4$. As we can see, the SOMARC/SNCC has always a performance loss compared to the SOMARC/JNCC. In the case of constellation expansion and $N_D = 1$, at the BLER of 10^{-2}, the loss is around 2 dB for $\eta = 4/3$ b./c.u., and 3 dB for $\eta = 8/3$ b./c.u.. The loss is much higher when we consider $N_D = 4$, attaining 3 dB for $\eta = 4/3$ b./c.u., and 4 dB for $\eta = 8/3$ b./c.u..

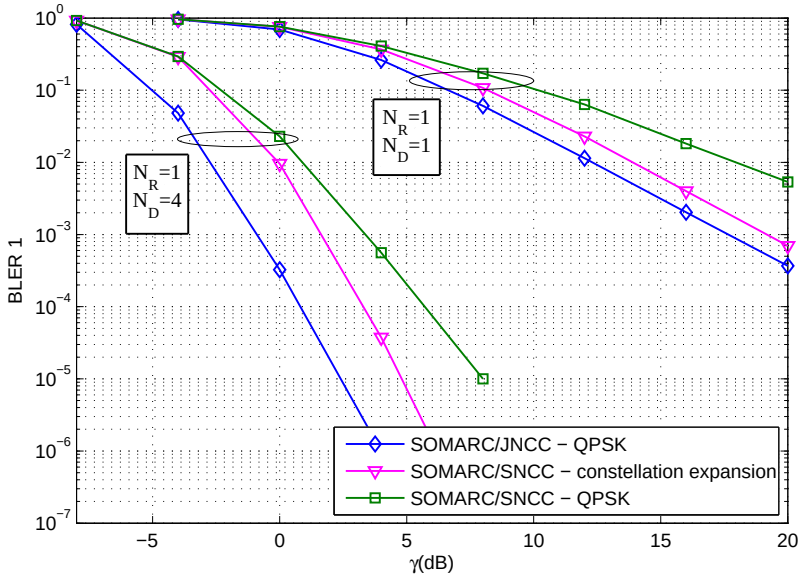

Figure 2.9: Individual outage probability (e.g., for S_1) - SOMARC/JNCC vs. SOMARC/SNCC - $\eta = 4/3$ b./c.u.

2.5.2 Performance of practical code design

In the sequel, the number of iterations I is set to 5 at the relay and to 10 (for $N_D = 1$) or 3 (for $N_D = 4$) at the destination. These numbers of iterations ensure convergence and allow

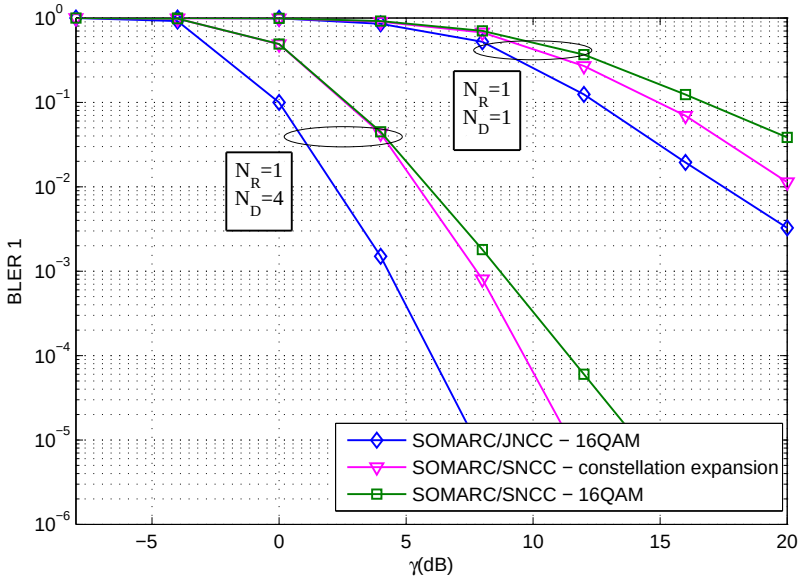

Figure 2.10: Individual outage probability (e.g., for S_1) - SOMARC/JNCC vs. SOMARC/SNCC - $\eta = 8/3$ b./c.u.

to very closely approach the performance of a Genie Aided (GA) receiver at sufficiently high SNR for the selected modulation and coding schemes, the Genie Aided (GA) receiver corresponding to the ideal case where the interference is known and perfectly removed.

2.5.2.1 Comparison of JNCC functions: XOR versus general scheme

In this section, we compare the performance of the two JNCC functions introduced in section (2.3.2.2) for SOMARC. The first one is based on $G_{R,|J|}$, and the second one is based on XOR followed by G_R. This experiment is carried out with $N_R = N_D = 1$ and with $N_R = 1$ and $N_D = 4$, and for the sum rate of $\eta = 4/3$ b./c.u.. As we are interested in comparing the JNCC functions, we assume that the source-to-relay links are error-free in this set of simulations. In our comparisons, we consider also two different coding schemes at the sources: (1) The two sources use identical turbo codes of rate-1/2 made of two 4-state rate-1/2 RSC encoders with generator matrix $\mathbf{G}_1 = [\ 1 \quad 5/7\ ]$ in octal representation, whose half of the parity bits are punctured; (2) The two sources use identical 64-state rate-1/2 RSC encoder with generator matrix $\mathbf{G}_2 = [\ 1 \quad 117/147\ ]$ [133]. Exhaustive simulations showed that those numbers of states yield the best performance/complexity trade-off. In both of the above schemes, the relay employs 4-state, 16-state or 64-state RSC encoders.

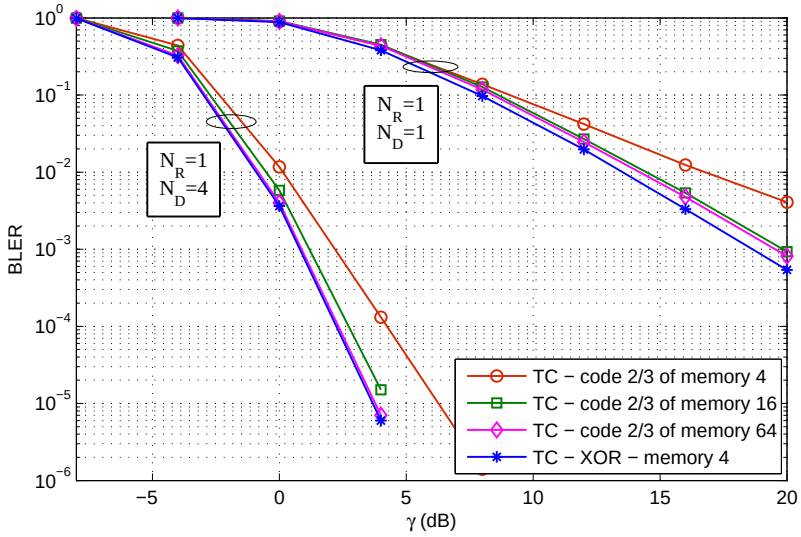

Figure 2.11: Joint BLER performance - error-free S-R links - Turbo Code (TC) at sources - JNCC based on XOR vs. JNCC based on double input binary linear code - $\eta = 4/3$ b./c.u.

These RSC encoders are defined by $[\ 1 \quad p/q\ ]$ and $\begin{bmatrix} 1 & 0 & p_1/q \\ 0 & 1 & p_2/q \end{bmatrix}$ for respective cases of XOR and general scheme, and in octal notation. In the case of 4-state RSC encoder, $p = 5$ and $q = 7$ for the XOR scheme, and $p_1 = 7$, $p_2 = 2$, and $q = 3$ for the general scheme. In the case of 16-state RSC encoder, $p = 21$ and $q = 37$ [133] for the XOR scheme, and $p_1 = 27$, $p_2 = 33$, and $q = 31$ for the general scheme. In the case of 64-state RSC encoder, $p = 117$ and $q = 147$ for the XOR scheme, and $p_1 = 52$, $p_2 = 36$, and $q = 115$ for the general scheme. The SISO decoders implement the BCJR algorithm [134]. The system performance is measured in terms of joint BLER which is defined as the probability to have at least one erroneously decoded information bit in either of the decoded blocks at the destination.

The simulation results for the first scheme (with turbo codes at sources) are depicted in Fig. 2.11. As we have seen that the performance of JNCC based on XOR is not affected by the memory order of the RSC encoder at the relay, only the joint BLER results for the memory order of 4 are depicted. As we see, the JNCC scheme based on XOR achieves the promised full diversity by construction, whatever the memory order of the RSC encoder. The general JNCC scheme also becomes full diversity for a sufficient memory order, but is not as good as the XOR scheme, especially in the case of $N_D = 1$.

Now, we analyze the joint BLER of the second scheme (with RSC encoders at sources). The simulation results are depicted in Fig. 2.12. Since the JNCC based on XOR performs

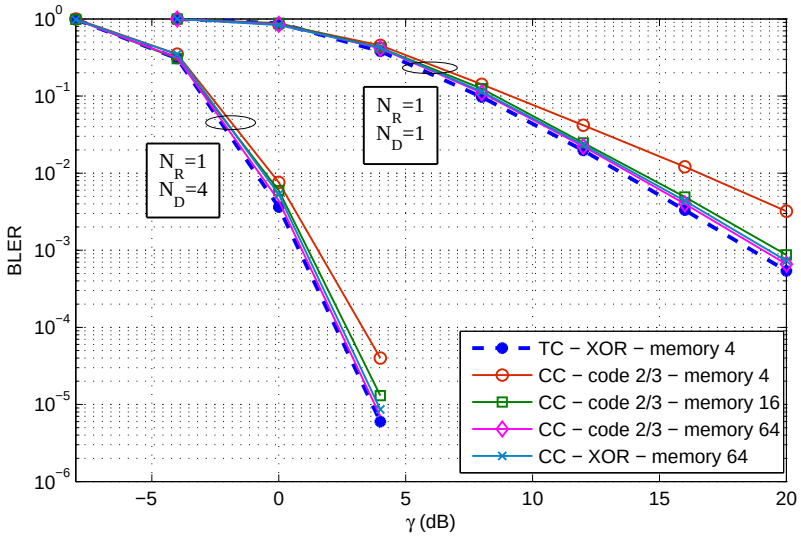

Figure 2.12: Joint BLER performance - error-free S-R links - Convolutional Code (CC) and Turbo Code (TC) at sources - JNCC based on XOR vs. JNCC based on double input binary linear code - $\eta = 4/3$ b./c.u.

slightly better when the memory order of the RSC encoder increases, only the joint BLER results for the memory order of 64 are depicted. As we see, here again, the JNCC scheme based on XOR achieves full diversity, whatever the memory order of the RSC encoder. The general JNCC scheme also becomes full diversity for a sufficient memory order and would exhibit better coding gain for less severe fading distribution (e.g., with receive antenna diversity) at the expense of more complex decoding. For comparison purposes, we have also plotted the best choice of the first scheme, which is the JNCC based on XOR with turbo codes and RSC encoder of memory order 4 at respectively the sources and the relay. Simulation results show that this scheme exhibits the best performance.

2.5.2.2 Gap to outage limits

Here, we first evaluate the gap between the individual BLER of practical designs for SO-MARC/JNCC and that of their corresponding information outage probability. The experiment is carried out for $\eta = 4/3$ b./c.u. and with the best coding schemes analyzed in section (2.5.2.1) for both cases of turbo codes and RSC encoders at the sources. Thus, in the first case, the sources use punctured turbo codes made of 4-state RSC encoders, and the relay uses JNCC based on XOR and an RSC encoder of memory order of 4. In the second case, the sources use 64-state RSC encoders, and the relay uses JNCC based on

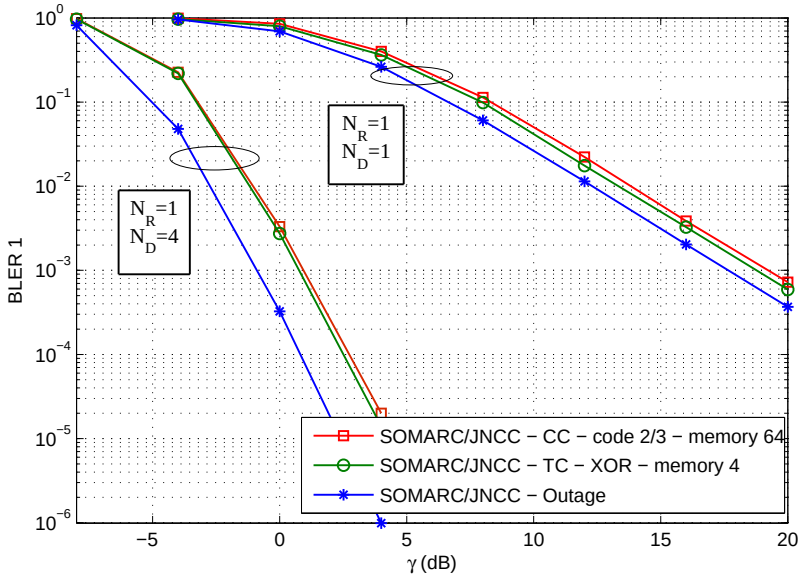

Figure 2.13: Individual BLER (e.g., for S_1) - Practical SOMARC/JNCC vs. outage limit - $\eta = 4/3$ b./c.u.

the double input 64-state RSC encoder. The corresponding results are demonstrated in Fig. 2.13. As expected, the JNCC scheme based on turbo codes provides the best results and performs 1 dB and 1.5 dB away from the information outage probability for respective cases of $N_D = 1$ and $N_D = 4$.

Next, we compare the individual BLER of practical designs for SOMARC/SNCC with their corresponding information outage probability. The experiment is carried out for $\eta = 4/3$ b./c.u. and for both cases of turbo codes and RSC encoders at both sources and the relay. In the first case, the sources and the relay use the punctured turbo codes made of 4-state rate-1/2 RSC encoders with generator matrix $\mathbf{G}_1$. In the second case, the sources and the relay employ rate-1/2 4-state, 16-state or 64-state RSC encoders with generator matrices $\mathbf{G}_1$, $\mathbf{G}_3 = [\ 1 \quad 21/37\ ]$ and $\mathbf{G}_2$, respectively. The constellation expansion is also performed at the relay. The simulation results are plotted in Fig. 2.14 for both $N_D = 1$ and $N_D = 4$. As we see, increasing the memory order of the RSC encoder improves the individual BLER of the second case. However, the turbo code remains the best choice which performs 1 dB away from the individual outage probability for both $N_D = 1$ and $N_D = 4$.

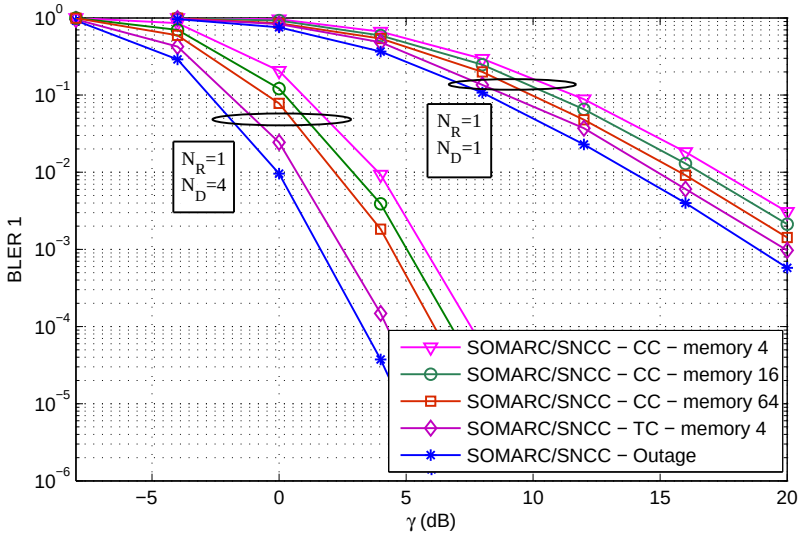

Figure 2.14: Individual BLER (e.g., for S_1) - Practical SOMARC/SNCC vs. outage limit - $\eta = 4/3$ b./c.u. - constellation expansion at the relay

2.5.2.3 Comparison of the different protocols

In this section, we first compare the individual BLER of practical code design for SOMARC/JNCC with that of the OMARC/JNCC. The JNCC in both protocols is based on XOR. In SOMARC/JNCC, the two sources use the punctured turbo codes made of 4-state rate-1/2 RSC encoders with generator matrix $\mathbf{G}_1$, and the relay uses the same RSC encoder. For OMARC/JNCC, we first imposed on the sources the use of same signal sets. In this case, the two sources transmit their information symbols without any coding, while the relay uses the 4-state rate-1/2 RSC encoder. The corresponding results demonstrated considerable gains in favour of our approach. We next carried out another experiment, where constellation expansion is employed for OMARC, as explained in the outage comparisons. Thus, in the case of OMARC with $\eta = 4/3$ b./c.u., both sources use the same turbo code as the SOMARC with 16QAM modulation, and the relay uses the 4-state rate-1/2 RSC encoder with QPSK constellation. Similarly, in the case of $\eta = 8/3$ b./c.u., both sources use the turbo code made of 4-state rate-1/2 RSC encoders with generator matrix $\mathbf{G}_1$, whose parity bits are punctured to result in a code of rate 2/3. They use then 64QAM constellation. The relay uses the same RSC encoder as the previous case with 16QAM modulation. The corresponding results are depicted in Fig. 2.15 for the spectral efficiency of $\eta = 4/3$ b./c.u., and in Fig. 2.16 for the spectral efficiency of $\eta = 8/3$ b./c.u., for both $N_D = 1$ and $N_D = 4$. Here again, the SOMARC outperforms the OMARC in most cases and the performance gains are considerable for $N_D = 4$. The exception is the case of

$\eta = 8/3$ b./c.u. and for $N_D = 1$, where the SOMARC starts to outperform the OMARC with constellation expansion at a relatively high SNR ($\gamma = 24$ dB).

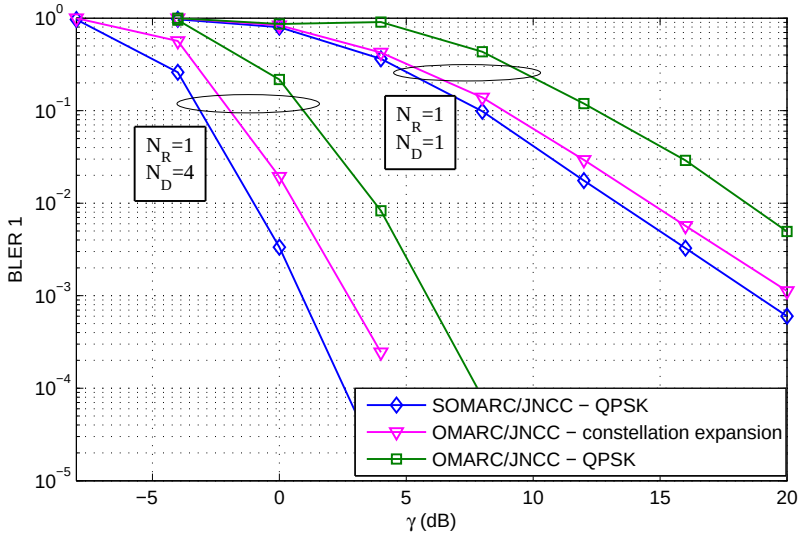

Figure 2.15: Individual BLER (e.g., for S_1) - SOMARC/JNCC vs. OMARC/JNCC - $\eta = 4/3$ b./c.u.

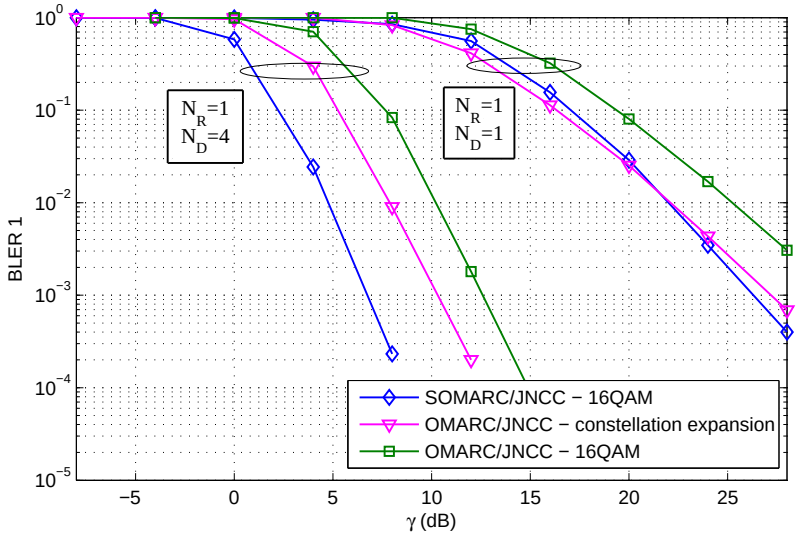

Figure 2.16: Individual BLER (e.g., for S_1) - SOMARC/JNCC vs. OMARC/JNCC - $\eta = 8/3$ b./c.u.

To pursue our comparison of practical designs, we compare the individual BLERs of

SOMARC/JNCC and SOMARC/SNCC. In SOMARC/SNCC, both sources use the same punctured turbo code as the SOMARC/JNCC, and the relay, as previously mentioned, has two choices: (1) It uses the same input alphabet as the case of SOMARC/JNCC and transmits its information symbols without any coding; (2) It performs constellation expansion. In case (2), for $\eta = 4/3$ b./c.u., the relay uses the same punctured turbo code as the sources with 16QAM modulation, and for $\eta = 8/3$ b./c.u., it uses the punctured turbo code of rate 2/3 made of 4-state rate-1/2 RSC encoders with generator matrix $\mathbf{G}_1$. It then uses 64QAM constellation. The corresponding results are depicted in Fig. 2.17 for the spectral efficiency of $\eta = 4/3$ b./c.u., and in Fig. 2.18 for the spectral efficiency of $\eta = 8/3$ b./c.u., for both $N_D = 1$ and $N_D = 4$. As we see, the SOMARC/JNCC outperforms the SOMARC/SNCC, and the power gains are approximately the same as the ones predicted by theoretical bounds.

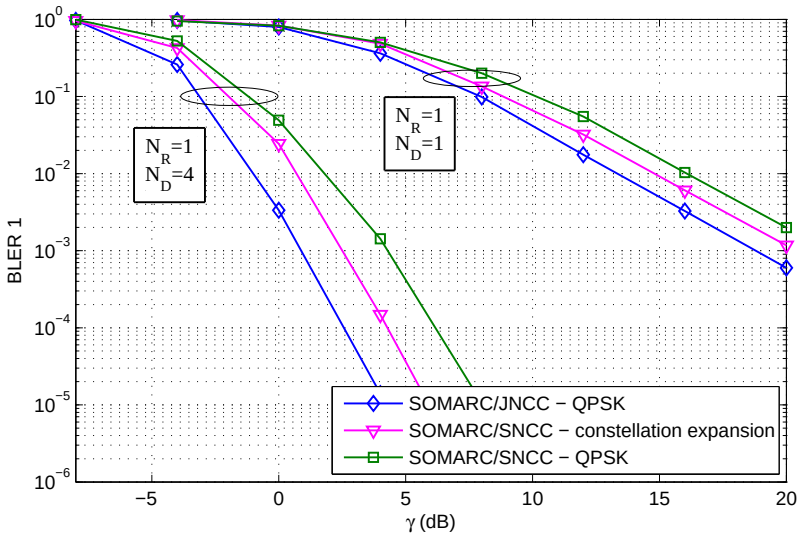

Figure 2.17: Individual BLER (e.g., for S_1) - SOMARC/JNCC vs. SOMARC/SNCC - $\eta = 4/3$ b./c.u.

2.6 Conclusion

In this chapter, we have studied JNCC for a new class of MARC, referred to as SOMARC, from both an information-theoretic and a practical code design perspective. We have derived the SOMARC individual information outage probability, conditional on JNCC (and SNCC used as a reference). We have also presented new JNCC schemes flexible in

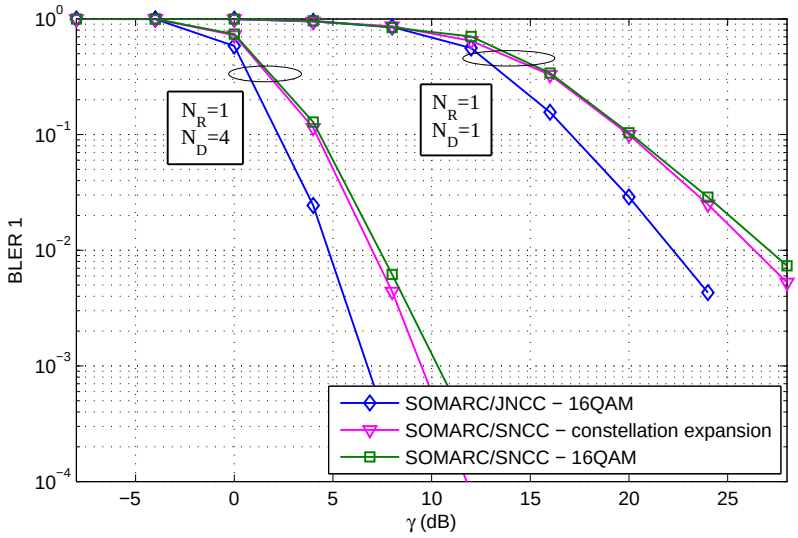

Figure 2.18: Individual BLER (e.g., for S_1) - SOMARC/JNCC vs. SOMARC/SNCC - $\eta = 8/3$ b./c.u.

terms of number of sources, encoders and modulations. For the 2-source symmetric case and targeted sum rates $\eta = 4/3$ b./c.u. and $\eta = 8/3$ b./c.u., we have shown that our proposed schemes are more efficient than (1) conventional distributed JNCC for OMARC; (2) conventional SNCC schemes. Moreover, the proposed SOMARC/JNCC performs very close to the outage limit (within 1.5 dB) for both cases of single and multiple receive antennas at the destination, and for the fixed sum rate of $\eta = 4/3$ b./c.u.. We have verified that the semi-orthogonal multiple access exhibits considerable gains over orthogonal multiple access, even in the case of a single receive antenna at the destination.

Chapter 3

Joint Network-Channel Coding for the Half-Duplex Non-Orthogonal MARC

In the previous chapter, we evaluated the performance of HD-SOMARC in which the sources were constrained to remain silent during the transmission phase of the relay. This necessitates extra signaling to inform the sources of the cooperation. However, if we allow the sources to transmit, only the destination node should be informed of the cooperation, which reduces significantly the control signaling overhead. At the same time, the sources can use better codes (additional parity bits), but since the source signals interfere with the relay signal, a more complex multiuser joint decoding is required at the destination. What we gain from a pure coding perspective could be lost due to the sub-optimality of iterative decoding. The other challenging problem is to design the codes able to perform well for the source-to-relay links in their partial version, and also to perform well at the destination in their full version (i.e., considering the additional parity bits of the sources during the second phase and those of the relay in case of cooperation). Motivated by the aforementioned points, we propose in this chapter a new class of MARC that we call Half-Duplex Non-Orthogonal MARC (HD-NOMARC or NOMARC) and is defined as follows: (1) Independent sources communicate with a single destination in the presence of a relay; (2) The relay is half-duplex and applies a Selective Decode and Forward (SDF) relaying strategy, i.e, it forwards only a deterministic function of the messages that it can decode without errors; (3) The sources are allowed to transmit simultaneously during both the listening phase and the transmission phase of the relay. During the first transmission phase, the sources simultaneously broadcast the first part of their messages, interfering at

The work presented in this chapter is submitted to IEEE Transaction on Wireless Communication. It was presented in part at IEEE PIMRC 2010, and in part at IEEE PIMRC 2012.

the relay and destination. During the second phase, they continue to transmit the second part of their messages, and thus interfere with the relay in case of transmission, but, at the same time, the destination benefits from stronger codes to perform joint detection and decoding. This is indeed the most general form of half-duplex relaying where the medium access is not orthogonal [112, 113]. Allowing collisions at the relay and the destination renders the reality of wireless environments and leverages better the broadcast nature of the radio channel than the OMARC. The proposed SDF in NOMARC is a modification of the relaying protocol presented in [135] so as to allow partial cooperation if some of the sources are successfully decoded at the relay and the others are not. Thus, it not only prevents the error propagation from the relay to the destination, but also decreases the individual BLER, i.e., the BLER for each source. As already mentioned in Chapter 2, this SDF approach has been analyzed in a variety of contributions for the OMARC using either JNCC [82] or SNCC [126]. Its theoretical and practical interests have also been confirmed in Chapter 2 for the HD-SOMARC. However, many issues need still to be addressed, including the impact of the multiple access interference during both transmission phases on the information outage probability. Based on a careful outage analysis, the NOMARC individual information outage probability (e.g., for S_1) is derived for both JNCC or SNCC. The individual information outage probability and the individual ϵ-outage achievable rate (e.g., for S1) are then numerically evaluated assuming independent Gaussian inputs or discrete independent identically and uniformly distributed inputs and compared with the ones of a OMARC at fixed energy budget per source (per available dimensions). As a second contribution, we propose practical JNCC designs for NOMARC that are flexible in terms of number of sources and MCS. Our designs are built on turbo codes, and rely on advanced (iterative) joint detection and decoding receiver architectures. We further demonstrate that they also guarantee the full diversity in the sense that they achieve the same diversity gain as the single-user case. The rationale behind our code construction has already been discussed in Chapter 2.

3.1 System Model

The M statistically independent sources $S_1, \ldots, S_M$ want to communicate with the destination D in the presence of a relay R. In order to create virtual uplink MIMO channels and to benefit from spatial multiplexing gains, we assume that the relay R and the destination D are equipped with N_R and N_D receive antennas. We consider that the baud rate of the sources and relay is $D = 1/T_s$ and the overall transmission time is fixed to T, thus the number of available channel uses to be shared between the sources and the relay is $N = DT$. We consider the case of Nyquist rate and cardinal sine transmission pulse shape,

i.e., $N = DT$ is the total number of available complex dimensions and D is the total bandwidth of the system. Our channel models are inspired by the following assumptions: (1) The delay spreads of the radio channels from the sources to the relay and the destination as well as from the relay to the destination are much lower than T_s ensuring no frequency selectivity; (2) the coherence time of all the aforementioned radio channels are supposed to be much larger than T. The Non-orthogonal transmission protocol is considered. The N available channel uses are divided into two successive time slots corresponding to the listening phase of the relay, say $N_1 = \alpha N$ channel uses, and to the transmission phase of the relay, say $N_2 = \bar{\alpha} N$ channel uses, with $\alpha \in [0, 1]$ and $\bar{\alpha} = 1 - \alpha$. Each source i broadcasts its message $\mathbf{u}_i \in \mathbb{F}_2^K$ of K information bits under the form of a modulated sequence during both transmission phases. Without loss of generality, the modulated sequences are chosen from the complex codebooks ζ_i of rate K/N and take the form of sequences $\mathbf{x}_i \in \zeta_i \subset \mathscr{X}_i^N$, $i \in \{1, \ldots, M\}$, where $\mathscr{X}_i \subset \mathbb{C}$ denote a complex signal set of cardinality $|\mathscr{X}_i| = 2^{q_i}$, with energy normalized to unity. During the first phase, the sources transmit the first part of their modulated sequences denoted by $\mathbf{x}_i^{(1)} \in \mathscr{X}_i^{\alpha N}$ which belongs to a complex codebook $\zeta_i^{(1)}$ of rate $K/(\alpha N)$. The corresponding received signals at the relay and destination are expressed as

$$\mathbf{y}_{R,k}^{(1)} = \sum_{i=1}^{M} \sqrt{P_{iR}} \mathbf{h}_{iR} x_{i,k}^{(1)} + \mathbf{n}_{R,k}^{(1)} \tag{3.1}$$

$$\mathbf{y}_{D,k}^{(1)} = \sum_{i=1}^{M} \sqrt{P_{iD}} \mathbf{h}_{iD} x_{i,k}^{(1)} + \mathbf{n}_{D,k}^{(1)} \tag{3.2}$$

for $k = 1, \ldots, \alpha N$. In (3.1) and (3.2), the channel fading vectors $\mathbf{h}_{iR} \in \mathbb{C}^{N_R}$, and $\mathbf{h}_{iD} \in \mathbb{C}^{N_D}$, $i \in \{1, \ldots, M\}$ are mutually independent, constant over the transmission of $\mathbf{x}_1$, …, $\mathbf{x}_M$ and change independently from one transmission of the sources to the next. The channel fading vectors $\mathbf{h}_{iR}$, $i \in \{1, \ldots, M\}$, are i.d. following the pdf $\mathcal{CN}(\mathbf{0}_{N_R}, \mathbf{I}_{N_R})$. The channel fading vectors $\mathbf{h}_{iD}$, $i \in \{1, \ldots, M\}$, are i.d. following the pdf $\mathcal{CN}(\mathbf{0}_{N_D}, \mathbf{I}_{N_D})$. The additive noise vectors $\mathbf{n}_{R,k}^{(1)}$ and $\mathbf{n}_{D,k}^{(1)}$ are independent and follow the pdf $\mathcal{CN}(\mathbf{0}_{N_R}, N_0 \mathbf{I}_{N_R})$ and $\mathcal{CN}(\mathbf{0}_{N_D}, N_0 \mathbf{I}_{N_D})$, respectively. $P_{ij} \propto (d_{ij}/d_0)^{-\kappa} P_i$, $i \in \{1, \ldots, M\}$, $j \in \{R, D\}$ is the average received energy per dimension and per antenna (in Joules/symbol), where d_{ij} is the distance between the transmitter and receiver, d_0 is a reference distance, κ is the path loss coefficient, with values typically in the range $[2, 6]$, and P_i is the transmit power (or energy per symbol) of S_i. Note that the shadowing could be included within P_{ij}. To fairly compare the performance with respect to other classes of MARC, in which the sources transmit only over a fraction of the available dimensions or channel uses N, we fix the total energy per available dimensions $NP_{0,i}$ spent by S_i, i.e., $P_i = P_{0,i}/\beta$. Here, β denotes the fraction

of N over which each source transmits. Thus, $\beta = 1$ in the case of NOMARC, $\beta = \alpha$ in the case of HD-SOMARC [136], and $\beta = \alpha/M$ in the case of OMARC supposing that the sources transmit in consecutive, equal duration, time slots. During the second phase, the sources continue to transmit the second part of their modulated sequences denoted by $\mathbf{x}_i^{(2)} \in \mathscr{X}_i^{\bar{\alpha}N}$, $i \in \{1, \ldots, M\}$. The relay uses a SDF approach, which depends on the number of correctly decoded messages. Let $J = \{j_1, j_2, \ldots, j_{|J|}\}$, $|J| \leq M$ denote the set of message indices with cardinality $|J|$ that have been successfully decoded. If $J = \emptyset$, the relay remains silent. Otherwise, according to the number of correctly decoded messages and the chosen network coding scheme, it transmits a modulated sequence of the form $\mathbf{x}_R^{(2)} \in \mathscr{X}_R^{\bar{\alpha}N}$, where $\mathscr{X}_R \subset \mathbb{C}$ is a complex constellation of order $|\mathscr{X}_R| = 2^{q_R}$ with energy normalized to unity. The modulated sequence $\mathbf{x}_R^{(2)}$ is chosen such that $(\mathbf{x}_{j_1}, \ldots, \mathbf{x}_{j_{|J|}}, \mathbf{x}_R)$ is a codeword on message $(\mathbf{u}_{j_1}, \ldots, \mathbf{u}_{j_{|J|}})$ belonging to a codebook $\zeta_{J,R}$ of rate $|J|K/N$. The received signal at the destination is expressed as

$$\mathbf{y}_{D,k}^{(2)} = \sum_{i=1}^{M} \sqrt{P_{iD}} \mathbf{h}_{iD} x_{i,k}^{(2)} + \theta \sqrt{P_{RD}} \mathbf{h}_{RD} x_{R,k}^{(2)} + \mathbf{n}_{D,k}^{(2)} \tag{3.3}$$

for $k = 1, \ldots, \bar{\alpha}N$. In (3.3), the channel fading vector $\mathbf{h}_{RD} \in \mathbb{C}^{N_D}$ follows the pdf $\mathcal{CN}(\mathbf{0}_{N_D}, \mathbf{I}_{N_D})$, is independent of $\mathbf{h}_{iD}$, $i \in \{1, \ldots, M\}$, constant over the transmission of $\mathbf{x}_R^{(2)}$ and changes independently from one transmission of the relay to another. The additive noise vector $\mathbf{n}_{D,k}^{(2)}$ is independent of $\mathbf{n}_{R,k}^{(1)}$ and $\mathbf{n}_{D,k}^{(1)}$, and follows the pdf $\mathcal{CN}(\mathbf{0}_{N_D}, N_0 \mathbf{I}_{N_D})$. $P_{RD} \propto (d_{RD}/d_0)^{-\kappa} P_R$, with P_R the transmit power of the relay, is the average receive power per dimension and per antenna at the destination. Here again, we fix the total energy per available dimensions $NP_{0,R}$ spent by the relay, i.e., $P_R = P_{0,R}/\bar{\alpha}$. The parameter θ is a discrete Bernoulli distributed random variable: $\theta = 1$ if the relay successfully decodes at least one source message, and $\theta = 0$ otherwise. Channel model (3.3) can be regarded as a family of MACs indexed by $\theta \in \{0, 1\}$ also called a two-state compound MAC [137].

Concerning the relay functionality, we distinguish the two cases of JNCC and SNCC:

- JNCC: The relay interleaves each message $\mathbf{u}_j$, $j \in J$, by π and applies a function $\Theta_{R,|J|}$

$$\Theta_{R,|J|} : \underbrace{\mathbb{F}_2^K \times \mathbb{F}_2^K \times \ldots \times \mathbb{F}_2^K}_{|J|} \to \mathbb{C}^{\bar{\alpha}N} \tag{3.4}$$

  to obtain the modulated sequence $\mathbf{x}_R^{(2)}$. In general, the function $\Theta_{R,|J|}$ is not a bijection on the interleaved correctly decoded messages. In practice, the relay would add some in-band signaling to make the destination aware of the set J. Finally, the relay signal, together with the source signals, forms a distributed joint network-channel

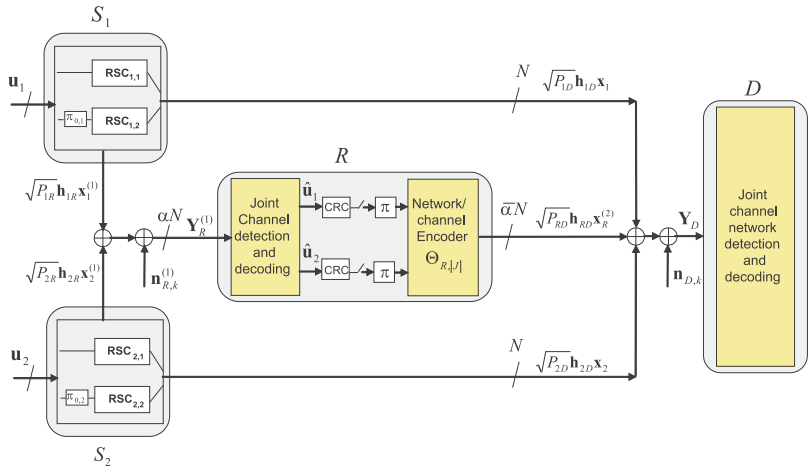

Figure 3.1: System model (relay cooperates)

codebook. The block diagram of the system model is depicted in Fig. 3.1 for the case of $M = 2$.

- SNCC: the relay sums the correctly decoded messages using XOR (or the addition in $\mathbb{F}_2$). The resulting vector $\mathbf{u}_R \in \mathbb{F}_2^K$ is then mapped to $\mathbf{x}_R$ using the codebook ζ_R of rate $K/\bar{\alpha}N$.

In the rest of the chapter, for the sake of notational simplicity, we consider $M = 2$ sources that transmit with an overall spectral efficiency $r = K/N$. For the specific case of SNCC, we can associate the same spectral efficiency r to the relay transmission. The generalization to the cases of $M > 2$ sources is straightforward.

3.2 Information-theoretic Analysis

The NOMARC breaks down into two MACs at the relay and destination corresponding to the first transmission phase, and one MAC at the destination corresponding to the second phase thanks to the SDF relaying function. Thus, its outage region is perfectly known conditional on a given channel state $\mathbf{H} = \begin{bmatrix} \mathbf{h}_{1R} & \mathbf{h}_{2R} & \mathbf{h}_{1D} & \mathbf{h}_{2D} & \mathbf{h}_{RD} \end{bmatrix}$. Let us define the independent input random variables $x_1^{(1)} \sim p(x_1^{(1)})$, $x_1^{(2)} \sim p(x_1^{(2)})$, $x_2^{(1)} \sim p(x_2^{(1)})$, $x_2^{(2)} \sim p(x_2^{(2)})$, and $x_R^{(2)} \sim p(x_R^{(2)})$ and the associated independent output random vectors $\mathbf{y}_D^{(1)}$, $\mathbf{y}_D^{(2)}$ and $\mathbf{y}_R^{(1)}$ whose channel transition conditional pdfs follows the ones associated to (3.2), (3.3) and (3.1), respectively. It follows that the mutual informations $I(x_1^{(1)}, x_2^{(1)}; \mathbf{y}_D^{(1)})$, $I(x_1^{(2)}, x_2^{(2)}, x_R^{(2)}; \mathbf{y}_D^{(2)})$ and $I(x_1^{(1)}, x_2^{(1)}; \mathbf{y}_R^{(1)})$ are perfectly defined by the pdfs $p(x_1^{(1)})$, $p(x_1^{(2)})$, $p(x_2^{(1)})$, $p(x_2^{(2)})$, $p(x_R^{(2)})$ and the aforementioned channel transition probabilities. It is clear

from our context that the mutual information conditional on any given channel state is maximized for the pdfs $p(x_1^{(1)})$, $p(x_1^{(2)})$, $p(x_2^{(1)})$, $p(x_2^{(2)})$, $p(x_R^{(2)})$ being circularly symmetric complex Gaussian pdfs. As a result, the latter pdfs minimize the information outage probabilities. However, in practice, $p(x_1^{(1)})$, $p(x_1^{(2)})$, $p(x_2^{(1)})$, $p(x_2^{(2)})$, $p(x_R^{(2)})$ are uniformly distributed pmfs (dirac comb pdfs) over the chosen constellation alphabets. That is why both cases are investigated in the following. We recall that in our analysis:

1. The theoretical bounds are derived conditional on both JNCC and SNCC.

2. The SDF relaying function is used under the hypothesis that all the links are prone to errors.

3. The sequences $\mathbf{x}_1^{(1)}$, $\mathbf{x}_1^{(2)}$, $\mathbf{x}_2^{(1)}$, $\mathbf{x}_2^{(2)}$, and $\mathbf{x}_R^{(2)}$ are the outcomes of independent discrete time i.i.d. processes whose associated pdfs are $p(x_1^{(1)})$, $p(x_1^{(2)})$, $p(x_2^{(1)})$, $p(x_2^{(2)})$, $p(x_R^{(2)})$ and their respective length is infinite ($N \to \infty$) such that the AEP holds.

4. The outage limit is either the individual information outage probability or the individual ϵ-outage achievable rate (e.g., for S_1). The efficiency of our proposed JNCC/JNCD is evaluated in terms of gap to the information outage probability, keeping in mind that the information outage probability remains a relevant measure of the best possible BLER even for finite code lengths [119].

3.2.1 Outage analysis of NOMARC/JNCC

As the relay uses a SDF approach, an evaluation of the source-to-relay channel quality has first to be processed. Let $\mathcal{E}_R(\mathbf{H})$ denote the outage event of the source-to-relay MAC conditional on $\mathbf{H}$. It corresponds to the case where the relay cannot decode both messages correctly, and can be expressed as

$$\mathcal{E}_R(\mathbf{H}) = \mathcal{E}_{R,1|2}(\mathbf{H}) \cup \mathcal{E}_{R,2|1}(\mathbf{H}) \cup \mathcal{E}_{R,1,2}(\mathbf{H}) \tag{3.5}$$

where $\mathcal{E}_{R,i|j}(\mathbf{H})$, $i,j \in \{1,2\}$, $j \neq i$ is the outage event of S_i if the information of S_j is known, and $\mathcal{E}_{R,1,2}(\mathbf{H})$ is the outage event of both sources at the relay. The three possible outage events are then given by

$$\mathcal{E}_{R,i|j}(\mathbf{H}) = \left\{ \alpha I(x_i^{(1)}; \mathbf{y}_R^{(1)} \mid x_j^{(1)}) < r \right\} \tag{3.6}$$

$$\mathcal{E}_{R,1,2}(\mathbf{H}) = \left\{ \alpha I(x_1^{(1)}, x_2^{(1)}; \mathbf{y}_R^{(1)}) < 2r \right\} \tag{3.7}$$

When the outage event $\mathcal{E}_R(\mathbf{H})$ holds, in order to verify whether only one of the messages $\mathbf{x}_i^{(1)}$ can be successfully decoded or not, we define the following outage event

$$\mathcal{E}_{R,i}(\mathbf{H}) = \left\{\alpha I(x_i^{(1)}; \mathbf{y}_R^{(1)}) < r\right\} \tag{3.8}$$

in which the relay treats the signal $\mathbf{x}_j^{(1)}$ as interference. Thus, the relay outage events for the SDF approach can be summarized as follows: (1) In case of $\mathcal{Q}_R^{(1)}(\mathbf{H}) = \bar{\mathcal{E}}_R(\mathbf{H})$, which indicates the complement of the outage event $\mathcal{E}_R(\mathbf{H})$, the relay cooperates with both sources; (2) In case of $\mathcal{Q}_R^{(2)}(\mathbf{H}) = \mathcal{E}_R(\mathbf{H}) \cap \bar{\mathcal{E}}_{R,1}(\mathbf{H})$ the relay cooperates only with S_1; (3) In case of $\mathcal{Q}_R^{(3)}(\mathbf{H}) = \mathcal{E}_R(\mathbf{H}) \cap \bar{\mathcal{E}}_{R,2}(\mathbf{H})$ the relay cooperates only with S_2; (4) Otherwise, in case of $\mathcal{Q}_R^{(4)}(\mathbf{H}) = \mathcal{E}_R(\mathbf{H}) \cap \mathcal{E}_{R,1}(\mathbf{H}) \cap \mathcal{E}_{R,2}(\mathbf{H})$ the relay does not cooperate. Now, depending on the relay transmission, we distinguish four outage events at the destination:

Case 1: The relay cooperates with both sources. The destination always receives the cooperative information from the relay during the second phase. Since the source-to-destination and the source-and-relay-to-destination MACs are non-interfering, they can be seen as two parallel MACs[1]. As a result, the outage at the destination occurs if the target rate exceeds the sum of the mutual informations of the two parallel MACs. Let $\mathcal{E}_D^{(1)}(\mathbf{H})$ denote the outage event at the destination conditional on $\mathbf{H}$. It can be expressed as

$$\mathcal{E}_D^{(1)}(\mathbf{H}) = \mathcal{E}_{D,1|2}^{(1)}(\mathbf{H}) \cup \mathcal{E}_{D,2|1}^{(1)}(\mathbf{H}) \cup \mathcal{E}_{D,1,2}^{(1)}(\mathbf{H}). \tag{3.9}$$

where

$$\mathcal{E}_{D,i|j}^{(1)}(\mathbf{H}) = \left\{\alpha I(x_i^{(1)}; \mathbf{y}_D^{(1)} \mid x_j^{(1)}) + \bar{\alpha} I(\widetilde{\mathbf{x}}_i^{(2)}; \widetilde{\mathbf{y}}_D^{(2)} \mid x_j^{(2)}) < r\right\} \tag{3.10}$$

for $i, j \in \{1, 2\}$ and $j \neq i$, and

$$\mathcal{E}_{D,1,2}^{(1)}(\mathbf{H}) = \left\{\alpha I(x_1^{(1)}, x_2^{(1)}; \mathbf{y}_D^{(1)}) + \bar{\alpha} I(x_1^{(2)}, x_2^{(2)}, x_R^{(2)}; \mathbf{y}_D^{(2)}) < 2r\right\}. \tag{3.11}$$

In (3.10), $\mathcal{E}_{D,i|j}^{(1)}(\mathbf{H})$, $i \in \{1, 2\}$ is the outage event of S_i if the information of S_j, $j \neq i$, is known, i.e., $x_j^{(1)}$ and $x_j^{(2)}$ are both known. In this case, $\mathbf{x}_R^{(2)}$ can be considered as a part of the codeword corresponding to S_i. Typically, this is the case when $\mathbf{x}_R^{(2)}$ is a codeword representing the XOR of the two source messages. Since the signals of S_i and the relay are independent (thanks to the JNCC interleaver π), the second term of the sum in (3.10) can

[1]Note that, on the other hand, their respective channel statistics are highly correlated, i.e., the source-to-destination channels remain static during the two transmission phases.

be derived from the equivalent MIMO channel

$$\tilde{\mathbf{y}}_D^{(2)} = \widetilde{\mathbf{H}}_i \, \mathbf{K}_i \, \widetilde{\mathbf{x}}_i^{(2)} + \mathbf{n}_D^{(2)} \tag{3.12}$$

where $\widetilde{\mathbf{y}}_D^{(2)} = \mathbf{y}_D^{(2)} - \sqrt{P_{jD}}\mathbf{h}_{jD}x_j^{(2)}$, $\widetilde{\mathbf{x}}_i^{(2)} = \left[x_i^{(2)} \; x_R^{(2)}\right]^\top$, $\widetilde{\mathbf{H}}_i = [\mathbf{h}_{iD} \; \mathbf{h}_{RD}]$, and $\mathbf{K}_i = \text{diag}(\sqrt{P_{iD}}, \sqrt{P_{RD}})$. The outage event in (3.11) corresponds to the constraint that the total throughput cannot exceed the sum of the mutual information of (1) a point-to-point MIMO channel with the aggregate received signals of the two sources which corresponds to the first phase, and (2) a point-to-point MIMO channel with the aggregate received signals of the two sources and the relay which corresponds to the second phase. When $\mathcal{E}_D^{(1)}(\mathbf{H})$ holds, the destination cannot decode both source messages correctly. As we are interested in calculating the outage event of S_1, we define the following event

$$\mathcal{E}_{D,1}^{(1)}(\mathbf{H}) = \left\{\alpha I(x_1^{(1)}; \mathbf{y}_D^{(1)}) + \bar{\alpha} I(x_1^{(2)}; \mathbf{y}_D^{(2)}) < r\right\} \tag{3.13}$$

in which the destination treats the signals $\mathbf{x}_2^{(1)}$, $\mathbf{x}_2^{(2)}$ and $\mathbf{x}_R^{(2)}$ as interferences. It is worth noting that the relay transmission in this case cannot help S_1 as it contains the interference from S_2. Finally, the outage event of S_1 is calculated as $\mathcal{O}_{D,1}^{(1)}(\mathbf{H}) = \mathcal{E}_D^{(1)}(\mathbf{H}) \cap \mathcal{E}_{D,1}^{(1)}(\mathbf{H})$.

Case 2: The relay cooperates with S_1. The outage event at the destination $\mathcal{E}_D^{(2)}(\mathbf{H})$ is calculated as

$$\mathcal{E}_D^{(2)}(\mathbf{H}) = \mathcal{E}_{D,1|2}^{(2)}(\mathbf{H}) \cup \mathcal{E}_{D,2|1}^{(2)}(\mathbf{H}) \cup \mathcal{E}_{D,1,2}^{(2)}(\mathbf{H}). \tag{3.14}$$

where

$$\mathcal{E}_{D,1|2}^{(2)}(\mathbf{H}) = \left\{\alpha I(x_1^{(1)}; \mathbf{y}_D^{(1)} \mid x_2^{(1)}) + \bar{\alpha} I(\widetilde{\mathbf{x}}_1^{(2)}; \widetilde{\mathbf{y}}_D^{(2)} \mid x_2^{(2)}) < r\right\} \tag{3.15}$$

$$\mathcal{E}_{D,2|1}^{(2)}(\mathbf{H}) = \left\{\alpha I(x_2^{(1)}; \mathbf{y}_D^{(1)} \mid x_1^{(1)}) + \bar{\alpha} I(x_2^{(2)}; \mathbf{y}_D^{(2)} \mid x_1^{(2)}, x_R^{(2)}) < r\right\} \tag{3.16}$$

$$\mathcal{E}_{D,1,2}^{(2)}(\mathbf{H}) = \left\{\alpha I(x_1^{(1)}, x_2^{(1)}; \mathbf{y}_D^{(1)}) + \bar{\alpha} I(x_1^{(2)}, x_2^{(2)}, x_R^{(2)}; \mathbf{y}_D^{(2)}) < 2r\right\} \tag{3.17}$$

In (3.15), $\widetilde{\mathbf{y}}_D^{(2)} = \mathbf{y}_D^{(2)} - \sqrt{P_{2D}}\mathbf{h}_{2D}x_2^{(2)}$, $\widetilde{\mathbf{x}}_1^{(2)} = \left[x_1^{(2)} \; x_R^{(2)}\right]^\top$, and the second term of the sum is deduced from an equivalent MIMO channel as in (3.12) with $i = 1$ and $j = 2$. Note that in (3.16), since the information of S_1 is supposed to be known and the relay cooperates only with S_1, the relay transmitted signal is known as well. Thus, there is no interference on the signal transmitted by S_2 during both transmission phases. Now, in order to calculate

the outage event of S_1, we define the following event

$$\mathcal{E}_{D,1}^{(2)}(\mathbf{H}) = \left\{ \alpha I(x_1^{(1)}; \mathbf{y}_D^{(1)}) + \bar{\alpha} I(\widetilde{\mathbf{x}}_1^{(2)}; \mathbf{y}_D^{(2)}) < r \right\} \tag{3.18}$$

in which the destination treats the signals $\mathbf{x}_2^{(1)}$ and $\mathbf{x}_2^{(2)}$ as interferences during the first and second transmission phases. The second term of the sum is deduced from the equivalent MIMO channel

$$\mathbf{y}_D^{(2)} = \widetilde{\mathbf{H}}_1 \mathbf{K}_1 \widetilde{\mathbf{x}}_1^{(2)} + \mathbf{n}_{eq}^{(2)} \tag{3.19}$$

where $\mathbf{n}_{eq}^{(2)} = \sqrt{P_{2D}}\mathbf{h}_{2D} x_2^{(2)} + \mathbf{n}_D^{(2)}$, $\widetilde{\mathbf{x}}_1^{(2)} = \left[x_1^{(2)} \; x_R^{(2)} \right]^\top$, $\widetilde{\mathbf{H}}_1 = [\mathbf{h}_{1D} \; \mathbf{h}_{RD}]$, and $\mathbf{K}_1 = \text{diag}(\sqrt{P_{1D}}, \sqrt{P_{RD}})$. Finally, the outage event of S_1 is calculated as $\mathcal{O}_{D,1}^{(2)}(\mathbf{H}) = \mathcal{E}_D^{(2)}(\mathbf{H}) \cap \mathcal{E}_{D,1}^{(2)}(\mathbf{H})$.

Case 3: The relay cooperates with S_2. Swapping the roles of S_1 and S_2, the outage event at the destination $\mathcal{E}_D^{(3)}(\mathbf{H})$ is identical to the previous case. In order to calculate the outage event of the source S_1, we define the event $\mathcal{E}_{D,1}^{(3)}(\mathbf{H})$ as in (3.13). Thus, the outage event of S_1 is calculated as $\mathcal{O}_{D,1}^{(3)}(\mathbf{H}) = \mathcal{E}_D^{(3)}(\mathbf{H}) \cap \mathcal{E}_{D,1}^{(3)}(\mathbf{H})$.

Case 4: The relay does not cooperate. The outage at the destination $\mathcal{E}_D^{(4)}(\mathbf{H})$ occurs if the target rate exceeds the sum of the mutual informations of the two parallel MACs. It yields

$$\mathcal{E}_D^{(4)}(\mathbf{H}) = \mathcal{E}_{D,1|2}^{(4)}(\mathbf{H}) \cup \mathcal{E}_{D,2|1}^{(4)}(\mathbf{H}) \cup \mathcal{E}_{D,1,2}^{(4)}(\mathbf{H}). \tag{3.20}$$

where

$$\mathcal{E}_{D,i|j}^{(4)}(\mathbf{H}) = \left\{ \alpha I(x_i^{(1)}; \mathbf{y}_D^{(1)} \mid x_j^{(1)}) + \bar{\alpha} I(x_i^{(2)}; \mathbf{y}_D^{(2)} \mid x_j^{(2)}) < r \right\} \tag{3.21}$$

for $i, j \in \{1, 2\}$ and $j \neq i$, and

$$\mathcal{E}_{D,1,2}^{(4)}(\mathbf{H}) = \left\{ \alpha I(x_1^{(1)}, x_2^{(1)}; \mathbf{y}_D^{(1)}) + \bar{\alpha} I(x_1^{(2)}, x_2^{(2)}; \mathbf{y}_D^{(2)}) < 2r \right\}. \tag{3.22}$$

The outage event of S_1 is then $\mathcal{O}_{D,1}^{(4)}(\mathbf{H}) = \mathcal{E}_D^{(4)}(\mathbf{H}) \cap \mathcal{E}_{D,1}^{(4)}(\mathbf{H})$, where $\mathcal{E}_{D,1}^{(4)}(\mathbf{H})$ is calculated as in (3.13) without the interference from the relay.

Finally, the outage event of S_1 for NOMARC based on JNCC, can be expressed as

$$\mathcal{O}_{D,1}(\mathbf{H}) = \bigcup_{i=1}^{4} \left(\mathcal{Q}_R^{(i)}(\mathbf{H}) \cap \mathcal{O}_{D,1}^{(i)}(\mathbf{H}) \right). \tag{3.23}$$

The above outage event is conditional on the channel state $\mathbf{H}$. The information outage

probability for S_1 is then obtained as

$$P_{out,1} = \int_{\mathbf{H}} [\mathcal{O}_{D,1}(\mathbf{H})] \;\; p(\mathbf{H}) d(\mathbf{H}) \tag{3.24}$$

where $p(\mathbf{H})$ is the pdf of $\mathbf{H}$. The ϵ-outage achievable rate of S_1 is defined as the largest rate of S_1 such that its corresponding information outage probability for a given transmission protocol, is smaller than or equal to ϵ.

3.2.2 Outage analysis of NOMARC/SNCC

In the case of SNCC/SNCD, we still have two MACs at the relay and destination corresponding to the first time slot, and one MAC at the destination corresponding to the second time slot. The outage event analysis at the relay remains the same as in (3.2.1). However, the SNCD strategy imposes a separate decoding of the relay and the sources. Thus, we end up with a three user MAC when the relay transmits.

Case 1: The relay cooperates with both sources. The source signals transmitted during the second phase are decoded jointly with those transmitted during the first phase, and the relay signal is decoded separately. If the message of S_1 cannot be correctly decoded, it can be recovered, provided that the destination can decode successfully the message of S_2 and the relay message during the second time slot (thanks to the Separate Network Coding). Let $S = \{1, 2, R\}$ stand for the set of transmitted signals with 1 for S_1, 2 for S_2, R for the relay. For simplicity, we adopt the convention that R is an index greater than 2. Let the overall three user MAC outage event conditional on $\mathbf{H}$ be $\mathcal{E}_D^{(1)}(\mathbf{H})$, it can be expressed as:

$$\mathcal{E}_D^{(1)}(\mathbf{H}) = \bigcup_{\forall\, \mathcal{I} \subset S} \mathcal{E}_{D,\, \mathcal{I}|\mathcal{I}^c}^{(1)}(\mathbf{H}) \tag{3.25}$$

where $\mathcal{I}^c$ the complement of the subset $\mathcal{I}$ in S. Clearly, $\mathcal{E}_{D,\mathcal{I}|\mathcal{I}^c}^{(1)}(\mathbf{H})$, for all $\mathcal{I} \subset S$, is the outage event of the transmit signals of subset $\mathcal{I}$ conditional to the perfect knowledge of the signals of subset $\mathcal{I}^c$. As a result, it yields

$$\mathcal{E}_{D,i|j,R}^{(1)}(\mathbf{H}) = \left\{ \alpha I(x_i^{(1)}; \mathbf{y}_D^{(1)} \mid x_j^{(1)}) + \bar{\alpha} I(x_i^{(2)}; \mathbf{y}_D^{(2)} \mid x_j^{(2)}, x_R^{(2)}) < r \right\} \tag{3.26}$$

$$\mathcal{E}_{D,i,R|j}^{(1)}(\mathbf{H}) = \left\{ \alpha I(x_i^{(1)}; \mathbf{y}_D^{(1)} \mid x_j^{(1)}) + \bar{\alpha} I(x_i^{(2)}, x_R^{(2)}; \mathbf{y}_D^{(2)} \mid x_j^{(2)}) < 2r \right\} \tag{3.27}$$

for $i, j \in \{1, 2\}$, $i \neq j$, and

$$\mathcal{E}^{(1)}_{D,R|1,2}(\mathbf{H}) = \left\{\bar{\alpha} I(x_R^{(2)}; \mathbf{y}_D^{(2)} \mid x_1^{(2)}, x_2^{(2)}) < r\right\} \tag{3.28}$$

$$\mathcal{E}^{(1)}_{D,1,2|R}(\mathbf{H}) = \left\{\alpha I(x_1^{(1)}, x_2^{(1)}; \mathbf{y}_D^{(1)}) + \bar{\alpha} I(x_1^{(2)}, x_2^{(2)}; \mathbf{y}_D^{(2)} \mid x_R^{(2)}) < 2r\right\} \tag{3.29}$$

$$\mathcal{E}^{(1)}_{D,1,2,R}(\mathbf{H}) = \left\{\alpha I(x_1^{(1)}, x_2^{(1)}; \mathbf{y}_D^{(1)}) + \bar{\alpha} I(x_1^{(2)}, x_2^{(2)}, x_R^{(2)}; \mathbf{y}_D^{(2)}) < 3r\right\}. \tag{3.30}$$

In the case that $\mathcal{E}^{(1)}_D(\mathbf{H})$ holds, the destination cannot decode all the three messages correctly. Thus, in order to calculate the outage event of S_1, we need to check the possibility of decoding error-free two messages out of three, considering the third one as interference. The corresponding outage events are derived in the sequel for each case.

- Treating $\mathbf{x}_R^{(2)}$ as interference:

$$\mathcal{E}^{(1)}_{D,1-2}(\mathbf{H}) = \mathcal{E}^{(1)}_{D,1|2}(\mathbf{H}) \cup \mathcal{E}^{(1)}_{D,2|1}(\mathbf{H}) \cup \mathcal{E}^{(1)}_{D,1,2}(\mathbf{H}) \tag{3.31}$$

  with

$$\mathcal{E}^{(1)}_{D,i|j}(\mathbf{H}) = \left\{\alpha I(x_i^{(1)}; \mathbf{y}_D^{(1)} \mid x_j^{(1)}) + \bar{\alpha} I(x_i^{(2)}; \mathbf{y}_D^{(2)} \mid x_j^{(2)}) < r\right\} \tag{3.32}$$

  for $i, j \in \{1, 2\}$, $i \neq j$, and

$$\mathcal{E}^{(1)}_{D,1,2}(\mathbf{H}) = \left\{\alpha I(x_1^{(1)}, x_2^{(1)}; \mathbf{y}_D^{(1)}) + \bar{\alpha} I(x_1^{(2)}, x_2^{(2)}; \mathbf{y}_D^{(2)}) < 2r\right\}. \tag{3.33}$$

- Treating $\mathbf{x}_j^{(1)}$ and $\mathbf{x}_j^{(2)}$, $j \in \{1, 2\}$ as interferences:

$$\mathcal{E}^{(1)}_{D,i-R}(\mathbf{H}) = \mathcal{E}^{(1)}_{D,i|R}(\mathbf{H}) \cup \mathcal{E}^{(1)}_{D,R|i}(\mathbf{H}) \cup \mathcal{E}^{(1)}_{D,i,R}(\mathbf{H}) \tag{3.34}$$

  for $i \in \{1, 2\}$, $i \neq j$, and with

$$\mathcal{E}^{(1)}_{D,i|R}(\mathbf{H}) = \left\{\alpha I(x_i^{(1)}; \mathbf{y}_D^{(1)}) + \bar{\alpha} I(x_i^{(2)}; \mathbf{y}_D^{(2)} \mid x_R^{(2)}) < r\right\} \tag{3.35}$$

$$\mathcal{E}^{(1)}_{D,R|i}(\mathbf{H}) = \left\{\bar{\alpha} I(x_R^{(2)}; \mathbf{y}_D^{(2)} \mid x_i^{(2)}) < r\right\} \tag{3.36}$$

$$\mathcal{E}^{(1)}_{D,i,R}(\mathbf{H}) = \left\{\alpha I(x_i^{(1)}; \mathbf{y}_D^{(1)}) + \bar{\alpha} I(x_i^{(2)}, x_R^{(2)}; \mathbf{y}_D^{(2)}) < 2r\right\}. \tag{3.37}$$

Finally, assuming that the outage events in (3.25), (3.31), and (3.34) hold, the message of S_1 is in outage if it can not be decoded correctly considering $\mathbf{x}_2^{(1)}$, $\mathbf{x}_2^{(2)}$ and $\mathbf{x}_R^{(2)}$ as interferences. We denote by $\mathcal{E}_{D,1}^{(1)}(\mathbf{H})$ the corresponding outage event which is given in (3.13). Finally, the outage event of S_1 is calculated as

$$\mathcal{O}_{D,1}^{(1)}(\mathbf{H}) = \left(\mathcal{E}_D^{(1)}(\mathbf{H}) \cap \left(\bigcap_{\substack{(i,j)\in S^2 \\ i<j}} \mathcal{E}_{D,i-j}^{(1)}(\mathbf{H}) \right) \cap \mathcal{E}_{D,1}^{(1)}(\mathbf{H}) \right). \tag{3.38}$$

Case 2: The relay cooperates with S_1. All the definitions of the outage events do no change, they are simply obtained by replacing the superscript $^{(1)}$ by $^{(2)}$. On the other hand, we need to define the following outage event $\mathcal{E}_{D,R}^{(2)}(\mathbf{H})$ that is expressed as

$$\mathcal{E}_{D,R}^{(2)}(\mathbf{H}) = \left\{ \bar{\alpha} I(x_R^{(2)}; \mathbf{y}_D^{(2)}) < r \right\} \tag{3.39}$$

considering $\mathbf{x}_1^{(2)}$ and $\mathbf{x}_2^{(2)}$ as interferences. Finally, the outage event of S_1 is calculated as:

$$\mathcal{O}_{D,1}^{(2)}(\mathbf{H}) = \left(\mathcal{E}_D^{(2)}(\mathbf{H}) \cap \left(\bigcap_{\substack{(i,j)\in S^2 \\ i<j}} \mathcal{E}_{D,i-j}^{(2)}(\mathbf{H}) \right) \cap \mathcal{E}_{D,1}^{(2)}(\mathbf{H}) \cap \mathcal{E}_{D,R}^{(2)}(\mathbf{H}) \right). \tag{3.40}$$

Case 3: The relay cooperates with S_2. We use the same approach as in Case 2. We should just take into account that, if the message of S_2 is decoded successfully, the interference of it could be removed during both transmission phases. Thus, the outage event of S_1 can be expressed as

$$\begin{aligned} \mathcal{O}_{D,1}^{(3)}(\mathbf{H}) \;=\; & \left(\mathcal{E}_D^{(3)}(\mathbf{H}) \cap \mathcal{E}_{D,1-2}^{(3)}(\mathbf{H}) \cap \mathcal{E}_{D,1-R}^{(3)}(\mathbf{H}) \cap \bar{\mathcal{E}}_{D,2-R}^{(3)}(\mathbf{H}) \cap \mathcal{E}_{D,1|2,R}^{(3)}(\mathbf{H}) \right) \cup \\ & \left(\mathcal{E}_D^{(3)}(\mathbf{H}) \cap \left(\bigcap_{\substack{(i,j)\in S^2 \\ i<j}} \mathcal{E}_{D,i-j}^{(3)}(\mathbf{H}) \right) \cap (\mathcal{A} \cup \mathcal{B} \cup \mathcal{C}) \right) \end{aligned} \tag{3.41}$$

where

$$\begin{aligned}\mathcal{A} &= \mathcal{E}_{D,1}^{(3)}(\mathbf{H}) \cap \mathcal{E}_{D,2}^{(3)}(\mathbf{H}) \cap \mathcal{E}_{D,R}^{(3)}(\mathbf{H}) \\ \mathcal{B} &= \mathcal{E}_{D,1}^{(3)}(\mathbf{H}) \cap \bar{\mathcal{E}}_{D,2}^{(3)}(\mathbf{H}) \cap \mathcal{E}_{D,R}^{(3)}(\mathbf{H}) \cap \mathcal{E}_{D,1|2,R}^{(3)}(\mathbf{H}) \\ \mathcal{C} &= \mathcal{E}_{D,1}^{(3)}(\mathbf{H}) \cap \mathcal{E}_{D,2}^{(3)}(\mathbf{H}) \cap \bar{\mathcal{E}}_{D,R}^{(3)}(\mathbf{H}) \cap \mathcal{E}_{D,1|2,R}^{(3)}(\mathbf{H}). \end{aligned} \tag{3.42}$$

Case 4: The relay does not cooperate. The outage event of S_1 is denoted by $\mathcal{O}_{D,1}^{(4)}(\mathbf{H})$, and is calculated as explained in Case 4 of section (3.2.1).

Finally, the outage event of S_1 in the error-prone NOMARC/SNCC can be expressed as

$$\mathcal{O}_{D,1}(\mathbf{H}) = \bigcup_{i=1}^{4} \left(\mathcal{Q}_R^{(i)}(\mathbf{H}) \cap \mathcal{O}_{D,1}^{(i)}(\mathbf{H}) \right). \tag{3.43}$$

Here again, the outage event $\mathcal{O}_{D,1}(\mathbf{H})$ is conditional on the channel state $\mathbf{H}$, and the information outage probability for S_1 is derived as

$$P_{out,1} = \int_{\mathbf{H}} [\mathcal{O}_{D,1}(\mathbf{H})] \;\; p(\mathbf{H}) d(\mathbf{H}). \tag{3.44}$$

3.2.3 Types of input distributions

We consider both Gaussian i.i.d. inputs and discrete i.i.d. inputs (for practical considerations as explained in Chapter 2) to calculate the mutual information. The corresponding expressions are given in Appendix B.

3.2.4 Information outage probability achieving codebooks

To achieve the information outage probability bounds, the codebooks ζ_1, ζ_2, $\zeta_1^{(1)}$, $\zeta_2^{(1)}$,ζ_{1R}, ζ_{2R} and ζ_{12R} should be universal codebooks. As defined in [127], a universal codebook of a given rate is a codebook that simultaneously achieves reliable communication over every channel that is not in outage for the chosen rate. Finally, it is worth stressing that, in practice, there exist codebooks with finite lengths whose performance are very close to the ones of universal codebooks. The simulation Section 3.5 examplifies such codebook constructions based on convolutional or turbo codes.

3.3 Joint Network Channel Coding and Decoding

In this section, we make explicit our proposed JNCC/JNCD approach. We explain the structure of the encoders, when and how JNCC is performed, and the structure of the corresponding multiuser receivers.

3.3.1 Coding at the sources

The messages of the two sources are binary vectors $\mathbf{u}_1 \in \mathbb{F}_2^K$ and $\mathbf{u}_2 \in \mathbb{F}_2^K$ of length K. Each source employs a BICM [128]. Binary vectors are first encoded with linear binary encoders $C_i : \mathbb{F}_2^K \to \mathbb{F}_2^{n_i}$, $i \in \{1,2\}$ into binary codewords $\mathbf{c}_1 \in \mathbb{F}_2^{n_1}$ and $\mathbf{c}_2 \in \mathbb{F}_2^{n_2}$ of respective lengths n_1 and n_2. The codes ζ_1 and ζ_2 are turbo codes. Each turbo code consists of two RSC encoders, concatenated in parallel using optimized semi-random interleavers $\pi_{0,1}$ and $\pi_{0,2}$. Let $\text{RSC}_{i,1}$ and $\text{RSC}_{i,2}$ denote the two RSC encoders of ζ_i, $i \in \{1,2\}$, defined by the generator matrices $\mathbf{G}_{i,1}(D)$ and $\mathbf{G}_{i,2}(D)$. Let $\mathbf{A}_i \in \mathbb{F}_2^{3\times P}$ denote the puncturing matrix associated to ζ_i, with P the puncturing period, and $a_{i;j,\ell} \in \{0,1\}$ where 0 implies puncturing. We assume that $\forall \ell = 1,\ldots,P$, $a_{i;1,\ell} = 1$ which means that the systematic bits are not punctured. Let also $\bar{\mathbf{A}}_i$ denote the complement of $\mathbf{A}_i$, i.e., $\bar{\mathbf{A}}_i + \mathbf{A}_i$ is a matrix filled with 1. The coded bits $\mathbf{c}_i$ are first punctured following the puncturing matrix $\mathbf{A}_i$. The resulting bits are then bit-interleaved using the interleavers $\Pi_i^{(1)}$ and reshaped as binary matrices $\mathbf{V}_i^{(1)} \in \mathbb{F}_2^{\alpha N \times q_i}$. Memoryless modulators based on one-to-one binary labeling maps $\phi_i : \mathbb{F}_2^{q_i} \to \mathscr{X}_i$ transform the binary arrays $\mathbf{V}_i^{(1)}$ into the complex vectors $\mathbf{x}_i^{(1)} \in \mathscr{X}_i^{\alpha N}$. For ϕ_i, we choose Gray labeling. For the second transmission phase, the coded bits that are punctured during the first phase (or equivalently, the coded bits $\mathbf{c}_i$ that are punctured following the puncturing matrix $\bar{\mathbf{A}}_i$) are bit-interleaved using the interleavers $\Pi_i^{(2)}$ and reshaped as two binary matrices $\mathbf{V}_i^{(2)} \in \mathbb{F}_2^{\bar{\alpha} N \times q_i}$. The same memoryless modulators based on labeling maps ϕ_i transform the binary arrays $\mathbf{V}_i^{(2)}$ into the complex vectors $\mathbf{x}_i^{(2)} \in \mathscr{X}_i^{\bar{\alpha} N}$. In the sequel, we denote by $v_{i,k,\ell}^{(\tau)} = \phi_{i,\ell}^{-1}(x_{i,k}^{(\tau)})$, $\tau \in \{1,2\}$, the ℓ-th bit of the binary labeling of each symbol $x_{i,k}^{(\tau)}$, $i \in \{1,2\}$, with $k = 1,\cdots,\alpha N$ for $\tau = 1$, and $k = 1,\cdots,\bar{\alpha} N$ for $\tau = 2$.

3.3.2 Relaying Function

Relay processing is divided into two steps: During the first time slot, based on (3.1), the relay performs a joint detection and decoding procedure to obtain the hard binary estimation of the information bits, $\hat{\mathbf{u}}_i \in \mathbb{F}_2^K$. Based on this estimation, the relay chooses a SDF approach for cooperation. Different cases can then be distinguished, depending on the number of successfully decoded messages. In the sequel, first, we briefly describe the relay detection and decoding algorithm, and then, we detail our proposed JNCC scheme.

3.3.2.1 Relay detection and decoding

The joint detection and decoding is performed in a suboptimal iterative way [129]. An inner SISO MAP detector generates extrinsic information on coded bits using the received signal (3.1) and a priori information coming from the outer SISO decoders SISO_1 and SISO_2 (referring to the decoding of ζ_1 and ζ_2). For the general case, the outer SISO decoder of S_i generates extrinsic information on both systematic and coded bits of S_i by activating the SISO decoder $\text{SISO}_{i,1}$ corresponding to $\text{RSC}_{i,1}$, and then $\text{SISO}_{i,2}$ corresponding to $\text{RSC}_{i,2}$. It is important to remember that each SISO decoding stage takes into account all the available a priori information on systematic bits [130] (and Algorithm 2 of Section 3.3.3.2). The extrinsic information on both source codewords is then interleaved and fed back to the detector, which in turn employs it as a priori information for the next iteration. It is worth noting that the proper (de)multiplexing and (de)puncturing are also performed if needed. The process is repeated until convergence. For the representation of the input/output soft information, we use log ratios of probabilities. The LAPPR on bit $v_{i,k,\ell}^{(1)} = \phi_{i,\ell}^{-1}(x_{i,k}^{(1)})$ delivered by the SISO MAP detector is defined as

$$\Lambda(v_{i,k,\ell}^{(1)}) = \log \frac{P(v_{i,k,\ell}^{(1)} = 1 | \mathbf{y}_{R,k}^{(1)})}{P(v_{i,k,\ell}^{(1)} = 0 | \mathbf{y}_{R,k}^{(1)})} \tag{3.45}$$

and, in practice, evaluated as

$$\Lambda(v_{i,k,\ell}^{(1)}) \simeq \log \frac{\sum_{a \in \mathscr{X}_i : \phi_{i,\ell}^{-1}(a)=1, b \in \mathscr{X}_j} P(\mathbf{y}_{R,k}^{(1)} | x_{i,k}^{(1)} = a, x_{j,k}^{(1)} = b) e^{\xi(a)+\xi(b)}}{\sum_{a \in \mathscr{X}_i : \phi_{i,\ell}^{-1}(a)=0, b \in \mathscr{X}_j} P(\mathbf{y}_{R,k}^{(1)} | x_{i,k}^{(1)} = a, x_{j,k}^{(1)} = b) e^{\xi(a)+\xi(b)}} \tag{3.46}$$

for $i, j \in \{1, 2\}, i \neq j$, with,

$$\xi(a) = \sum_{\ell'=1}^{\log_2 |\mathscr{X}_i|} \phi_{i,\ell'}^{-1}(a) E(v_{i,k,\ell'}^{(1)}) \tag{3.47}$$

$$\xi(b) = \sum_{\ell'=1}^{\log_2 |\mathscr{X}_j|} \phi_{j,\ell'}^{-1}(b) E(v_{j,k,\ell'}^{(1)}) \tag{3.48}$$

where $\{E(v_{i,k,\ell}^{(1)})\}$ and $\{E(v_{j,k,\ell}^{(1)})\}$ are LAPRs on bits $v_{i,k,\ell}^{(1)}$ and $v_{j,k,\ell}^{(1)}$ provided by the SISO decoders SISO_1 and SISO_2. The extrinsic information on bit $v_{i,k,\ell}^{(1)}$ is given by $L(v_{i,k,\ell}^{(1)}) = \Lambda(v_{i,k,\ell}^{(1)}) - E(v_{i,k,\ell}^{(1)})$, and after de-interleaving, feeds the corresponding outer SISO decoder.

3.3.2.2 JNCC

As previously mentioned, the relay chooses a SDF approach for cooperation, which is based on the number of successfully decoded messages, the knowledge of which being ensured by using CRC codes for each source message. Let $J = \{j_1, \ldots, j_{|J|}\}$, $|J| \leq 2$ denote the set of message indices that have been successfully decoded. For the case where $J = \emptyset$, the relay does not cooperate. Otherwise, it combines all the correctly decoded messages by XOR, i.e., $\mathbf{u}_R = \mathbf{u}_{j_1} \oplus \ldots \oplus \mathbf{u}_{j_{|J|}}$, and interleaves the resulting vector by π. Interestingly, the interleaver commutes with the XOR. The interleaved vector is then encoded to $\mathbf{c}_R$ using a binary linear encoder $C_R : \mathbb{F}_2^K \to \mathbb{F}_2^{n_R}$. For C_R, we choose an RSC encoder defined by the generator matrix $G_R(D)$, referred to as RSC_R. A linear transformation $\Omega : \mathbb{F}_2^{n_R} \to \mathbb{F}_2^{n'_R}$ is applied which selects the parity bits of $\mathbf{c}_R$ to obtain the new vector $\mathbf{c}'_R \in \mathbb{F}_2^{n_R}$, $n'_R < n_R$. The vector $\mathbf{c}'_R$ is bit-interleaved using the interleaver $\Pi_R^{(2)}$ and reshaped as a binary matrix $\mathbf{V}_R^{(2)} \in \mathbb{F}_2^{\bar{\alpha}N \times q_R}$. Finally, a memoryless modulator based on a one-to-one binary labeling map $\phi_R : \mathbb{F}_2^{q_R} \to \mathscr{X}_R$ transforms the binary array $\mathbf{V}_R^{(2)}$ into the complex vector $\mathbf{x}_R^{(2)} \in \mathscr{X}_R^{\bar{\alpha}N}$. For ϕ_R, we choose Gray labeling. In the sequel, we denote by $v_{R,k,\ell}^{(2)} = \phi_{R,\ell}^{-1}(x_{R,k}^{(2)})$ the ℓ-th bit of the binary labeling of each symbol $x_{R,k}^{(2)}$ for and $k = 1, \cdots, \bar{\alpha}N$. Finally, to let the destination detect which of the messages are included in the relay signal, the relay transmits side information (additional bits) to indicate its state to the receiver.

The proposed coding scheme which is based on XOR operation, ensures full diversity for the OMARC using SNCC [126] or JNCC [82]. As shown in Appendix A, the high SNR slope of the outage probability of MAC versus SNR (in dB scale), for the critical case of just one receive antenna, is the same as the one of the orthogonal MAC. Thus, the full diversity design for OMARC remains valid when we have collisions at the relay and destination. Furthermore, the proposed design simplifies the decoder structure, and is optimal in terms of diversity and coding gain whatever the memory order of the RSC encoder [131,136,138].

3.3.3 JNCD at the Destination

The JNCD at the destination depends on the side information received from the relay: In case 1, where the relay has successfully decoded both source messages, the combination of the systematic and parity bits of the two sources and of the additional joint network-channel parity bits forwarded by the relay form two distributed turbo codes. In case 2 (case 3), where the relay has successfully decoded the information of S_1 (S_2), one distributed turbo code is formed at the destination corresponding to S_1 (S_2), and a separate turbo decoder corresponding to C_2 (C_1) is used to decode the information of the other source. In these cases, at the end of the second transmission phase, the destination starts to detect and decode the original data, processing the received signals (3.2) and (3.3), with $\theta = 1$ in

(3.3). To accomplish this, we again resort to a suboptimal iterative procedure. Extrinsic information on coded bits circulates between two SISO MAP detectors corresponding to two transmission phases and the outer decoders, while, at the same time, extrinsic information on systematic bits circulates between the SISO decoders of each turbo code. Finally, in case 4, where the relay does not cooperate, the destination applies iterative detection and decoding, processing the received signal (3.2) and (3.3), with $\theta = 0$ in (3.3), and using the two separate turbo decoders corresponding to C_1 and C_2. The destination knows whether the relay transmits or not. This knowledge may come from an in-band dedicated control signal. Otherwise, this knowledge should be learned by means of advanced multiuser detection methods, e.g., [139]. This last topic is out of the scope of this thesis.

3.3.3.1 SISO MAP Detectors

The first SISO MAP detector computes the LAPPR $\Lambda(v_{i,k,\ell}^{(1)})$ with $v_{i,k,\ell}^{(1)} = \phi_{i,\ell}^{-1}(x_{i,k}^{(1)})$, $i \in \{1,2\}$, using the received signal (3.2) and a priori information coming from the outer SISO decoders. Expression is similar to (3.46) substituting $\mathbf{y}_{D,k}^{(1)}$ for $\mathbf{y}_{R,k}^{(1)}$. We now turn to the second SISO MAP detector. If the relay stays silent, the second SISO MAP detector computes the LAPPR $\Lambda(v_{i,k,\ell}^{(2)})$ with $v_{i,k,\ell}^{(2)} = \phi_{i,\ell}^{-1}(x_{i,k}^{(2)})$, $i \in \{1,2\}$, using the received signal (3.3) with $\theta = 0$, and a priori information coming from the turbo decoders corresponding to C_1 and C_2. Expression is similar to (3.46) substituting $\mathbf{y}_{D,k}^{(2)}$ for $\mathbf{y}_{R,k}^{(1)}$. If the relay cooperates (successful selective relaying), the second SISO MAP detector must also deliver soft information on the additional relay parity bits. The LAPPR on bit $v_{R,k,\ell}^{(2)} = \phi_{R,\ell}^{-1}(x_{R,k}^{(2)})$ is defined as

$$\Lambda(v_{R,k,\ell}^{(2)}) = \log \frac{P(v_{R,k,\ell}^{(2)} = 1 | \mathbf{y}_{D,k}^{(2)})}{P(v_{R,k,\ell}^{(2)} = 0 | \mathbf{y}_{D,k}^{(2)})} \tag{3.49}$$

and, in practice, evaluated as

$$\Lambda(v_{R,k,\ell}^{(2)}) \simeq \log \frac{\sum_{c \in \mathscr{X}_R : \phi_{R,\ell}^{-1}(c)=1, a \in \mathscr{X}_1, b \in \mathscr{X}_2} P(\mathbf{y}_{D,k}^{(2)} | x_{1,k}^{(2)} = a, x_{2,k}^{(2)} = b, x_{R,k}^{(2)} = c) e^{\xi(a)+\xi(b)+\xi(c)}}{\sum_{c \in \mathscr{X}_R : \phi_{R,\ell}^{-1}(c)=0, a \in \mathscr{X}_1, b \in \mathscr{X}_2} P(\mathbf{y}_{D,k}^{(2)} | x_{1,k}^{(2)} = a, x_{2,k}^{(2)} = b, x_{R,k}^{(2)} = c) e^{\xi(a)+\xi(b)+\xi(c)}} \tag{3.50}$$

with

$$\xi(a) = \sum_{\ell'=1}^{\log_2 |\mathscr{X}_1|} \phi_{1,\ell'}^{-1}(a) E(v_{1,k,\ell'}^{(2)}) \tag{3.51}$$

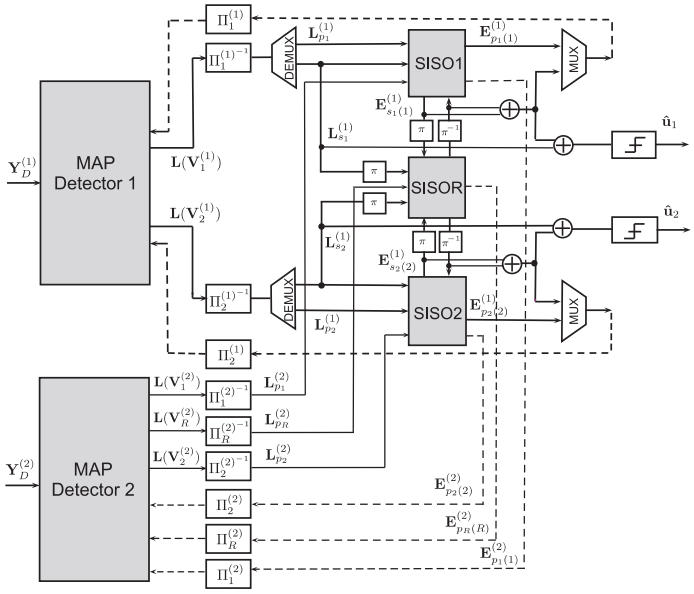

Figure 3.2: JNCD at the destination (relay cooperates with both sources)

where $\{E(v_{1,k,\ell}^{(2)})\}$ is the LAPR on bit $v_{1,k,\ell}^{(2)}$ provided by SISO_1,

$$\xi(b) = \sum_{\ell'=1}^{\log_2|\mathscr{X}_2|} \phi_{2,\ell'}^{-1}(b) E(v_{2,k,\ell'}^{(2)}) \tag{3.52}$$

where $\{E(v_{2,k,\ell}^{(2)})\}$ is the LAPR on bit $v_{2,k,\ell}^{(2)}$ provided by SISO_2, and

$$\xi(c) = \sum_{\ell'=1}^{\log_2|\mathscr{X}_R|} \phi_{R,\ell'}^{-1}(c) E(v_{R,k,\ell'}^{(2)}) \tag{3.53}$$

where $\{E(v_{R,k,\ell}^{(2)})\}$ is the LAPR on bit $v_{R,k,\ell}^{(2)}$ provided by the SISO decoder SISO_R corresponding to the relay joint network-channel encoder (XOR followed by C_R). The LAPPRs $\Lambda(v_{i,k,\ell}^{(2)})$, $i \in \{1,2\}$ are evaluated in the same manner. The extrinsic information on $v_{1,k,\ell}^{(2)}$ is given by $L(v_{1,k,\ell}^{(2)}) = \Lambda(v_{1,k,\ell}^{(2)}) - E(v_{1,k,\ell}^{(2)})$ and, after de-interleaving, feeds SISO_1. The extrinsic information on $v_{2,k,\ell}^{(2)}$ is given by $L(v_{2,k,\ell}^{(2)}) = \Lambda(v_{2,k,\ell}^{(2)}) - E(v_{2,k,\ell}^{(2)})$ and, after de-interleaving, feeds SISO_2. The extrinsic information on $v_{R,k,\ell}^{(2)}$ is given by $L(v_{R,k,\ell}^{(2)}) = \Lambda(v_{R,k,\ell}^{(2)}) - E(v_{R,k,\ell}^{(2)})$ and, after de-interleaving, feeds SISO_R.

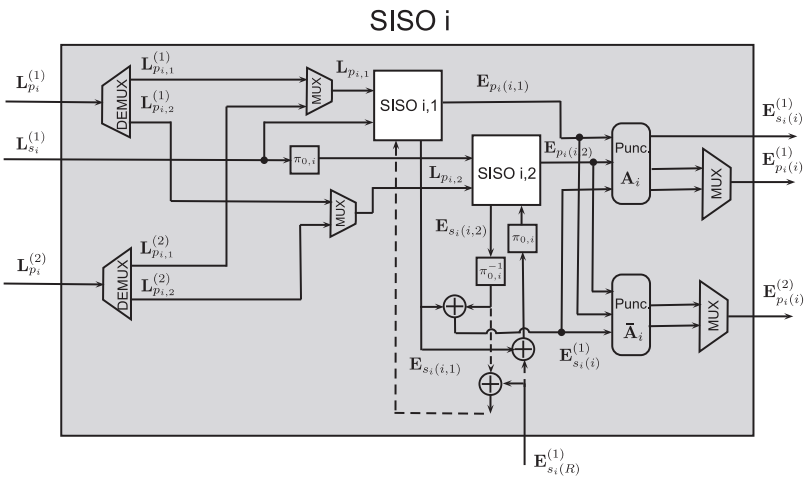

Figure 3.3: SISO decoder SISO_i

3.3.3.2 Message-Passing Schedule

A recapitulative block diagram of the JNCD is depicted in Fig. 3.2. In this paragraph, we detail the message-passing for the case where the relay cooperates with both sources. The SISO decoder SISO_i corresponds to C_i, $i \in \{1,2\}$, and SISO_R corresponds to the relay encoder (XOR followed by C_R) which is viewed as a systematic encoder on the two source messages [131]. Each SISO_i, $i \in \{1,2\}$, is made up of the two SISO decoders $\text{SISO}_{i,1}$ and $\text{SISO}_{i,2}$. Let $\mathbf{L}_{s_i}^{(\tau)}$, $\mathbf{L}_{p_i}^{(\tau)}$, $i \in \{1,2,R\}$ and $\tau \in \{1,2\}$, denote the soft information of the systematic and parity bits of transmitter i obtained from the activation of SISO MAP detector τ (related to transmission phase τ). We now come to description of the SISO_i, $i \in \{1,2\}$ inputs and outputs. Let denote by $\mathbf{L}_{p_{i,1}}^{(\tau)}$, $\mathbf{L}_{p_{i,2}}^{(\tau)}$ the soft information of the parity bits transmitted during phase τ related to $\text{SISO}_{i,1}$ and $\text{SISO}_{i,2}$. These soft information are derived from $\mathbf{L}_{p_i}^{(\tau)}$ after proper demultiplexing as depicted in Fig. 3.3. Following the puncturing pattern $\mathbf{A}_i$, $\mathbf{L}_{p_{i,1}}^{(1)}$ and $\mathbf{L}_{p_{i,1}}^{(2)}$ are multiplexed to form the parity bits soft information $\mathbf{L}_{p_{i,1}}$ corresponding to $\text{SISO}_{i,1}$. The same operation is carried out on $\mathbf{L}_{p_{i,2}}^{(1)}$ and $\mathbf{L}_{p_{i,2}}^{(2)}$ to obtain $\mathbf{L}_{p_{i,2}}$. After the activation of $\text{SISO}_{i,1}$ and $\text{SISO}_{i,2}$, two extrinsic information on the systematic bits corresponding to C_i are available, namely, $\mathbf{E}_{s_i(i,1)}$ and $\mathbf{E}_{s_i(i,2)}$. They are summed up after proper (re)-interleaving of $\mathbf{E}_{s_i(i,2)}$ to get the total extrinsic information $\mathbf{E}_{s_i(i)}^{(1)} = \mathbf{E}_{s_i(i,1)} + \pi_{0,i}^{-1}(\mathbf{E}_{s_i(i,2)})$ as depicted in Fig. 3.3. It is important to stress that the systematic bits are not punctured and belongs to the first transmission phase. On the other hand, the two extrinsic information on parity bits $\mathbf{E}_{p_i(i,1)}$ and $\mathbf{E}_{p_i(i,1)}$, obtained from $\text{SISO}_{i,1}$ and $\text{SISO}_{i,2}$, respectively, need to be punctured and multiplexed to obtain the extrinsic information on the parity bits corresponding to the transmission phases

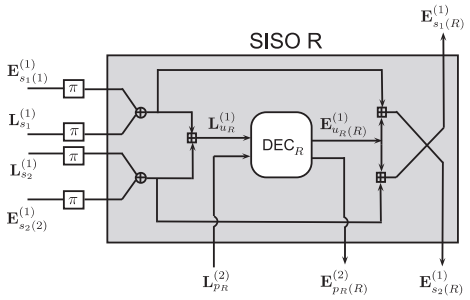

Figure 3.4: XOR decoder

1 and 2. More specifically, applying the puncturing pattern $\mathbf{A}_i$ on $\left[\mathbf{E}^{(1)\top}_{s_i(i)}\ \mathbf{E}^{\top}_{p_i(i,1)}\ \mathbf{E}^{\top}_{p_i(i,2)}\right]^{\top}$ followed by multiplexing, it yields $\mathbf{E}^{(1)}_{s_i(i)}$ and $\mathbf{E}^{(1)}_{p_i(i)}$ which is the extrinsic information on the parity bits related to the first transmission phase. Similarly, by applying $\bar{\mathbf{A}}_i$ followed by multiplexing, it yields $\mathbf{E}^{(2)}_{p_i(i)}$ which is the extrinsic information on the parity bits related to the second transmission phase. Finally, we define $\mathbf{E}^{(1)}_{s_i(R)}$ and $\mathbf{E}^{(2)}_{p_R(R)}$ as the extrinsic information on the systematic and parity bits generated by SISO$_R$, respectively. We now have defined all the messages involved in our message passing schedule. The first SISO MAP detector generates the LAPPRs for the systematic and parity bits in $\mathbf{V}^{(1)}_1$ using $\mathbf{E}^{(1)}_{s_1(1)}+\pi^{-1}(\mathbf{E}^{(1)}_{s_1(R)})$ and $\mathbf{E}^{(1)}_{p_1(1)}$, respectively (after proper multiplexing interleaving). It also generates the LAPPRs for the systematic and parity bits in $\mathbf{V}^{(1)}_2$ using $\mathbf{E}^{(1)}_{s_2(2)}+\pi^{-1}(\mathbf{E}^{(1)}_{s_2(R)})$ and $\mathbf{E}^{(1)}_{p_2(2)}$, respectively. The second MAP detector generates the LAPPRs for the parity bits in $\mathbf{V}^{(2)}_1$ using $\mathbf{E}^{(2)}_{p_1(1)}$, for the parity bits in $\mathbf{V}^{(2)}_2$ using $\mathbf{E}^{(2)}_{p_2(2)}$, and for the parity bits in $\mathbf{V}^{(2)}_R$ using $\mathbf{E}^{(2)}_{p_R(R)}$ (after proper interleaving). Then, the two distributed turbo decoders are activated and calculate the extrinsic information for both the systematic and parity bits which are fed back to the SISO MAP detectors. Let us now detail the decoding of SISO$_R$ which is depicted in Fig. 3.4. The SISO decoder corresponding to C_R (DEC$_R$) must collect all the a priori information $\mathbf{L}^{(1)}_{u_R}$ on $\mathbf{u}_R$. Denoting $\mathbf{L}^{(1)}_1 = \pi(\mathbf{L}^{(1)}_{s_1} + \mathbf{E}^{(1)}_{s_1(1)})$ and $\mathbf{L}^{(1)}_2 = \pi(\mathbf{L}^{(1)}_{s_2} + \mathbf{E}^{(1)}_{s_2(2)})$, it yields, taking into account the XOR constraint node (see, e.g., [132]),

$$L^{(1)}_{u_R,k} = L^{(1)}_{1,k} \boxplus L^{(1)}_{2,k} = \log \frac{e^{L^{(1)}_{1,k}} + e^{L^{(1)}_{2,k}}}{1 + e^{(L^{(1)}_{1,k}+L^{(1)}_{2,k})}}. \tag{3.54}$$

Note, that the independence between the messages should hold in order to apply (3.54). Finally, the SISO$_R$ computes at its output, the extrinsic information $\mathbf{E}^{(1)}_{s_i(R)}$ from $\mathbf{L}^{(1)}_j$ and $\mathbf{E}^{(1)}_{u_R(R)}$, $i,j \in \{1,2\}$, $i \neq j$, where $\mathbf{E}^{(1)}_{u_R(R)}$ is the extrinsic information on $\mathbf{u}_R$ computed by the SISO decoder corresponding to C_R. The message-passing schedule for the JNCD at

each iteration, and the final hard decisions are recapitulated in the Algorithm 2.

Algorithm 2 : JNCD at the destination

(Initialization)
Set all the a priori information to zero.

(Iterations)
Iterate until convergence:

1. Activate the first SISO MAP detector using the received signal $\mathbf{Y}_D^{(1)}$ and the messages $\mathbf{E}_{s_1(1)}^{(1)} + \pi^{-1}(\mathbf{E}_{s_1(R)}^{(1)})$, $\mathbf{E}_{p_1(1)}^{(1)}$ and $\mathbf{E}_{s_2(2)}^{(1)} + \pi^{-1}(\mathbf{E}_{s_2(R)}^{(1)})$, $\mathbf{E}_{p_2(2)}^{(1)}$.

2. Activate the second SISO MAP detector using the received signal $\mathbf{Y}_D^{(2)}$ and the messages $\mathbf{E}_{p_1(1)}^{(2)}$, and $\mathbf{E}_{p_2(2)}^{(2)}$, and $\mathbf{E}_{p_R(R)}^{(2)}$.

3. Activate simultaneously the SISO decoders SISO_1 and SISO_2

   (a) Activate simultaneously the $\text{SISO}_{1,1}$ and $\text{SISO}_{2,1}$ with the messages $\mathbf{L}_{s_1}^{(1)}$, $\mathbf{L}_{p_{1,1}}$ and $\mathbf{L}_{s_2}^{(1)}$, $\mathbf{L}_{p_{2,1}}$ provided by the MAP detectors, and $\pi_{0,1}^{-1}(\mathbf{E}_{s_1(1,2)}) + \pi^{-1}(\mathbf{E}_{s_1(R)}^{(1)})$ and $\pi_{0,2}^{-1}(\mathbf{E}_{s_2(2,2)}) + \pi^{-1}(\mathbf{E}_{s_2(R)}^{(1)})$, which are derived from the previous iteration.

   (b) Activate simultaneously the $\text{SISO}_{1,2}$ and $\text{SISO}_{2,2}$ with, respectively, the messages $\pi_{0,1}(\mathbf{L}_{s_1}^{(1)})$, $\mathbf{L}_{p_{1,2}}$ and $\pi_{0,2}(\mathbf{L}_{s_2}^{(1)})$, $\mathbf{L}_{p_{2,2}}$ provided by the MAP detectors, and $\pi_{0,1}(\mathbf{E}_{s_1(1,1)}) + \pi_{0,1} \circ \pi^{-1}(\mathbf{E}_{s_1(R)}^{(1)})$ and $\pi_{0,2}(\mathbf{E}_{s_2(2,1)}) + \pi_{0,2} \circ \pi^{-1}(\mathbf{E}_{s_2(R)}^{(1)})$.

4. Activate the SISO decoder SISO_R with the message $\mathbf{L}_{p_R}^{(2)}$ provided by the second MAP detector, and $\mathbf{L}_1^{(1)} = \pi(\mathbf{L}_{s_1}^{(1)} + \mathbf{E}_{s_1(1)}^{(1)})$ and $\mathbf{L}_2^{(1)} = \pi(\mathbf{L}_{s_2}^{(1)} + \mathbf{E}_{s_2(2)}^{(1)})$.

(Hard decisions)
Combine all available information concerning systematic bits $\mathbf{u}_1$ and $\mathbf{u}_2$:

$$\mathbf{L}_{s_1}^{(1)} + \mathbf{E}_{s_1(1,1)} + \pi_{0,1}^{-1}(\mathbf{E}_{s_1(1,2)}) + \pi^{-1}(\mathbf{E}_{s_1(R)}^{(1)}) \rightarrow \hat{\mathbf{u}}_1$$
$$\mathbf{L}_{s_2}^{(1)} + \mathbf{E}_{s_2(2,1)} + \pi_{0,2}^{-1}(\mathbf{E}_{s_2(2,2)}) + \pi^{-1}(\mathbf{E}_{s_2(R)}^{(1)}) \rightarrow \hat{\mathbf{u}}_2$$

3.4 Separate Network Channel Coding and Decoding

As previously mentioned, the SNCC scheme is based on the XOR operation at the relay, and the network-coded signal is separately decoded at the destination. Thus, in case of NOMARC/SNCC, a joint detection and decoding procedure similar to section (3.3.3) is performed at the destination, with the exception that the SISO_i and SISO_R do not exchange

information. We use the same notations as in section (3.3.3.2), and we further denote by $\mathbf{L}_{c_R}^{(2)}$ and $\mathbf{L}_{s_R}^{(2)}$ the soft information of the coded bits and the systematic bits of the relay generated by the second MAP detector, and by $\mathbf{E}_{c_R(R)}^{(2)}$ and $\mathbf{E}_{s_R(R)}^{(2)}$ the extrinsic information on the coded bits and the systematic bits generated by the SISO decoder corresponding to C_R. For the case where the relay cooperates with both sources, the message-passing schedule for the SNCD at each iteration and the final hard decisions are recapitulated in the Algorithm 3. Finally, the hard decisions of channel decoders are given to the network decoder. If at least two out of three channel output estimates are error-free, the network decoder can retrieve both source messages.

3.5 Numerical Results

In this section, we provide some numerical results to evaluate the effectiveness of our approach. In our comparisons, we consider both NOMARC and OMARC using JNCC or SNCC. We also consider the MAC reference system in which both sources transmit simultaneously to the destination during the available number of channel uses N. We start by detailing the topology of the network. For the sake of simplicity, we consider a symmetric MARC and MAC, i.e., $d_{1R} = d_{2R}$ and $d_{1D} = d_{2D}$. The average energy per available dimension allocated to the two sources is the same, i.e., $P_{0,1} = P_{0,2} = P_0$. We fix the same path loss factor, i.e., $\kappa = 3$, free distance, i.e., $d_0 = 1$ and noise power spectral density, i.e., $N_0 = 1$, for all links. In the case of relay assisted communication schemes, due to the half-duplex nature of the relay, the listening and the transmission time slots of the relay are separated in time. For NOMARC, we have $P_1 = P_2 = P_0$ (since the sources are active during the two transmission phases) and $P_R = P_{0,R}/\bar{\alpha}$. For OMARC, the two sources transmit in consecutive, equal duration, time slots occupying $\alpha N/2$ channel uses while the relay keeps $\bar{\alpha}N$ channel uses. It comes that $P_1 = P_2 = 2P_0/\alpha$ and $P_R = P_{0,R}/\bar{\alpha}$. For MAC, we have again $P_1 = P_2 = P_0$. Let us choose $\alpha = \alpha_0 = 2/3$ and $P_{0,R} = \frac{\bar{\alpha}_0}{\alpha_0} P_0 = 1/2P_0$ as references in order to compare our results with [136]. For simulation purposes, two different configurations are considered: In the first configuration, we fix the number of receive antennas to one both at the relay and destination, i.e., $N_R = N_D = 1$. The geometry is chosen such that $d_{ij} = d$ which yields, taking [136] as a reference, $P_{RD} = \frac{\bar{\alpha}_0}{\bar{\alpha}}\gamma$, $P_{ij} = \alpha_0\gamma$ for NOMARC, $P_{RD} = \frac{\bar{\alpha}_0}{\bar{\alpha}}\gamma$, $P_{ij} = \frac{2\alpha_0}{\alpha}\gamma$ for OMARC, and $P_{iD} = \alpha_0\gamma$ for MAC, $i \in \{1, 2\}$, $j \in \{R, D\}$, where γ is the received SNR per symbol or dimension for $\alpha = 2/3$ in the case of SOMARC [136]. In the second configuration, we increase the number of receive antennas at the destination to 4, i.e., $N_R = 1$ and $N_D = 4$. The geometry is chosen such that $d_{iR} = d_1$ and $d_{iD} = d_{RD} = d$ with $(d_1/d)^{-3} = 100$, $i \in \{1, 2\}$. It yields $P_{iR} = 100\alpha_0\gamma$ (or $\gamma + 20 + 10\log_{10}(\alpha_0)$ in dB), $P_{iD} = \alpha_0\gamma$ and $P_{RD} = \frac{\bar{\alpha}_0}{\bar{\alpha}}\gamma$ for NOMARC which translates

Algorithm 3 : SNCD at the destination

(Initialization)
Set all the a priori information to zero.

(Iterations)
Iterate until convergence:

1. Activate the first SISO MAP detector using the received signal $\mathbf{Y}_D^{(1)}$ and the messages $\mathbf{E}_{s_1(1)}^{(1)}$, $\mathbf{E}_{p_1(1)}^{(1)}$ and $\mathbf{E}_{s_2(2)}^{(1)}$, $\mathbf{E}_{p_2(2)}^{(1)}$.

2. Activate the second SISO MAP detector using the received signal $\mathbf{Y}_D^{(2)}$ and the messages $\mathbf{E}_{p_1(1)}^{(2)}$, and $\mathbf{E}_{p_2(2)}^{(2)}$, and $\mathbf{E}_{c_R(R)}^{(2)}$.

3. Activate simultaneously the SISO decoders SISO_1, SISO_2, and the one corresponding to C_R

   (a) SISO_1 and SISO_2:

      i. Activate simultaneously the $\text{SISO}_{1,1}$ and $\text{SISO}_{2,1}$ with the messages $\mathbf{L}_{s_1}^{(1)}$, $\mathbf{L}_{p_{1,1}}$ and $\mathbf{L}_{s_2}^{(1)}$, $\mathbf{L}_{p_{2,1}}$ provided by the MAP detectors, and $\pi_{0,1}^{-1}(\mathbf{E}_{s_1(1,2)})$ and $\pi_{0,2}^{-1}(\mathbf{E}_{s_2(2,2)})$, which are derived from the previous iteration.

      ii. Activate simultaneously the $\text{SISO}_{1,2}$ and $\text{SISO}_{2,2}$ with, respectively, the messages $\pi_{0,1}(\mathbf{L}_{s_1}^{(1)})$, $\mathbf{L}_{p_{1,2}}$ and $\pi_{0,2}(\mathbf{L}_{s_2}^{(1)})$, $\mathbf{L}_{p_{2,2}}$ provided by the MAP detectors, and $\pi_{0,1}(\mathbf{E}_{s_1(1,1)}^{(1)})$ and $\pi_{0,2}(\mathbf{E}_{s_2(2,1)}^{(1)})$.

   (b) SISO decoder corresponding to C_R: Activate the SISO decoder with $\mathbf{L}_{c_R}^{(2)}$ provided by the second MAP detector (in the case of turbo codes at the relay, this SISO decoder is composed of two inner SISO decoders that should be activated one after another by taking into account all the available a priori information on systematic bits).

(Hard decisions)
Combine all available information concerning systematic bits $\mathbf{u}_1$, $\mathbf{u}_2$, and $\mathbf{u}_R$:

$$\begin{aligned}\mathbf{L}_{s_1}^{(1)} + \mathbf{E}_{s_1(1,1)}^{(1)} + \pi_{0,1}^{-1}(\mathbf{E}_{s_1(1,2)}^{(1)}) &\rightarrow \hat{\mathbf{u}}_1\\ \mathbf{L}_{s_2}^{(1)} + \mathbf{E}_{s_2(2,1)}^{(1)} + \pi_{0,2}^{-1}(\mathbf{E}_{s_2(2,2)}^{(1)}) &\rightarrow \hat{\mathbf{u}}_2\\ \mathbf{L}_{s_R}^{(2)} + \mathbf{E}_{s_R(R)}^{(2)} &\rightarrow \hat{\mathbf{u}}_R\end{aligned}$$

(Network Decoding)
If one out of the two source messages, let's say $\hat{\mathbf{u}}_i$, is detected with errors and $\hat{\mathbf{u}}_R$ is error free, then

$$\mathbf{u}_i = \mathbf{u}_j \oplus \mathbf{u}_R, \ i \neq j$$

into $P_{iR} = \frac{200\alpha_0}{\alpha}\gamma$, $P_{iD} = \frac{2\alpha_0}{\alpha}\gamma$ and $P_{RD} = \frac{\bar{\alpha}_0}{\bar{\alpha}}\gamma$ for OMARC, $i \in \{1, 2\}$. P_{iD} in case of MAC remains unchanged. Each message of the sources has length $K = 1024$ information bits. In our proposed JNCC, the complex signal sets $\mathscr{X}_1$, $\mathscr{X}_2$, and $\mathscr{X}_R$ used in BICM are either QPSK or 16QAM constellation (Gray labeling) and their corresponding sum rates are $\eta = 4/3$ bits per channel use (b./c.u) and $\eta = 8/3$ b./c.u, respectively.

3.5.1 Optimization of the parameter α

In the first set of simulations, we consider the ϵ-outage achievable rate $C_\epsilon(\gamma)$ of S_1 to optimize the parameter α in NOMARC/JNCC, i.e., the fraction of time that the relay should listen. In our analysis, we consider Gaussian i.i.d. inputs and we fix $\epsilon = 10^{-2}$. Both cases of $N_D = 1$ and $N_D = 4$ are also considered. We choose $\alpha = 2/3$ as a reference to calculate the values of P_{ij} and P_{RD}, $i \in \{1, 2\}$, $j \in \{R, D\}$. The corresponding results are depicted in Fig. 3.5 and Fig. 3.6 for the respective cases of $N_D = 1$ and $N_D = 4$. Obviously, the optimum α depends on the overall spectral efficiency of interest. When α is too small, the relay may not be able to decode the messages correctly and thus it does not cooperate with the sources during the second phase. On the other hand, the transmission of the sources during the second phase does not suffer from the interference due to the relay. However, if α is too large, the relay cannot help much to the transmission of the source signals even if it acquires a lot of information during the first phase. The simulation results show that, for the data rates of 0.2 b./c.u and higher in the case of $N_D = 1$, and 0.1 b./c.u and higher in the case of $N_D = 4$, $\alpha = 2/3$ gives the best performance. It is worth noting that this optimum value for α may change for other network topologies and configurations. In the sequel, we fix $\alpha = \alpha_0 = 2/3$ for simulation purposes.

3.5.2 Information-theoretic comparison of the protocols

3.5.2.1 Individual ϵ-outage achievable rate with Gaussian inputs

In the second set of simulations, we consider the ϵ-outage achievable rate of S_1, and we compare the individual ϵ-outage achievable rate $C_\epsilon(\gamma)$ of JNCC and SNCC for the NOMARC and the OMARC. We also compare the individual ϵ-outage achievable rate of the aforementioned schemes with that of the MAC. In our analysis, we fix $\epsilon = 10^{-2}$. The number of receive antennas at the destination is either $N_D = 1$ or $N_D = 4$. The corresponding results are depicted in Fig. 3.7. As we can see, the ϵ-outage achievable rate for the NOMARC is always higher than the ϵ-outage achievable rate for the OMARC regardless of the network channel coding strategy (i.e., JNCC or SNCC); Especially, in the case of $N_D = 4$, JNCC with orthogonal multiple access (OMARC/JNCC) is strictly suboptimal and the

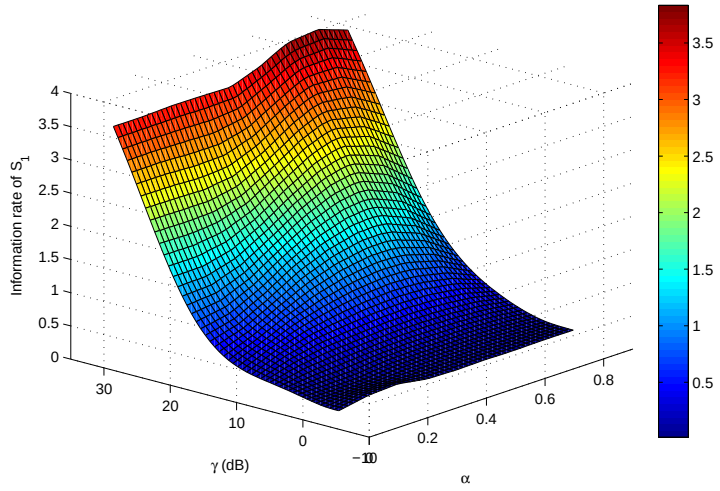

Figure 3.5: Individual ϵ-outage achievable rate for different values of α - $\epsilon = 10^{-2}$ - NOMARC/JNCC - $N_R = 1$, $N_D = 1$

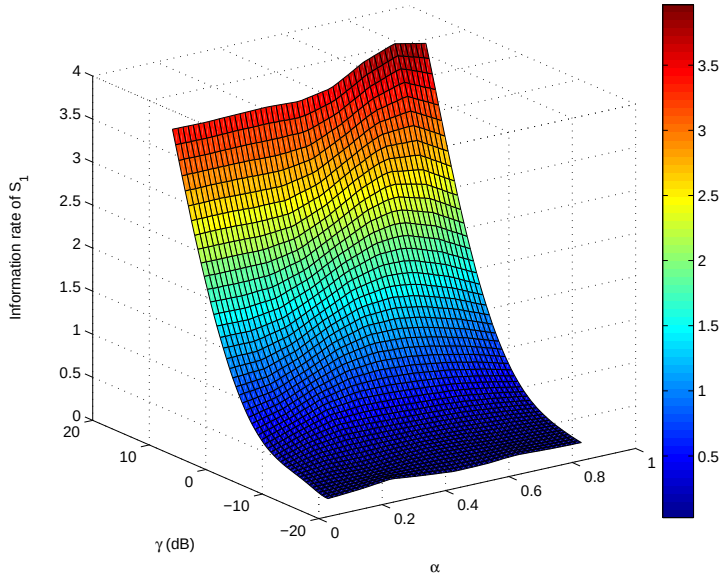

Figure 3.6: Individual ϵ-outage achievable rate for different values of α - $\epsilon = 10^{-2}$ - NOMARC/JNCC - $N_R = 1$, $N_D = 4$

ϵ-outage achievable rate gain of NOMARC/JNCC versus OMARC/JNCC for individual rates above 2b./c.u. is more than 6 dB. This results from the fact that, in the presence of multiple receive antennas, a non-orthogonal MAC can better exploit the available degrees

of freedom. Moreover, even in the case of $N_D = 1$ which is not a priori favorable for a MAC, we see that NOMARC/JNCC can provide an ϵ-outage achievable rate gain of approximately 4 dB for data rates above 2 b./c.u., and more than 6 dB for the data rates above 3 b./c.u.. In Fig. 3.7, we also see that the JNCC schemes outperform the SNCC ones for both transmission protocols. For the data rate of 2 b./c.u., the ϵ-outage achievable rate gains are about 5 dB and 3 dB in case of NOMARC for the respective cases of $N_D = 1$ and $N_D = 4$, 3 dB and 4 dB in case of OMARC with respectively $N_D = 1$ and $N_D = 4$. Finally, it is interesting to see that only NOMARC/JNCC always outperforms MAC. This is not the case for NOMARC/SNCC or OMARC, whose individual ϵ-outage achievable rate becomes lower than that of the MAC, beyond a certain threshold for γ, as can be seen in Fig. 3.7. As our last experiment in this section, we consider the NOMARC/JNCC and we apply a slight modification on the SDF relaying strategy: we assume that the relay transmits only if both source messages are correctly decoded. This approach can possibly reduces the number of interfering signals during the second transmission phase. The corresponding ϵ-outage achievable rate $C_\epsilon(\gamma)$ results are depicted in Fig. 3.7 under the caption of NOMARC/JNCC/Joint selection. As expected, the ϵ-outage achievable rate of NOMARC/JNCC/Joint selection performs very close to that of the NOMARC/JNCC at high SNR. But in the case of $N_D = 1$, and for low data rates and low to medium SNR, it has a loss of around 1 dB with respect to NOMARC/JNCC. The performance gap between the two approaches is less obvious in the case of $N_D = 4$, since the SNRs of source-to-relay links are quite large and the relay decodes both messages correctly almost all the time.

3.5.2.2 Individual information outage probability with discrete inputs

In the third set of simulations, our purpose is first to compare the individual outage probability of NOMARC/JNCC and OMARC/JNCC, and for the fixed sum rates of $\eta = 4/3$ and $\eta = 8/3$ b./c.u.. In order to achieve the same spectral efficiency as the NOMARC, we consider two approaches for OMARC: (1) We impose on the transmitters to use the same input alphabet as in the case of NOMARC, which makes sense if we want to preserve the same level of PAPR; (2) We employ constellation expansion for the sources in OMARC. In the first approach, the two sources have no other choice but to transmit their information symbols without any coding, and thus, from a theoretical perspective ($N \to \infty$), the system is always in outage. In the second approach, the sources increase the cardinality of their modulation while preserving the same spectral efficiency, which makes room for coding. Thus, the information outage probability of NOMARC with QPSK is compared with the information outage probability of OMARC with 16QAM at the sources and QPSK at the relay. Similarly, the the information outage probability of NOMARC with 16QAM

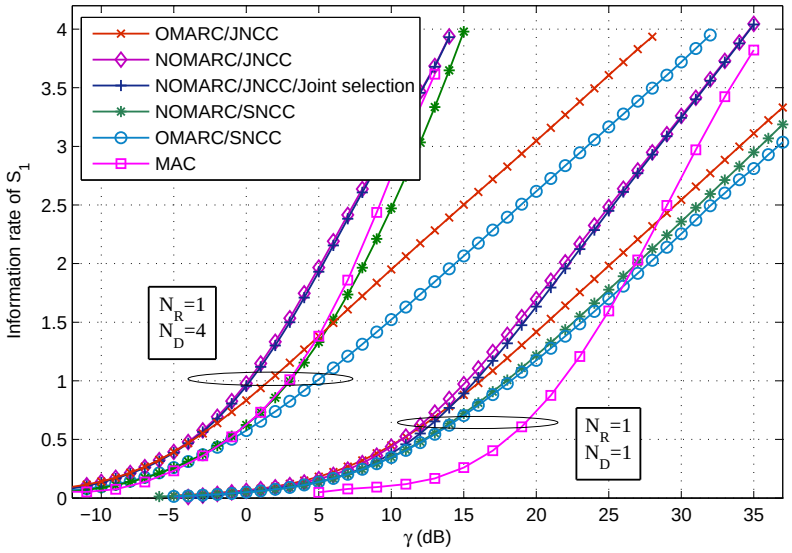

Figure 3.7: Individual ϵ-outage achievable rate - $\epsilon = 10^{-2}$ - NOMARC vs. OMARC - JNCC vs. SNCC

is compared with the the information outage probability of OMARC with 64QAM at the sources and 16QAM at the relay. The corresponding results are depicted in Fig. 3.8 for the sum rate of $\eta = 4/3$ b./c.u. and in Fig. 3.9 for the sum rate of $\eta = 8/3$ b./c.u., for both $N_D = 1$ and $N_D = 4$. As we can see, in all cases, the information outage probability of NOMARC is smaller than the one of OMARC. Considering the second approach, for $\eta = 8/3$ b./c.u., and at the BLER of 10^{-2}, the power gain is approximately equal to 3 dB for $N_D = 1$ and becomes even larger for $N_D = 4$, attaining 4 dB at the BLER of 10^{-2}, which reconfirms the sub-optimality of the orthogonal multiple access in case of multiple receive antennas.

To pursue our analysis, we compare the individual information outage probabilities of NOMARC/JNCC and NOMARC/SNCC. Here again, to keep the same spectral efficiency for the SNCC case, we have the aforementioned two approaches. Using the first approach, the outage events corresponding to the relay-to-destination channel always hold in the case of NOMARC/SNCC. This explains the difference of slopes between the two curves in the corresponding figures. In the second approach, constellation expansion is employed for the relay-to-destination channel. Thus, in NOMARC/SNCC, the relay uses 16QAM for $\eta = 4/3$ b./c.u., and 64QAM for $\eta = 8/3$ b./c.u. The corresponding results are depicted in Fig. 3.10 and Fig. 3.11 for both $N_D = 1$ and $N_D = 4$. As we can see, the NOMARC/SNCC has always a performance loss compared to the NOMARC/JNCC. In the case of constellation

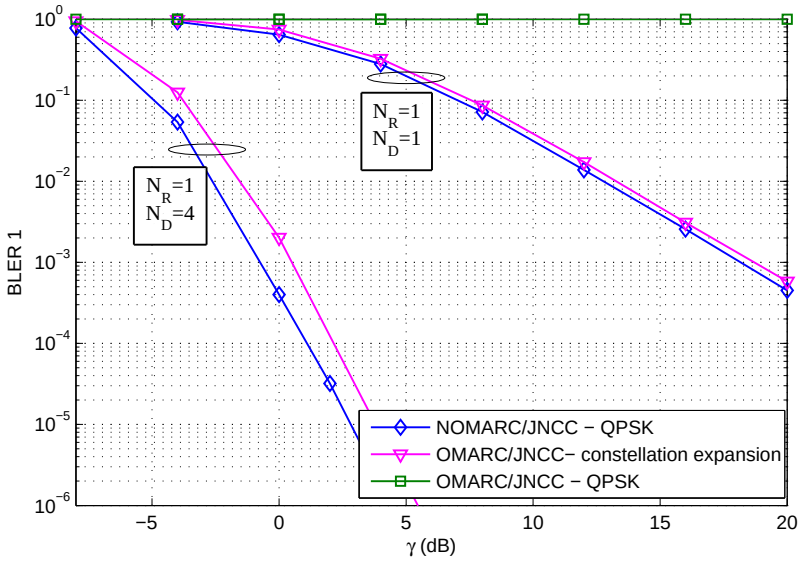

Figure 3.8: Individual outage probability (e.g., for S_1) - NOMARC/JNCC vs. OMARC/JNCC - $\eta = 4/3$ b./c.u.

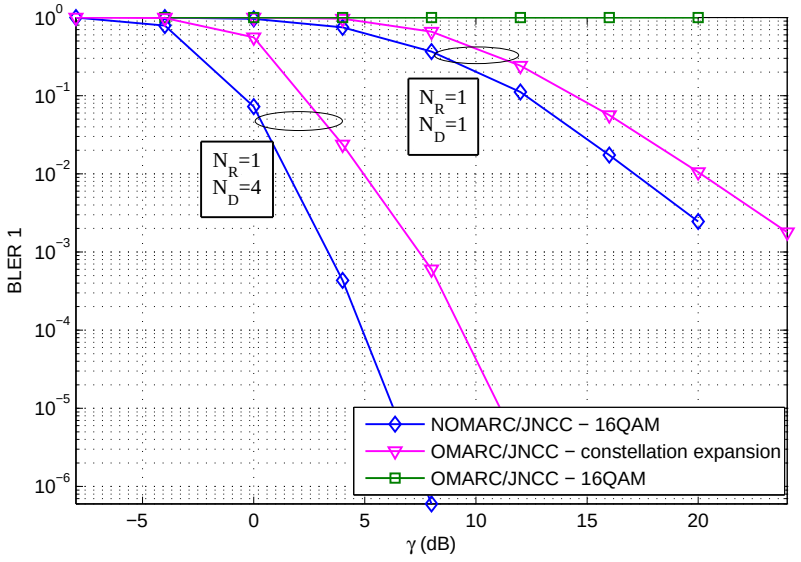

Figure 3.9: Individual outage probability (e.g., for S_1) - NOMARC/JNCC vs. OMARC/JNCC - $\eta = 8/3$ b./c.u.

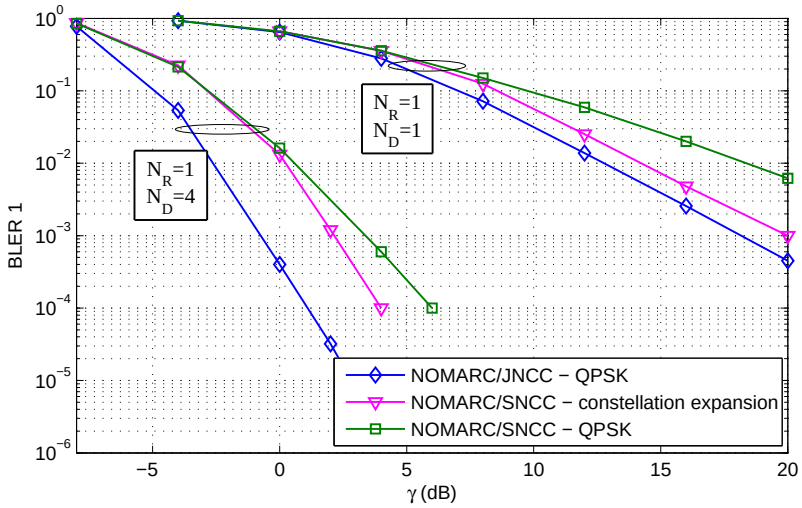

Figure 3.10: Individual outage probability (e.g., for S_1) - NOMARC/JNCC vs. NOMARC/SNCC - $\eta = 4/3$ b./c.u.

expansion and $N_D = 1$, at the BLER of 10^{-2}, the loss is around 1.5 dB for $\eta = 4/3$ b./c.u., and 3 dB for $\eta = 8/3$ b./c.u.. The loss is much higher when we consider $N_D = 4$, attaining 3 dB for $\eta = 4/3$ b./c.u., and 3.5 dB for $\eta = 8/3$ b./c.u..

3.5.3 Performance of practical code design

In the sequel, the number of iterations I is set to 5 at the relay and to 10 (for $N_D = 1$) or 3 (for $N_D = 4$) at the destination. These numbers of iterations ensure convergence and allow to very closely approach the performance of a Genie Aided (GA) receiver at sufficiently high SNR for the selected modulation and coding schemes, the Genie Aided (GA) receiver corresponding to the ideal case where the interference is known and perfectly removed.

3.5.3.1 Gap to outage limits

In this section, we first evaluate the gap between the individual BLER of practical designs for NOMARC/JNCC and that of their corresponding information outage probability. The experiment is carried out for $\eta = 4/3$ b./c.u.. In our comparisons, we assume that both sources use identical turbo codes of rate-1/3 made of two 4-state rate-1/2 RSC encoders with generator matrices $\mathbf{G}_{i,1} = \mathbf{G}_{i,2} = [\ 1 \quad 5/7\ ]$, $i \in \{1, 2\}$, in octal representation. We also consider two different puncturing matrices at the sources: (1) $\mathbf{A}_1 = \mathbf{A}_2 = \begin{bmatrix} 1 & 1 \\ 1 & 0 \\ 0 & 1 \end{bmatrix}$;

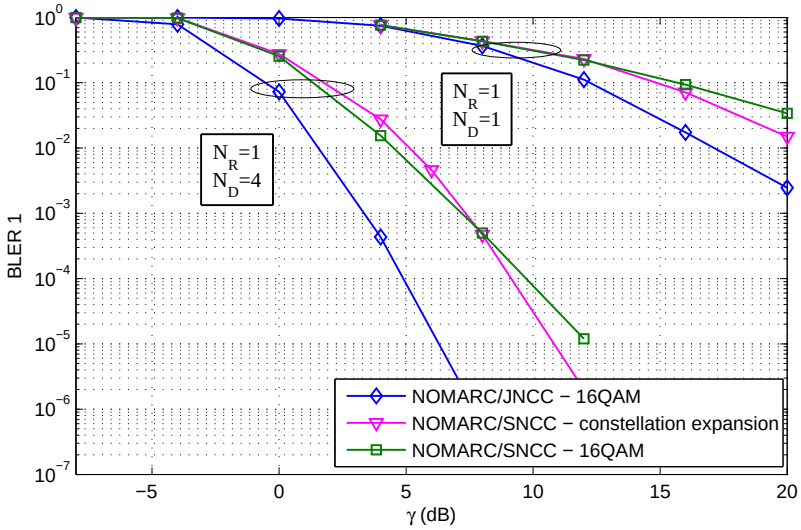

Figure 3.11: Individual outage probability (e.g., for S_1) - NOMARC/JNCC vs. NOMARC/SNCC - $\eta = 8/3$ b./c.u.

(2) $\mathbf{A}_1 = \mathbf{A}_2 = \begin{bmatrix} 1 & 1 \\ 1 & 1 \\ 0 & 0 \end{bmatrix}$. The two coding schemes corresponding to the above puncturing matrices are denoted respectively by TC 1 and TC 2. In both schemes, the JNCC at the relay is based on XOR followed by a 4-state rate-1/2 RSC encoder with generator matrix $\mathbf{G}_R = [\ 1 \quad 5/7\ ]$. Exhaustive simulations showed that those numbers of states yield the best performance/complexity trade-off. The corresponding simulation results are demonstrated in Fig. 3.12. As we can see, the JNCC scheme based on TC 1 provides the lower individual BLER, since it results in a turbo code even during the first transmission phase. Thus, in TC 1, the relay can also benefit from the error correction of the turbo code. The gap between TC 1 and TC 2 is less obvious in the case of $N_D = 4$, which is probably due to the high SNRs of the source-to-relay links. Finally, we see that the JNCC scheme based on TC 1 performs only about 0.5 dB and 2 dB away from the information outage probability for the respective cases of $N_D = 1$ and $N_D = 4$.

Next, we compare the individual BLER of practical designs for NOMARC/SNCC versus their corresponding information outage probability. The experiment is carried out for $\eta = 4/3$ b./c.u. and for the case of TC 1 at both sources. The relay also uses a turbo code of rate-1/2 made of two identical 4-state rate-1/2 RSC encoders with generator matrix $\mathbf{G}_R$, whose half of the parity bits are punctured. The constellation expansion is then performed at the relay. The simulation results are plotted in Fig. 3.13 for both $N_D = 1$ and $N_D = 4$. As we can see, with the chosen coding schemes, the individual BLER of practical design

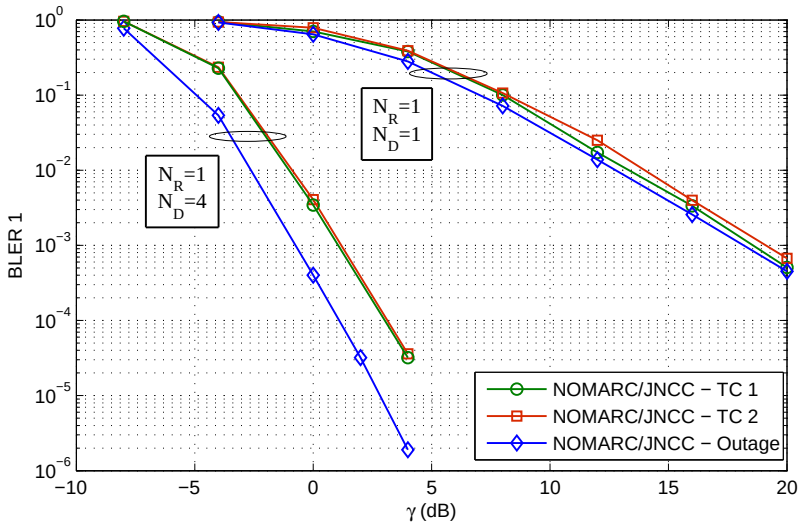

Figure 3.12: Individual BLER (e.g., for S_1) - Practical NOMARC/JNCC vs. outage limit - $\eta = 4/3$ b./c.u.

for NOMARC/SNCC is only about 1 dB and 1.5 dB away from the individual outage probability for the respective cases of $N_D = 1$ and $N_D = 4$.

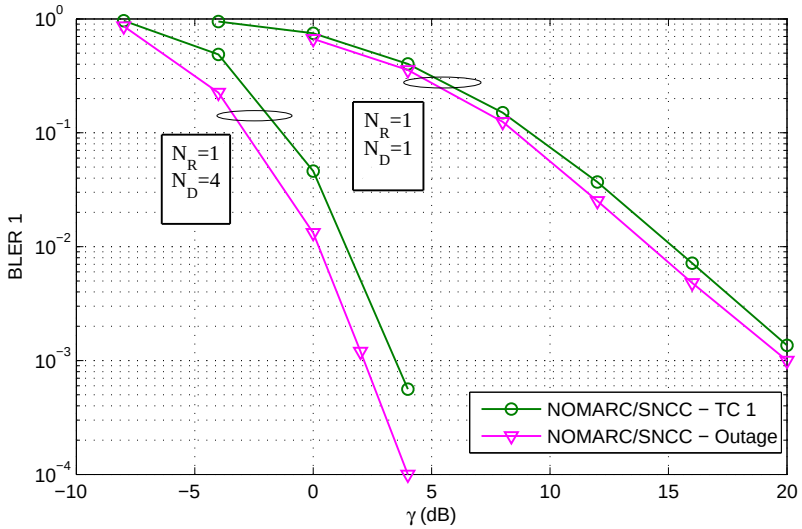

Figure 3.13: Individual BLER (e.g., for S_1) - Practical NOMARC/SNCC vs. outage limit - $\eta = 4/3$ b./c.u. - constellation expansion at the relay

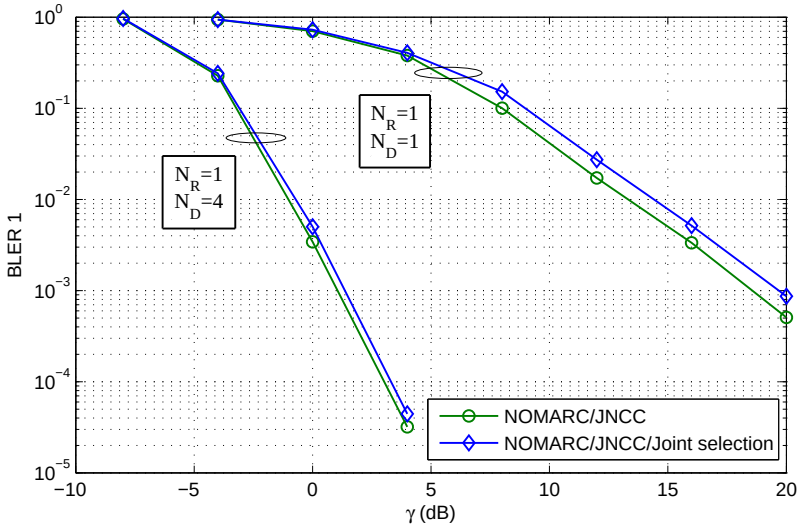

Figure 3.14: Individual BLER (e.g., for S_1) - NOMARC/JNCC vs. NOMARC/JNCC/Joint selection - $\eta = 4/3$ b./c.u.

3.5.3.2 Comparison of the different protocols

In this section, we first compare the individual BLER of practical code design for NOMARC/JNCC with that of the NOMARC/JNCC/Joint selection. In both protocols, the sources use the coding scheme of TC 1 and the relay uses XOR and a 4-state rate-1/2 RSC encoder with generator matrix $\mathbf{G}_R$. The corresponding results are depicted in Fig. 3.14 for the spectral efficiency of $\eta = 4/3$ b./c.u., and in Fig. 3.15 for the spectral efficiency of $\eta = 8/3$ b./c.u., for both $N_D = 1$ and $N_D = 4$. As we can see, in the case of $\eta = 4/3$ b./c.u. and for $N_D = 1$, NOMARC/JNCC outperforms NOMARC/JNCC/Joint selection and the power gain is around 1 dB which is the same as the one predicted by the theoretical bounds for low data rates.

As a second step in our comparisons of practical designs, we compare the individual BLER of NOMARC/JNCC with that of the OMARC/JNCC. For OMARC/JNCC, we first imposed on the sources the use of the same signal sets. In this case, the two sources transmit their information symbols without any coding, while the relay uses the 4-state rate-1/2 RSC encoder with generator matrix $\mathbf{G}_R$. The corresponding results demonstrated considerable gains in favour of our approach. We next carried out another experiment, where constellation expansion is employed for OMARC, as explained in the outage comparisons. Thus, in the case of OMARC with $\eta = 4/3$ b./c.u., both sources use a turbo code of rate-1/2 made of two 4-state rate-1/2 RSC encoders with generator matrices $\mathbf{G}_{i,1}$ and $\mathbf{G}_{i,2}$, $i \in \{1, 2\}$, whose half of the parity bits are punctured. They use then 16QAM

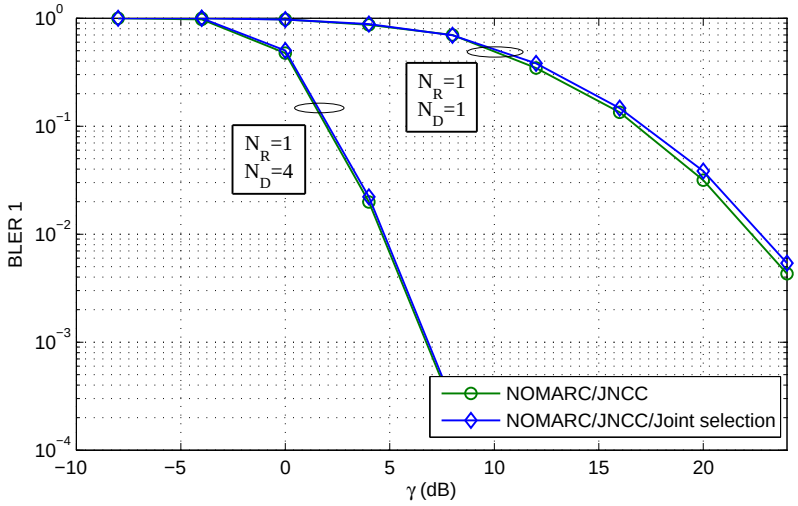

Figure 3.15: Individual BLER (e.g., for S_1) - NOMARC/JNCC vs. NOMARC/JNCC/Joint selection - $\eta = 8/3$ b./c.u.

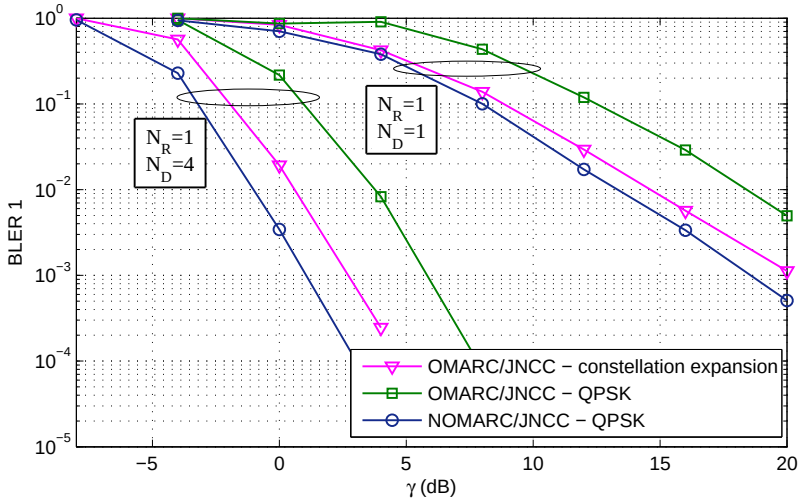

Figure 3.16: Individual BLER (e.g., for S_1) - NOMARC/JNCC vs. OMARC/JNCC - $\eta = 4/3$ b./c.u.

constellation. The relay uses the 4-state rate-1/2 RSC encoder with generator matrix $\mathbf{G}_R$ and it uses QPSK constellation. Similarly, in the case of $\eta = 8/3$ b./c.u., both sources use the same turbo code as the previous case, but with the parity bits that are punctured to result in a code of rate 2/3. They use then 64QAM constellation. The relay uses the same RSC encoder as the previous case with 16QAM modulation. The corresponding results are

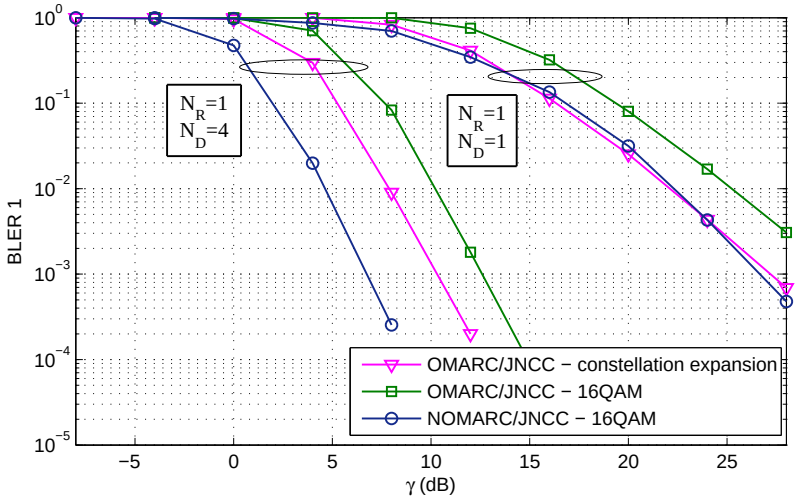

Figure 3.17: Individual BLER (e.g., for S_1) - NOMARC/JNCC vs. OMARC/JNCC - $\eta = 8/3$ b./c.u.

depicted in Fig. 3.16 for the spectral efficiency of $\eta = 4/3$ b./c.u., and in Fig. 3.17 for the spectral efficiency of $\eta = 8/3$ b./c.u., for both $N_D = 1$ and $N_D = 4$. Here again, the NOMARC outperforms the OMARC in most cases and the performance gains are considerable for $N_D = 4$. The exception is the case of $\eta = 8/3$ b./c.u. and for $N_D = 1$, where the NOMARC starts to outperform the OMARC with constellation expansion at a relatively high SNR ($\gamma = 24$ dB).

To pursue our comparison of practical designs, we compare the individual BLERs of NOMARC/JNCC and NOMARC/SNCC. In NOMARC/SNCC, both sources use the coding scheme of TC 1, and the relay, as previously mentioned, has two choices: (1) it uses the same input alphabet as the case of NOMARC/JNCC and transmits its information symbols without any coding; (2) it performs constellation expansion. In case (2), for $\eta = 4/3$ b./c.u., the relay uses a turbo code of rate-1/2 made of two identical 4-state rate-1/2 RSC encoders with generator matrix $\mathbf{G}_R$, whose half of the parity bits are punctured. It uses then 16QAM modulation. For $\eta = 8/3$ b./c.u., the relay uses the same turbo code as the previous case but with the parity bits that are punctured to give the code rate of 2/3. It then uses 64QAM constellation. The corresponding results are depicted in Fig. 3.18 for the spectral efficiency of $\eta = 4/3$ b./c.u., and in Fig. 3.19 for the spectral efficiency of $\eta = 8/3$ b./c.u., for both $N_D = 1$ and $N_D = 4$. As we see, the NOMARC/JNCC outperforms the NOMARC/SNCC, and the power gains are approximately the same as the ones predicted by theoretical bounds.

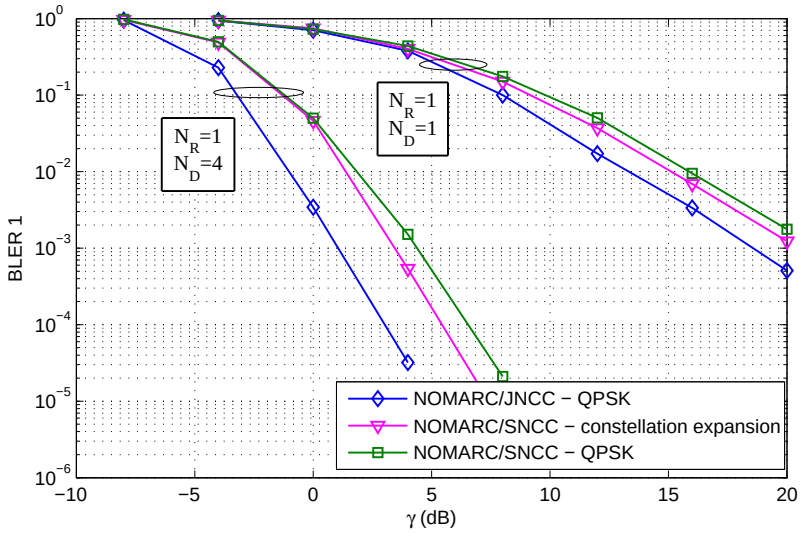

Figure 3.18: Individual BLER (e.g., for S_1) - NOMARC/JNCC vs. NOMARC/SNCC - $\eta = 4/3$ b./c.u.

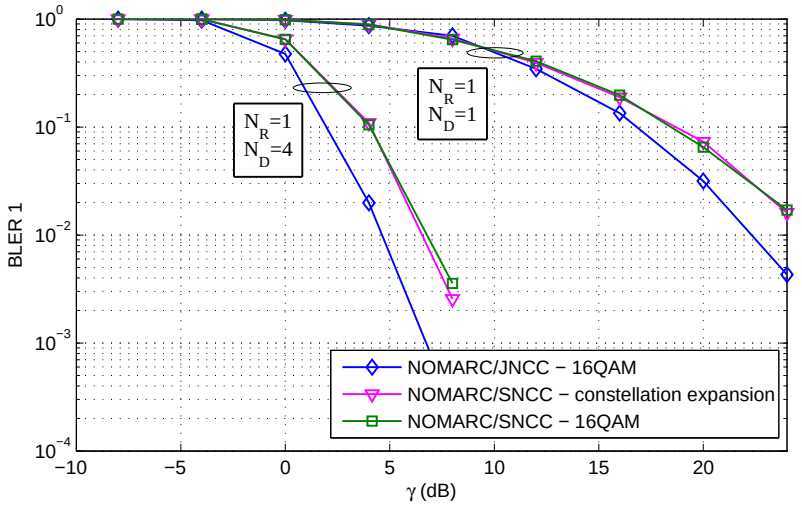

Figure 3.19: Individual BLER (e.g., for S_1) - NOMARC/JNCC vs. NOMARC/SNCC - $\eta = 8/3$ b./c.u.

3.6 Conclusion

We have studied JNCC for a new class of MARC, referred to as NOMARC, from both an information-theoretic and a practical code design perspective. We have derived the NOMARC individual information outage probability, conditional on JNCC (and SNCC

used as a reference). We have also presented new JNCC schemes flexible in terms of number of sources, encoders and modulations. For the 2-source symmetric case and targeted sum rates $\eta = 4/3$ b./c.u. and $\eta = 8/3$ b./c.u., we have shown that our proposed schemes are more efficient than (1) conventional distributed JNCC for OMARC; (2) conventional SNCC schemes. Moreover, the proposed NOMARC/JNCC performs very close to the outage limit (within 2 dB) for both cases of single and multiple receive antennas at the destination, and for the fixed sum rate of $\eta = 4/3$ b./c.u.. We have verified that the non-orthogonal multiple access exhibits considerable gains over orthogonal multiple access, even in the case of a single receive antenna at the destination.

Chapter 4

Joint Network-Channel Coding for the Full-Duplex Non-Orthogonal MARC

In previous chapters, we introduced and analyzed two different classes of MARC with a half-duplex relay. As already mentioned, a full-duplex relay can achieve a higher capacity than its half-duplex counterpart from a theoretical point of view. Besides, full-duplex relays were shown to be feasible recently. This inspires further theoretical analysis and design of practical JNCC schemes for the full-duplex MARC. In this chapter, as a first contribution, we propose a new class of MARC that we call Full-Duplex Non-Orthogonal MARC (FD-NOMARC) and is defined as follows: (1) Independent sources communicate with a single destination in the presence of a relay; (2) The relay is full-duplex and applies a Selective Decode and Forward (SDF) relaying strategy, i.e, it forwards only a deterministic function of the messages that it can decode without errors; (3) The sources and relays are allowed to transmit simultaneously. A new transmission protocol adapted to this class of MARC is proposed which combines several ideas found in [5] [114] [112] [71]. Following [5], we consider superposition block Markov encoding. During the first (initial) block transmission, the sources simultaneously broadcast their messages, interfering at the relay and at the destination. The destination simply stores the received interfering signals. The relay jointly decodes the messages of the sources, and linearly combines the correctly decoded ones to produce its own message to be transmitted during the next block transmission. Note that the processing delay at the relay is typically neglected in our system model. In case of unsuccessful decoding of all the messages, it does nothing and will remain silent during the next block transmission. During the second block transmission, the sources broadcast new messages to both the relay and the destination. The relay jointly decodes

This chapter was presented in part at IEEE ICUMT 2010.

the messages of the sources and applies the same procedure as before. At the same time, if selective decoding was successful during the previous block transmission, the relay transmits its produced message to the destination. The destination continues to store all received interfering signals. The process is repeated for subsequent blocks. Once all blocks have been received, the destination starts to decode. This type of decoding may introduce significant delays but provides the best performance. It is worth noting that, the destination always knows whether the relay cooperates or not, but depending on the coding strategy, the sources may or may not be informed of the cooperation. Allowing collisions at the relay and the destination renders the reality of wireless environments and leverages better the broadcast nature of the radio channel than the OMARC. The proposed SDF in FD-NOMARC is a modification of the relaying protocol presented in [140] so as to allow partial cooperation if some of the sources are successfully decoded at the relay and the others are not. Thus, it not only prevents the error propagation from the relay to the destination, but also decreases the individual BLER, i.e., the BLER for each source. As already mentioned in Chapter 2, this SDF approach has been analyzed in a variety of contributions for the OMARC using either JNCC [82] or SNCC [126]. Its theoretical and practical interests have also been confirmed in Chapter 2 for the HD-SOMARC, and in Chapter 3 for the HD-NOMARC. While these information-theoretic analyses with selective relaying has provided insight into the behavior of the system, especially in the presence of multiple access interferences, many issues need still to be addressed, including the impact of a full-duplex relay. Based on the achievable rates in [8, 27, 115] for full-duplex MARC with decode and forward relaying protocol, the FD-NOMARC joint information outage probability is derived conditional on JNCC, superposition block Markov encoding, and block by block decoding (or backward decoding) at the destination. The joint information outage probability and the joint ϵ-outage achievable rate are then numerically evaluated assuming independent Gaussian inputs or discrete independent identically and uniformly distributed inputs and compared with the ones of a OMARC at fixed energy budget per source (per available dimensions). As a second contribution, we propose practical JNCC designs for FD-NOMARC that are flexible in terms of number of sources and MCS. Our designs are built on turbo codes, and rely on advanced (iterative) joint detection and decoding receiver architectures. Furthermore, contrary to block by block decoding, the proposed decoding approach operates over all the transmitted blocks. The performance of the proposed designs are then compared with the derived information outage probabilities, which can be considered as lower bounds on the theoretical performance of our designs. Finally, we demonstrate that our designs also guarantee the full diversity in the sense that they achieve the same diversity gain as the single-user case. The rationale behind our code construction has already been discussed in Chapter 2.

4.1 System Model

The M statistically independent sources $S_1, \ldots, S_M$ want to communicate with the destination D in the presence of a relay R. In order to create virtual uplink MIMO channels and to benefit from spatial multiplexing gains, we assume that the relay R and the destination D are equipped with N_R and N_D receive antennas. We consider that the baud rate of the sources and relay is $D = 1/T_s$ and the overall transmission time is fixed to T, thus the number of available channel uses to be shared between the sources and the relay is $N = DT$. We consider the case of Nyquist rate and cardinal sine transmission pulse shape, i.e., $N = DT$ is the total number of available complex dimensions and D is the total bandwidth of the system. Our channel models are inspired by the following assumptions: (1) The delay spreads of the radio channels from the sources to the relay and the destination as well as from the relay to the destination are much lower than T_s ensuring no frequency selectivity; (2) the coherence time of all the aforementioned radio channels are supposed to be much larger than T. Following [5], we consider superposition block Markov encoding. The number of block transmission is fixed, say $B+1$. Assume that, in each block transmission $b = 0, \cdots, B-1$, the sources have K information bits to transmit over N channel uses, and during the last block transmission B, the sources remain silent. This necessitates extra signaling to inform the sources of the cooperation. Each source i broadcasts its message $\mathbf{u}_i^{(b)} \in \mathbb{F}_2^K$ of K information bits under the form of a modulated sequence. Without loss of generality, the modulated sequences are chosen from the complex codebooks ζ_i of rate K/N and take the form of sequences $\mathbf{x}_i^{(b)} \in \zeta_i \subset \mathscr{X}_i^N$, $i \in \{1, \ldots, M\}$, where $\mathscr{X}_i \subset \mathbb{C}$ denote a complex signal set of cardinality $|\mathscr{X}_i| = 2^{q_i}$, with energy normalized to unity. At the relay, the received signal is expressed as

$$\mathbf{y}_{R,k}^{(b)} = \sum_{i=1}^{M} \sqrt{P_{iR}} \mathbf{h}_{iR}^{(b)} x_{i,k}^{(b)} + \mathbf{n}_{R,k}^{(b)} \tag{4.1}$$

for $k = 1, \ldots, N$. The received samples form the matrix $\mathbf{Y}_R^{(b)} \in \mathbb{C}^{N_R \times N}$. In (4.1), the channel fading vectors $\mathbf{h}_{iR}^{(b)} \in \mathbb{C}^{N_R}$, $i \in \{1, \ldots, M\}$ are mutually independent, constant over the transmission of $\mathbf{x}_1^{(b)}$, ..., $\mathbf{x}_M^{(b)}$ and change independently from one block transmission of the sources to the next. The channel fading vectors $\mathbf{h}_{iR}^{(b)}$, $i \in \{1, \ldots, M\}$, are identically distributed (i.d.) following the pdf $\mathcal{CN}(\mathbf{0}_{N_R}, \mathbf{I}_{N_R})$. The additive noise vectors $\mathbf{n}_{R,k}^{(b)}$ are independent and follow the pdf $\mathcal{CN}(\mathbf{0}_{N_R}, N_0 \mathbf{I}_{N_R})$. $P_{iR} \propto (d_{iR}/d_0)^{-\kappa} P_i$, $i \in \{1, \ldots, M\}$ is the average received energy per dimension and per antenna (in Joules/symbol), where d_{iR} is the distance between the transmitter and receiver, d_0 is a reference distance, κ is the path loss coefficient, with values typically in the range $[2, 6]$, and P_i is the transmit

power (or energy per symbol) of S_i. Note that the shadowing could be included within P_{ij}. To fairly compare the performance with respect to other classes of MARC, in which the relay operates in half-duplex mode and the number of available dimensions or channel uses is N', and in order to take into account the number of block transmissions in case of FD-NOMARC during which the sources transmit their information, we fix: (1) the sum rate of the system, i.e., $\eta = \frac{MK}{N'} = \frac{MKB}{N(B+1)}$ which yields $\frac{N}{N'} = \frac{B}{B+1}$; (2) the total energy per available dimensions N' and transmitted blocks $(B+1)N'P_{0,i}$ spent by S_i, i.e., $P_i = P_{0,i}/\beta$. Here, β takes into account both the fraction of N' and the fraction of $B+1$ over which each source transmits. Thus, $\beta = \frac{N}{N'} \cdot \frac{B}{B+1} = \left(\frac{B}{B+1}\right)^2$ in the case of FD-NOMARC, $\beta = 1$ in the case of HD-NOMARC [141], $\beta = \alpha$ in the case of HD-SOMARC [136], where α represents the fraction of N' corresponding to the listening phase of the relay, and $\beta = \alpha/M$ in the case of OMARC supposing that the sources transmit in consecutive, equal duration, time slots. Let us now consider the received signals at the destination. During the first block transmission, the received signal at the destination is expressed as

$$\mathbf{y}_{D,k}^{(0)} = \sum_{i=1}^{M} \sqrt{P_{iD}} \mathbf{h}_{iD}^{(0)} x_{i,k}^{(0)} + \mathbf{n}_{D,k}^{(0)} \tag{4.2}$$

for $k = 1, \cdots, N$. For subsequent block transmissions, the relay uses a SDF approach and can either transmit or stay silent, depending on the number of correctly decoded messages during the previous block transmission. Let $J^{(b-1)} \subset \{1, \ldots, M\}$ denote the set of message indices with cardinality $|J^{(b-1)}| \leq M$ that have been successfully decoded during the block transmission $(b-1)$. If $J^{(b-1)} = \emptyset$, the relay remains silent during the block transmission b. Otherwise, according to the number of correctly decoded messages and the chosen network coding scheme, it transmits a modulated sequence of the form $\mathbf{x}_R^{(b)} \in \mathscr{X}_R^N$, where $\mathscr{X}_R \subset \mathbb{C}$ is a complex constellation of order $|\mathscr{X}_R| = 2^{q_R}$ with energy normalized to unity. The modulated sequence $\mathbf{x}_R^{(b)}$ is chosen such that $\left(\left\{\mathbf{x}_j^{(b-1)}, j \in J^{(b-1)}\right\}, \mathbf{x}_R^{(b)}\right)$ is a codeword on message $\left\{\mathbf{u}_j^{(b-1)}, j \in J^{(b-1)}\right\}$ belonging to a codebook $\zeta_{J^{(b-1)},R}$ of rate $|J^{(b-1)}|K/N$. The received signals at the destination during the block transmissions $b \in \{1, \ldots, B\}$ are expressed as

$$\mathbf{y}_{D,k}^{(b)} = \sum_{i=1}^{M} \sqrt{P_{iD}} \mathbf{h}_{iD}^{(b)} x_{i,k}^{(b)} + \theta^{(b)} \sqrt{P_{RD}} \mathbf{h}_{RD}^{(b)} x_{R,k}^{(b)} + \mathbf{n}_{D,k}^{(b)} \tag{4.3}$$

$$\mathbf{y}_{D,k}^{(B)} = \theta^{(B)} \sqrt{P_{RD}} \mathbf{h}_{RD}^{(B)} x_{R,k}^{(B)} + \mathbf{n}_{D,k}^{(B)} \tag{4.4}$$

for $k = 1, \ldots, \bar{\alpha}N$. In (4.2), (4.3) and (4.4), the channel fading vectors $\mathbf{h}_{iD}^{(b)} \in \mathbb{C}^{N_D}$, $i \in \{1, \ldots, M\}$ are mutually independent and follow the pdf $\mathcal{CN}(\mathbf{0}_{N_D}, \mathbf{I}_{N_D})$. They are

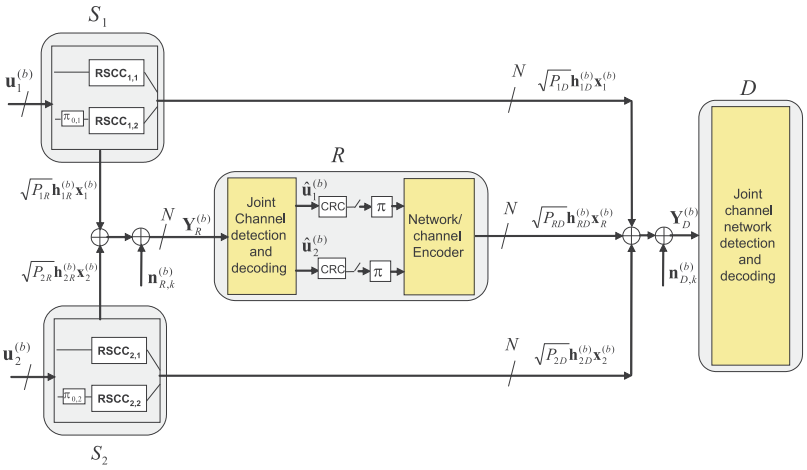

Figure 4.1: System model (relay cooperates)

constant over the transmission of $\mathbf{x}_1^{(b)}, \ldots, \mathbf{x}_M^{(b)}$ and change independently from one block transmission of the sources to the next. The channel fading vector $\mathbf{h}_{RD}^{(b)} \in \mathbb{C}^{N_D}$ follows the pdf $\mathcal{CN}(\mathbf{0}_{N_D}, \mathbf{I}_{N_D})$, is independent of $\mathbf{h}_{iD}^{(b)}$, $i \in \{1, \ldots, M\}$, constant over the transmission of $\mathbf{x}_R^{(b)}$ and changes independently from one block transmission of the relay to another. The additive noise vector $\mathbf{n}_{D,k}^{(b)}$ is independent of $\mathbf{n}_{R,k}^{(b)}$ and $\mathbf{n}_{D,k}^{(b)}$, and follows the pdf $\mathcal{CN}(\mathbf{0}_{N_D}, N_0\mathbf{I}_{N_D})$. $P_{iD} \propto (d_{iD}/d_0)^{-\kappa} P_i$, $i \in \{1, \ldots, M\}$, and $P_{RD} \propto (d_{RD}/d_0)^{-\kappa} P_R$, with P_R the transmit power of the relay, are the average received power per dimension and per antenna at the destination. Here again, we fix the total energy per available dimensions N' and transmitted blocks $(B+1)N'P_{0,R}$ spent by the relay, i.e., $P_R = P_{0,R}/\rho$, where $\rho = \frac{N}{N'} \cdot \frac{B}{B+1} = \left(\frac{B}{B+1}\right)^2$ in the case of FD-NOMARC, and $\rho = \bar{\alpha}$ for all the cases of OMARC, HD-SOMARC, and HD-NOMARC. The parameter $\theta^{(b)}$ is a discrete Bernoulli distributed random variable: $\theta^{(b)} = 1$ if the relay successfully decodes at least one source message during the previous block transmission, and $\theta^{(b)} = 0$ otherwise. Channel model (4.3) can be regarded as a family of MACs indexed by $\theta^{(b)} \in \{0, 1\}$ also called a two-state compound MAC [137]. Concerning the relay functionality, the relay interleaves each message $\mathbf{u}_j^{(b-1)}$, $j \in J^{(b-1)}$, $b \in \{1, \ldots, B\}$, by π and applies a function $\Theta_{R,|J^{(b-1)}|}$

$$\Theta_{R,|J^{(b-1)}|} : \underbrace{\mathbb{F}_2^K \times \mathbb{F}_2^K \times \ldots \times \mathbb{F}_2^K}_{|J^{(b-1)}|} \to \mathbb{C}^N \tag{4.5}$$

to obtain the modulated sequence $\mathbf{x}_R^{(b)}$. In general, the function $\Theta_{R,|J^{(b-1)}|}$ is not a bijection on the interleaved correctly decoded messages. In practice, the relay would add some in-band signaling to make the destination aware of the set J. Finally, the relay signal,

together with the source signals, forms a distributed joint network-channel codebook. The block diagram of the system model is depicted in Fig. 4.1 for the case of $M = 2$. In the rest of the chapter, for the sake of notational simplicity, we consider $M = 2$ sources that transmit with an overall spectral efficiency $r = K/N$. The generalization to the cases of $M > 2$ sources is straightforward.

4.2 Information-theoretic Analysis

The achievable rates for full-duplex MARC with decode and forward relaying strategy was derived in [8, 27, 115] conditional on JNCC, superposition block Markov encoding and backward decoding. Here, we extend the results to the case of FD-NOMARC in which the SDF relaying strategy is applied. Thus, the outage region of FD-NOMARC is perfectly known conditional on a given channel state $\mathbf{H} = \begin{bmatrix} \mathbf{h}_{1R} & \mathbf{h}_{2R} & \mathbf{h}_{1D} & \mathbf{h}_{2D} & \mathbf{h}_{RD} \end{bmatrix}$. Let us define the independent input random variables $x_1 \sim p(x_1)$, $x_2 \sim p(x_2)$, and $x_R \sim p(x_R)$ and the associated independent output random vectors $\mathbf{y}_R$ and $\mathbf{y}_D$ whose channel transition conditional pdfs follow the ones associated to (4.1) and (4.3), respectively. It is clear from our context that the mutual information conditional on any given channel state is maximized for the pdfs $p(x_1)$, $p(x_2)$, $p(x_R)$ being circularly symmetric complex Gaussian pdfs. As a result, the latter pdfs minimize the information outage probabilities. However, in practice, $p(x_1)$, $p(x_2)$, $p(x_R)$ are uniformly distributed pmfs (dirac comb pdfs) over the chosen constellation alphabets. That is why both cases are investigated in the following. We recall that in our analysis:

1. The theoretical bounds are derived conditional on JNCC, superposition block Markov encoding and backward decoding.

2. The SDF relaying function is used under the hypothesis that all the links are prone to errors.

3. The sequences $\mathbf{x}_1$, $\mathbf{x}_2$, and $\mathbf{x}_R$ are the outcomes of independent discrete time i.i.d. processes whose associated pdfs are $p(x_1)$, $p(x_2)$, $p(x_R)$ and their respective length is infinite ($N \to \infty$) such that the AEP holds.

4. The outage limit is either the joint information outage probability or the joint ϵ-outage achievable rate. The efficiency of our proposed JNCC/JNCD is evaluated in terms of gap to the information outage probability, keeping in mind that the information outage probability remains a relevant measure of the best possible BLER even for finite code lengths [119].

4.2.1 Outage analysis of FD-NOMARC/JNCC

As the relay uses a SDF approach, an evaluation of the source-to-relay channel quality has first to be processed. Let $\mathcal{E}_R(\mathbf{H})$ denote the outage event of the source-to-relay MAC conditional on $\mathbf{H}$. It corresponds to the case where the relay cannot decode both messages correctly, and can be expressed as

$$\mathcal{E}_R(\mathbf{H}) = \mathcal{E}_{R,1|2}(\mathbf{H}) \cup \mathcal{E}_{R,2|1}(\mathbf{H}) \cup \mathcal{E}_{R,1,2}(\mathbf{H}) \tag{4.6}$$

where $\mathcal{E}_{R,i|j}(\mathbf{H})$, $i,j \in \{1,2\}$, $j \neq i$ is the outage event of S_i if the information of S_j is known, and $\mathcal{E}_{R,1,2}(\mathbf{H})$ is the outage event of both sources at the relay. The three possible outage events are then given by

$$\mathcal{E}_{R,i|j}(\mathbf{H}) = \{I(x_i; \mathbf{y}_R \mid x_j) < r\} \tag{4.7}$$

$$\mathcal{E}_{R,1,2}(\mathbf{H}) = \{I(x_1, x_2; \mathbf{y}_R) < 2r\} \tag{4.8}$$

When the outage event $\mathcal{E}_R(\mathbf{H})$ holds, in order to verify whether only one of the messages $\mathbf{x}_i$ can be successfully decoded or not, we define the following outage event

$$\mathcal{E}_{R,i}(\mathbf{H}) = \{I(x_i; \mathbf{y}_R) < r\} \tag{4.9}$$

in which the relay treats the signal $\mathbf{x}_j$ as interference. Thus, the relay outage events for the SDF approach can be summarized as follows: (1) In case of $\mathcal{Q}_R^{(1)}(\mathbf{H}) = \bar{\mathcal{E}}_R(\mathbf{H})$, which indicates the complement of the outage event $\mathcal{E}_R(\mathbf{H})$, the relay cooperates with both sources; (2) In case of $\mathcal{Q}_R^{(2)}(\mathbf{H}) = \mathcal{E}_R(\mathbf{H}) \cap \bar{\mathcal{E}}_{R,1}(\mathbf{H})$ the relay cooperates only with S_1; (3) In case of $\mathcal{Q}_R^{(3)}(\mathbf{H}) = \mathcal{E}_R(\mathbf{H}) \cap \bar{\mathcal{E}}_{R,2}(\mathbf{H})$ the relay cooperates only with S_2; (4) Otherwise, in case of $\mathcal{Q}_R^{(4)}(\mathbf{H}) = \mathcal{E}_R(\mathbf{H}) \cap \mathcal{E}_{R,1}(\mathbf{H}) \cap \mathcal{E}_{R,2}(\mathbf{H})$ the relay does not cooperate. Now, depending on the relay transmission, we distinguish four outage events at the destination:

Case 1: The relay cooperates with both sources. The destination always receives the cooperative information from the relay. Following [115], the outage at the destination occurs if the target rate exceeds the mutual informations of the source-and-relay-to-destination MAC. Let $\mathcal{E}_D^{(1)}(\mathbf{H})$ denote the outage event at the destination conditional on $\mathbf{H}$. It can be expressed as

$$\mathcal{O}_D^{(1)}(\mathbf{H}) = \mathcal{E}_{D,1|2}^{(1)}(\mathbf{H}) \cup \mathcal{E}_{D,2|1}^{(1)}(\mathbf{H}) \cup \mathcal{E}_{D,1,2}^{(1)}(\mathbf{H}). \tag{4.10}$$

where

$$\mathcal{E}^{(1)}_{D,i|j}(\mathbf{H}) = \{I(x_i, x_R; \mathbf{y}_D \mid x_j) < r\} \tag{4.11}$$

for $i, j \in \{1, 2\}$ and $j \neq i$, and

$$\mathcal{E}^{(1)}_{D,1,2}(\mathbf{H}) = \{I(x_1, x_2, x_R; \mathbf{y}_D) < 2r\}\,. \tag{4.12}$$

In (4.11), $\mathcal{E}^{(1)}_{D,i|j}(\mathbf{H})$, $i \in \{1, 2\}$ is the outage event of S_i if the information of S_j, $j \neq i$, is known, i.e., x_j is known. In this case, $\mathbf{x}_R$ can be considered as a part of the codeword corresponding to S_i. Typically, this is the case when $\mathbf{x}_R$ is a codeword representing the XOR of the two source messages. The outage event in (4.12) corresponds to the constraint that the total throughput cannot exceed the sum of the mutual information of a point-to-point MIMO channel with the aggregate received signals of the two sources and the relay. When $\mathcal{O}^{(1)}_D(\mathbf{H})$ holds, the destination cannot decode both source messages correctly, which corresponds to the joint outage event at the destination.

Case 2: The relay cooperates with S_1. The joint outage event at the destination $\mathcal{O}^{(2)}_D(\mathbf{H})$ is calculated as

$$\mathcal{O}^{(2)}_D(\mathbf{H}) = \mathcal{E}^{(2)}_{D,1|2}(\mathbf{H}) \cup \mathcal{E}^{(2)}_{D,2|1}(\mathbf{H}) \cup \mathcal{E}^{(2)}_{D,1,2}(\mathbf{H}). \tag{4.13}$$

where

$$\mathcal{E}^{(2)}_{D,1|2}(\mathbf{H}) = \{I(x_1, x_R; \mathbf{y}_D \mid x_2) < r\} \tag{4.14}$$

$$\mathcal{E}^{(2)}_{D,2|1}(\mathbf{H}) = \{I(x_2; \mathbf{y}_D \mid x_1, x_R) < r\} \tag{4.15}$$

$$\mathcal{E}^{(2)}_{D,1,2}(\mathbf{H}) = \{I(x_1, x_2, x_R; \mathbf{y}_D) < 2r\}\,. \tag{4.16}$$

Case 3: The relay cooperates with S_2. Swapping the roles of S_1 and S_2, the joint outage event at the destination $\mathcal{O}^{(3)}_D(\mathbf{H})$ is identical to the previous case.

Case 4: The relay does not cooperate. The joint outage at the destination $\mathcal{O}^{(4)}_D(\mathbf{H})$ occurs if the target rate exceeds the sum of the mutual informations of the source-to-destination MAC. It yields

$$\mathcal{O}^{(4)}_D(\mathbf{H}) = \mathcal{E}^{(4)}_{D,1|2}(\mathbf{H}) \cup \mathcal{E}^{(4)}_{D,2|1}(\mathbf{H}) \cup \mathcal{E}^{(4)}_{D,1,2}(\mathbf{H}). \tag{4.17}$$

where

$$\mathcal{E}^{(4)}_{D,i|j}(\mathbf{H}) = \{I(x_i; \mathbf{y}_D \mid x_j) < r\} \tag{4.18}$$

for $i, j \in \{1, 2\}$ and $j \neq i$, and

$$\mathcal{E}_{D,1,2}^{(4)}(\mathbf{H}) = \{I(x_1, x_2; \mathbf{y}_D) < 2r\}. \tag{4.19}$$

Finally, the joint outage event for FD-NOMARC based on JNCC, can be expressed as

$$\mathcal{O}_D(\mathbf{H}) = \bigcup_{i=1}^{4} \left(\mathcal{Q}_R^{(i)}(\mathbf{H}) \cap \mathcal{O}_D^{(i)}(\mathbf{H}) \right). \tag{4.20}$$

The above outage event is conditional on the channel state $\mathbf{H}$. The joint information outage probability is then obtained as

$$P_{out} = \int_{\mathbf{H}} [\mathcal{O}_D(\mathbf{H})] \;\; p(\mathbf{H}) d(\mathbf{H}) \tag{4.21}$$

where $p(\mathbf{H})$ is the pdf of $\mathbf{H}$. The joint ϵ-outage achievable rate is defined as the largest rate of each source (e.g. S_1) such that the joint information outage probability for a given transmission protocol, is smaller than or equal to ϵ.

As already mentioned, the above outage analysis is conditional on the backward decoding at the destination, which is different from our proposed practical decoding for FD-NOMARC (see Section 4.3.3). Thus, the resulting theoretical bounds can be viewed as lower bounds to the exact outage limits of our proposed designs for FD-NOMARC. The latter may be obtained by taking into account the joint decoding of the all transmitted blocks, and is left for future work.

4.2.2 Types of input distributions

We consider both Gaussian i.i.d. inputs and discrete i.i.d. inputs (for practical considerations as explained in Chapter 2) to calculate the mutual information. The corresponding expressions are given in Appendix B.

4.2.3 Information outage probability achieving codebooks

To achieve the information outage probability bounds, the codebooks ζ_1, ζ_2,ζ_{1R}, ζ_{2R} and ζ_{12R} should be universal codebooks. As defined in [127], a universal codebook of a given rate is a codebook that simultaneously achieves reliable communication over every channel that is not in outage for the chosen rate. Finally, it is worth stressing that, in practice,

there exist codebooks with finite lengths whose performance are very close to the ones of universal codebooks. The simulation Section 4.4 examplifies such codebook constructions based on convolutional or turbo codes.

4.3 Joint Network Channel Coding and Decoding

In this section, we make explicit our proposed JNCC/JNCD approach. We explain the structure of the encoders, when and how JNCC is performed, and the structure of the corresponding multiuser receivers.

4.3.1 Coding at the sources

There are two different approaches for the transmission of source messages. The sources can either (1) transmit their messages in each block $b = 0, \cdots, B$, as in [114] [112], or (2) transmit only in blocks $b = 0, \cdots, B-1$, and stay silent during the last transmission block. In this case, the block B received at the destination, corresponds only to the relay transmitted symbols. Concerning the first approach, there is no rate loss but the last messages of both sources cannot benefit from the relay cooperation. Moreover, the sources do not need to be informed of the cooperation. In the second approach, all the source messages benefit from the relay cooperation, but it implies a rate loss of $\frac{1}{B+1}$ which approaches 0 as B increases. This second approach also reduces the delay processing of the last received block at the destination. However, extra signaling is needed to inform the sources of the cooperation. Here, we consider the second approach. Thus, in each block transmission $b = 0, \cdots, B-1$, the messages of the two sources are binary vectors $\mathbf{u}_1^{(b)} \in \mathbb{F}_2^K$ and $\mathbf{u}_2^{(b)} \in \mathbb{F}_2^K$ of length K. Each source employs a BICM [128]. Binary vectors are first encoded with linear binary encoders $C_i : \mathbb{F}_2^K \rightarrow \mathbb{F}_2^{n_i}$, $i \in \{1, 2\}$ into binary codewords $\mathbf{c}_1^{(b)} \in \mathbb{F}_2^{n_1}$ and $\mathbf{c}_2^{(b)} \in \mathbb{F}_2^{n_2}$ of respective lengths n_1 and n_2. The codes ζ_1 and ζ_2 are in general punctured turbo codes, consisting of two RSC encoders, denoted by $\text{RSC}_{i,1}$ and $\text{RSC}_{i,2}$, $i = \{1, 2\}$, concatenated in parallel using optimized semi-random interleavers $\pi_{0,i}$. The coded bits $\mathbf{c}_1^{(b)}$ and $\mathbf{c}_2^{(b)}$ are then interleaved using interleavers Π_1 and Π_2, and reshaped as two binary matrices $\mathbf{V}_1^{(b)} \in \mathbb{F}_2^{N \times q_1}$ and $\mathbf{V}_2^{(b)} \in \mathbb{F}_2^{N \times q_2}$. Memoryless modulators based on one-to-one binary labeling maps $\phi_1 : \mathbb{F}_2^{q_1} \rightarrow \mathscr{X}_1$ and $\phi_2 : \mathbb{F}_2^{q_2} \rightarrow \mathscr{X}_2$ transform the binary arrays $\mathbf{V}_1^{(b)}$ and $\mathbf{V}_2^{(b)}$ into the complex vectors $\mathbf{x}_1^{(b)} \in \mathscr{X}_1^N$ and $\mathbf{x}_2^{(b)} \in \mathscr{X}_2^N$. For ϕ_1 and ϕ_2, we choose Gray labeling. In the sequel, we denote by $v_{i,k,\ell}^{(b)} = \phi_{i,\ell}^{-1}(x_{i,k}^{(b)})$ the ℓ-th bit of the binary labeling of each symbol $x_{i,k}^{(b)}$ for $i \in \{1, 2\}$ and $k = 1, \cdots, N$.

4.3.2 Relaying Function

During each block transmission $b = 0, \cdots, B-1$, relay processing is divided in two steps: During the first time slot, based on (4.1), the relay performs a joint detection and decoding procedure to obtain the hard binary estimation of the information bits, $\hat{\mathbf{u}}_i^{(b)} \in \mathbb{F}_2^K$. Based on this estimation, the relay chooses a SDF approach for cooperation. Different cases can then be distinguished, depending on the number of successfully decoded messages. In the sequel, first, we briefly describe the relay detection and decoding algorithm, and then, we detail our proposed JNCC scheme.

4.3.2.1 Relay detection and decoding

The joint detection and decoding is performed in a suboptimal iterative way [129]. An inner SISO MAP detector generates extrinsic information on coded bits using the received signal (4.1) and a priori information coming from the outer SISO decoders SISO_1 and SISO_2 (referring to the decoding of ζ_1 and ζ_2). For the general case, the outer SISO decoder of S_i generates extrinsic information on both systematic and coded bits of S_i by activating the SISO decoder $\text{SISO}_{i,1}$ corresponding to $\text{RSC}_{i,1}$, and then $\text{SISO}_{i,2}$ corresponding to $\text{RSC}_{i,2}$. It is important to remember that each SISO decoding stage takes into account all the available a priori information on systematic bits [130] (and Algorithm 4 of Section 4.3.3.2). The extrinsic information on both source codewords is then interleaved and fed back to the detector, which in turn employs it as a priori information for the next iteration. It is worth noting that the proper (de)multiplexing and (de)puncturing are also performed if needed. The process is repeated until convergence. For the representation of the input/output soft information, we use log ratios of probabilities. The LAPPR on bit $v_{i,k,\ell}^{(b)} = \phi_{i,\ell}^{-1}(x_{i,k}^{(b)})$ delivered by the SISO MAP detector is defined as

$$\Lambda(v_{i,k,\ell}^{(b)}) = \log \frac{P(v_{i,k,\ell}^{(b)} = 1 | \mathbf{y}_{R,k}^{(b)})}{P(v_{i,k,\ell}^{(b)} = 0 | \mathbf{y}_{R,k}^{(b)})} \tag{4.22}$$

and, in practice, evaluated as

$$\Lambda(v_{i,k,\ell}^{(b)}) \simeq \log \frac{\sum_{a_i \in \mathscr{X}_i : \varphi_{i,\ell}^{-1}(a_i)=1, a_j \in \mathscr{X}_j} P(\mathbf{y}_{R,k}^{(b)} | x_{i,k}^{(b)} = a_i, x_{j,k}^{(b)} = a_j) e^{\xi(a_i)+\xi(a_j)}}{\sum_{a_i \in \mathscr{X}_i : \varphi_{i,\ell}^{-1}(a_i)=0, a_j \in \mathscr{X}_j} P(\mathbf{y}_{R,k}^{(b)} | x_{i,k}^{(b)} = a_i, x_{j,k}^{(b)} = a_j) e^{\xi(a_i)+\xi(a_j)}} \tag{4.23}$$

for $i, j \in \{1, 2\}, i \neq j$, with,

$$\xi(a_1) = \sum_{\ell'=1}^{\log_2|\mathscr{X}_1|} \phi_{1,\ell'}^{-1}(a_1) E(v_{1,k,\ell'}^{(b)}) \tag{4.24}$$

$$\xi(a_2) = \sum_{\ell'=1}^{\log_2|\mathscr{X}_2|} \phi_{2,\ell'}^{-1}(a_2) E(v_{2,k,\ell'}^{(b)}) \tag{4.25}$$

where $\{E(v_{i,k,\ell}^{(b)})\}$ and $\{E(v_{j,k,\ell}^{(b)})\}$ are LAPRs on bits $v_{i,k,\ell}^{(b)}$ and $v_{j,k,\ell}^{(b)}$ provided by the SISO decoders SISO_1 and SISO_2. The extrinsic information on bit $v_{i,k,\ell}^{(b)}$ is given by $L(v_{i,k,\ell}^{(b)}) = \Lambda(v_{i,k,\ell}^{(b)}) - E(v_{i,k,\ell}^{(b)})$, and after de-interleaving, feeds the corresponding outer SISO decoder.

4.3.2.2 JNCC

As previously mentioned, the relay chooses a SDF approach for cooperation, which is based on the number of successfully decoded messages, the knowledge of which being ensured by using CRC codes for each source message. Let $J^{(b)} \subset \{1, 2\}$, $|J| \leq 2$ denote the set of message indices that have been successfully decoded during the block transmission b. For the case where $J^{(b)} = \emptyset$, the relay does not cooperate during the block transmission $b + 1$. Otherwise, it combines all the correctly decoded messages by XOR, i.e., $\mathbf{u}_R^{(b+1)} = \bigoplus_{j \in J^{(b)}} \mathbf{u}_j^{(b)}$, and interleaves the resulting vector by π. Interestingly, the interleaver commutes with the XOR. The interleaved vector is then encoded to $\mathbf{c}_R^{(b+1)}$ using a binary linear encoder $C_R : \mathbb{F}_2^K \to \mathbb{F}_2^{n_R}$. For C_R, we choose an RSC encoder defined by the generator matrix $G_R(D)$, referred to as RSC_R. A linear transformation $\Omega : \mathbb{F}_2^{n_R} \to \mathbb{F}_2^{n'_R}$ is applied which selects the parity bits of $\mathbf{c}_R^{(b+1)}$ to obtain the new vector $\bar{\mathbf{c}}_R^{(b+1)} \in \mathbb{F}_2^{n'_R}$, $n'_R < n_R$. The vector $\bar{\mathbf{c}}_R^{(b+1)}$ is bit-interleaved using the interleaver Π_R and reshaped as a binary matrix $\mathbf{V}_R^{(b+1)} \in \mathbb{F}_2^{\bar{\alpha}N \times q_R}$. Finally, a memoryless modulator based on a one-to-one binary labeling map $\phi_R : \mathbb{F}_2^{q_R} \to \mathscr{X}_R$ transforms the binary array $\mathbf{V}_R^{(b+1)}$ into the complex vector $\mathbf{x}_R^{(b+1)} \in \mathscr{X}_R^{\bar{\alpha}N}$. For ϕ_R, we choose Gray labeling. In the sequel, we denote by $v_{R,k,\ell}^{(b+1)} = \phi_{R,\ell}^{-1}(x_{R,k}^{(b+1)})$ the ℓ-th bit of the binary labeling of each symbol $x_{R,k}^{(b+1)}$ for and $k = 1, \cdots, \bar{\alpha}N$. Finally, to let the destination detect which of the messages are included in the relay signal, the relay transmits side information (additional bits) to indicate its state to the receiver.

The proposed coding scheme which is based on XOR operation, ensures full diversity for the OMARC using SNCC [126] or JNCC [82]. As shown in Appendix A, the high SNR slope of the outage probability of MAC versus SNR (in dB scale), for the critical case of just one receive antenna, is the same as the one of the orthogonal MAC. Thus, the full diversity

design for OMARC remains valid when we have collisions at the relay and destination. Furthermore, the proposed design simplifies the decoder structure, and is optimal in terms of diversity and coding gain whatever the memory order of the RSC encoder [131,136,138].

4.3.3 JNCD at the Destination

Once the destination has received the $B+1$ transmission blocks, it starts to detect/decode the original data $\mathbf{u}_i^{(b)}$, $i \in \{1,2\}$, $b = 0, \cdots, B-1$. To accomplish this, we again resort to a suboptimal iterative procedure, where B SISO MAP detectors and one SISO demapper (corresponding to the last received block from the relay) are activated in parallel. Two consecutive MAP detectors b and $b+1$ are potentially involved in decoding one particular information block of each source depending on whether the relay transmits at block $b+1$ or not. The destination has access to this knowledge, which may either come from an in-band dedicated control signal, or be learned by means of advanced multiuser detection methods, e.g., [139]. This last topic is out of the scope of this thesis.

4.3.3.1 SISO MAP Detectors

For the first block transmission, the SISO MAP detector computes the LAPPR $\Lambda(v_{i,k,\ell}^{(0)})$ with $v_{i,k,\ell}^{(0)} = \phi_{i,\ell}^{-1}(x_{i,k}^{(0)})$, $i \in \{1,2\}$, using the received signal (4.2). Expression is similar to (4.23) substituting $\mathbf{y}_{D,k}^{(0)}$ for $\mathbf{y}_{R,k}^{(0)}$. For subsequent block transmissions $b = 1, \ldots B-1$, the SISO MAP detector computes the LAPPR $\Lambda(v_{i,k,\ell}^{(b)})$ with $v_{i,k,\ell}^{(b)} = \phi_{i,\ell}^{-1}(x_{i,k}^{(b)})$, $i \in \{1,2\}$, using the received signal (4.3). If the relay stays silent, the SISO MAP detector computes $\Lambda(v_{i,k,\ell}^{(b)})$ using the received signal (4.3) with $\theta^{(b)} = 0$, and a priori information coming from the turbo decoders corresponding to C_1 and C_2. If the relay transmits, the SISO MAP detector not only computes $\Lambda(v_{i,k,\ell}^{(b)})$, but also the LAPPR $\Lambda(v_{R,k,\ell}^{(b)})$ with $v_{R,k,\ell}^{(b)} = \phi_{i,\ell}^{-1}(x_{i,k}^{(b)})$, using the received signal (4.3) with $\theta^{(b)} = 1$, and a priori information coming from SISO_1, SISO_2 and SISO_R which corresponds to the relay joint network-channel encoder (XOR followed by C_R). The LAPPR on bit $v_{R,k,\ell}^{(b)} = \phi_{R,\ell}^{-1}(x_{R,k}^{(b)})$ is defined as

$$\Lambda(v_{R,k,\ell}^{(b)}) = \log \frac{P(v_{R,k,\ell}^{(b)} = 1 | \mathbf{y}_{D,k}^{(b)})}{P(v_{R,k,\ell}^{(b)} = 0 | \mathbf{y}_{D,k}^{(b)})} \tag{4.26}$$

and, in practice, evaluated as

$$\Lambda(v_{R,k,\ell}^{(b)}) \simeq$$

$$\log \frac{\sum_{a_R \in \mathscr{X}_R : \phi_{R,\ell}^{-1}(a_R)=1, a_1 \in \mathscr{X}_1, a_2 \in \mathscr{X}_2} P(\mathbf{y}_{D,k}^{(b)} | x_{1,k}^{(b)} = a_1, x_{2,k}^{(b)} = a_2, x_{R,k}^{(b)} = a_R) e^{\xi(a_1)+\xi(a_2)+\xi(a_R)}}{\sum_{a_R \in \mathscr{X}_R : \phi_{R,\ell}^{-1}(a_R)=0, a_1 \in \mathscr{X}_1, a_2 \in \mathscr{X}_2} P(\mathbf{y}_{D,k}^{(b)} | x_{1,k}^{(b)} = a_1, x_{2,k}^{(b)} = a_2, x_{R,k}^{(b)} = a_R) e^{\xi(a_1)+\xi(a_2)+\xi(a_R)}} \tag{4.27}$$

with

$$\xi(a_1) = \sum_{\ell'=1}^{\log_2|\mathscr{X}_1|} \phi_{1,\ell'}^{-1}(a_1) E(v_{1,k,\ell'}^{(b)}) \tag{4.28}$$

where $\{E(v_{1,k,\ell}^{(b)})\}$ is the LAPR on bit $v_{1,k,\ell}^{(b)}$ provided by SISO_1,

$$\xi(a_2) = \sum_{\ell'=1}^{\log_2|\mathscr{X}_2|} \phi_{2,\ell'}^{-1}(a_2) E(v_{2,k,\ell'}^{(b)}) \tag{4.29}$$

where $\{E(v_{2,k,\ell}^{(b)})\}$ is the LAPR on bit $v_{2,k,\ell}^{(b)}$ provided by SISO_2, and

$$\xi(a_R) = \sum_{\ell'=1}^{\log_2|\mathscr{X}_R|} \phi_{R,\ell'}^{-1}(a_R) E(v_{R,k,\ell'}^{(b)}) \tag{4.30}$$

where $\{E(v_{R,k,\ell}^{(b)})\}$ is the LAPR on bit $v_{R,k,\ell}^{(b)}$ provided by SISO_R. The LAPPRs $\Lambda(v_{i,k,\ell}^{(b)})$, $i \in \{1,2\}$ are evaluated in the same manner. The extrinsic information on $v_{1,k,\ell}^{(b)}$ is given by $L(v_{1,k,\ell}^{(b)}) = \Lambda(v_{1,k,\ell}^{(b)}) - E(v_{1,k,\ell}^{(b)})$ and, after de-interleaving, feeds SISO_1. The extrinsic information on $v_{2,k,\ell}^{(b)}$ is given by $L(v_{2,k,\ell}^{(b)}) = \Lambda(v_{2,k,\ell}^{(b)}) - E(v_{2,k,\ell}^{(b)})$ and, after de-interleaving, feeds SISO_2. The extrinsic information on $v_{R,k,\ell}^{(b)}$ is given by $L(v_{R,k,\ell}^{(b)}) = \Lambda(v_{R,k,\ell}^{(b)}) - E(v_{R,k,\ell}^{(b)})$ and, after de-interleaving, feeds SISO_R. Obviously, for the last transmission block B, if the relay transmits, the LAPPRs $\Lambda(v_{R,k,\ell}^{(B)})$ should be calculated by using a SISO demapper.

4.3.3.2 Message-Passing Schedule

A recapitulative block diagram of the JNCD is depicted in Fig. 4.2. In this paragraph, we detail the message-passing for the case where the relay cooperates with both sources, and for $b = 1, \ldots B-1$. We also consider the case of turbo codes at the sources, i.e., each C_i, $i \in \{1,2\}$ consists of two RSC encoders separated by $\pi_{0,i}$. The generalization to other cases is straightforward. The SISO decoder SISO_i corresponds to C_i, $i \in \{1,2\}$, and SISO_R corresponds to the relay encoder (XOR followed by C_R) which is viewed as a systematic encoder on the two source messages [131]. Each SISO_i, $i \in \{1,2\}$, is made up of the two SISO decoders $\text{SISO}_{i,1}$ and $\text{SISO}_{i,2}$. Channel detectors and decoders exchange iteratively

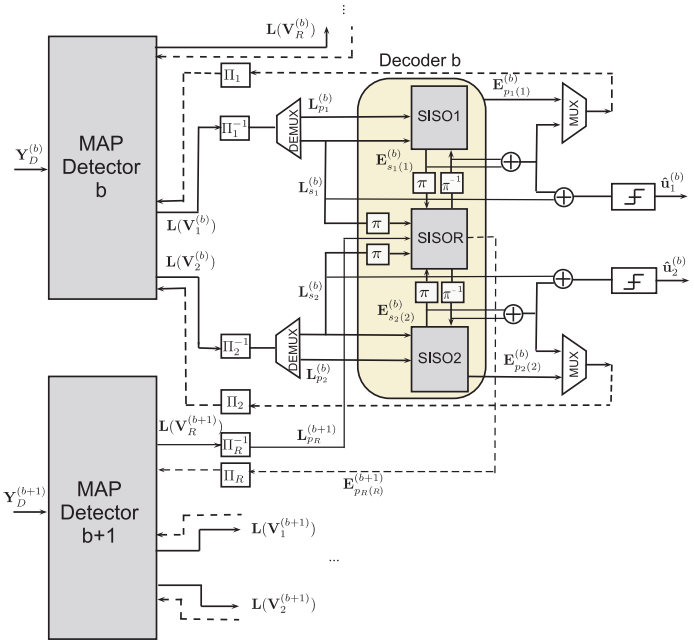

Figure 4.2: JNCD of the block b at the destination (relay cooperates with both sources)

the extrinsic soft information. Two consecutive MAP detectors are involved in decoding one particular block of each source. Let $\mathbf{L}_{s_i}^{(b)}$, $\mathbf{L}_{p_i}^{(b)}$, and $\mathbf{L}_{p_R}^{(b+1)}$ $(i \in \{1,2\})$ denote respectively the soft information of the systematic and parity bits of the two sources and the relay, obtained from the two consecutive channel MAP detectors b and $b+1$. It is worth noting that the proper (de)multiplexing and (de)puncturing are also performed if needed. In Fig. 4.2, the (de)puncturing is included in the blocks corresponding to (de)multiplexing. Let also denote by $\mathbf{E}_{s_i(j)}^{(b)}$, $\mathbf{E}_{p_i(j)}^{(b)}$, and $\mathbf{E}_{p_R(j)}^{(b+1)}$ the extrinsic information generated by the SISO_j, $j \in \{1,2,R\}$. Similarly, let $\mathbf{L}_{p_{i,1}}^{(b)}$ and $\mathbf{L}_{p_{i,2}}^{(b)}$ denote respectively the soft information of the parity bits corresponding to $\text{SISO}_{i,1}$ and $\text{SISO}_{i,2}$ obtained from the MAP detector b, $\mathbf{E}_{s_i(i,1)}^{(b)}$ and $\mathbf{E}_{s_i(i,2)}^{(b)}$ denote respectively the extrinsic information on systematic bits corresponding to the block b of each source, and generated by $\text{SISO}_{i,1}$ and $\text{SISO}_{i,2}$, and $\mathbf{E}_{p_i(i,1)}^{(b)}$ and $\mathbf{E}_{p_i(i,2)}^{(b)}$ denote respectively the extrinsic information on parity bits corresponding to the block b of each source, and generated by $\text{SISO}_{i,1}$ and $\text{SISO}_{i,2}$.

First, the channel MAP detectors generate the LAPPRs for the coded bits by using the a priori information from the B decoders. The MAP detectors b and $b+1$ are involved in decoding the block b of each source. They take respectively $\mathbf{E}_{s_1(1)}^{(b)} + \pi^{-1}(\mathbf{E}_{s_1(R)}^{(b)})$, $\mathbf{E}_{p_1(1)}^{(b)}$, $\mathbf{E}_{s_2(2)}^{(b)} + \pi^{-1}(\mathbf{E}_{s_2(R)}^{(b)})$, $\mathbf{E}_{p2(2)}^{(b)}$, and $\mathbf{E}_{p_R(R)}^{(b+1)}$ as the a priori knowledge about the systematic and parity bits from the decoder b. It is worth stressing that $\mathbf{E}_{s_1(1)}^{(b)} = \mathbf{E}_{s_1(1,1)}^{(b)} + \pi_{0,1}^{-1}(\mathbf{E}_{s_1(1,2)}^{(b)})$,

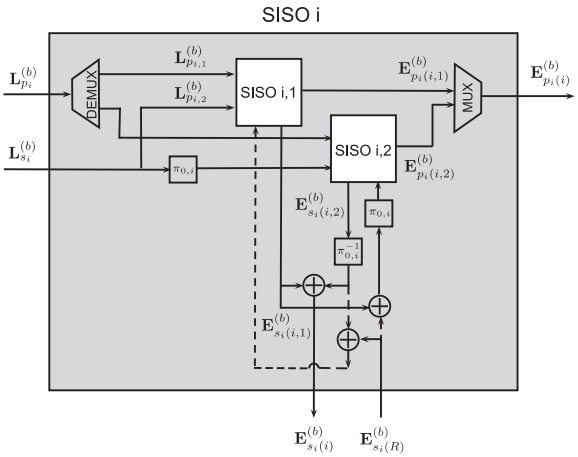

Figure 4.3: SISO decoder SISO_i

and $\mathbf{E}^{(b)}_{s_2(2)} = \mathbf{E}^{(b)}_{s_2(2,1)} + \pi^{-1}_{0,2}(\mathbf{E}^{(b)}_{s_2(2,2)})$, as depicted in Fig. 4.3. Then, the two distributed turbo decoders of decoder b are activated and calculate the extrinsic information for both the systematic bits and the parity bits which are fed back to the MAP detectors b and $b+1$.

In the case of an XOR encoding scheme (full diversity by construction), we detail in Fig. 4.4 and hereafter, the low complexity implementation of SISO_R. As depicted in Fig. 4.4, the SISO decoder corresponding to C_R (DEC_R) should collect all the a priori information $\mathbf{L}^{(b+1)}_{u_R}$ on $\mathbf{u}^{(b+1)}_R$. Denoting $\mathbf{L}^{(b)}_1 = \pi(\mathbf{L}^{(b)}_{s_1} + \mathbf{E}^{(b)}_{s_1(1)})$ and $\mathbf{L}^{(b)}_2 = \pi(\mathbf{L}^{(b)}_{s_2} + \mathbf{E}^{(b)}_{s_2(2)})$, it yields, taking into account the XOR constraint node (see, e.g., [132]),

$$L_{u^{(b+1)}_R,k} = L^{(b)}_{1,k} \boxplus L^{(b)}_{2,k} = \log \frac{e^{L^{(b)}_{1,k}} + e^{L^{(b)}_{2,k}}}{1 + e^{(L^{(b)}_{1,k} + L^{(b)}_{2,k})}}. \tag{4.31}$$

Note, that independency between messages should hold in order to apply (4.31).

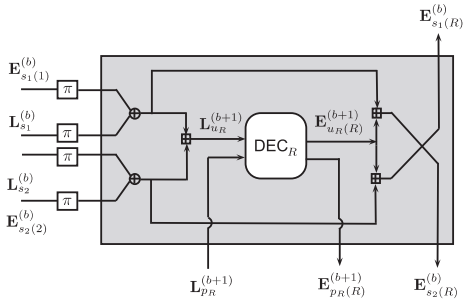

Figure 4.4: XOR decoder

Finally, SISO_R computes at its output, the extrinsic information $\mathbf{E}_{s_i(R)}^{(b)}$ from $\mathbf{L}_j^{(b)}$ and $\mathbf{E}_{u_R(R)}^{(b+1)}$, $i,j \in \{1,2\}$, $i \neq j$, where $\mathbf{E}_{u_R(R)}^{(b+1)}$ is the extrinsic information on $\mathbf{u}_R^{(b+1)}$ computed by the decoder corresponding to C_R. The succession of the decoding procedure of block b at each iteration, and the final hard decisions are detailed in the Algorithm 4.

4.4 Numerical Results

In this section, we provide some numerical results to evaluate the effectiveness of our approach. In our comparisons, we consider both FD-NOMARC and OMARC using JNCC. We start by detailing the topology of the network. For the sake of simplicity, we consider a symmetric MARC, i.e., $d_{1R} = d_{2R}$ and $d_{1D} = d_{2D}$. The average energy per available dimension allocated to the two sources is the same, i.e., $P_{0,1} = P_{0,2} = P_0$. We fix the same path loss factor, i.e., $\kappa = 3$, free distance, i.e., $d_0 = 1$ and noise power spectral density, i.e., $N_0 = 1$, for all links. We fix $B = 5$ for FD-NOMARC, which yields $P_1 = P_2 = 36/25P_0$, and $P_R = 36/25P_{0,R}$. In OMARC, the two sources transmit in consecutive, equal duration, time slots occupying $\alpha N'/2$ channel uses while the relay, which operates in half-duplex mode, keeps $\bar{\alpha}N'$ channel uses, where $\frac{N}{N'} = \frac{B}{B+1} = \frac{5}{6}$. We choose $\alpha = 2/3$ and $P_{0,R} = \frac{\bar{\alpha}}{\alpha}P_0 = 1/2P_0$ as references in order to compare our results with [136, 141]. It comes that $P_1 = P_2 = 3P_0$ and $P_R = 3P_{0,R}$ for OMARC. For simulation purposes, two different configurations are considered: In the first configuration, we fix the number of receive antennas to one both at the relay and destination, i.e., $N_R = N_D = 1$. The geometry is chosen such that $d_{ij} = d$ which yields, taking [136] as a reference, $P_{RD} = \bar{\alpha}\left(\frac{B+1}{B}\right)^2\gamma = 12/25\gamma$, $P_{ij} = \alpha\left(\frac{B+1}{B}\right)^2\gamma = 24/25\gamma$ for FD-NOMARC and $P_{RD} = \gamma$, $P_{ij} = 2\gamma$ for OMARC, $i \in \{1,2\}$, $j \in \{R,D\}$, where γ is the received SNR per symbol or dimension for $\alpha = 2/3$ in the case of HD-SOMARC [136]. In the second configuration, we increase the number of receive antennas at the destination to 4, i.e., $N_R = 1$ and $N_D = 4$. The geometry is chosen such that $d_{iR} = d_1$ and $d_{iD} = d_{RD} = d$ with $(d_1/d)^{-3} = 100$, $i \in \{1,2\}$. It yields $P_{iR} = 100\alpha\left(\frac{B+1}{B}\right)^2\gamma = 96\gamma$ (or $\gamma + 10\log_{10}(96)$ in dB), $P_{iD} = 24/25\gamma$ and $P_{RD} = 12/25\gamma$ for FD-NOMARC which translates into $P_{iR} = 200\gamma$, $P_{iD} = 2\gamma$ and $P_{RD} = \gamma$ for OMARC, $i \in \{1,2\}$. Each message of the sources has length $K = 1024$ information bits. In our proposed JNCC, the complex signal sets $\mathscr{X}_1$, $\mathscr{X}_2$, and $\mathscr{X}_R$ used in BICM are either QPSK or 16QAM constellation (Gray labeling) and their corresponding sum rates are $\eta = 4/3$ b./c.u and $\eta = 8/3$ b./c.u, respectively.

Algorithm 4 : JNCD at the destination

(Initialization)

1. Start when all the $B+1$ transmitted blocks have been received.
2. Set all the a priori information to zero.

(Iterations)
Iterate until convergence:

1. Activate in parallel, the B SISO MAP detectors and the SISO MAP demapper:
   (a) Activate the first SISO MAP detector using $\mathbf{Y}_D^{(0)}$, and the messages $\mathbf{E}_{s_1(1)}^{(0)} + \pi^{-1}(\mathbf{E}_{s_1(R)}^{(0)})$, $\mathbf{E}_{p_1(1)}^{(0)}$ and $\mathbf{E}_{s_2(2)}^{(0)} + \pi^{-1}(\mathbf{E}_{s_2(R)}^{(0)})$, $\mathbf{E}_{p_2(2)}^{(0)}$, where $\mathbf{E}_{s_i(i)}^{(b)} = \mathbf{E}_{s_i(i,1)}^{(b)} + \pi_{0,i}^{-1}(\mathbf{E}_{s_i(i,2)}^{(b)})$.
   (b) Activate each SISO MAP detector b, $b \in \{1, \ldots, B-1\}$ using $\mathbf{Y}_D^{(b)}$, and the messages $\mathbf{E}_{s_1(1)}^{(b)} + \pi^{-1}(\mathbf{E}_{s_1(R)}^{(b)})$, $\mathbf{E}_{p_1(1)}^{(b)}$ and $\mathbf{E}_{s_2(2)}^{(b)} + \pi^{-1}(\mathbf{E}_{s_2(R)}^{(b)})$, $\mathbf{E}_{p_2(2)}^{(b)}$ and $\mathbf{E}_{p_R(R)}^{(b)}$.
   (c) Activate the SISO MAP demapper B using $\mathbf{Y}_D^{(B)}$, and the message $\mathbf{E}_{p_R(R)}^{(B)}$.
2. Activate the B parallel decoders. At each decoder b, $b \in \{0, \ldots, B-1\}$:
   (a) Activate simultaneously the SISO decoders SISO_1 and SISO_2
      i. Activate simultaneously $\text{SISO}_{1,1}$ and $\text{SISO}_{2,1}$ with the messages $\mathbf{L}_{s_1}^{(b)}$, $\mathbf{L}_{p_{1,1}}^{(b)}$ and $\mathbf{L}_{s_2}^{(b)}$, $\mathbf{L}_{p_{2,1}}^{(b)}$ provided by the MAP detector b, and $\pi_{0,1}^{-1}(\mathbf{E}_{s_1(1,2)}^{(b)}) + \pi^{-1}(\mathbf{E}_{s_1(R)}^{(b)})$ and $\pi_{0,2}^{-1}(\mathbf{E}_{s_2(2,2)}^{(b)}) + \pi^{-1}(\mathbf{E}_{s_2(R)}^{(b)})$, which are derived from the previous iteration.
      ii. Activate simultaneously the $\text{SISO}_{1,2}$ and $\text{SISO}_{2,2}$ with, respectively, the messages $\pi_{0,1}(\mathbf{L}_{s_1}^{(b)})$, $\mathbf{L}_{p_{1,2}}^{(b)}$ and $\pi_{0,2}(\mathbf{L}_{s_2}^{(b)})$, $\mathbf{L}_{p_{2,2}}^{(b)}$ provided by the MAP detector b, and $\pi_{0,1}(\mathbf{E}_{s_1(1,1)}^{(b)}) + \pi_{0,1} \circ \pi^{-1}(\mathbf{E}_{s_1(R)}^{(b)})$ and $\pi_{0,2}(\mathbf{E}_{s_2(2,1)}^{(b)}) + \pi_{0,2} \circ \pi^{-1}(\mathbf{E}_{s_2(R)}^{(b)})$.
   (b) Activate the SISO decoder SISO_R with the messages $\mathbf{L}_{p_R}^{(b+1)}$ provided by the MAP detector b+1 (or by the MAP demapper for the last transmitted block), and $\mathbf{L}_1^{(b)} = \pi(\mathbf{L}_{s_1}^{(b)} + \mathbf{E}_{s_1(1)}^{(b)})$ and $\mathbf{L}_2^{(b)} = \pi(\mathbf{L}_{s_2}^{(b)} + \mathbf{E}_{s_2(2)}^{(b)})$.

(Hard decisions)
Combine all the available information on the systematic bits $\mathbf{u}_1^{(b)}$ and $\mathbf{u}_2^{(b)}$:

$$\mathbf{L}_{s_1}^{(b)} + \mathbf{E}_{s_1(1,1)}^{(b)} + \pi_{0,1}^{-1}(\mathbf{E}_{s_1(1,2)}^{(b)}) + \pi^{-1}(\mathbf{E}_{s_1(R)}^{(b)}) \rightarrow \hat{\mathbf{u}}_1^{(b)}$$
$$\mathbf{L}_{s_2}^{(b)} + \mathbf{E}_{s_2(2,1)}^{(b)} + \pi_{0,2}^{-1}(\mathbf{E}_{s_2(2,2)}^{(b)}) + \pi^{-1}(\mathbf{E}_{s_2(R)}^{(b)}) \rightarrow \hat{\mathbf{u}}_2^{(b)}$$

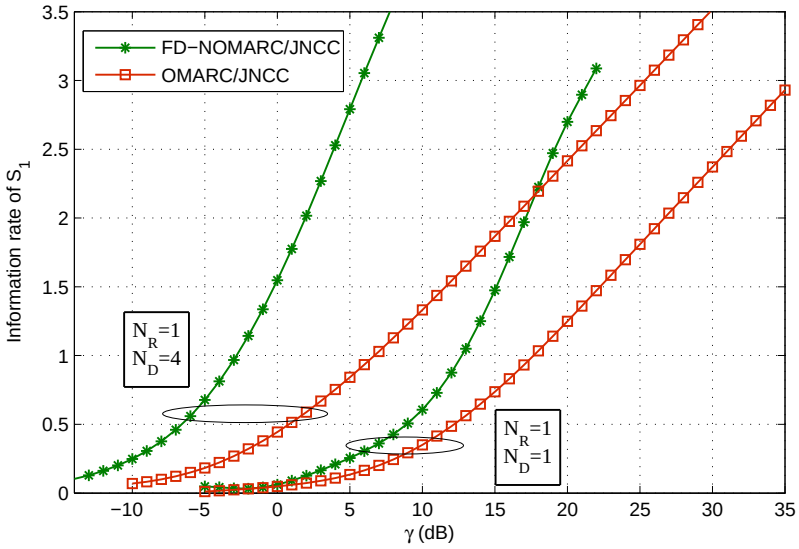

Figure 4.5: Joint ϵ-outage achievable rate - $\epsilon = 10^{-2}$ - FD-NOMARC/JNCC vs. OMARC/JNCC

4.4.1 Joint ϵ-outage achievable rate comparison of the protocols

In the first set of simulations, we consider the joint ϵ-outage achievable rate $C_\epsilon(\gamma)$, under Gaussian i.i.d. inputs, and we compare the $C_\epsilon(\gamma)$ of FD-NOMARC/JNCC conditional on backward decoding and the $C_\epsilon(\gamma)$ of OMARC/JNCC. In our analysis, we fix $\epsilon = 10^{-2}$. The number of receive antennas at the destination is either $N_D = 1$ or $N_D = 4$. The corresponding results are depicted in Fig. 4.5. As we can see, the joint ϵ-outage achievable rate for the FD-NOMARC/JNCC is always higher than the joint ϵ-outage achievable rate for the OMARC/JNCC; Especially, in the case of $N_D = 4$, JNCC with half-duplex relay and orthogonal multiple access (OMARC/JNCC) is strictly suboptimal and the joint ϵ-outage achievable rate gain of FD-NOMARC/JNCC versus OMARC/JNCC for individual rates above 2b./c.u. is more than 14 dB. This results from the fact that, in the presence of multiple receive antennas, a non-orthogonal MAC can better exploit the available degrees of freedom. Moreover, even in the case of $N_D = 1$ which is not a priori favorable for a MAC, we see that the use of full-duplex relay and backward decoding in FD-NOMARC/JNCC can provide an ϵ-outage achievable rate gain of more than 9 dB for data rates above 2 b./c.u..

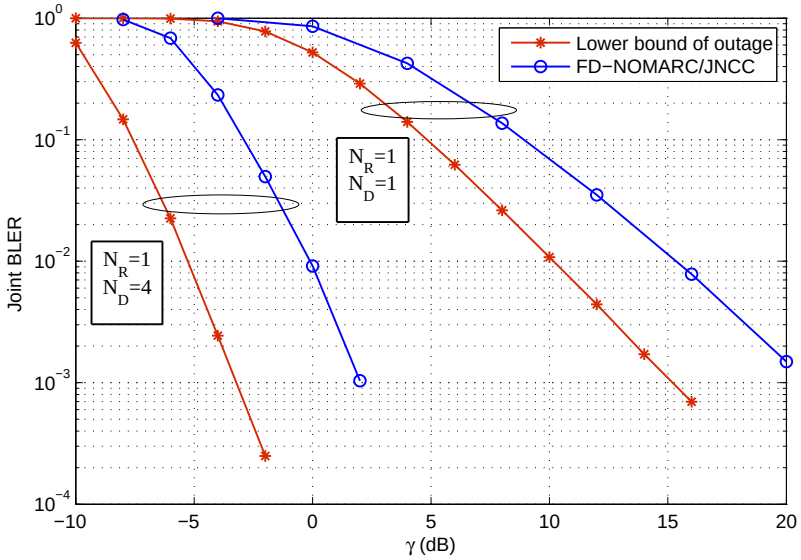

Figure 4.6: Joint BLER - Practical FD-NOMARC/JNCC vs. lower bound of outage limit - $\eta = 4/3$ b./c.u.

4.4.2 Performance of practical code design

In the sequel, the number of iterations I is set to 5 at the relay and to 10 (for $N_D = 1$) or 3 (for $N_D = 4$) at the destination. These numbers of iterations ensure convergence and allow to very closely approach the performance of a Genie Aided (GA) receiver at sufficiently high SNR for the selected modulation and coding schemes, the Genie Aided (GA) receiver corresponding to the ideal case where the interference is known and perfectly removed.

4.4.2.1 Gap to outage limits

In this section, we evaluate the gap between the joint BLER of practical designs for FD-NOMARC/JNCC and that of the lower bounds on their corresponding information outage probability. Here, the joint information outage probabilities are computed under discrete independent identically uniformly distributed inputs. Joint BLER is defined as the probability to have at least one erroneously decoded information bit in either of the decoded blocks at the destination. The experiment is carried out for $\eta = 4/3$ b./c.u.. In our comparisons, we assume that both sources use identical turbo codes of rate-1/3 made of two 4-state rate-1/2 RSC encoders with generator matrices $\mathbf{G}_{i,1} = \mathbf{G}_{i,2} = [\ 1 \quad 5/7\ ]$, $i \in \{1, 2\}$, in octal representation, whose one quarter of the parity bits are punctured. The JNCC at the relay is based on XOR, followed by a 4-state rate-1/4 RSC encoder with

generator matrix $\mathbf{G}_R = [\ 1 \quad 5/7 \quad 4/7 \quad 6/7\ ]$ [142] whose one sixth of the parity bits are punctured. Exhaustive simulations showed that those numbers of states yield the best performance/complexity trade-off. The corresponding results are demonstrated in Fig. 4.6. As we see, there is around 5 dB gap between the proposed JNCC designs and the lower bounds on the information outage probability for both $N_D = 1$ and $N_D = 4$. This is mainly due to the difference between the decoding strategies in practical designs and theoretical bounds. The backward decoding which is used in theoretical analyses, can not be implemented in practice.

4.4.2.2 Comparison of the different protocols

In this section, we compare the individual BLER (e.g. for S_1) of FD-NOMARC/JNCC with that of the OMARC/JNCC. In FD-NOMARC/JNCC, the two sources use the punctured turbo codes made of 4-state rate-1/2 RSC encoders with generator matrices $\mathbf{G}_{i,1}$ and $\mathbf{G}_{i,2}$, and the relay uses the RSC encoder with generator matrix $\mathbf{G}_R$ whose one sixth of the parity bits are punctured. For OMARC/JNCC, we first imposed on the sources the use of the same signal sets. In this case, the two sources transmit their information symbols without any coding, while the relay uses the 4-state rate-1/2 RSC encoder with generator matrix $\mathbf{G}'_R = [\ 1 \quad 5/7\ ]$. The corresponding results demonstrated considerable gains in favour of our approach. We next carried out another experiment, where constellation expansion is employed for OMARC. In this approach, the sources increase the cardinality of their modulation while preserving the same spectral efficiency, which makes room for coding. Thus, in the case of OMARC with $\eta = 4/3$ b./c.u., both sources use a turbo code of rate-1/2 made of two 4-state rate-1/2 RSC encoders with generator matrices $\mathbf{G}_{i,1}$ and $\mathbf{G}_{i,2}$, $i \in \{1, 2\}$, whose half of the parity bits are punctured. They use then 16QAM constellation. The relay uses the 4-state rate-1/2 RSC encoder with generator matrix $\mathbf{G'}_R$ and it uses QPSK constellation. Similarly, in the case of $\eta = 8/3$ b./c.u., both sources use the same turbo code as the previous case, but with the parity bits that are punctured to result in a code of rate 2/3. They use then 64QAM constellation. The relay uses the same RSC encoder as the previous case with 16QAM modulation. The corresponding results are depicted in Fig. 4.7 for the spectral efficiency of $\eta = 4/3$ b./c.u., and in Fig. 4.8 for the spectral efficiency of $\eta = 8/3$ b./c.u., for both $N_D = 1$ and $N_D = 4$. Here again, the FD-NOMARC outperforms the OMARC in most cases and the performance gains are considerable for $N_D = 4$. The exception is the case of $\eta = 8/3$ b./c.u. and for $N_D = 1$, where the FD-NOMARC starts to outperform the OMARC with constellation expansion at a relatively high SNR ($\gamma = 28$ dB). This is certainly due to the sub-optimality of the MAP detectors in FD-NOMARC.

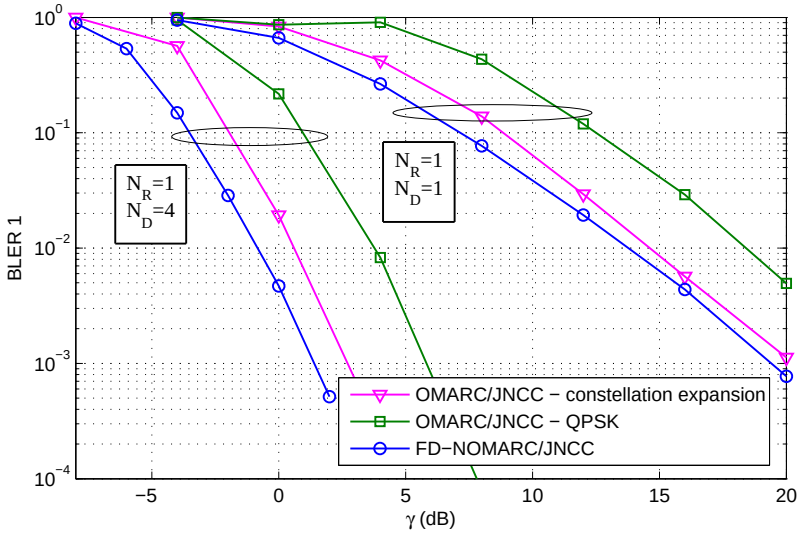

Figure 4.7: Individual BLER (e.g., for S_1) - FD-NOMARC/JNCC vs. OMARC/JNCC - $\eta = 4/3$ b./c.u.

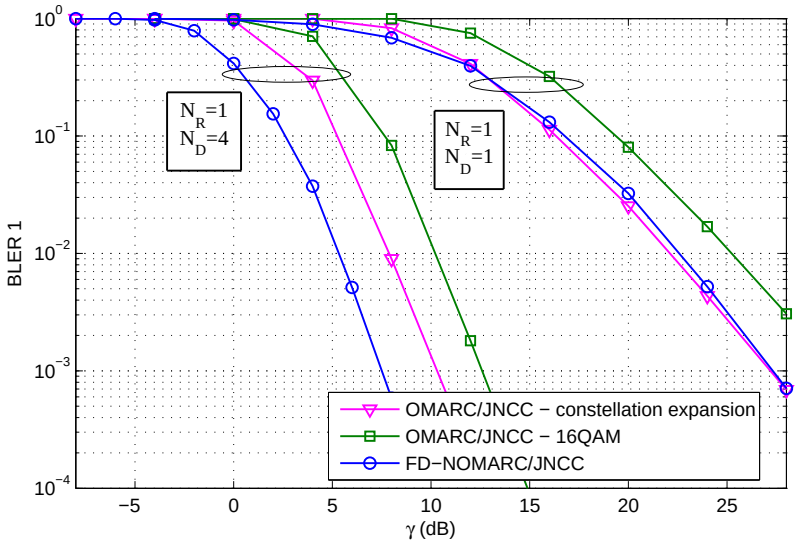

Figure 4.8: Individual BLER (e.g., for S_1) - FD-NOMARC/JNCC vs. OMARC/JNCC - $\eta = 8/3$ b./c.u.

4.5 Conclusion

We have studied JNCC for a new class of MARC, referred to as FD-NOMARC, from both an information-theoretic and a practical code design perspective. We have derived the FD-NOMARC joint information outage probability, conditional on JNCC, superposition block Markov coding, and backward decoding. This provides lower bounds on the information outage probability of our practical designs. We have also presented new JNCC schemes flexible in terms of number of sources, encoders and modulations. For the 2-source symmetric case and targeted sum rates $\eta = 4/3$ b./c.u. and $\eta = 8/3$ b./c.u., we have shown that our proposed schemes are more efficient than conventional distributed JNCC for OMARC. We have also verified that the non-orthogonal multiple access exhibits considerable gains over orthogonal multiple access, even in the case of a single receive antenna at the destination.

Chapter 5

Joint Network-Channel Coding for the Half-Duplex Semi-Orthogonal MAMRC

In this chapter, we extend the network model by considering multiple relays which help multiple sources to communicate with a destination. The relays operate in half-duplex mode. All nodes in the network are informed that they cooperate. We propose a new class of MAMRC that we call Half-Duplex Semi-Orthogonal MAMRC (HD-SOMAMRC or SOMAMRC) and is defined as follows: (1) Independent sources communicate with a single destination in the presence of multiple relays; (2) The relays are half-duplex and apply a Selective Decode and Forward (SDF) strategy, i.e, each relay forwards only a deterministic function of the messages that it can decode without errors; (3) The sources are allowed to transmit simultaneously during the listening phase of the relays, but are constrained to remain silent during their transmission phases. The relays are also allowed to transmit simultaneously all together. Allowing collisions at the relay and the destination renders the reality of wireless environments and leverages better the broadcast nature of the radio channel than the Orthogonal MAMRC (OMAMRC). Furthermore, the proposed SDF in SOMAMRC not only prevents the error propagation from the relay to the destination, but also decreases the individual BLER, i.e., the BLER for each source. As already mentioned in Chapter 2, this SDF approach has been analyzed in a variety of contributions for the OMARC using either JNCC [82] or SNCC [126]. Its theoretical and practical interests have also been confirmed in Chapter 2 for the HD-SOMARC, in Chapter 3 for the HD-NOMARC, and in Chapter 4 for the FD-NOMARC. It has also been studied in [92] for OMAMRC/SNCC. While these information-theoretic analyses have provided insight into the behavior of the system, many issues need still to be addressed in case of MAMRC,

The work presented in this chapter will be submitted to IEEE Transaction on Wireless Communication.

including the impact of JNCC and the multiple access interferences. Based on a careful outage analysis, the SOMAMRC individual information outage probability (e.g., for S_1) is derived for both JNCC or SNCC. The individual information outage probability and the individual ϵ-outage achievable rate (e.g., for S1) are then numerically evaluated assuming independent Gaussian inputs or discrete independent identically and uniformly distributed inputs and compared with the ones of a OMAMRC at fixed energy budget per source (per available dimensions). As a second contribution, we propose practical JNCC designs for SOMAMRC that are flexible in terms of number of sources and relays, and MCS. Our designs are built on convolutional codes and turbo codes, and rely on advanced (iterative) joint detection and decoding receiver architectures. We further demonstrate that they also guarantee the full diversity in the sense that they achieve the same diversity gain as the single-user case. As already discussed in Chapter 2, in the large SNR regime, the MACs at the relays and at the destination turn into $ML+M+L$ independent BECs (corresponding to ML source-to-relay links and $M+L$ source-to-destination and relay-to-destination links). We claim that our proposed JNCC schemes are full diversity since the BLER of each source decays as ϵ^{L+1} where ϵ is the probability of each link to be in erasure.

5.1 System Model

The M statistically independent sources $S_1, \ldots, S_M$ want to communicate with the destination D in the presence of L relays $R_1, \ldots, R_L$. In order to create virtual uplink MIMO channels and to benefit from spatial multiplexing gains, we assume that the relays R_ℓ, $\ell \in \{1, \ldots, L\}$ and the destination D are equipped with N_{R_ℓ} and N_D receive antennas. We consider that the baud rate of the sources and relays is $D = 1/T_s$ and the overall transmission time is fixed to T, thus the number of available channel uses to be shared between the sources and the relays is $N = DT$. We consider the case of Nyquist rate and cardinal sine transmission pulse shape, i.e., $N = DT$ is the total number of available complex dimensions and D is the total bandwidth of the system. Our channel models are inspired by the following assumptions: (1) The delay spreads of the radio channels from the sources to the relay and the destination as well as from the relay to the destination are much lower than T_s ensuring no frequency selectivity; (2) the coherence time of all the aforementioned radio channels are supposed to be much larger than T. The Semi-orthogonal transmission protocol is considered. The N available channel uses are divided into two successive time slots corresponding to the listening phase of the relays, say $N_1 = \alpha N$ channel uses, and to the transmission phase of the relays, say $N_2 = \bar{\alpha} N$ channel uses, with $\alpha \in [0, 1]$ and $\bar{\alpha} = 1 - \alpha$. Each source i broadcasts its messages $\mathbf{u}_i \in \mathbb{F}_2^K$ of K information bits under the form of a modulated sequence during the first transmission phase. Without loss of generality, the

modulated sequences are chosen from the complex codebooks ζ_i of rate $K/(\alpha N)$ and take the form of sequences $\mathbf{x}_i \in \zeta_i \subset \mathscr{X}_i^{\alpha N}$, $i \in \{1, \ldots, M\}$, where $\mathscr{X}_i \subset \mathbb{C}$ denote a complex signal set of cardinality $|\mathscr{X}_i| = 2^{q_i}$, with energy normalized to unity. The corresponding received signals at the relays and destination are expressed as

$$\mathbf{y}_{R_\ell,k}^{(1)} = \sum_{i=1}^{M} \sqrt{P_{iR_\ell}} \mathbf{h}_{iR_\ell} x_{i,k} + \mathbf{n}_{R_\ell,k}^{(1)} \tag{5.1}$$

$$\mathbf{y}_{D,k}^{(1)} = \sum_{i=1}^{M} \sqrt{P_{iD}} \mathbf{h}_{iD} x_{i,k} + \mathbf{n}_{D,k}^{(1)} \tag{5.2}$$

for $\ell \in \{1, \ldots, L\}$ and $k = 1, \ldots, \alpha N$. In (5.1) and (5.2), the channel fading vectors $\mathbf{h}_{iR_\ell} \in \mathbb{C}^{N_{R_\ell}}$, and $\mathbf{h}_{iD} \in \mathbb{C}^{N_D}$, $i \in \{1, \ldots, M\}$ are mutually independent, constant over the transmission of $\mathbf{x}_1$, ..., $\mathbf{x}_M$ and change independently from one transmission of the sources to the next. The channel fading vectors $\mathbf{h}_{iR_\ell}$, $i \in \{1, \ldots, M\}$, $\ell \in \{1, \ldots, L\}$, are identically distributed (i.d.) following the pdf $\mathcal{CN}(\mathbf{0}_{N_{R_\ell}}, \mathbf{I}_{N_{R_\ell}})$. The channel fading vectors $\mathbf{h}_{iD}$, $i \in \{1, \ldots, M\}$, are i.d. following the pdf $\mathcal{CN}(\mathbf{0}_{N_D}, \mathbf{I}_{N_D})$. The additive noise vectors $\mathbf{n}_{R_\ell,k}^{(1)}$ and $\mathbf{n}_{D,k}^{(1)}$ are independent and follow the pdf $\mathcal{CN}(\mathbf{0}_{N_{R_\ell}}, N_0\mathbf{I}_{N_{R_\ell}})$ and $\mathcal{CN}(\mathbf{0}_{N_D}, N_0\mathbf{I}_{N_D})$, respectively. $P_{ij} \propto (d_{ij}/d_0)^{-\kappa} P_i$, $i \in \{1, \ldots, M\}$, $j \in \{R_1, \cdots, R_L, D\}$, is the average received energy per dimension and per antenna (in Joules/symbol), where d_{ij} is the distance between the transmitter and receiver, d_0 is a reference distance, κ is the path loss coefficient, with values typically in the range $[2, 6]$, and P_i is the transmit power (or energy per symbol) of S_i. Note that the shadowing could be included within P_{ij}. To fairly compare the performance with respect to α, we fix the total energy per available dimensions $NP_{0,i}$ (recall that N is the number of available dimensions or channel uses) spent by S_i, i.e., $P_i = P_{0,i}/\alpha$. During the second phase, the sources are silent. Each relay uses a SDF approach, which depends on the number of correctly decoded messages. Let $J_\ell \subset \{1, \cdots, M\}$ denote the set of message indices with cardinality $|J_\ell| \leq M$ that have been successfully decoded at R_ℓ. If $J_\ell = \emptyset$, R_ℓ remains silent. Otherwise, according to the number of correctly decoded messages and the chosen network coding scheme, it transmits a modulated sequence of the form $\mathbf{x}_{R_\ell} \in \mathscr{X}_{R_\ell}^{\tilde{\alpha} N}$, where $\mathscr{X}_{R_\ell} \subset \mathbb{C}$ is a complex constellation of order $|\mathscr{X}_{R_\ell}| = 2^{q_{R_\ell}}$ with energy normalized to unity. The modulated sequences $\mathbf{x}_{R_\ell}$ are chosen such that $(\{\mathbf{x}_i, i \in J_\ell\}, \mathbf{x}_{R_\ell})$ is a codeword on message $(\{\mathbf{u}_i, i \in J_\ell\})$ belonging to a codebook ζ_{J_ℓ,R_ℓ} of rate $|J_\ell|K/N$. The received signal at the destination is expressed as

$$\mathbf{y}_{D,k}^{(2)} = \sum_{\ell=1}^{L} \theta_\ell \sqrt{P_{R_\ell D}} \mathbf{h}_{R_\ell D} x_{R_\ell,k} + \mathbf{n}_{D,k}^{(2)} \tag{5.3}$$

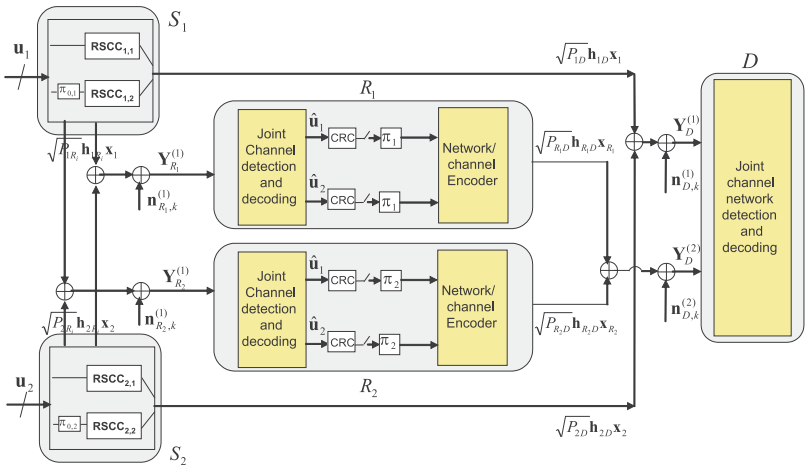

Figure 5.1: System model (relay cooperates)

for $k = 1, \ldots, \bar{\alpha}N$. In (5.3), the channel fading vectors $\mathbf{h}_{R_\ell D} \in \mathbb{C}^{N_D}$ are mutually independent and follow the pdf $\mathcal{CN}(\mathbf{0}_{N_D}, \mathbf{I}_{N_D})$. They are independent of $\mathbf{h}_{iD}$, $i \in \{1, \ldots, M\}$, constant over the transmission of $\mathbf{x}_{R_\ell}$ and changes independently from one transmission of the relays to another. The additive noise vector $\mathbf{n}_{D,k}^{(2)}$ is independent of $\mathbf{n}_{R_\ell,k}^{(1)}$ and $\mathbf{n}_{D,k}^{(1)}$, and follows the pdf $\mathcal{CN}(\mathbf{0}_{N_D}, N_0\mathbf{I}_{N_D})$. $P_{R_\ell D} \propto (d_{R_\ell D}/d_0)^{-\kappa} P_{R_\ell}$, with P_{R_ℓ} the transmit power of R_ℓ, is the average received power per dimension and per antenna at the destination. Here again, we fix the total energy per available dimensions NP_{0,R_ℓ} spent by R_ℓ, i.e., $P_{R_\ell} = P_{0,R_\ell}/\bar{\alpha}$. The parameter θ_ℓ is a discrete Bernoulli distributed random variable: $\theta_\ell = 1$ if the relay R_ℓ successfully decodes at least one source message, and $\theta_\ell = 0$ otherwise.

Concerning the relay functionalities, we distinguish the two cases of JNCC and SNCC:

- JNCC: The relay R_ℓ interleaves each message $\mathbf{u}_i$, $i \in J_\ell$, by π_ℓ and applies a function $\Theta_{R_\ell,|J_\ell|}$

$$\Theta_{R_\ell,|J_\ell|} : \underbrace{\mathbb{F}_2^K \times \mathbb{F}_2^K \times \ldots \times \mathbb{F}_2^K}_{|J_\ell|} \to \mathbb{C}^{\bar{\alpha}N} \tag{5.4}$$

  to obtain the modulated sequence $\mathbf{x}_{R_\ell}$. In general, the function $\Theta_{R_\ell,|J_\ell|}$ is not a bijection on the interleaved correctly decoded messages. In practice, each relay would add some in-band signaling to make the destination aware of the set J_ℓ. Finally, the relay signals, together with the source signals, form a distributed joint network-channel codebook. The block diagram of the system model is depicted in Fig. 5.1 for the case of $M = L = 2$.

- SNCC: The relay R_ℓ combines linearly the messages $\mathbf{u}_i$, $i \in J_\ell$ in $\mathbb{F}_q$, which is then mapped to $\mathbf{x}_{R_\ell}$ using the codebook ζ_{R_ℓ} of rate $K/\bar{\alpha}N$.

5.2 Information-theoretic Analysis

In this section, for the sake of notational simplicity, we consider $M = 2$ sources and $L = 2$ relays. The sources transmit with an overall spectral efficiency $r = K/N$. For the specific case of SNCC, we can associate the same spectral efficiency r to the relay transmissions. The generalization to the cases of $M, L > 2$ is straightforward. The SOMAMRC breaks down into three MACs at the relays and destination corresponding to the first transmission phase, and one MAC at the destination corresponding to the second phase, thanks to the SDF relaying function. Thus, its outage region is perfectly known conditional on a given channel state $\mathbf{H} = \left[\begin{array}{cccccccc} \mathbf{h}_{1R_1} & \mathbf{h}_{1R_2} & \mathbf{h}_{2R_1} & \mathbf{h}_{2R_2} & \mathbf{h}_{1D} & \mathbf{h}_{2D} & \mathbf{h}_{R_1D} & \mathbf{h}_{R_2D} \end{array} \right]$. Let us define the independent input random variables $x_i \sim p(x_i)$ and $x_{R_i} \sim p(x_{R_i})$, $i \in \{1, 2\}$, and the associated independent output random vectors $\mathbf{y}_D^{(1)}$, $\mathbf{y}_D^{(2)}$ and $\mathbf{y}_{R_i}^{(1)}$ whose channel transition conditional pdfs follow the ones associated to (5.2), (5.3), and (5.1), respectively. It follows that the mutual informations $I(x_1, x_2; \mathbf{y}_D^{(1)})$, $I(x_{R_1}, x_{R_2}; \mathbf{y}_D^{(2)})$ and $I(x_1, x_2; \mathbf{y}_R^{(1)})$ are perfectly defined by the pdfs $p(x_i)$, $p(x_{R_i})$ and the aforementioned channel transition probabilities. It is clear from our context that the mutual information conditional on any given channel state is maximized for the pdfs $p(x_i)$, $p(x_{R_i})$ being circularly symmetric complex Gaussian pdfs. As a result, the latter pdfs minimize the information outage probabilities. However, in practice, $p(x_i)$, $p(x_{R_i})$ are uniformly distributed pmfs (dirac comb pdfs) over the chosen constellation alphabets. That is why both cases are investigated in the following. We recall that in our analysis:

1. The theoretical bounds are derived conditional on both JNCC and SNCC.

2. The SDF relaying function is used under the hypothesis that all the links are prone to errors.

3. The sequences $\mathbf{x}_i$ and $\mathbf{x}_{R_i}$, $i \in \{1, 2\}$, are the outcomes of independent discrete time i.i.d. processes whose associated pdfs are $p(x_i)$ and $p(x_{R_i})$ and their respective length is infinite ($N \to \infty$) such that the AEP holds.

4. The outage limit is either the individual information outage probability or the individual ϵ-outage achievable rate (e.g., for S_1). The efficiency of our proposed JNCC/JNCD is evaluated in terms of gap to the information outage probability, keeping in mind that the information outage probability remains a relevant measure of the best possible BLER even for finite code lengths [119].

5.2.1 Outage analysis of SOMAMRC/JNCC

As each relay uses a SDF approach, an evaluation of the source-to-relay channel qualities has first to be processed. Let $\mathcal{E}_{R_\ell}(\mathbf{H})$ denote the outage event of the MAC between the sources and the relay R_ℓ, $\ell \in \{1,2\}$, conditional on $\mathbf{H}$. It corresponds to the case where R_ℓ cannot decode both messages correctly, and can be expressed as

$$\mathcal{E}_{R_\ell}(\mathbf{H}) = \mathcal{E}_{R_\ell,1|2}(\mathbf{H}) \cup \mathcal{E}_{R_\ell,2|1}(\mathbf{H}) \cup \mathcal{E}_{R_\ell,1,2}(\mathbf{H}) \tag{5.5}$$

where $\mathcal{E}_{R_\ell,i|j}(\mathbf{H})$, $i,j \in \{1,2\}$, $j \neq i$ is the outage event of S_i if the information of S_j is known, and $\mathcal{E}_{R_\ell,1,2}(\mathbf{H})$ is the outage event of both sources at R_ℓ. The three possible outage events are then given by

$$\mathcal{E}_{R_\ell,i|j}(\mathbf{H}) = \left\{\alpha I(x_i; \mathbf{y}_{R_\ell}^{(1)} \mid x_j) < r\right\} \tag{5.6}$$

$$\mathcal{E}_{R_\ell,1,2}(\mathbf{H}) = \left\{\alpha I(x_1, x_2; \mathbf{y}_{R_\ell}^{(1)}) < 2r\right\} \tag{5.7}$$

When the outage event $\mathcal{E}_{R_\ell}(\mathbf{H})$ holds, in order to verify whether only one of the messages $\mathbf{x}_i$ can be successfully decoded or not, we define the following outage event

$$\mathcal{E}_{R_\ell,i}(\mathbf{H}) = \left\{\alpha I(x_i; \mathbf{y}_{R_\ell}^{(1)}) < r\right\} \tag{5.8}$$

in which R_ℓ treats the signal $\mathbf{x}_j$ as interference. Thus, the outage events of R_ℓ for the SDF approach can be summarized as follows: (1) In case of $\mathcal{Q}_{R_\ell}^{(1)}(\mathbf{H}) = \bar{\mathcal{E}}_{R_\ell}(\mathbf{H})$, which indicates the complement of the outage event $\mathcal{E}_{R_\ell}(\mathbf{H})$, R_ℓ cooperates with both sources; (2) In case of $\mathcal{Q}_{R_\ell}^{(2)}(\mathbf{H}) = \mathcal{E}_{R_\ell}(\mathbf{H}) \cap \bar{\mathcal{E}}_{R_\ell,1}(\mathbf{H})$, R_ℓ cooperates only with S_1; (3) In case of $\mathcal{Q}_{R_\ell}^{(3)}(\mathbf{H}) = \mathcal{E}_{R_\ell}(\mathbf{H}) \cap \bar{\mathcal{E}}_{R_\ell,2}(\mathbf{H})$, R_ℓ cooperates only with S_2; (4) Otherwise, in case of $\mathcal{Q}_{R_\ell}^{(4)}(\mathbf{H}) = \mathcal{E}_{R_\ell}(\mathbf{H}) \cap \mathcal{E}_{R_\ell,1}(\mathbf{H}) \cap \mathcal{E}_{R_\ell,2}(\mathbf{H})$, R_ℓ does not cooperate. Now, depending on both relay transmissions, sixteen different outage events can be distinguished at the destination. In the sequel, Case m,n corresponds to the case of having the outage event $\mathcal{Q}_{R_1}^{(m)}$ at R_1 and $\mathcal{Q}_{R_2}^{(n)}$ at R_2, $m,n \in \{1,\cdots,4\}$.

Case 1,1: Both relays cooperate with both sources. The destination always receives the cooperative information from both relays during the second phase. Since the source-to-destination and the relay-to-destination MACs are orthogonal, they can be seen as two parallel MACs. As a result, the outage at the destination occurs if the target rate exceeds the sum of the mutual informations of the two parallel MACs. Let $\mathcal{E}_D^{(1,1)}(\mathbf{H})$ denote the

outage event at the destination conditional on $\mathbf{H}$. It can be expressed as

$$\mathcal{E}_D^{(1,1)}(\mathbf{H}) = \mathcal{E}_{D,1|2}^{(1,1)}(\mathbf{H}) \cup \mathcal{E}_{D,2|1}^{(1,1)}(\mathbf{H}) \cup \mathcal{E}_{D,1,2}^{(1,1)}(\mathbf{H}). \tag{5.9}$$

where

$$\mathcal{E}_{D,i|j}^{(1,1)}(\mathbf{H}) = \left\{ \alpha I(x_i; \mathbf{y}_D^{(1)} \mid x_j) + \bar{\alpha} I(\widetilde{\mathbf{x}}; \mathbf{y}_D^{(2)}) < r \right\} \tag{5.10}$$

for $i, j \in \{1, 2\}$ and $j \neq i$, and

$$\mathcal{E}_{D,1,2}^{(1,1)}(\mathbf{H}) = \left\{ \alpha I(x_1, x_2; \mathbf{y}_D^{(1)}) + \bar{\alpha} I(x_{R_1}, x_{R_2}; \mathbf{y}_D^{(2)}) < 2r \right\}. \tag{5.11}$$

In (5.10), $\mathcal{E}_{D,i|j}^{(1,1)}(\mathbf{H})$, $i \in \{1, 2\}$ is the outage event of S_i if the information of S_j, $j \neq i$, is known. In this case, $\mathbf{x}_{R_1}$ and $\mathbf{x}_{R_2}$ can be considered as part of the codewords of S_i. Since the signals of R_1 and R_2 are independent (thanks to the JNCC interleavers π_1 and π_2), the second term of the sum in (5.10) can be derived from the equivalent MIMO channel

$$\mathbf{y}_D^{(2)} = \widetilde{\mathbf{H}}\, \mathbf{K}\, \widetilde{\mathbf{x}} + \mathbf{n}_D^{(2)} \tag{5.12}$$

where $\widetilde{\mathbf{x}} = [x_{R_1} \;\; x_{R_2}]^\top$, $\widetilde{\mathbf{H}} = [\mathbf{h}_{R_1 D} \;\; \mathbf{h}_{R_2 D}]$, and $\mathbf{K} = \text{diag}(\sqrt{P_{R_1 D}}, \sqrt{P_{R_2 D}})$. The outage event in (5.11) corresponds to the constraint that the total throughput cannot exceed the sum of the mutual informations of (1) a point-to-point MIMO channel with the aggregate received signals of the two sources corresponding to the first phase, and (2) a point-to-point MIMO channel with the aggregate received signals of the two relays corresponding to the second phase. When $\mathcal{E}_D^{(1,1)}(\mathbf{H})$ holds, the destination cannot decode both source messages correctly. As we are interested in calculating the outage event of S_1, we define the following event

$$\mathcal{E}_{D,1}^{(1,1)}(\mathbf{H}) = \left\{ \alpha I(x_1; \mathbf{y}_D^{(1)}) < r \right\} \tag{5.13}$$

in which the destination treats the signal $\mathbf{x}_2$ as interference. It is worth noting that the relay transmissions in this case cannot help S_1 as they contain the interference from S_2. Finally, the outage event of S_1 is calculated as $\mathcal{O}_{D,1}^{(1,1)}(\mathbf{H}) = \mathcal{E}_D^{(1,1)}(\mathbf{H}) \cap \mathcal{E}_{D,1}^{(1,1)}(\mathbf{H})$.

Case 1,2 - Case 2,1: One of the relays cooperates with both sources and the other cooperates only with S_1. Let first consider the Case 1,2. The outage event at the destination $\mathcal{E}_D^{(1,2)}(\mathbf{H})$ is calculated as

$$\mathcal{E}_D^{(1,2)}(\mathbf{H}) = \mathcal{E}_{D,1|2}^{(1,2)}(\mathbf{H}) \cup \mathcal{E}_{D,2|1}^{(1,2)}(\mathbf{H}) \cup \mathcal{E}_{D,1,2}^{(1,2)}(\mathbf{H}). \tag{5.14}$$

where

$$\mathcal{E}_{D,1|2}^{(1,2)}(\mathbf{H}) = \left\{\alpha I(x_1; \mathbf{y}_D^{(1)} \mid x_2) + \bar{\alpha} I(\widetilde{\mathbf{x}}; \mathbf{y}_D^{(2)}) < r\right\} \tag{5.15}$$

$$\mathcal{E}_{D,2|1}^{(1,2)}(\mathbf{H}) = \left\{\alpha I(x_2; \mathbf{y}_D^{(1)} \mid x_1) + \bar{\alpha} I(x_{R_1}; \mathbf{y}_D^{(2)} \mid x_{R_2}) < r\right\} \tag{5.16}$$

$$\mathcal{E}_{D,1,2}^{(1,2)}(\mathbf{H}) = \left\{\alpha I(x_1, x_2; \mathbf{y}_D^{(1)}) + \bar{\alpha} I(x_{R_1}, x_{R_2}; \mathbf{y}_D^{(2)}) < 2r\right\} \tag{5.17}$$

In (5.15), $\widetilde{\mathbf{x}} = [x_{R_1} \ x_{R_2}]^\top$, and the second term of the sum is deduced from an equivalent MIMO channel as in (5.12). Note that in (5.16), since the information of S_1 is supposed to be known and R_2 cooperates only with S_1, the transmitted signal from R_2 is known as well. Thus, there is no interference on the signal transmitted by R_1 during the second transmission phase. Now, in order to calculate the outage event of S_1, we define the following event

$$\mathcal{E}_{D,1}^{(1,2)}(\mathbf{H}) = \left\{\alpha I(x_1; \mathbf{y}_D^{(1)}) + \bar{\alpha} I(x_{R_2}; \mathbf{y}_D^{(2)}) < r\right\} \tag{5.18}$$

in which the destination treats the signal $\mathbf{x}_2$ and $\mathbf{x}_{R_1}$ as interferences during the first and second transmission phases. Finally, the outage event of S_1 is calculated as $\mathcal{O}_{D,1}^{(1,2)}(\mathbf{H}) = \mathcal{E}_D^{(1,2)}(\mathbf{H}) \cap \mathcal{E}_{D,1}^{(1,2)}(\mathbf{H})$. The outage event $\mathcal{O}_{D,1}^{(2,1)}(\mathbf{H})$ is calculated in a similar manner, by swapping the roles of R_1 and R_2.

Case 1,3 - Case 3,1: One of the relays cooperates with both sources and the other cooperates only with S_2. Let first consider the Case 1,3. Swapping the roles of S_1 and S_2, the outage event at the destination $\mathcal{E}_D^{(1,3)}(\mathbf{H})$ is identical to the Case 1,2. In order to calculate the outage event of the source S_1, we define the event $\mathcal{E}_{D,1}^{(1,3)}(\mathbf{H})$ as in (5.13). Thus, the outage event of S_1 is calculated as $\mathcal{O}_{D,1}^{(1,3)}(\mathbf{H}) = \mathcal{E}_D^{(1,3)}(\mathbf{H}) \cap \mathcal{E}_{D,1}^{(1,3)}(\mathbf{H})$. The outage event $\mathcal{O}_{D,1}^{(3,1)}(\mathbf{H})$ is calculated in a similar manner, by swapping the roles of R_1 and R_2.

Case 2,2: Both relays cooperate only with S_1. The outage event at the destination $\mathcal{E}_D^{(2,2)}(\mathbf{H})$ is calculated as

$$\mathcal{E}_D^{(2,2)}(\mathbf{H}) = \mathcal{E}_{D,1|2}^{(2,2)}(\mathbf{H}) \cup \mathcal{E}_{D,2|1}^{(2,2)}(\mathbf{H}) \cup \mathcal{E}_{D,1,2}^{(2,2)}(\mathbf{H}). \tag{5.19}$$

where

$$\mathcal{E}_{D,1|2}^{(2,2)}(\mathbf{H}) = \left\{\alpha I(x_1; \mathbf{y}_D^{(1)} \mid x_2) + \bar{\alpha} I(\widetilde{\mathbf{x}}; \mathbf{y}_D^{(2)}) < r\right\} \tag{5.20}$$

$$\mathcal{E}_{D,2|1}^{(2,2)}(\mathbf{H}) = \left\{\alpha I(x_2; \mathbf{y}_D^{(1)} \mid x_1) < r\right\} \tag{5.21}$$

$$\mathcal{E}_{D,1,2}^{(2,2)}(\mathbf{H}) = \left\{\alpha I(x_1, x_2; \mathbf{y}_D^{(1)}) + \bar{\alpha} I(x_{R_1}, x_{R_2}; \mathbf{y}_D^{(2)}) < 2r\right\}. \tag{5.22}$$

In (5.20), $\widetilde{\mathbf{x}} = [x_{R_1} \ x_{R_2}]^\top$, and as already mentioned, the second term of the sum is deduced from an equivalent MIMO channel. In order to calculate the outage event of S_1, we define the following event

$$\mathcal{E}_{D,1}^{(2,2)}(\mathbf{H}) = \left\{ \alpha I(x_1; \mathbf{y}_D^{(1)}) + \bar{\alpha} I(\widetilde{\mathbf{x}}; \mathbf{y}_D^{(2)}) < r \right\} \tag{5.23}$$

in which the destination treats the signal $\mathbf{x}_2$ as interference during the first transmission phase. Finally, the outage event of S_1 is calculated as $\mathcal{O}_{D,1}^{(2,2)}(\mathbf{H}) = \mathcal{E}_D^{(2,2)}(\mathbf{H}) \cap \mathcal{E}_{D,1}^{(2,2)}(\mathbf{H})$.

Case 3,3: Both relays cooperate only with S_2. Swapping the roles of S_1 and S_2, the outage event at the destination $\mathcal{E}_D^{(3,3)}(\mathbf{H})$ is identical to the Case 2,2. In order to calculate the outage event of the source S_1, we define the event $\mathcal{E}_{D,1}^{(3,3)}(\mathbf{H})$ as in (5.13). Thus, the outage event of S_1 is calculated as $\mathcal{O}_{D,1}^{(3,3)}(\mathbf{H}) = \mathcal{E}_D^{(3,3)}(\mathbf{H}) \cap \mathcal{E}_{D,1}^{(3,3)}(\mathbf{H})$.

Case 2,3 - Case 3,2: One of the relays cooperates only with S_1 and the other cooperates only with S_2. Let first consider the Case 2,3. The outage event at the destination $\mathcal{E}_D^{(2,3)}(\mathbf{H})$ is calculated as

$$\mathcal{E}_D^{(2,3)}(\mathbf{H}) = \mathcal{E}_{D,1|2}^{(2,3)}(\mathbf{H}) \cup \mathcal{E}_{D,2|1}^{(2,3)}(\mathbf{H}) \cup \mathcal{E}_{D,1,2}^{(2,3)}(\mathbf{H}). \tag{5.24}$$

where

$$\mathcal{E}_{D,1|2}^{(2,3)}(\mathbf{H}) = \left\{ \alpha I(x_1; \mathbf{y}_D^{(1)} \mid x_2) + \bar{\alpha} I(x_{R_1}; \mathbf{y}_D^{(2)} \mid x_{R_2}) < r \right\} \tag{5.25}$$

$$\mathcal{E}_{D,2|1}^{(2,3)}(\mathbf{H}) = \left\{ \alpha I(x_2; \mathbf{y}_D^{(1)} \mid x_1) + \bar{\alpha} I(x_{R_2}; \mathbf{y}_D^{(2)} \mid x_{R_1}) < r \right\} \tag{5.26}$$

$$\mathcal{E}_{D,1,2}^{(2,3)}(\mathbf{H}) = \left\{ \alpha I(x_1, x_2; \mathbf{y}_D^{(1)}) + \bar{\alpha} I(x_{R_1}, x_{R_2}; \mathbf{y}_D^{(2)}) < 2r \right\}. \tag{5.27}$$

In order to calculate the outage event of S_1, we define the following event

$$\mathcal{E}_{D,1}^{(2,3)}(\mathbf{H}) = \left\{ \alpha I(x_1; \mathbf{y}_D^{(1)}) + \bar{\alpha} I(x_{R_1}; \mathbf{y}_D^{(2)}) < r \right\} \tag{5.28}$$

in which the destination treats the signal $\mathbf{x}_2$ and $\mathbf{x}_{R_2}$ as interferences during the first and second transmission phases. Finally, the outage event of S_1 is calculated as $\mathcal{O}_{D,1}^{(2,3)}(\mathbf{H}) = \mathcal{E}_D^{(2,3)}(\mathbf{H}) \cap \mathcal{E}_{D,1}^{(2,3)}(\mathbf{H})$. The outage event $\mathcal{O}_{D,1}^{(3,2)}(\mathbf{H})$ is calculated in a similar manner, by swapping the roles of R_1 and R_2.

Case m,4 - Case 4,n: In these cases, at least, one of the relays does not cooperate, and thus, the SOMAMRC becomes HD-SOMARC. The outage events $\mathcal{O}_{D,1}^{(m,4)}(\mathbf{H})$ and $\mathcal{O}_{D,1}^{(4,n)}(\mathbf{H})$, $m, n \in \{1, \cdots, 4\}$, are calculated as in the case of HD-SOMARC/JNCC [136].

Finally, the outage event of S_1 in the error-prone SOMAMRC/JNCC, can be expressed as

$$\mathcal{O}_{D,1}(\mathbf{H}) = \bigcup_{m,n=1}^{4} \left(\mathcal{Q}_{R_1}^{(m)}(\mathbf{H}) \cap \mathcal{Q}_{R_2}^{(n)}(\mathbf{H}) \cap \mathcal{O}_{D,1}^{(m,n)}(\mathbf{H}) \right). \tag{5.29}$$

The above outage event is conditional on the channel state $\mathbf{H}$. The information outage probability for S_1 is then obtained as

$$P_{out,1} = \int_{\mathbf{H}} [\mathcal{O}_{D,1}(\mathbf{H})] \;\; p(\mathbf{H}) d(\mathbf{H}) \tag{5.30}$$

where $p(\mathbf{H})$ is the pdf of $\mathbf{H}$. The ϵ-outage achievable rate of S_1 is defined as the largest rate of S_1 such that its corresponding information outage probability for a given transmission protocol, is smaller than or equal to ϵ.

5.2.2 Outage analysis of SOMAMRC/SNCC

In the case of SNCC/SNCD, we still have three MACs at the relays and destination corresponding to the first time slot, and one MAC at the destination corresponding to the second time slot. The outage event analysis at the relays remains the same as in (5.2.1). However, the received signals at the destination from the sources and the relays are now decoded separately. Therefore, the outage event analyses at the destination related to the first and second time slots exactly follows the one of the relays. More specifically, the outage events $\mathcal{E}_D(\mathbf{H})$, $\mathcal{E}_{D,1}(\mathbf{H})$, $\mathcal{E}_{D,2}(\mathbf{H})$ are defined similarly to $\mathcal{E}_{R_\ell}(\mathbf{H})$, $\mathcal{E}_{R_\ell,1}(\mathbf{H})$, $\mathcal{E}_{R_\ell,2}(\mathbf{H})$ (by replacing the subscript R_ℓ by D). $\mathcal{E}_{RD}(\mathbf{H})$, $\mathcal{E}_{RD,1}(\mathbf{H})$, $\mathcal{E}_{RD,2}(\mathbf{H})$ which correspond to the relay-to-destination MAC, are also defined similarly to $\mathcal{E}_{R_\ell}(\mathbf{H})$, $\mathcal{E}_{R_\ell,1}(\mathbf{H})$, $\mathcal{E}_{R_\ell,2}(\mathbf{H})$, i.e., by replacing $\mathbf{y}_{R_\ell}^{(1)}$ by $\mathbf{y}_D^{(2)}$, x_i by x_{R_i}, and α by $\bar{\alpha}$. Now, depending on the relays transmitted signals, we distinguish the following cases at the destination:

Case 1,1: Both relays cooperate with both sources. If the message of S_1 cannot be correctly decoded from the source-to-destination MAC, it can be recovered, provided that the destination can decode successfully, at least, two out of the three messages corresponding to S_2, R_1 and R_2. Thus, the outage event of S_1 is calculated as

$$\begin{aligned} \mathcal{O}_{D,1}^{(1,1)}(\mathbf{H}) &= \left(\mathcal{E}_D(\mathbf{H}) \cap \left(\bigcap_{i=1,2} \mathcal{E}_{D,i}(\mathbf{H}) \right) \cap \mathcal{E}_{RD}(\mathbf{H}) \right) \\ &\cup \left(\mathcal{E}_D(\mathbf{H}) \cap \bar{\mathcal{E}}_{D,2}(\mathbf{H}) \cap \mathcal{E}_{RD}(\mathbf{H}) \cap \left(\bigcap_{i=1,2} \mathcal{E}_{RD,i}(\mathbf{H}) \right) \right). \end{aligned} \tag{5.31}$$

Case 1,2 - Case 2,1: One of the relays cooperates with both sources and the other cooperates only with S_1. Let first consider the Case 1,2. The outage event of S_1 is calculated as

$$\begin{aligned}\mathcal{O}_{D,1}^{(1,2)}(\mathbf{H}) &= \left(\mathcal{E}_D(\mathbf{H}) \cap \left(\bigcap_{i=1,2} \mathcal{E}_{D,i}(\mathbf{H})\right) \cap \mathcal{E}_{RD}(\mathbf{H}) \cap \mathcal{E}_{RD,2}(\mathbf{H})\right) \\ &\cup \left(\mathcal{E}_D(\mathbf{H}) \cap \bar{\mathcal{E}}_{D,2}(\mathbf{H}) \cap \mathcal{E}_{RD}(\mathbf{H}) \cap \left(\bigcap_{i=1,2} \mathcal{E}_{RD,i}(\mathbf{H})\right)\right). \end{aligned} \tag{5.32}$$

The outage event $\mathcal{O}_{D,1}^{(2,1)}(\mathbf{H})$ is calculated in a similar manner, by swapping the roles of R_1 and R_2.

Case 1,3 - Case 3,1: One of the relays cooperates with both sources and the other cooperates only with S_2. Let first consider the Case 1,3. If the message of S_2 is decoded successfully from one of the two MACs corresponding to the first or second time slot, the interference of it could be removed from the other MAC which becomes then a point-to-point channel. Let denote by $\mathcal{E}_{D,1|2}(\mathbf{H})$ and $\mathcal{E}_{RD,1|2}(\mathbf{H})$ the outage events corresponding to S_1 and R_1 if the message of S_2 is known, i.e. $\mathbf{x}_2$ and $\mathbf{x}_{R_2}$ are both known. The outage event of S_1 is then derived as

$$\begin{aligned}\mathcal{O}_{D,1}^{(1,3)}(\mathbf{H}) =& \left(\mathcal{E}_D(\mathbf{H}) \cap \bar{\mathcal{E}}_{D,2}(\mathbf{H}) \cap \mathcal{E}_{RD,1|2}(\mathbf{H})\right) \cup \left(\mathcal{E}_{RD}(\mathbf{H}) \cap \bar{\mathcal{E}}_{RD,2}(\mathbf{H}) \cap \mathcal{E}_{D,1|2}(\mathbf{H})\right) \\ &\cup \left(\mathcal{E}_D(\mathbf{H}) \cap \left(\bigcap_{i=1,2} \mathcal{E}_{D,i}(\mathbf{H})\right) \cap \mathcal{E}_{RD}(\mathbf{H}) \cap \mathcal{E}_{RD,2}(\mathbf{H})\right) \end{aligned} \tag{5.33}$$

The outage event $\mathcal{O}_{D,1}^{(3,1)}(\mathbf{H})$ is calculated in a similar manner, by swapping the roles of R_1 and R_2.

Case 2,2: Both relays cooperate only with S_1. We define

$$\mathcal{E}_{\widetilde{RD}}(\mathbf{H}) = \left\{\bar{\alpha} I(\widetilde{\mathbf{x}}; \mathbf{y}_D^{(2)}) < r\right\} \tag{5.34}$$

which is derived from an equivalent MIMO channel as in (5.12) with $\widetilde{\mathbf{x}} = [x_{R_1} \;\; x_{R_2}]^\top$. The outage event of S_1 is then calculated as

$$\mathcal{O}_{D,1}^{(2,2)}(\mathbf{H}) = \left(\mathcal{E}_D(\mathbf{H}) \cap \mathcal{E}_{D,1}(\mathbf{H}) \cap \mathcal{E}_{\widetilde{RD}}(\mathbf{H})\right). \tag{5.35}$$

Case 3,3: Both relays cooperate only with S_2. We define $\mathcal{E}_{\widetilde{RD}}(\mathbf{H})$ as in (5.34). The outage event of S_1 is then calculated as

$$\mathcal{O}_{D,1}^{(3,3)}(\mathbf{H}) = \left(\mathcal{E}_D(\mathbf{H}) \cap \mathcal{E}_{D,1}(\mathbf{H}) \cap \mathcal{E}_{\widetilde{RD}}(\mathbf{H})\right) \cup \left(\bar{\mathcal{E}}_{\widetilde{RD}}(\mathbf{H}) \cap \mathcal{E}_{D,1|2}(\mathbf{H})\right). \tag{5.36}$$

Case 2,3 - Case 3,2: One of the relays cooperates only with S_1 and the other cooperates only with S_2. Let first consider the Case 2,3. The outage event of S_1 is calculated as

$$\begin{aligned}\mathcal{O}_{D,1}^{(2,3)}(\mathbf{H}) &= \left(\mathcal{E}_D(\mathbf{H}) \cap \left(\bigcap_{i=1,2} \mathcal{E}_{D,i}(\mathbf{H})\right) \cap \mathcal{E}_{RD}(\mathbf{H}) \cap \left(\bigcap_{i=1,2} \mathcal{E}_{RD,i}(\mathbf{H})\right)\right) \\ &\cup \left(\mathcal{E}_{RD}(\mathbf{H}) \cap \bar{\mathcal{E}}_{RD,2}(\mathbf{H}) \cap \mathcal{E}_{D,1|2}(\mathbf{H})\right) \\ &\cup \left(\mathcal{E}_D(\mathbf{H}) \cap \bar{\mathcal{E}}_{D,2}(\mathbf{H}) \cap \mathcal{E}_{RD,1|2}(\mathbf{H})\right). \end{aligned} \tag{5.37}$$

The outage event $\mathcal{O}_{D,1}^{(3,2)}(\mathbf{H})$ is calculated in a similar manner, by swapping the roles of R_1 and R_2.

Case m,4 - Case 4,n: In these cases, at least, one of the relays does not cooperate, and thus, the SOMAMRC becomes HD-SOMARC. The outage events $\mathcal{O}_{D,1}^{(m,4)}(\mathbf{H})$ and $\mathcal{O}_{D,1}^{(4,n)}(\mathbf{H})$, $m, n \in \{1, \cdots, 4\}$, are calculated as in the case of HD-SOMARC/SNCC (see Section 2.2.2 of Chapter 2).

Finally, the outage event of S_1 in the error-prone SOMAMRC/SNCC can be expressed as

$$\mathcal{O}_{D,1}(\mathbf{H}) = \bigcup_{m,n=1}^{4} \left(\mathcal{Q}_{R_1}^{(m)}(\mathbf{H}) \cap \mathcal{Q}_{R_2}^{(n)}(\mathbf{H}) \cap \mathcal{O}_{D,1}^{(m,n)}(\mathbf{H})\right). \tag{5.38}$$

Here again, the outage event $\mathcal{O}_{D,1}(\mathbf{H})$ is conditional on the channel state $\mathbf{H}$, and the information outage probability for S_1 is derived as

$$P_{out,1} = \int_{\mathbf{H}} \left[\mathcal{O}_{D,1}(\mathbf{H})\right] \; p(\mathbf{H}) d(\mathbf{H}). \tag{5.39}$$

5.2.3 Types of input distributions

We consider both Gaussian i.i.d. inputs and discrete i.i.d. inputs (for practical considerations as explained in Chapter 2) to calculate the mutual information. The corresponding expressions are given in Appendix B.

5.2.4 Information outage probability achieving codebooks

To achieve the information outage probability bounds, the codebooks ζ_i, ζ_{iR_j}, ζ_{12R_j}, $i, j \in \{1, 2\}$, should be universal codebooks. As defined in [127], a universal codebook of a given rate is a codebook that simultaneously achieves reliable communication over every channel that is not in outage for the chosen rate. Finally, it is worth stressing that, in practice, there exist codebooks with finite lengths whose performance are very close to the ones of universal codebooks. The simulation Section 5.5 exemplifies such codebook constructions based on convolutional or turbo codes.

5.3 Joint Network Channel Coding and Decoding

In this section, we make explicit our proposed JNCC/JNCD approach. We explain the structure of the encoders, when and how JNCC is performed, and the structure of the corresponding multiuser receivers.

5.3.1 Coding at the sources

The messages of the sources are binary vectors $\mathbf{u}_i \in \mathbb{F}_2^K$ of length K, $i \in \{1, \cdots, M\}$. Each source employs a BICM [128]. Binary vectors are first encoded with linear systematic binary encoders $C_i : \mathbb{F}_2^K \to \mathbb{F}_2^{n_i}$, $i = \{1, \cdots, M\}$ into binary codewords $\mathbf{c}_i \in \mathbb{F}_2^{n_i}$ of respective lengths n_i. The codes ζ_i are in general punctured turbo codes, consisting of two RSC encoders, denoted by $\text{RSC}_{i,1}$ and $\text{RSC}_{i,2}$, concatenated in parallel using optimized semi-random interleavers $\pi_{0,i}$. The coded bits are then interleaved using interleavers Π_i and reshaped as two binary matrices $\mathbf{V}_i \in \mathbb{F}_2^{\alpha N \times q_i}$. Memoryless modulators based on one-to-one binary labeling maps $\phi_i : \mathbb{F}_2^{q_i} \to \mathscr{X}_i$ transform the binary arrays $\mathbf{V}_i$ into the complex vectors $\mathbf{x}_i \in \mathscr{X}_i^{\alpha N}$. For ϕ_i, we choose Gray labeling. In the sequel, we denote by $v_{i,k,m} = \phi_{i,m}^{-1}(x_{i,k})$ the m-th bit of the binary labeling of each symbol $x_{i,k}$ for $i \in \{1, \cdots, M\}$ and $k = 1, \cdots, \alpha N$.

5.3.2 Relaying Functions

The processing at each relay is divided in two steps: During the first time slot, based on (5.1), each relay performs a joint detection and decoding procedure to obtain the hard binary estimation of the information bits, $\hat{\mathbf{u}}_i \in \mathbb{F}_2^K$. Based on this estimation, each relay chooses a SDF approach for cooperation. Different cases can then be distinguished, depending on the number of successfully decoded messages. In the sequel, first, we briefly describe

the detection and decoding algorithm at each relay, and then, we detail our proposed JNCC scheme.

5.3.2.1 Relay detection and decoding

The joint detection and decoding is performed in a suboptimal iterative way [129]. An inner SISO MAP detector generates extrinsic information on coded bits using the received signal (5.1) and a priori information coming from the outer SISO decoders SISO_i (referring to the decoding of ζ_i, $i \in \{1, \cdots, M\}$). For the general case of turbo codes at the sources, the outer SISO decoder of S_i generates extrinsic information on both systematic and coded bits of S_i by activating the SISO decoder $\text{SISO}_{i,1}$ corresponding to $\text{RSC}_{i,1}$, and then $\text{SISO}_{i,2}$ corresponding to $\text{RSC}_{i,2}$. It is important to remember that each SISO decoding stage takes into account all the available a priori information on systematic bits [130] (and Algorithm 5 of Section 5.3.3.2). The extrinsic information on the source codewords is then interleaved and fed back to the detector, which in turn employs it as a priori information for the next iteration. It is worth noting that the proper (de)multiplexing and (de)puncturing are also performed if needed. The process is repeated until convergence. For the representation of the input/output soft information, we use log ratios of probabilities. At R_ℓ, $\ell \in \{1, \cdots, L\}$, the LAPPR on bit $v_{i,k,m} = \phi_{i,m}^{-1}(x_{i,k})$ delivered by the SISO MAP detector is defined as

$$\Lambda(v_{i,k,m}) = \log \frac{P(v_{i,k,m} = 1 | \mathbf{y}_{R_\ell,k}^{(1)})}{P(v_{i,k,m} = 0 | \mathbf{y}_{R_\ell,k}^{(1)})} \tag{5.40}$$

and, in practice, evaluated as

$$\Lambda(v_{i,k,m}) \simeq \log \frac{\sum_{b_1 \in \mathscr{X}_1, \cdots, b_M \in \mathscr{X}_M : \phi_{i,m}^{-1}(b_i)=1} P(\mathbf{y}_{R_\ell,k}^{(1)} | x_{1,k} = b_1, \cdots, x_{M,k} = b_M) e^{\sum_{j=1}^{M} \xi(b_j)}}{\sum_{b_1 \in \mathscr{X}_1, \cdots, b_M \in \mathscr{X}_M : \phi_{i,m}^{-1}(b_i)=0} P(\mathbf{y}_{R_\ell,k}^{(1)} | x_{1,k} = b_1, \cdots, x_{M,k} = b_M) e^{\sum_{j=1}^{M} \xi(b_j)}} \tag{5.41}$$

for $i, j \in \{1, \cdots, M\}$, $\ell \in \{1, \cdots, L\}$, with,

$$\xi(b_j) = \sum_{m'=1}^{\log_2 |\mathscr{X}_j|} \phi_{j,m'}^{-1}(b_j) E(v_{j,k,m'}) \tag{5.42}$$

where $\{E(v_{j,k,m})\}$ is LAPR on bit $v_{j,k,m}$ provided by the SISO decoders SISO_j. The extrinsic information on bit $v_{i,k,m}$ is given by $L(v_{i,k,m}) = \Lambda(v_{i,k,m}) - E(v_{i,k,m})$, and after de-interleaving, feeds the corresponding outer SISO decoder.

5.3.2.2 JNCC

As previously mentioned, each relay chooses a SDF approach for cooperation, which is based on the number of successfully decoded messages, the knowledge of which being ensured by using CRC codes for each source message. Let $J_\ell \subset \{1, \cdots, M\}$, $|J_\ell| \leq M$ denote the set of message indices that have been successfully decoded at R_ℓ, $\ell \in \{1, \cdots, L\}$. For the case where $J_\ell = \emptyset$, R_ℓ does not cooperate. Otherwise, it interleaves each message $\mathbf{u}_i$, $i \in J_\ell$, by π_ℓ. Memoryless bit to algebraic symbol converter

$$\psi : \underbrace{\mathbb{F}_2 \times \mathbb{F}_2 \times \cdots \times \mathbb{F}_2}_{\log_2(q)} \rightarrow \mathbb{F}_q, \;\; q > 2 \tag{5.43}$$

transforms the interleaved binary vectors into the symbols $\mathbf{w}_i \in \mathbb{F}_q^W$ with $W = \left\lceil \frac{K}{\log_2(q)} \right\rceil$, supposing that each symbol in $\mathbb{F}_q$ has a binary representation containing $\log_2(q)$ bits. The symbols $\mathbf{w}_i$ are then combined linearly in $\mathbb{F}_q$. Let $\mathbf{a}_\ell^{J_\ell} = \begin{bmatrix} a_{1,\ell} & a_{2,\ell} & \cdots & a_{M,\ell} \end{bmatrix}^\top$ with $a_{i,\ell} \in \mathbb{F}_q$ and $\{a_{i,\ell} = 0\}_{i \notin J_\ell}$, denote the vector of network coding coefficients associated to R_ℓ. It follows that $\mathbf{w}_{R_\ell} = \sum_{i \in J_\ell} a_{i,\ell} \mathbf{w}_i$. The vector $\mathbf{u}_{R_\ell} \in \mathbb{F}_2^K$ is then obtained from $\mathbf{w}_{R_\ell}$ by applying ψ^{-1}. In the sequel, we denote by $b_i = \psi_i^{-1}(w)$, $b_i \in \mathbb{F}_2$, the binary representation of each symbol $w \in \mathbb{F}_q$, for $w = \psi(b_1, \cdots, b_{\log_2(q)})$. The vector $\mathbf{u}_{R_\ell}$ is then encoded to $\mathbf{c}_{R_\ell}$ using a binary linear encoder $C_{R_\ell} : \mathbb{F}_2^K \rightarrow \mathbb{F}_2^{n_{R_\ell}}$. For C_{R_ℓ}, we choose an RSC encoder defined by the generator matrix $G_{R_\ell}(D)$, referred to as RSC_{R_ℓ}. A linear transformation $\Omega : \mathbb{F}_2^{n_{R_\ell}} \rightarrow \mathbb{F}_2^{n'_{R_\ell}}$ is applied which selects the parity bits of $\mathbf{c}_{R_\ell}$ to obtain the new vector $\mathbf{c}'_{R_\ell} \in \mathbb{F}_2^{n'_{R_\ell}}$, $n'_{R_\ell} < n_{R_\ell}$. The vector $\mathbf{c}'_{R_\ell}$ is bit-interleaved using the interleaver Π_{R_ℓ} and reshaped as a binary matrix $\mathbf{V}_{R_\ell} \in \mathbb{F}_2^{\bar{\alpha}N \times q_{R_\ell}}$. Finally, a memoryless modulator based on a one-to-one binary labeling map $\phi_{R_\ell} : \mathbb{F}_2^{q_{R_\ell}} \rightarrow \mathscr{X}_{R_\ell}$ transforms the binary array $\mathbf{V}_{R_\ell}$ into the complex vector $\mathbf{x}_{R_\ell} \in \mathscr{X}_{R_\ell}^{\bar{\alpha}N}$. For ϕ_{R_ℓ}, we choose Gray labeling. In the sequel, we denote by $v_{R_\ell,k,m} = \phi_{R_\ell,m}^{-1}(x_{R_\ell,k})$ the m-th bit of the binary labeling of each symbol $x_{R_\ell,k}$ for $k = 1, \cdots, \bar{\alpha}N$ and $\ell = 1, \cdots, L$. Finally, to let the destination detect which of the messages are included in relay signals, each relay transmits side information (additional bits) to indicate its state to the receiver.

As already mentioned, the vectors $\mathbf{a}_\ell$ should be chosen such that the maximum available diversity which is equal to $L + 1$ can be attained. In other words, the following property should hold: if any L links, between the ML source-to-relay links and $M + L$ source-to-destination and relay-to-destination links, are in outage, it should always be possible to retrieve the M source messages. In general, in order to find the network codes meeting the above property, all the possible outage configurations of the ML source-to-relay links should be considered. Let consider an outage configuration of the source-to-relay links containing

$Q \in \{0, 1, \cdots, L\}$ links in outage. The systematic generator matrix $\mathbf{T} = [\mathbf{I}_M \ \mathbf{G}]$, with $\mathbf{G}$ representing the L vectors $\mathbf{a}_\ell$, $\ell \in \{1, \cdots, L\}$, corresponding to each relay, should satisfy the following condition: If any $L-Q$ columns of the matrix $\mathbf{T}$ are eliminated, the remaining $M+Q$ columns have a rank of at least equal to M. The existence of such network coding vectors has been proved in [92] for finite fields of sufficiently high cardinality. However, for large M and L, the exhaustive research becomes extremely complicated. One of the solutions that is usually adopted is to choose a sufficiently high order field and to randomly and independently draw the network coding components. The maximum diversity is not ensured in this case, but the diversity order is in general close to optimal.

In the rest of the chapter, we are interested in small structures and for the sake of notational simplicity, we consider $M = 2$ sources and $L = 2$ relays. Therefore, the network coding vectors that are chosen (in GF(4)) ensure the maximum diversity. This is verified in [92] for the OMARC using SNCC. As shown in Appendix A, the high SNR slope of the outage probability of MAC versus SNR (in dB scale), for the critical case of just one receive antenna, is the same as the one of the orthogonal MAC. Thus, the full diversity design for OMARC remains valid when we have collisions at the relay and destination. Furthermore, as we show later by numerical results, the proposed design ensures full diversity in the case of JNCC.

5.3.3 JNCD at the Destination

The JNCD at the destination depends on the side information received from each relay. As already explained in Section 5.2, sixteen different cases can happen, depending on the error-free decoded messages at each relay. Here, we distinguish six representative scenarios which lead to a change in the JNCD approach. (i) In the case where both relays have successfully decoded both source messages, two distributed turbo codes are formed at the destination, in which the decoders corresponding to C_1 and C_2 exchange information with both of the decoders corresponding to C_{R_1} and C_{R_2}. (ii) In the case where R_ℓ has successfully decoded both source messages and R_m has successfully decoded the information of S_i, $i, \ell, m \in \{1, 2\}$, $\ell \neq m$, we still have two distributed turbo codes at the destination, but the decoder corresponding to C_{R_m} exchange information only with the decoder corresponding to C_i. (iii) In the case where R_ℓ has successfully decoded the information of S_i and R_m has successfully decoded the information of S_j, $i, j, \ell, m \in \{1, 2\}$, $i \neq j$, $\ell \neq m$, we still have two distributed turbo codes at the destination, in which the decoder corresponding to C_{R_ℓ} exchange information only with the decoder corresponding to C_i, and the decoder corresponding to C_{R_m} exchange information only with the decoder corresponding to C_j. (iv) In the case where both relays has successfully decoded the information of S_i, one

distributed turbo code is formed at the destination in which the decoders corresponding to C_i, C_{R_1} and C_{R_2} exchange information, and a separate decoder is used to decode the information of the other source. (v) In the case where one of the relays, say R_ℓ, does not cooperate, the system is equivalent to HD-SOMARC [136]. In all of these cases, at the end of the second transmission time slot, the destination starts to detect and decode the original data, processing the received signals (5.2) and (5.3) (with $\theta_1 = \theta_2 = 1$ for the scenarios $1, \cdots, 4$, and $\theta_\ell = 0$ for the scenario 5). (vi) Finally, in the case where both relays do not cooperate, the destination applies iterative detection and decoding, processing the received signal (5.2), and using the two separate decoders corresponding to C_1 and C_2. Here again, we resort to a suboptimal iterative procedure. Extrinsic information on coded bits circulates between SISO MAP detectors corresponding to both transmission phases (or between SISO MAP detector and demapper in case of $\theta_\ell = 0$) and the outer decoders, while, at the same time, extrinsic information on systematic bits circulates between the SISO decoders of each code.

5.3.3.1 SISO MAP Detector and Demapper

The first SISO MAP detector computes the LAPPR $\Lambda(v_{i,k,m})$ with $v_{i,k,m} = \phi_{i,m}^{-1}(x_{i,k})$, $i \in \{1, 2\}$, using the received signal (5.2) and a priori information coming from the outer SISO decoders. Expression is similar to (5.41) substituting $\mathbf{y}_{D,k}^{(1)}$ for $\mathbf{y}_{R_\ell,k}^{(1)}$. We now turn to the second SISO MAP detector or demapper (depending on the relays cooperation). If both relays cooperate, the second SISO MAP detector should deliver soft information on the additional parity bits coming from both relays. Thus, it computes the LAPPR $\Lambda(v_{R_\ell,k,m})$ with $v_{R_\ell,k,m} = \phi_{R_\ell,m}^{-1}(x_{R_\ell,k})$, $\ell \in \{1, 2\}$, using the received signal (5.3) with $\theta_\ell = 1$, and a priori information coming from the SISO decoders SISO_{R_1} and SISO_{R_2} corresponding to the relays joint network-channel encoders (network codes in $\mathbb{F}_4$ followed by C_{R_1} and C_{R_2}). Expression is similar to (5.41) substituting $\mathbf{y}_{D,k}^{(2)}$ for $\mathbf{y}_{R_\ell,k}^{(1)}$. If just one of the relays, say R_1, cooperates, instead of a SISO MAP detector, a SISO MAP demapper is used which delivers soft information on the additional parity bits coming from R_1. The LAPPR on bit $v_{R_1,k,m} = \phi_{R_1,m}^{-1}(x_{R_1,k})$ is defined as

$$\Lambda(v_{R_1,k,m}) = \log \frac{P(v_{R_1,k,m} = 1|\mathbf{y}_{D,k}^{(2)})}{P(v_{R_1,k,m} = 0|\mathbf{y}_{D,k}^{(2)})}. \tag{5.44}$$

and evaluated as

$$\Lambda(v_{R_1,k,m}) \simeq \log \frac{\sum_{c\in\mathscr{X}_{R_1}:\phi^{-1}_{R_1,m}(c)=1} P(\mathbf{y}^{(2)}_{D,k}|x_{R_1,k}=c)e^{\xi(c)}}{\sum_{c\in\mathscr{X}_{R_1}:\phi^{-1}_{R_1,m}(c)=0} P(\mathbf{y}^{(2)}_{D,k}|x_{R_1,k}=c)e^{\xi(c)}} \tag{5.45}$$

with

$$\xi(c) = \sum_{m'=1}^{\log_2|\mathscr{X}_{R_1}|} \phi^{-1}_{R,m'}(c)E(v_{R_1,k,m'}) \tag{5.46}$$

where $\{E(v_{R_1,k,m})\}$ is the LAPR on bit $v_{R_1,k,m}$ provided by the SISO decoder SISO_{R_1} corresponding to the relay joint network-channel encoder (network codes in $\mathbb{F}_4$ followed by C_{R_1}). Finally, the extrinsic information on $v_{R_1,k,m}$ is given by $L(v_{R_1,k,m}) = \Lambda(v_{R_1,k,m}) - E(v_{R_1,k,m})$ and, after de-interleaving, feeds SISO_{R_1}.

5.3.3.2 Message-Passing Schedule

A recapitulative block diagram of the JNCD is depicted in Fig. 5.2. In this paragraph, we detail the message-passing for the case where both relays cooperate with both sources. We also consider the case of turbo codes at the sources, i.e., each C_i, $i \in \{1,2\}$ consists of two RSC encoders separated by $\pi_{0,i}$. The generalization to other cases is straightforward. The SISO decoder SISO_i corresponds to C_i, $i \in \{1,2\}$, and SISO_{R_i} corresponds to the relay encoder (network codes in $\mathbb{F}_4$ followed by C_{R_i}). Each SISO_i, $i \in \{1,2\}$, is made up of the two SISO decoders $\text{SISO}_{i,1}$ and $\text{SISO}_{i,2}$. Let $\mathbf{L}_{s_i}$, $\mathbf{L}_{p_i}$, and $\mathbf{L}_{p_{R_i}}$, $i \in \{1,2\}$, denote respectively the soft information of the systematic and parity bits of the sources and relays, obtained from the channel MAP detectors corresponding to both transmission phases. It is worth noting that the proper (de)multiplexing and (de)puncturing are also performed if needed. In Fig. 5.2, the (de)puncturing is included in the blocks corresponding to (de)multiplexing. Let also denote by $\mathbf{E}_{s_i(j)}$, $\mathbf{E}_{p_i(j)}$, and $\mathbf{E}_{p_{R_i}(j)}$ the extrinsic information generated by SISO_j, $j \in \{1,2,R_1,R_2\}$. Similarly, let $\mathbf{L}_{p_{i,1}}$ and $\mathbf{L}_{p_{i,2}}$ denote respectively the soft information of the parity bits corresponding to $\text{SISO}_{i,1}$ and $\text{SISO}_{i,2}$ obtained from the first MAP detector, $\mathbf{E}_{s_i(i,1)}$ and $\mathbf{E}_{s_i(i,2)}$ denote respectively the extrinsic information on systematic bits generated by $\text{SISO}_{i,1}$ and $\text{SISO}_{i,2}$, and $\mathbf{E}_{p_i(i,1)}$ and $\mathbf{E}_{p_i(i,2)}$ denote respectively the extrinsic information on parity bits generated by $\text{SISO}_{i,1}$ and $\text{SISO}_{i,2}$.

The first SISO MAP detector generates the LAPPRs for the systematic and parity bits in $\mathbf{V}_1$ using $\mathbf{E}_{s_1(1)} + \pi_1^{-1}(\mathbf{E}_{s_1(R_1)}) + \pi_2^{-1}(\mathbf{E}_{s_1(R_2)})$ and $\mathbf{E}_{p_1(1)}$, respectively (after proper multiplexing interleaving). It also generates the LAPPRs for the systematic and parity bits in $\mathbf{V}_2$ using $\mathbf{E}_{s_2(2)} + \pi_1^{-1}(\mathbf{E}_{s_2(R_1)}) + \pi_2^{-1}(\mathbf{E}_{s_2(R_2)})$ and $\mathbf{E}_{p_2(2)}$, respectively. It is worth

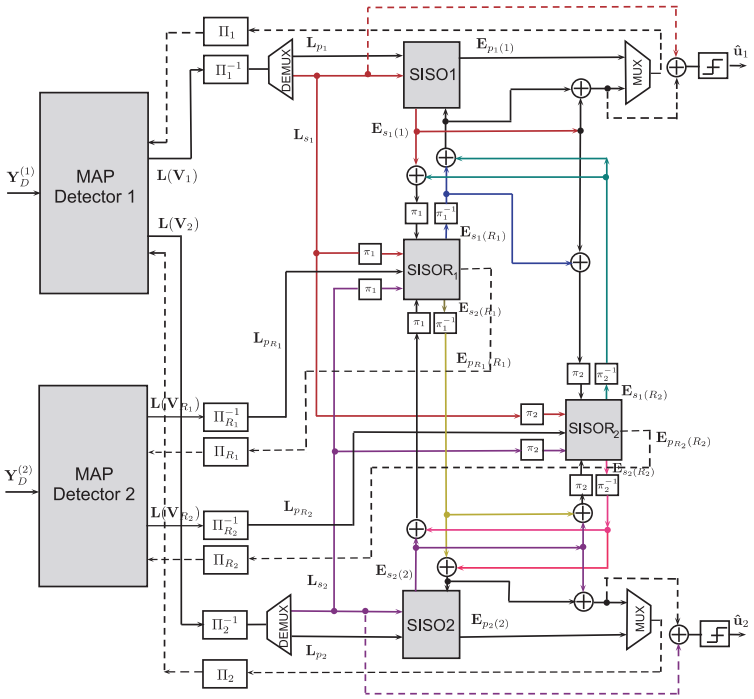

Figure 5.2: JNCD at the destination (both relays cooperate with both sources)

stressing that $\mathbf{E}_{s_1(1)} = \mathbf{E}_{s_1(1,1)} + \pi_{0,1}^{-1}(\mathbf{E}_{s_1(1,2)})$, and $\mathbf{E}_{s_2(2)} = \mathbf{E}_{s_2(2,1)} + \pi_{0,2}^{-1}(\mathbf{E}_{s_2(2,2)})$, as depicted in Fig. 5.3. The second SISO MAP detector generates the LAPPRs for the parity bits in $\mathbf{V}_{R_1}$ and $\mathbf{V}_{R_2}$ using $\mathbf{E}_{p_{R_1}(R_1)}$ and $\mathbf{E}_{p_{R_2}(R_2)}$. Then, the two distributed decoders are activated and calculate the extrinsic information for both the systematic and parity bits which are fed back to the SISO MAP detectors.

Hereafter, we detail the low complexity implementations of SISO_{R_i}. Let first introduce some definitions and notations which will be used to detail the structure of SISO_{R_i}.

- A bit to symbol or symbol to bit soft conversion:

  Let w be a random symbol taking values in $\mathbb{F}_q$ and $w = \psi(b_1, \cdots, b_M)$, $M = \log_2(q)$, $b_i \in \mathbb{F}_2$. We define

$$\begin{aligned} L^a(w) &= \log \frac{P(w=a)}{P(w=0)}, & \forall a \in \mathbb{F}_q \\ L(b_i) &= \log \frac{P(b_i=1)}{P(b_i=0)}, & i \in \{1, \cdots, M\} \end{aligned} \tag{5.47}$$

We first consider the bit to algebraic symbol conversion. We have

$$\begin{aligned} P(w=a) &= P(b_1=\psi_1^{-1}(a),\cdots,b_M=\psi_M^{-1}(a)) \\ &= \prod_{i=1}^{M} P(b_i=\psi_i^{-1}(a)) \\ &= \frac{\exp\left(\sum_{i=1}^{M}\psi_i^{-1}(a)L(b_i)\right)}{\prod_{i=1}^{M}\left(1+\exp\left(L(b_i)\right)\right)} \end{aligned} \tag{5.48}$$

Thus, we conclude

$$L^a(w)=\sum_{i=1}^{M}\psi_i^{-1}(a)L(b_i). \tag{5.49}$$

Now, we consider the algebraic symbol to bit conversion. Let $j\in\{0,1\}$, we have

$$\begin{aligned} P(b_i=j) &= \sum_{a\in\mathbb{F}_q} P(b_i=j,w=a) \\ &= \sum_{a\in\mathbb{F}_q} P(b_i=j|w=a)P(w=a) \\ &= \sum_{a\in\mathbb{F}_q,\psi_i^{-1}(a)=j} P(w=a) \\ &= \sum_{a\in\mathbb{F}_q,\psi_i^{-1}(a)=j} \exp\left(L^a(w)\right)P(w=0) \end{aligned} \tag{5.50}$$

Thus, we conclude

$$L(b_i)=\log\left(\frac{\sum_{a\in\mathbb{F}_q,\psi_i^{-1}(a)=1}\exp(L^a(w))}{\sum_{a\in\mathbb{F}_q,\psi_i^{-1}(a)=0}\exp(L^a(w))}\right). \tag{5.51}$$

- Algebraic constraint node:

  Let $w_1,\cdots,w_{M+1}$ be arbitrary symbols in $\mathbb{F}_q$ and let consider the function

$$f(w_1,\cdots,w_{M+1})=\left[\sum_{k=1}^{M}a_kw_k=w_{M+1}\right],\qquad a_k\in\mathbb{F}_q. \tag{5.52}$$

  Let also $i\in\{1,\cdots,M+1\}$ and $J=\{1\le j\le M+1; j\neq i\}$.

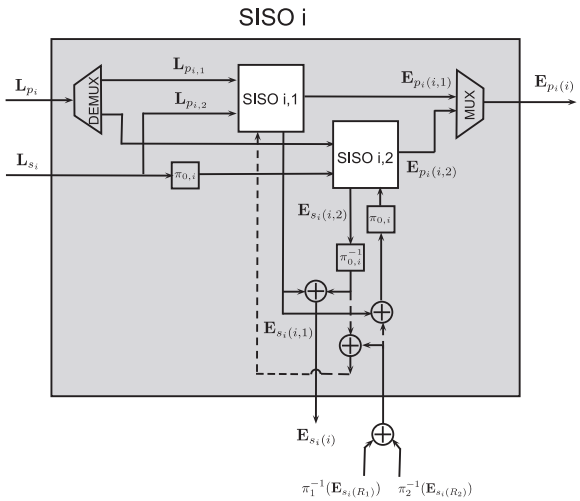

Figure 5.3: SISO decoder SISO_i in case of compound codes at sources

We define $\sum_{a_1,\cdots,a_M;i} : \underbrace{\mathbb{R}^q \times \mathbb{R}^q \times \cdots \mathbb{R}^q}_{M} \to \mathbb{R}$ such that

$$\begin{aligned}\sum\nolimits_{a_1,\cdots,a_M;i}\left(\{L^{r_k}(w_k)\}_{k\in J}\right) &= \log\frac{P\left(\sum_{k=1}^{M} a_k w_k = w_{M+1} | w_i = s\right)}{P\left(\sum_{k=1}^{M} a_k w_k = w_{M+1} | w_i = 0\right)} \\ &= \log\left(\frac{\sum_{\left(\{r_k\in\mathbb{F}_q\}_{k\in J}\right)} e^{\sum_{k\in J} L^{r_k}(w_k)} f\left(\{w_k = r_k\}_{k\in J}, w_i = s\right)}{\sum_{\left(\{r_k\in\mathbb{F}_q\}_{k\in J}\right)} e^{\sum_{k\in J} L^{r_k}(w_k)} f\left(\{w_k = r_k\}_{k\in J}, w_i = 0\right)}\right) \end{aligned} \tag{5.53}$$

where $r_k, s \in \mathbb{F}_q$. ■

SISO_{R_i} corresponds to the network coding vector $\mathbf{a}_i^{1,2} = \begin{bmatrix} a_{1i} & a_{2i} \end{bmatrix}^\top$. For the case of $M = 2$ sources and $L = 2$ relays, we choose $\mathbf{a}_1^{1,2} = \begin{bmatrix} 1 & 1 \end{bmatrix}^\top$ and $\mathbf{a}_2^{1,2} = \begin{bmatrix} 1 & 2 \end{bmatrix}^\top$ whose coefficients are defined in $\mathbb{F}_4$. As depicted in Fig. 5.4, the SISO decoders corresponding to C_{R_i} (DEC_{R_i}) should collect all the a priori information $\mathbf{L}_{u_{R_i}}$ on $\mathbf{u}_{R_i}$, $i \in \{1,2\}$. Let $\mathbf{L}_{1R_i} = \pi_i(\mathbf{L}_{s_1} + \mathbf{E}_{s_1(1)} + \pi_j^{-1}(\mathbf{E}_{s_1(R_j)}))$ and $\mathbf{L}_{2R_i} = \pi_i(\mathbf{L}_{s_2} + \mathbf{E}_{s_2(2)}) + \pi_j^{-1}(\mathbf{E}_{s_2(R_j)}))$, $j \in \{1,2\}$, $j \neq i$. Let $L^s_{1R_i,k'}$ and $L^s_{2R_i,k'}$, $s \in \mathbb{F}_4$, denote the soft information in $\mathbb{F}_4$ which is derived from the a priori information $L_{1R_i,k}$ and $L_{2R_i,k}$ using (5.49). Taking into account the algebraic constraint node and using (5.53), we have

$$L^s_{u_{R_i},k'} = \sum\nolimits_{a_{1,i},a_{2,i};3}\left(L^{r_1}_{1R_2,k'}, L^{r_2}_{2R_2,k'}\right), \qquad \forall r_1, r_2 \in \mathbb{F}_4 \tag{5.54}$$

$L_{u_{R_i},k}$ is then calculated using (5.51) which feeds DEC_{R_i}. Let denote by $E_{u_{R_i}(R_i),k}$ the

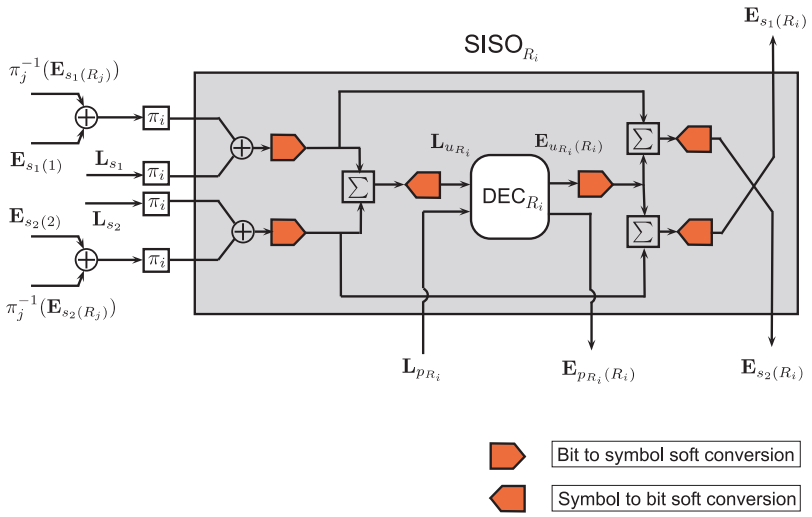

Figure 5.4: Algebraic decoder

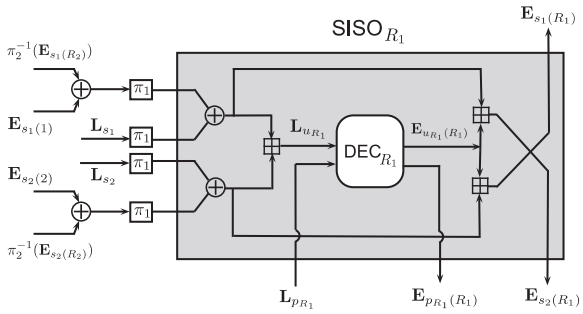

Figure 5.5: Equivalent XOR decoder for SISO$_{R_1}$

extrinsic information on $\mathbf{u}_{R_i}$ computed by the decoder corresponding to C_{R_i}. After proper bit to symbol soft conversions, $E^s_{s_1(R_i),k'}$ and $E^s_{s_2(R_i),k'}$ are obtained as

$$\begin{aligned} E^s_{s_1(R_i),k'} &= \sum\nolimits_{a_{1,i},a_{2,i};1} \left(L^{r_2}_{2R_i,k'}, E^{r_3}_{u_{R_i}(R_i),k'} \right), \qquad \forall r_2, r_3 \in \mathbb{F}_4 \\ E^s_{s_2(R_i),k'} &= \sum\nolimits_{a_{1,i},a_{2,i};2} \left(L^{r_1}_{1R_i,k'}, E^{r_3}_{u_{R_i}(R_i),k'} \right), \qquad \forall r_1, r_3 \in \mathbb{F}_4 \end{aligned} \tag{5.55}$$

Finally, $\mathbf{E}_{s_1(R_i)}$ and $\mathbf{E}_{s_2(R_i)}$ are derived after symbol to bit soft conversions. It is worth noting that, interestingly, SISO$_{R_1}$ which corresponds to $\mathbf{a}_1^{1,2} = \begin{bmatrix} 1 & 1 \end{bmatrix}^\top$ can also be implemented as in Fig. 5.5, where $\boxplus$ denote the XOR constraint node.

The message-passing schedule for the JNCD at each iteration, and the final hard decisions are recapitulated in the Algorithm 5.

Algorithm 5 : JNCD at the destination

(Initialization)
Set all the a priori information to zero.
(Iterations)
Iterate until convergence:

1. Activate the first SISO MAP detector using the received signal $\mathbf{Y}_D^{(1)}$, and the messages $\mathbf{E}_{s_1(1)} + \pi_1^{-1}(\mathbf{E}_{s_1(R_1)}) + \pi_2^{-1}(\mathbf{E}_{s_1(R_2)})$, $\mathbf{E}_{p_1(1)}$ and $\mathbf{E}_{s_2(2)} + \pi_1^{-1}(\mathbf{E}_{s_2(R_1)}) + \pi_2^{-1}(\mathbf{E}_{s_2(R_2)})$, $\mathbf{E}_{p_2(2)}$, where $\mathbf{E}_{s_i(i)} = \mathbf{E}_{s_i(i,1)} + \pi_{0,i}^{-1}(\mathbf{E}_{s_i(i,2)})$.

2. Activate the second SISO MAP detector using the received signal $\mathbf{Y}_D^{(2)}$, and the messages $\mathbf{E}_{p_{R_1}(R_1)}$ and $\mathbf{E}_{p_{R_2}(R_2)}$.

3. Activate simultaneously the SISO decoders SISO_1 and SISO_2

   (a) Activate simultaneously $\text{SISO}_{1,1}$ and $\text{SISO}_{2,1}$ with the messages $\mathbf{L}_{s_1}$, $\mathbf{L}_{p_{1,1}}$ and $\mathbf{L}_{s_2}$, $\mathbf{L}_{p_{2,1}}$ provided by the first MAP detector, and $\pi_{0,1}^{-1}(\mathbf{E}_{s_1(1,2)}) + \pi_1^{-1}(\mathbf{E}_{s_1(R_1)}) + \pi_2^{-1}(\mathbf{E}_{s_1(R_2)})$ and $\pi_{0,2}^{-1}(\mathbf{E}_{s_2(2,2)}) + \pi_1^{-1}(\mathbf{E}_{s_2(R_1)}) + \pi_2^{-1}(\mathbf{E}_{s_2(R_2)})$, which are derived from the previous iteration.

   (b) Activate simultaneously the $\text{SISO}_{1,2}$ and $\text{SISO}_{2,2}$ with, respectively, the messages $\pi_{0,1}(\mathbf{L}_{s_1})$, $\mathbf{L}_{p_{1,2}}$ and $\pi_{0,2}(\mathbf{L}_{s_2})$, $\mathbf{L}_{p_{2,2}}$ provided by the first MAP detector, and $\pi_{0,1}(\mathbf{E}_{s_1(1,1)}) + \pi_{0,1} \circ \pi_1^{-1}(\mathbf{E}_{s_1(R_1)}) + \pi_{0,1} \circ \pi_2^{-1}(\mathbf{E}_{s_1(R_2)})$ and $\pi_{0,2}(\mathbf{E}_{s_2(2,1)}) + \pi_{0,2} \circ \pi_1^{-1}(\mathbf{E}_{s_2(R_1)}) + \pi_{0,2} \circ \pi_2^{-1}(\mathbf{E}_{s_2(R_2)})$.

4. Activate the SISO decoder SISO_{R_1} with the messages $\mathbf{L}_{p_{R_1}}$ provided by the second MAP detector, and $\mathbf{L}_{1R_1} = \pi_1(\mathbf{L}_{s_1} + \mathbf{E}_{s_1(1)} + \pi_2^{-1}(\mathbf{E}_{s_1(R_2)}))$ and $\mathbf{L}_{2R_1} = \pi_1(\mathbf{L}_{s_2} + \mathbf{E}_{s_2(2)} + \pi_2^{-1}(\mathbf{E}_{s_2(R_2)}))$.

5. Activate the SISO decoder SISO_{R_2} with the messages $\mathbf{L}_{p_{R_2}}$ provided by the second MAP detector, and $\mathbf{L}_{1R_2} = \pi_2(\mathbf{L}_{s_1} + \mathbf{E}_{s_1(1)} + \pi_1^{-1}(\mathbf{E}_{s_1(R_1)})$ and $\mathbf{L}_{2R_2} = \pi_2(\mathbf{L}_{s_2} + \mathbf{E}_{s_2(2)} + \pi_1^{-1}(\mathbf{E}_{s_2(R_1)}))$.

(Hard decisions)
Combine all the available information on the systematic bits $\mathbf{u}_1$ and $\mathbf{u}_2$:

$$\mathbf{L}_{s_1} + \mathbf{E}_{s_1(1,1)} + \pi_{0,1}^{-1}(\mathbf{E}_{s_1(1,2)}) + \pi_1^{-1}(\mathbf{E}_{s_1(R_1)}) + \pi_2^{-1}(\mathbf{E}_{s_1(R_2)}) \rightarrow \hat{\mathbf{u}}_1$$
$$\mathbf{L}_{s_2} + \mathbf{E}_{s_2(2,1)} + \pi_{0,2}^{-1}(\mathbf{E}_{s_2(2,2)}) + \pi_1^{-1}(\mathbf{E}_{s_2(R_1)}) + \pi_2^{-1}(\mathbf{E}_{s_2(R_2)}) \rightarrow \hat{\mathbf{u}}_2$$

5.4 Separate Network Channel Coding and Decoding

As previously mentioned, in the SNCC scheme, the network-coded signals provided by the relays are separately decoded at the destination. Thus, in case of SOMAMRC/SNCC, a joint detection and decoding procedure similar to section (5.3.2.1) is performed at the destination on the signal received during the first transmission phase, and a separate decoding is performed on the signal received from the the relays during the second phase. If both relays transmit, the latter would be done similar to section (5.3.2.1). It is worth noting that, when one of the relays cooperates with just one source whose message is retrieved error-free from either of the transmission phases, the interference corresponding to this message can then be removed during the decoding procedure corresponding to the other transmission phase. Finally, the channel decoders make hard decisions and output the estimates to the network decoder. When both relays cooperate with both sources, if at least two out of four channel output estimates are error-free, the network decoder can retrieve both source messages.

5.5 Numerical Results

In this section, we provide some numerical results to evaluate the effectiveness of our approach. In our comparisons, we consider both SOMAMRC and OMAMRC using JNCC or SNCC. We start by detailing the topology of the network. For the sake of simplicity, we consider a symmetric MAMRC, i.e., $d_{1R_1} = d_{2R_1} = d_{1R_2} = d_{2R_2}$, $d_{R_1D} = d_{R_2D}$, and $d_{1D} = d_{2D}$. The average energy per available dimension allocated to the two sources is the same, i.e., $P_{0,1} = P_{0,2} = P_0$. We fix the same path loss factor, i.e., $\kappa = 3$, free distance, i.e., $d_0 = 1$ and noise power spectral density, i.e., $N_0 = 1$, for all links. Due to the half-duplex nature of the relays, the transmission time slot of the sources and the relay are separated in time. For SOMAMRC, we have $P_1 = P_2 = P_0/\alpha$ and $P_{R_1} = P_{R_2} = P_{0,R}/\bar{\alpha}$. In OMAMRC, the two sources and the relays transmit in consecutive, equal duration, time slots. Thus, the first two time slots are dedicated to the sources, and the last two time slots are dedicated to the relays. It comes that $P_1 = P_2 = 2P_0/\alpha$ and $P_{R_1} = P_{R_2} = 2P_{0,R}/\bar{\alpha}$. Let us choose $\alpha = \alpha_0 = 2/3$ and $P_{0,R} = \frac{\bar{\alpha}_0}{\alpha_0} P_0 = 1/2P_0$ as references in order to compare our results with [136, 141]. For simulation purposes, two different configurations are considered: In the first configuration, we fix the number of receive antennas to one both at the relays and destination, i.e., $N_{R_1} = N_{R_2} = N_D = 1$. The geometry is chosen such that $d_{ij} = d_{R_1D} = d_{R_2D} = d$ which yields $P_{ij} = \frac{\alpha_0}{\alpha}\gamma$, $P_{R_1D} = P_{R_2D} = \frac{2\bar{\alpha}_0}{\bar{\alpha}}\gamma$ for SOMAMRC and $P_{ij} = \frac{2\alpha_0}{\alpha}\gamma$, $P_{R_1D} = P_{R_2D} = \frac{\bar{\alpha}_0}{\bar{\alpha}}\gamma$ for OMAMRC, $i \in \{1, 2\}$, $j \in \{R_1, R_2, D\}$ where γ is the received SNR per symbol or dimension. In the second configuration, we increase the

number of receive antennas at the destination to 4, i.e. , $N_{R_1} = N_{R_2} = 1$ and $N_D = 4$. The geometry is chosen such that $d_{iR_\ell} = d_1$, $i, \ell \in \{1, 2\}$, and $d_{iD} = d_{R_1 D} = d_{R_2 D} = d$ with $(d_1/d)^{-3} = 100$. It yields $P_{iR_\ell} = \frac{100\alpha_0}{\alpha}\gamma$ (or $\gamma + 20 + 10\log_{10}(\frac{\alpha_0}{\alpha})$ in dB), $P_{iD} = \frac{\alpha_0}{\alpha}\gamma$ and $P_{R_1 D} = P_{R_2 D} = \frac{\bar{\alpha}_0}{\bar{\alpha}}\gamma$ for SOMAMRC which translates into $P_{iR_\ell} = \frac{200\alpha_0}{\alpha}\gamma$, $P_{iD} = \frac{2\alpha_0}{\alpha}\gamma$ and $P_{R_1 D} = P_{R_2 D} = \frac{2\bar{\alpha}_0}{\bar{\alpha}}\gamma$ for OMAMRC, $i \in \{1, 2\}$. Each message of the sources has length $K = 1024$ information bits. The network coding vectors are chosen as $\mathbf{a}_1^{1,2} = \begin{bmatrix} 1 & 1 \end{bmatrix}^\top$, and $\mathbf{a}_2^{1,2} = \begin{bmatrix} 1 & 2 \end{bmatrix}^\top$. In our proposed JNCC, the complex signal sets $\mathscr{X}_1$, $\mathscr{X}_2$, $\mathscr{X}_{R_1}$ and $\mathscr{X}_{R_2}$ used in BICM are either QPSK or 16QAM constellation (Gray labeling) and their corresponding sum rates are $\eta = 4/3$ b./c.u. and $\eta = 8/3$ b./c.u., respectively.

5.5.1 Optimization of the parameter α

In the first set of simulations, we consider the ϵ-outage achievable rate $C_\epsilon(\gamma)$ of S_1 to optimize the parameter α in SOMAMRC/JNCC, i.e., the fraction of time that the relays should listen. In our analysis, we consider Gaussian i.i.d. inputs and we fix $\epsilon = 10^{-2}$. Both cases of $N_D = 1$ and $N_D = 4$ are also considered. We choose $\alpha = 2/3$ as a reference to calculate the values of P_{ij} and $P_{R_i D}$, $i \in \{1, 2\}$, $j \in \{R_1, R_2, D\}$. The corresponding results are depicted in Fig. 5.6 for the case of $N_D = 1$. Obviously, the optimum α depends on the overall spectral efficiency of interest. When α is too small, the relays may not be able to decode the messages correctly and thus they do not cooperate with the sources during the second phase. However, if α is too large, the relays cannot help much to the transmission of the source signals even if they acquire a lot of information during the first phase. The simulation results show that, in the case of $N_D = 1$ and for the data rates in the range of $[0.1, 2]$ b./c.u., $\alpha = 2/3$ gives the best performance. However, the best choice of α becomes $\alpha = 0.8$ for the the data rates of 2.5 b./c.u. and higher. In the case of $N_D = 4$ and for the data rates of 0.1 b./c.u and higher $\alpha = 2/3$ remains the optimal choice. It is worth noting that this optimum value for α may change for other network topologies and configurations. In the sequel, we fix $\alpha = \alpha_0 = 2/3$ for simulation purposes.

5.5.2 Information-theoretic comparison of the protocols

5.5.2.1 Individual ϵ-outage achievable rate with Gaussian inputs

In the first set of simulations, we consider the ϵ-outage achievable rate of S_1, and we compare the individual ϵ-outage achievable rate $C_\epsilon(\gamma)$ of JNCC and SNCC for the SOMAMRC and the OMAMRC. In our analysis, we fix $\epsilon = 10^{-2}$. The number of receive antennas at the destination is either $N_D = 1$ or $N_D = 4$. The corresponding results are depicted in Fig. 5.7. As we can see, the ϵ-outage achievable rate for the SOMAMRC is always higher

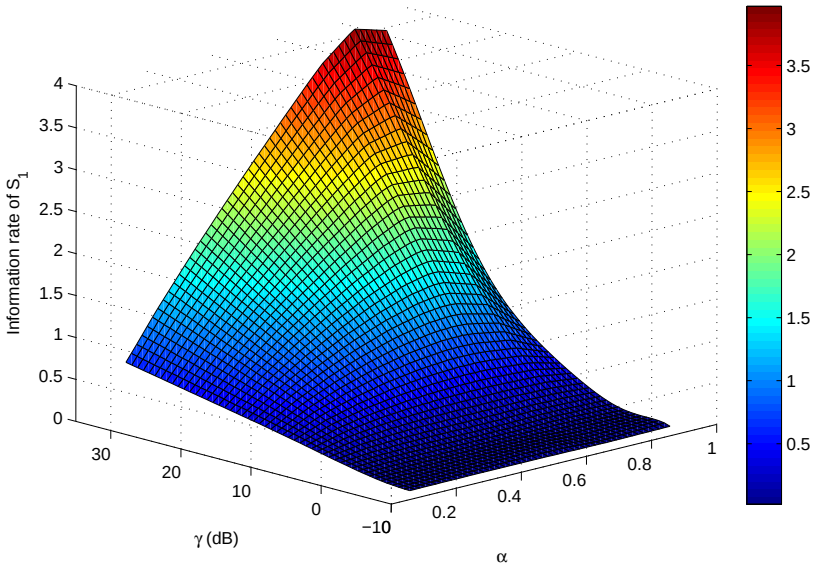

Figure 5.6: Individual ϵ-outage achievable rate for different values of α - $\epsilon = 10^{-2}$ - SOMAMRC/JNCC - $N_R = 1$, $N_D = 1$

than the ϵ-outage achievable rate for the OMAMRC regardless of the network channel coding strategy (i.e., JNCC or SNCC); Especially, in the case of $N_D = 4$, JNCC with orthogonal multiple access (OMAMRC/JNCC) is strictly suboptimal and the ϵ-outage achievable rate gain of SOMAMRC/JNCC versus OMAMRC/JNCC for individual rates above 2.5 b./c.u. is more than 5 dB. This results from the fact that, in the presence of multiple receive antennas, a non-orthogonal MAC can better exploit the available degrees of freedom. Moreover, even in the case of $N_D = 1$ which is not a priori favorable for a MAC, we see that SOMAMRC/JNCC can provide an ϵ-outage achievable rate gain of approximately 3 dB for data rates above 2 b./c.u.. Finally, the JNCC schemes outperform the SNCC ones for both transmission protocols. For the data rate of 2 b./c.u., the ϵ-outage achievable rate gains are about 9 dB and 6 dB in case of SOMAMRC for respectively $N_D = 1$ and $N_D = 4$, 10 dB and 9 dB in case of OMAMRC with respectively $N_D = 1$ and $N_D = 4$.

5.5.2.2 Individual information outage probability with discrete inputs

In the second set of simulations, our purpose is first to compare the individual outage probability of SOMAMRC/JNCC and OMAMRC/JNCC, and for the fixed sum rates of $\eta = 4/3$ and $\eta = 8/3$ b./c.u.. In order to achieve the same spectral efficiency as the SOMAMRC,

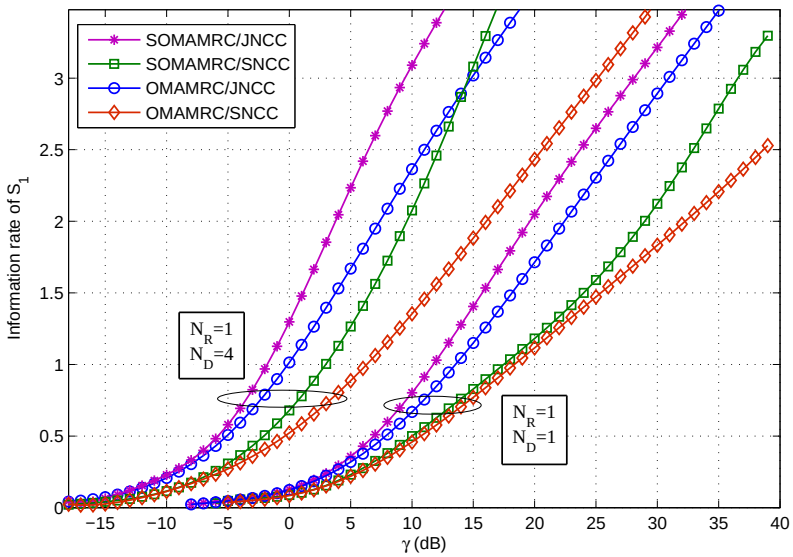

Figure 5.7: Individual ϵ-outage achievable rate - $\epsilon = 10^{-2}$ - SOMAMRC vs. OMAMRC - JNCC vs. SNCC

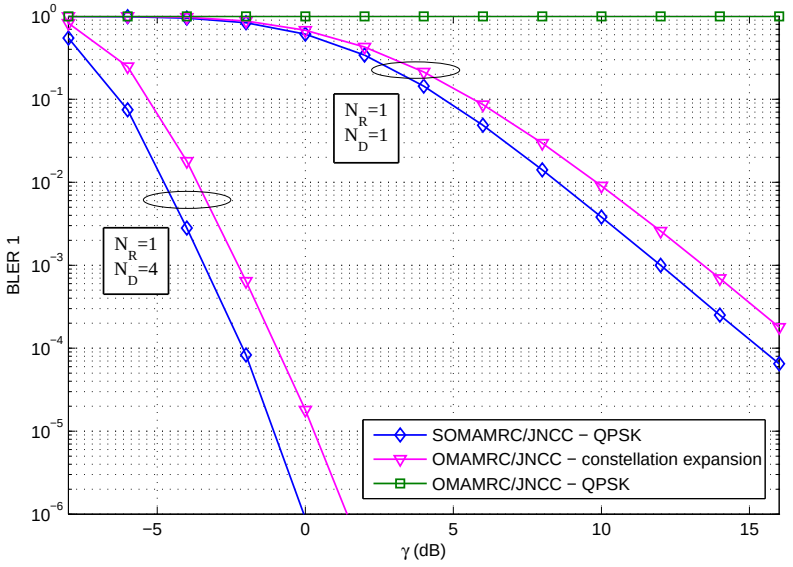

Figure 5.8: Individual outage probability (e.g., for S_1) - SOMAMRC/JNCC vs. OMAMRC/JNCC - $\eta = 4/3$ b./c.u.

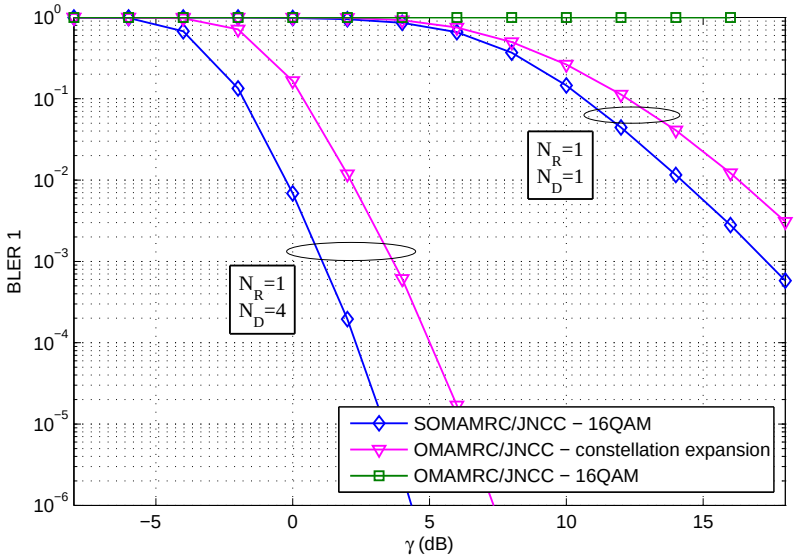

Figure 5.9: Individual outage probability (e.g., for S_1) - SOMAMRC/JNCC vs. OMAMRC/JNCC - $\eta = 8/3$ b./c.u.

we consider two approaches for OMAMRC: (1) We impose on the transmitters to use the same input alphabet as in the case of SOMAMRC, which makes sense if we want to preserve the same level of PAPR; (2) We employ constellation expansion for the sources and relays in OMAMRC. In the first approach, the two sources have no other choice but to transmit their information symbols without any coding, and thus, from a theoretical perspective ($N \rightarrow \infty$), the system is always in outage. In the second approach, the sources and relays increase the cardinality of their modulation while preserving the same spectral efficiency, which makes room for coding. Thus, the information outage probability of SOMAMRC with QPSK is compared with the information outage probability of OMAMRC with 16QAM at both sources and relays. Similarly, the information outage probability of SOMAMRC with 16QAM is compared with the information outage probability of OMAMRC with 64QAM at the sources and relay. The corresponding results are depicted in Fig. 5.8 for the sum rate of $\eta = 4/3$ b./c.u. and in Fig. 5.9 for the sum rate of $\eta = 8/3$ b./c.u., for both $N_D = 1$ and $N_D = 4$. As we can see, in all cases, the information outage probability of SOMAMRC is smaller than the one of OMAMRC. Considering the second approach, for $\eta = 8/3$ b./c.u., and at the BLER of 10^{-2}, the power gain is approximately equal to 2 dB for $N_D = 1$ and becomes even larger for $N_D = 4$, attaining 2.5 dB at the BLER of 10^{-2}, which reconfirms the sub-optimality of the orthogonal multiple access in case of multiple receive antennas.

To pursue our analysis, we compare the individual information outage probabilities

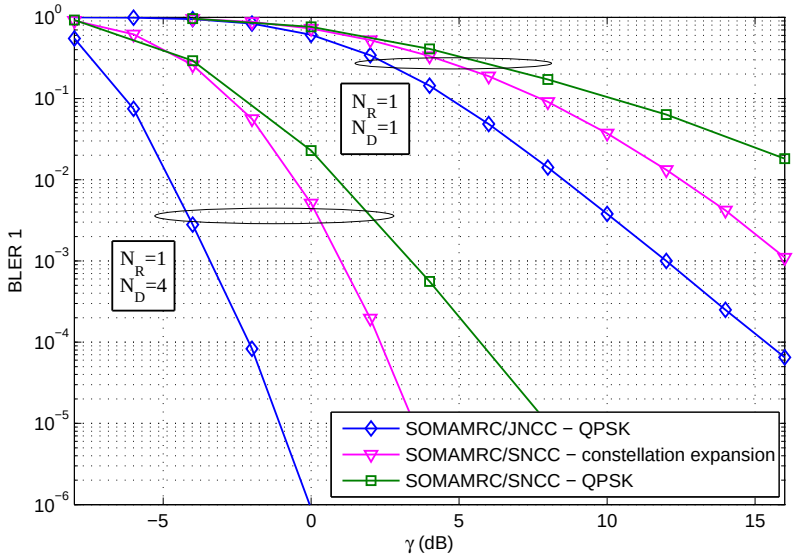

Figure 5.10: Individual outage probability (e.g., for S_1) - SOMAMRC/JNCC vs. SOMAMRC/SNCC - $\eta = 4/3$ b./c.u.

of SOMAMRC/JNCC and SOMAMRC/SNCC. Here again, to keep the same spectral efficiency for the SNCC case, we have the aforementioned two approaches. Using the first approach, the relay-to-destination channel is always in outage in the case of SOMAMRC/SNCC, and thus it leads to the performance of a MAC corresponding to the first transmission time slot. This explains the difference of slopes between the two curves in the corresponding figures. In the second approach, constellation expansion is employed for the relay-to-destination channel. Thus, in SOMAMRC/SNCC, the relays use 16QAM for $\eta = 4/3$ b./c.u., and 64QAM for $\eta = 8/3$ b./c.u.. The corresponding results are depicted in Fig. 5.10 and Fig. 5.11 for both $N_D = 1$ and $N_D = 4$. As we can see, the SOMAMRC/SNCC has always a performance loss compared to the SOMAMRC/JNCC. In the case of constellation expansion and $N_D = 1$, at the BLER of 10^{-2}, the loss is around 4 dB for $\eta = 4/3$ b./c.u., and becomes much higher and attains 7 dB for $\eta = 8/3$ b./c.u.. In the case of $N_D = 4$, the loss is around 5 dB for both $\eta = 4/3$ b./c.u., and $\eta = 8/3$ b./c.u..

5.5.3 Performance of practical code design

In the sequel, the number of iterations I is set to 5 at the relays and to 10 (for $N_D = 1$) or 3 (for $N_D = 4$) at the destination. These numbers of iterations ensure convergence and allow to very closely approach the performance of a Genie Aided (GA) receiver at sufficiently

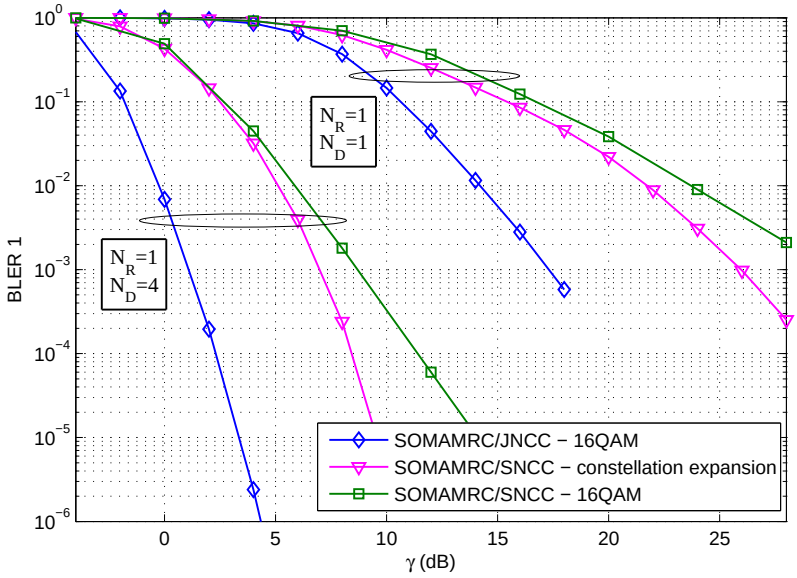

Figure 5.11: Individual outage probability (e.g., for S_1) - SOMAMRC/JNCC vs. SOMAMRC/SNCC - $\eta = 8/3$ b./c.u.

high SNR for the selected modulation and coding schemes, the Genie Aided (GA) receiver corresponding to the ideal case where the interference is known and perfectly removed.

5.5.3.1 Gap to outage limits

Here, we evaluate the gap between the individual BLER of practical designs for SOMAMRC/JNCC and that of their corresponding information outage probability. The experiment is carried out for $\eta = 4/3$ b./c.u.. The two sources use identical turbo codes of rate-1/2 made of two 4-state rate-1/2 RSC encoders with generator matrix $\mathbf{G}_1 = [\ 1 \quad 5/7\ ]$ in octal representation, whose half of the parity bits are punctured. The JNCC at the relays is based on the network coding vectors $\mathbf{a}_1^{1,2}$ and $\mathbf{a}_2^{1,2}$ in $\mathbb{F}_4$, followed by a 4-state rate-1/2 RSC encoder with generator matrix $\mathbf{G}_R = [\ 1 \quad 5/7\ ]$. Exhaustive simulations showed that those numbers of states yield the best performance/complexity trade-off. The corresponding results are demonstrated in Fig. 5.12. As we see, the proposed JNCC scheme performs 1.5 dB and 2.5 dB away from the information outage probability for respective cases of $N_D = 1$ and $N_D = 4$.

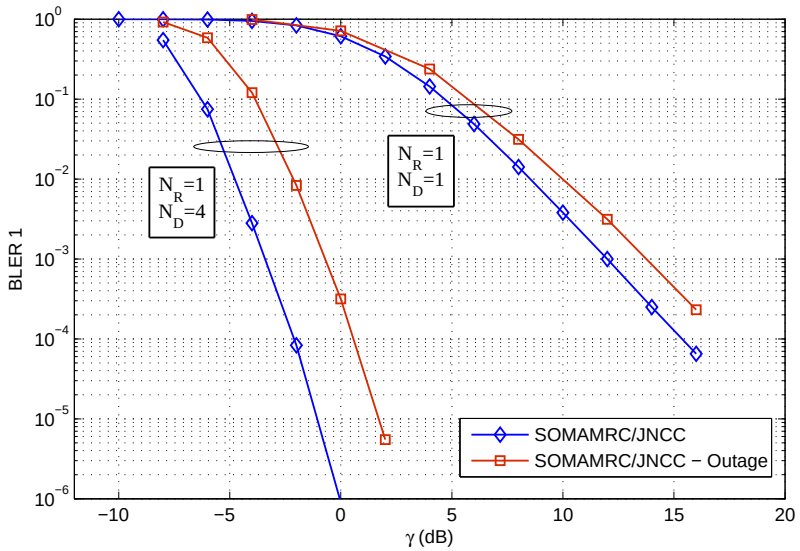

Figure 5.12: Individual BLER (e.g., for S_1) - Practical SOMAMRC/JNCC vs. outage limit - $\eta = 4/3$ b./c.u.

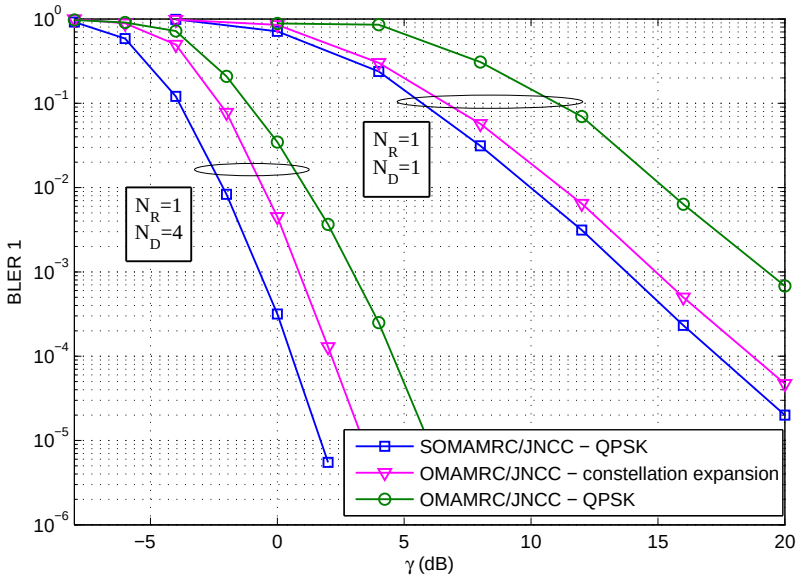

Figure 5.13: Individual BLER (e.g., for S_1) - SOMAMRC/JNCC vs. OMAMRC/JNCC - $\eta = 4/3$ b./c.u.

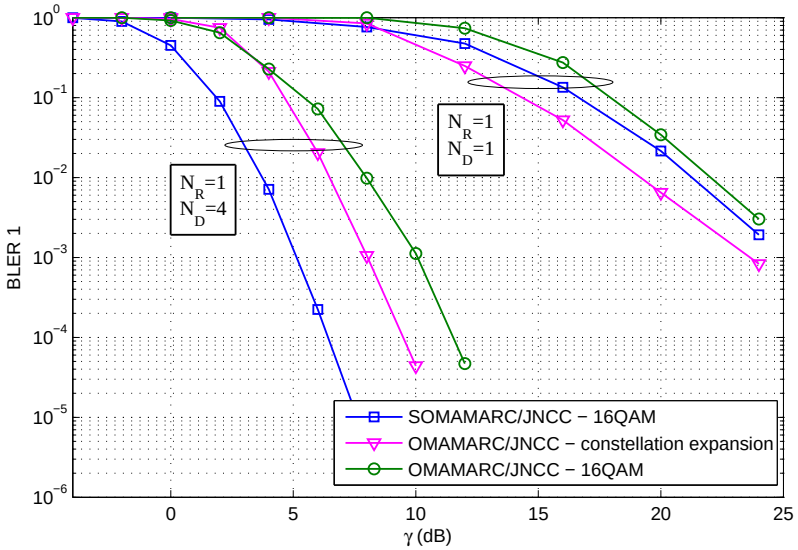

Figure 5.14: Individual BLER (e.g., for S_1) - SOMAMRC/JNCC vs. OMAMRC/JNCC - $\eta = 8/3$ b./c.u.

5.5.3.2 Comparison of the different protocols

In this section, we compare the individual BLER of practical code designs for the SOMAMRC/JNCC with that of the OMAMRC/JNCC. The JNCC in both protocols is based on the vectors $\mathbf{a}_1^{1,2}$ and $\mathbf{a}_2^{1,2}$. In SOMAMRC/JNCC, the two sources use the punctured turbo codes made of 4-state rate-1/2 RSC encoders with generator matrix $\mathbf{G}_1$, and the relays use the same RSC encoder. For OMAMRC/JNCC, we first imposed on the sources and the relay the use of same signal sets. In this case, the two sources transmit their information symbols without any coding, while the relays use the 4-state rate-1/2 RSC encoder whose half of the parity bits are punctured. The corresponding results demonstrated considerable gains in favour of our approach. We next carried out another experiment, where constellation expansion is employed for OMAMRC, as explained in the outage comparisons. Thus, in the case of OMAMRC with $\eta = 4/3$ b./c.u., both sources use the same turbo code as the SOMAMRC with 16QAM modulation, and the relays use the 4-state rate-1/2 RSC encoder with 16QAM constellation. Similarly, in the case of $\eta = 8/3$ b./c.u., both sources use the turbo code made of 4-state rate-1/2 RSC encoders with generator matrix $\mathbf{G}_1$, whose parity bits are punctured to result in a code of rate 2/3. They use then 64QAM constellation. The relays use the same RSC encoder as the previous case whose 1/4 of the parity bits are punctured. They also use 64QAM constellation. The corresponding results are depicted in Fig. 5.13 for the spectral efficiency of $\eta = 4/3$ b./c.u., and in Fig.

5.14 for the spectral efficiency of $\eta = 8/3$ b./c.u., for both $N_D = 1$ and $N_D = 4$. Here again, the SOMAMRC outperforms the OMAMRC in most cases and the performance gains are considerable for $N_D = 4$. The exception is the case of $\eta = 8/3$ b./c.u. and for $N_D = 1$, where the SOMAMRC performs around 1 dB worse than the OMAMRC. This is probably due to the multiuser detectors in SOMAMRC which suffer from high order modulations.

5.6 Conclusion

We have studied JNCC for a new class of MAMRC, referred to as SOMAMRC, from both an information-theoretic and a practical code design perspective. We have derived the SOMAMRC individual information outage probability, conditional on JNCC (and SNCC used as a reference). We have also presented new JNCC schemes flexible in terms of number of sources, encoders and modulations. For the 2-source symmetric case and targeted sum rates $\eta = 4/3$ b./c.u. and $\eta = 8/3$ b./c.u., we have shown that our proposed schemes are more efficient than (1) conventional distributed JNCC for OMAMRC; (2) conventional SNCC schemes. Moreover, the proposed SOMAMRC/JNCC performs very close to the outage limit for both cases of single and multiple receive antennas at the destination, and for the fixed sum rate of $\eta = 4/3$ b./c.u.. We have verified that the semi-orthogonal multiple access exhibits considerable gains over orthogonal multiple access, even in the case of a single receive antenna at the destination.

Chapter 6

Relaying Functions for the Half-Duplex Semi-Orthogonal MARC

In Chapter 2, we evaluated the performance of HD-SOMARC, in which the sources were constrained to remain silent during the transmission phase of the relay, and the relay employed an SDF relaying approach. However, since the interference generated by the relay at the destination does not impact the overall performance (contrary to HD-NOMARC, FD-NOMARC and HD-SOMAMRC), the choice of the relaying function is an interesting degree of freedom that remains to be exploited and optimized. In this chapter, we consider the JNCC approach and we compare the SDF relaying with two Soft Decode and Forward (SoDF) relaying functions: one based on log a posterior probability ratios (LAPPRs) [116] and the other based on Mean Square Error (MSE) estimate [117]. In fact, SoDF can be considered as an alternative approach to SDF, which does not need any signal overhead. Our proposed JNCC is generic and can be easily extended to arbitrary signal constellations, so as to enhance the system spectral efficiency.

6.1 System Model

The M statistically independent sources $S_1, \ldots, S_M$ want to communicate with the destination D in the presence of a relay R. We assume that the relay R and the destination D are equipped with N_R and N_D receive antennas. Let N be the total number of available complex dimensions to be shared between the sources and the relay. The semi-orthogonal transmission protocol is considered. The N available channel uses are divided into two suc-

This chapter was presented in part at IEEE ISTC 2010.

cessive time slots corresponding to the listening phase of the relay, say $N_1 = \alpha N$ channel uses, and to the transmission phase of the relay, say $N_2 = \bar{\alpha} N$ channel uses, with $\alpha \in [0, 1]$ and $\bar{\alpha} = 1 - \alpha$. Each source i broadcasts its messages $\mathbf{u}_i \in \mathbb{F}_2^K$ of K information bits under the form of a modulated sequence during the first transmission phase. Without loss of generality, the modulated sequences are chosen from the complex codebooks ζ_i of rate $K/(\alpha N)$ and take the form of sequences $\mathbf{x}_i \in \zeta_i \subset \mathscr{X}_i^{\alpha N}$, $i \in \{1, \ldots, M\}$, where $\mathscr{X}_i \subset \mathbb{C}$ denote a complex signal set of cardinality $|\mathscr{X}_i| = 2^{q_i}$, with energy normalized to unity. The corresponding received signals at the relay and destination are expressed as

$$\mathbf{y}_{R,k}^{(1)} = \sum_{i=1}^{M} \sqrt{P_{iR}} \mathbf{h}_{iR} x_{i,k} + \mathbf{n}_{R,k}^{(1)} \tag{6.1}$$

$$\mathbf{y}_{D,k}^{(1)} = \sum_{i=1}^{M} \sqrt{P_{iD}} \mathbf{h}_{iD} x_{i,k} + \mathbf{n}_{D,k}^{(1)} \tag{6.2}$$

for $k = 1, \ldots, \alpha N$. In (6.1) and (6.2), the channel fading vectors $\mathbf{h}_{iR} \in \mathbb{C}^{N_R}$, and $\mathbf{h}_{iD} \in \mathbb{C}^{N_D}$, $i \in \{1, \ldots, M\}$ are mutually independent, constant over the transmission of $\mathbf{x}_1$, …, $\mathbf{x}_M$ and change independently from one transmission of the sources to the next. The channel fading vectors $\mathbf{h}_{iR}$, $i \in \{1, \ldots, M\}$, are identically distributed following the pdf $\mathcal{CN}(\mathbf{0}_{N_R}, \mathbf{I}_{N_R})$. The channel fading vectors $\mathbf{h}_{iD}$, $i \in \{1, \ldots, M\}$, are i.d. following the pdf $\mathcal{CN}(\mathbf{0}_{N_D}, \mathbf{I}_{N_D})$. The additive noise vectors $\mathbf{n}_{R,k}^{(1)}$ and $\mathbf{n}_{D,k}^{(1)}$ are independent and follow the pdf $\mathcal{CN}(\mathbf{0}_{N_R}, N_0 \mathbf{I}_{N_R})$ and $\mathcal{CN}(\mathbf{0}_{N_D}, N_0 \mathbf{I}_{N_D})$. $P_{ij} \propto (d_{ij}/d_0)^{-\kappa} P_i$, $i \in \{1, \ldots, M\}$, $j \in \{R, D\}$ is the average received energy per dimension and per antenna (in Joules/symbol), where d_{ij} is the distance between the transmitter and receiver, d_0 is a reference distance, κ is the path loss coefficient, with values typically in the range $[2, 6]$, and P_i is the transmit power (or energy per symbol) of S_i. Note that the shadowing could be included within P_{ij}. To fairly compare the performance with respect to α, we fix the total energy per available dimensions $NP_{0,i}$ (recall that N is the number of available dimensions or channel uses) spent by S_i, i.e., $P_i = P_{0,i}/\alpha$. During the second phase, the sources are silent. The relay can either use an analog transmission scheme or a digital one. Therefore, in the most general case, the transmitted signals from the relay could be of the form $\tilde{\mathbf{x}}_R \in \mathbb{C}^{\bar{\alpha} N}$ with energy normalized to unity. The received signal at the destination is expressed as

$$\mathbf{y}_{D,k}^{(2)} = \sqrt{P_{RD}} \mathbf{h}_{RD} \tilde{x}_{R,k} + \mathbf{n}_{D,k}^{(2)} \tag{6.3}$$

for $k = 1, \ldots, \bar{\alpha} N$. In (6.3), the channel fading vector $\mathbf{h}_{RD} \in \mathbb{C}^{N_D}$ follows the pdf $\mathcal{CN}(\mathbf{0}_{N_D}, \mathbf{I}_{N_D})$, is independent of $\mathbf{h}_{iD}$, $i \in \{1, \ldots, M\}$, constant over the transmission of

$\mathbf{x}_R$ and changes independently from one transmission of the relay to another. The additive noise vector $\mathbf{n}_{D,k}^{(2)}$ is independent of $\mathbf{n}_{R,k}^{(1)}$ and $\mathbf{n}_{D,k}^{(1)}$, and follows the pdf $\mathcal{CN}(\mathbf{0}_{N_D}, N_0\mathbf{I}_{N_D})$. $P_{RD} \propto (d_{RD}/d_0)^{-\kappa} P_R$, with P_R the transmit power of the relay, is the average received power per dimension and per antenna at the destination. Here again, we fix the total energy per available dimensions $NP_{0,R}$ spent by the relay, i.e., $P_R = P_{0,R}/\bar{\alpha}$. In the rest of the paper, for the sake of notational simplicity, we consider $M = 2$ sources that transmit with an overall spectral efficiency $r = K/N$. The generalization to the cases of $M > 2$ sources is straightforward.

6.2 Joint Network Channel Coding and Decoding

In this section, we discuss different relaying schemes for MARC, in the context of JNCC and for the semi-orthogonal transmission protocol. We explain the structure of the encoders, how JNCC is performed for each relay functionality, and the structure of the corresponding multiuser receiver.

6.2.1 Coding at the Sources

The messages of the two sources are binary vectors $\mathbf{u}_1 \in \mathbb{F}_2^K$ and $\mathbf{u}_2 \in \mathbb{F}_2^K$ of length K. Each source employs a BICM [128]. Binary vectors are first encoded with linear systematic binary encoders $C_i : \mathbb{F}_2^K \to \mathbb{F}_2^{n_i}$, $i = \{1, 2\}$ into binary codewords $\mathbf{c}_i \in \mathbb{F}_2^{n_i}$ of respective lengths n_i. The codes ζ_i are punctured turbo codes, consisting of two RSC encoders, denoted by $\text{RSC}_{i,1}$ and $\text{RSC}_{i,2}$, concatenated in parallel using optimized semi-random interleavers $\pi_{0,i}$. The coded bits are then interleaved using interleavers Π_i and reshaped as two binary matrices $\mathbf{V}_i \in \mathbb{F}_2^{\alpha N \times q_i}$. Memoryless modulators based on one-to-one binary labeling maps $\phi_i : \mathbb{F}_2^{q_i} \to \mathscr{X}_i$ transform the binary arrays $\mathbf{V}_i$ into the complex vectors $\mathbf{x}_i \in \mathscr{X}_i^{\alpha N}$. For ϕ_i, we choose Gray labeling.

6.2.2 JNCC and Relaying Functions

Relay processing is divided in two steps: During the first transmission phase, based on (6.1), the relay performs an iterative MAP detection and turbo-decoding procedure. Depending on the relaying function, it obtains either the real-valued vectors $\boldsymbol{\lambda}_i \in \mathbb{R}^K$ representing the LAPPRs on $u_{i,k}$, $i \in \{1, 2\}$, $k = 1, \cdots, K$, or the hard binary estimation of the latter, $\hat{\mathbf{u}}_i \in \mathbb{F}_2^K$. Note that such iterative procedure is detailed in [131] for convolutional codes at the sources, and in the previous chapters for the general case of turbo codes which is inspired from [130]. At the second phase, the relay interleaves the derived values using an

interleaver π, constructs and forwards the signal $\tilde{\mathbf{x}}_R$ to the destination. The determination of $\tilde{\mathbf{x}}_R$ depends on the relaying function and will be detailed in the sequel. Now, let us define the relay coding and modulation scheme. It is based on an interleaver π followed by the XOR operation and a binary linear encoder $C_R : \mathbb{F}_2^K \to \mathbb{F}_2^{n_R}$ which yields the binary vector $\mathbf{c}_R \in \mathbb{F}_2^{n_R}$, a linear transformation $\Omega : \mathbb{F}_2^{n_R} \to \mathbb{F}_2^{n'_R}$ which selects the $n'_R \leq n_R$ entries of $\mathbf{c}_R$ to obtain the new vector $\mathbf{c}'_R \in \mathbb{F}_2^{n'_R}$ (Ω typically removes the systematic bits), a bit interleaver Π_R which reshapes the vector $\mathbf{c}'_R$ into a binary matrix $\mathbf{V}_R \in \mathbb{F}_2^{\bar{\alpha}N \times q_R}$, and finally, a memoryless modulator based on a one-to-one binary labeling map $\phi_R : \mathbb{F}_2^{q_R} \to \mathscr{X}_R$ which transforms the binary array $\mathbf{V}_R$ into the modulated vector $\mathbf{x}_R \in \mathscr{X}_R^{\bar{\alpha}N}$. $\mathscr{X}_R \subset \mathbb{C}$ is a complex constellation of order $|\mathscr{X}_R| = 2^{q_R}$ with energy normalized to unity. For ϕ_R, we choose Gray labeling. In the sequel, we denote by $v_{R,k,\ell} = \phi_{R,\ell}^{-1}(x_{R,k})$ the ℓ-th bit of the binary labeling of each symbol $x_{R,k}$ for $k = 1, \cdots, \bar{\alpha}N$. For C_R, we choose the RSC encoder defined by the generator matrix $G_R(D) = \left[\begin{array}{cc} 1 & \frac{p(D)}{q(D)} \end{array} \right]$.

6.2.2.1 Digital Selective Relaying

The relay makes hard decision to obtain the estimates of the information bits, i.e., $\hat{\mathbf{u}}_i$, $i \in \{1, 2\}$. It interleaves by π all the correctly decoded messages, the knowledge of which being ensured in practice by using two CRC codes for each source message. It then adds them together (XOR operation). Using the aforementioned coding and modulation scheme, it yields then the symbol sequence $\tilde{\mathbf{x}}_R = \mathbf{x}_R \in \mathcal{X}_R^{\bar{\alpha}N}$ to be transmitted to the destination.

6.2.2.2 Analog Soft Information Relaying

In the soft relaying scheme, the relay makes use of the derived LAPPRs on the informations bits, i.e., $\boldsymbol{\lambda}_i \in \mathbb{R}^K$ for $i \in \{1, 2\}$, interleaves them by π, and combines them, taking into account the XOR constraint node (see, e.g., [132]),

$$\lambda_{u_R,k} = \lambda_{1,k} \boxplus \lambda_{2,k} = \log \frac{e^{\lambda_{1,k}} + e^{\lambda_{2,k}}}{1 + e^{(\lambda_{1,k} + \lambda_{2,k})}}. \tag{6.4}$$

Note, that the independence between the messages should hold in order to apply (6.4). It then performs a soft encoding by applying the sum-product algorithm [143] to the code C_R. The latter (followed by the linear transformation Ω) yields the LAPPRs on the parity bits $c'_{R,k}$, which should be transmitted to the destination (after being interleaved by Π_R) in a proper way. Hereafter, we denote by $\boldsymbol{\lambda}_{R,k} \in \mathbb{R}^{q_R}$, $k = 1, \ldots, \bar{\alpha}N$, the LAPPRs on the interleaved parity bits $v_{R,k,\ell}$ at the relay.

One approach of soft relaying, is to transmit the LAPPRs $\lambda_{R,k,\ell}$ (two LAPPRs can be

transmitted for one channel use through in phase and quadrature branches). The LAPPRs are assumed at the destination to be observations of a binary input AWGN channel as in [116]. Clearly they should be normalized to ensure a given transmission power P_{RD}.

Another approach, based on MSE estimate, is proposed in [117] which is proved to be the optimal relay function in terms of SNR in the uncoded case. Interestingly, this approach needs the same number of channel uses from the relay to destination as the selective relaying (independently of the modulation order). Here, we apply this approach to the coded case. Let $x_{R,k}$ be the unknown symbols that would result from the genie aided knowledge of $\mathbf{u}_1$ and $\mathbf{u}_2$ within the selective relaying framework. Clearly, minimizing the Signal to Interference Ratio (SINR) at the destination, where the interference is simply $\sqrt{P_{RD}}\mathbf{h}_{RD}(\tilde{x}_{R,k}-x_{R,k})$, comes down to minimizing the MSE $\mathbb{E}\{|\tilde{x}_{R,k}-x_{R,k}|^2|\mathbf{Y}_R^{(1)}\}$. Since, this is not tractable, we rather consider the MSE $\mathbb{E}\{|\tilde{x}_{R,k}-x_{R,k}|^2|\boldsymbol{\lambda}_{R,k}\}$ which should be a good approximation of the optimal solution. Therefore, the chosen relay function (whose energy is normalized to unity) is given by

$$\tilde{x}_{R,k} = \frac{1}{\sqrt{\tilde{\sigma}^2}}\mathbb{E}\{x_{R,k}|\boldsymbol{\lambda}_{R,k}\} \tag{6.5}$$

with

$$\tilde{\sigma}^2 = \frac{1}{\bar{\alpha}N}\sum_{k=1}^{\bar{\alpha}N}|\mathbb{E}\{x_{R,k}|\boldsymbol{\lambda}_{R,k}\}|^2. \tag{6.6}$$

Let $v_{j,\ell} = \phi_{R,\ell}^{-1}(x_j)$, $x_j \in \mathscr{X}_R$, $j = 0, \cdots, |\mathscr{X}_R|-1$. Then, assuming perfect interleaving Π_R, we have

$$\mathbb{E}\{x_{R,k}|\boldsymbol{\lambda}_{R,k}\} = \sum_{j=0}^{|\mathscr{X}_R|-1} x_j \left(\prod_{\ell=1}^{q_R}\frac{e^{v_{j,\ell}\lambda_{R,k,\ell}}}{1+e^{\lambda_{R,k,\ell}}}\right). \tag{6.7}$$

The signals transmitted from the relay $\tilde{x}_{R,k}$, can then be viewed as an estimation followed by a normalizing energy factor as in [117]. Thus, their corresponding received signals at the destination can be expressed as

$$\begin{aligned}\mathbf{y}_{D,k}^{(2)} &= \sqrt{P_{RD}}\mathbf{h}_{RD}\tilde{x}_{R,k} + \mathbf{n}_{D,k}^{(2)} \\ &= \sqrt{P_{RD}}\mathbf{h}_{RD}(\beta x_{R,k} + e_{u,k}) + \mathbf{n}_{D,k}^{(2)} \\ &= \sqrt{P_{RD}}\mathbf{h}_{RD}\beta x_{R,k} + \mathbf{n}_{eq,k}\end{aligned} \tag{6.8}$$

where $\mathbf{n}_{eq,k} = \sqrt{P_{RD}}\mathbf{h}_{RD}e_{u,k} + \mathbf{n}_{D,k}^{(2)}$ are considered as i.i.d. random complex circularly symmetric Gaussian noise samples at the destination and $e_{u,k}$ is the uncorrelated estimation

error with respect to $x_{R,k}$. It is straight forward to calculate $\beta^2 = \tilde{\sigma}^2$, as well as the error variance $\mathbb{E}\{|e_u|^2\} = 1 - \tilde{\sigma}^2$. Finally, we have

$$\mathbf{y}_{D,k}^{(2)} = \sqrt{P_{RD}}\mathbf{h}_{RD}\tilde{\sigma}x_{R,k} + \mathbf{n}_{eq,k} \tag{6.9}$$

with $\mathbb{E}\{\mathbf{n}_{eq}\} = \mathbf{0}_{N_D}$, and

$$\mathbf{R}_{eq} = \mathbb{E}\{\mathbf{n}_{eq}\mathbf{n}_{eq}^{\dagger}\} = P_{RD}(1-\tilde{\sigma}^2)\mathbf{h}_{RD}\mathbf{h}_{RD}^{\dagger} + N_0\mathbf{I}_{N_D}. \tag{6.10}$$

6.2.3 JNCD at the destination

The JNCD at the destination is conditional to the relay functionality. In the case of selective relaying, the JNCD is already discussed in Chapter 2 (Section 2.3.3). In the case of soft relaying, the combination of the systematic and parity bits of both sources, and of the additional JNC parity bits forwarded by the relay form two distributed codes. Thus, at the end of the second transmission phase, the destination starts to detect and decode the original data, processing the received signals (6.2) and (6.3). To accomplish this, we again resort to a suboptimal iterative procedure. Extrinsic information on coded bits circulate between SISO MAP detector and demapper corresponding to two transmission phases and the outer decoders, while, at the same time, extrinsic information on systematic bits circulate between the SISO decoders of each distributed code. The reader is referred to Chapter 2 for the SISO MAP detector and demapper key equations (Section 2.3.3.1), the overall receiver architecture details and the message-passing schedule (Section 2.3.3.2). We should just point out that the calculation of $P(\mathbf{y}_{D,k}^{(2)}|x_{R,k} = c)$ in the selective relaying is according to

$$P(\mathbf{y}_{D,k}^{(2)}|x_{R,k} = c) \propto e^{-\frac{\|\mathbf{y}_{D,k}^{(2)} - \sqrt{P_{RD}}\mathbf{h}_{RD}c\|^2}{N_0}} \tag{6.11}$$

while in the soft MSE estimate relaying, based on the equivalent model of $\mathbf{y}_{D,k}^{(2)}$ in (6.9), we have

$$P(\mathbf{y}_{D,k}^{(2)}|x_{R,k} = c) \propto e^{-(\mathbf{y}_{D,k}^{(2)} - \sqrt{P_{RD}}\mathbf{h}_{RD}\tilde{\sigma}c)^{\dagger}\mathbf{R}_{eq}^{-1}(\mathbf{y}_{D,k}^{(2)} - \sqrt{P_{RD}}\mathbf{h}_{RD}\tilde{\sigma}c)}. \tag{6.12}$$

6.3 Performance Evaluation

In this section, we provide some numerical results to compare different relaying functions (SDF, LAPPR transmission, and MSE estimate) in the half duplex MARC with semi-orthogonal transmission protocol. It is worth noting that in [144], we showed that SoDF

could outperform by around 2 dB the joint selective DF in some extreme cases. Here, we want to verify if it can outperform the SDF approach as well. For the sake of simplicity, we consider a symmetric MARC, i.e., $d_{1R} = d_{2R}$ and $d_{1D} = d_{2D}$. The average energy per available dimension allocated to the two sources is the same, i.e., $P_{0,1} = P_{0,2} = P_0$. We fix the same path loss factor, i.e., $\kappa = 3$, free distance, i.e., $d_0 = 1$ and noise power spectral density, i.e., $N_0 = 1$, for all links. Due to the half-duplex nature of the relay, the transmission time slot of the sources and the relay are separated in time. We have $P_1 = P_2 = P_0/\alpha$. The relay, in case of cooperation, transmits always at $P_R = P_{0,R}/\bar{\alpha}$. Each message of the sources has length $K = 1024$ information bits. The system performance is measured in terms of individual BLER (for example for S_1). For simulation purposes, two different configurations are considered:

(1) In the first configuration, we fix $\alpha = 2/3$. The number of receive antennas is fixed to one both at the relay and destination, i.e., $N_R = N_D = 1$. The geometry is chosen such that $d_{ij} = d_{RD} = d$ which yields $P_{i,j} = P_{RD} = \gamma$, $i \in \{1, 2\}$, $j \in \{R, D\}$ where γ is the received SNR per symbol or dimension. The two sources use identical turbo codes of rate-1/2 made of two 4-state rate-1/2 RSC encoders with generator matrix $\mathbf{G}_1 = [\ 1 \quad 5/7\ ]$ in octal representation, whose half of the parity bits are punctured. The relay uses XOR followed by the 4-state rate-1/2 RSC encoder. The complex signal sets $\mathscr{X}_1$, $\mathscr{X}_2$, and $\mathscr{X}_R$ used in BICM are either QPSK or 16QAM constellations (Gray labeling) and the corresponding sum rates are $\eta = 4/3$ b./c.u. and $\eta = 8/3$ b./c.u., respectively. The number of iterations I is set to 5 at the relay and to 10 at the destination. These numbers of iterations ensure convergence and allow to very closely approach the performance of a Genie Aided (GA) receiver at sufficiently high SNR for the selected modulation and coding schemes, the Genie Aided (GA) receiver corresponding to the ideal case where the interference is known and perfectly removed. The corresponding results are depicted in Fig. 6.1. As we see, with the chosen coding schemes, the SDF relaying performs slightly better than the soft relaying functions. The exception is the case of 16QAM and for the SNRs beyond 22 dB, where SoDF slightly outperforms the SDF. It is worth stressing that in the case of LAPPR transmission for 16QAM, twice as much channel uses are dedicated to the relay-to-destination link. Moreover, interestingly, the LAPPR transmission for 16QAM performs very close to the MSE estimate which tends to confirm that the MSE estimate relaying function is efficient for high order modulations.

(2) To pursue our comparison analysis, we then consider another somehow extreme case in which the two sources transmit directly their uncoded information symbols, and the relay uses XOR followed by the 4-state rate-1/2 RSC encoder. It yields $\alpha = 1/2$. The sum rates for QPSK and 16QAM modulation becomes respectively $\eta = 2$ and $\eta = 4$ b./c.u.. We increase the number of receive antennas at the destination to 2, i.e., $N_R = 2$ and $N_D = 2$.

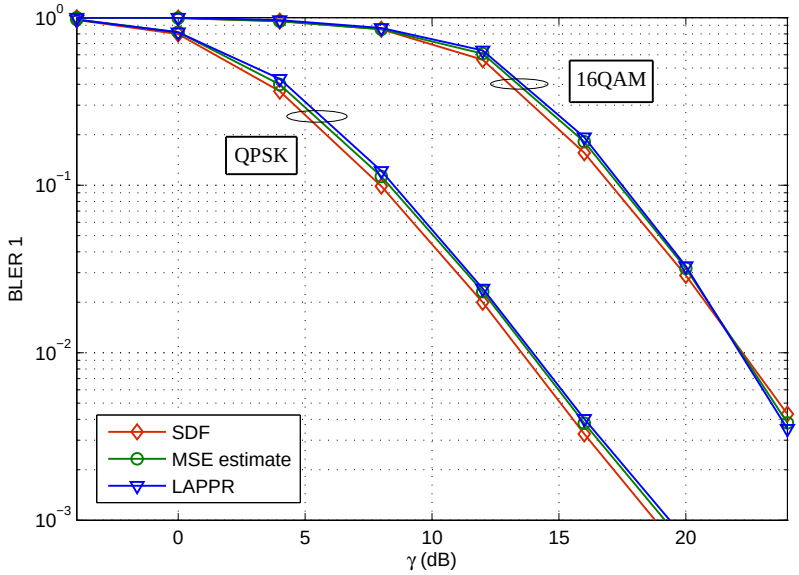

Figure 6.1: Individual BLER (e.g., for S_1) - Different relaying functions in semi-orthogonal half-duplex MARC - $N_R = 1$, $N_D = 1$ - $\alpha = 2/3$

The value of P_{RD} is fixed to 25 dB. The geometry is chosen such that $d_{ij} = d$ which yields $P_{i,j} = \gamma$, $i \in \{1, 2\}$, $j \in \{R, D\}$. There is no iteration at the relay, and we fix the number of iterations at the destination to 10. The corresponding results showed the same trends as the previous case.

Clearly, the performance gap between the soft and hard selective relaying depends on the coding schemes used at the sources and the relay, as well as, the characteristics of the radio links. However, according to the simulation results, it seems that soft relaying cannot do much better compared to the SDF one, even if it remains an interesting approach in comparison to the Detect-and-Forward relaying considering both the uncoded [117] and coded performance [124].

6.4 Conclusions

In this chapter, we discussed different relaying functions in the context of JNCC for the half duplex MARC with semi-orthogonal transmission protocol, and for a given spectral efficiency. Simulation results showed that SDF works well in most of the configurations and just in some extreme cases, SoDF relaying functions (based on LAPPR or MSE estimate) can slightly outperform the hard selective one. The potential gains then highly depend on

the chosen configurations. They also tend to confirm that the MSE estimate is an efficient LAPPR compression function for high order modulation.

Chapter 7

Conclusions and Research Perspectives

In regards to the emerging interest for cooperative communication and network coding, this thesis was initiated with the goal of study and design of practical network coding schemes for different scenarios of wireless communication and from the physical layer perspective. Contrary to the traditional literature, the superposition and broadcast nature of wireless medium have both been exploited in our studies, and they have enlightened the potential benefits of interference management in spite of the practical considerations. Furthermore, different ways of implementing cooperation, including practical relaying protocols have been investigated in a realistic wireless environment. In the following, we highlight the main contributions that have been achieved in this thesis:

- We tackled, theoretically and in practice, the problem of JNCC for a MARC in the presence of multiple access interferences, and for both of the relay operating modes, namely, half-duplex and full-duplex. To this end, we have introduced and studied three new classes of MARC, referred to as HD-SOMARC, HD-NOMARC, and FD-NOMARC:

  - HD-SOMARC: The sources transmit simultaneously during the listening phase of the relay, but are constrained to remain silent during the relay transmission phase; The relay is half-duplex and applies an SDF strategy, i.e, it forwards only a deterministic function of the error-free decoded messages. We have derived the HD-SOMARC individual information outage probability, conditional on JNCC

(and SNCC used as a reference). We have also presented new JNCC schemes flexible in terms of number of sources, encoders and modulations. For the 2-source symmetric case and targeted sum rates $\eta = 4/3$ b./c.u. and $\eta = 8/3$ b./c.u., we have shown that our proposed schemes are more efficient than (1) conventional distributed JNCC for OMARC; (2) conventional SNCC schemes. Moreover, the proposed HD-SOMARC/JNCC performs very close to the outage limit for both cases of single and multiple receive antennas at the destination, and for the fixed sum rate of $\eta = 4/3$ b./c.u.. We have also verified that the semi-orthogonal multiple access exhibits considerable gains over orthogonal multiple access, even in the case of a single receive antenna at the destination.

- HD-NOMARC: We removed the constraint of SOMARC in which the sources remain silent during the transmission phase of the relay. This class of MARC reduces significantly the number of signaling, since only the destination node should be informed of the cooperation. We have derived the HD-NOMARC individual information outage probability, conditional on JNCC and SNCC. Using the outage analysis, we have optimized the fraction of available channel uses during which the relay should listen and those during which the sources and the relay should transmit. The optimal allocation was then applied to our practical designs. We have presented new JNCC schemes flexible in terms of number of sources, encoders and modulations, and we have shown that they are more efficient than (1) conventional distributed JNCC for OMARC; (2) conventional SNCC schemes. Moreover, the proposed HD-NOMARC/JNCC performs very close to the outage limit for both cases of single and multiple receive antennas at the destination, and for the fixed sum rate of $\eta = 4/3$ b./c.u..
- FD-NOMARC: Full-duplex relays were shown to be feasible recently, and thus, as a last step, we relaxed the half duplex constraint of the relay. We have derived the FD-NOMARC joint information outage probability, conditional on JNCC, superposition block Markov coding, and backward decoding. This provides lower bounds on the information outage probability of our practical designs. We have also presented new JNCC designs together with advanced receiver architectures at the destination, which, contrary to block by block decoding, operate over all the transmitted blocks. For the 2-source symmetric case and targeted sum rates $\eta = 4/3$ b./c.u. and $\eta = 8/3$ b./c.u., we have shown that our proposed schemes are more efficient than conventional distributed JNCC for OMARC.

- We extended the network model by considering multiple relays which help multiple sources to communicate with a destination. A new class of MAMRC, referred

to as HD-SOMAMRC was then proposed, in which (1) the relays operate in half-duplex mode; (2) During the listening phase of the relays, the sources transmit simultaneously, but they remain silent during their transmission phases. The relays are also allowed to transmit simultaneously all together; (3) the relays apply an SDF relaying approach. We then studied JNCC for HD-SOMAMRC from both an information-theoretic and a practical code design perspective. We have derived the HD-SOMAMRC individual information outage probability, conditional on JNCC and SNCC. Using the outage analysis, we have optimized the fraction of available channel uses during which the relays should listen and those during which the relays should transmit. We have also presented new practical JNCC schemes, in which binary channel coding and non binary network coding were combined. The appropriate receiver architectures were also derived. Both theoretic analyses and simulations have demonstrated that the proposed HD-SOMAMRC/JNCC can fully exploit the spatial diversity, and have significant benefits compared to the existing schemes. Moreover, the proposed HD-SOMAMRC/JNCC performs very close to the outage limit for both cases of single and multiple receive antennas at the destination, and for the fixed sum rate of $\eta = 4/3$ b./c.u..

- Finally, different relaying functions were discussed in the context of HD-SOMARC with JNCC. In HD-SOMARC, contrary to other classes of MARC, the relaying function is an interesting degree of freedom to be optimized, thanks to the interference free transmission of the relay. We have compared the SDF function proposed in preceding parts of the thesis with two analog relaying functions: one based on LAPPR and the other based on MSE estimate. The simulation results showed that SDF works well in most of the configurations and just in some extreme cases, soft relaying functions (based on LAPPR or MSE estimate) can slightly outperform the hard selective one. They also tend to confirm that the MSE estimate is an efficient LAPPR compression function for high order modulation.

To conclude, some possible directions for future research are listed below:

- We have shown that our proposed designs for HD-SOMARC, HD-NOMARC and HD-SOMAMRC perform very close to the outage limit for the fixed sum rate of $\eta = 4/3$ b./c.u.. However, coding gain optimization should still be carried out for large signal constellations. In the case of FD-NOMARC, the individual information outage probabilities should first be derived, conditional on joint decoding of all the transmitted blocks. This allows us to measure the gap between our proposed schemes

and the exact outage limits, and to strive to achieve the theoretical limits by further coding gain optimization.

In order to optimize the coding gain, it is also important to compute the union (upper) bounds on the error performance using specific codes, which would then serve as a basis to find the optimal code. These bounds are known to be tight for medium to large SNR. To this end, tools and techniques from [118–120] should be used together with the knowledge on the exact Weight Enumerator Functions (WEFs) of convolutional codes and the average WEFs of turbo codes [121, 122]. Such analysis is conducted for OMARC with BPSK and under AWGN channel in [123]. However, the performance analysis in case of non-orthogonal transmission and under slow fading channels remain an open issue for future works. The derived bounds would also be used to predict the performance of the system at very low bit or block error rates and could also serve as a benchmark for sub-optimal iterative decoding algorithms.

- Regarding the MAMRC, non-binary channel coding at the sources and relays could be investigated, especially in case of JNCC. In this case, as the coding and modulation schemes at the sources and relays are defined in the non-binary field where the network coding coefficients are chosen, there is no more need to employ the bit to symbol or symbol to bit conversion. This may improve the performance, but at the same time it could be restrictive in terms of spectral efficiency. A possible design based on LDPC code was treated in [95] for OMAMRC. Further code design could be conducted based on non binary turbo coding.

- In this thesis, we have only considered the HD-SOMAMRC. However, it would be worth investigating practical designs and theoretical bounds for the more complex Half-Duplex Non-Orthogonal MAMRC (HD-NOMAMRC) and Full-Duplex Non-Orthogonal MAMRC (FD-NOMAMRC). In HD-NOMAMRC, the constraint that the sources remain silent during the transmission phase of the relays, is removed, and in FD-NOMAMRC, the half duplex constraint of the relays is also relaxed. The task is not a straightforward generalization of the current results.

- It remains unclear if there exists a better practical relaying function than SDF in the context of HD-NOMARC, FD-NOMARC, and HD-SOMAMRC. However, better relaying functions than the proposed SDF or MSE estimate could be explored in the context of half-duplex MARC with semi-orthogonal transmission protocol. A possible perspective is to consider the PNC approach. As already mentioned, PNC has mainly been studied in the case of two-phase TWRC, where both sources also act as a destination, and a separate destination is absent. Thus, one of the network-encoded messages is perfectly known at each source. Moreover, since there is no direct

link between the sources, they only receive the broadcast transmission of the relay during the second phase, which leads to a diversity order of one (as in the case of multi-hop networks). Hence, studying PNC in situations where cooperative diversity can be exploited, such as MARC, remains a subject of interest. Using the PNC approach, the relay decodes the addition modulo 2 of the source messages from the superimposed received signal. To further reduce the error propagation from the relay to the destination, we can consider joint decode-and-forward PNC; here, the relay transmits if it can successfully decode the XOR of the messages. The probability of the latter is always greater than the probability of joint successful decoding of each source message. Therefore, the relay is more often active which may improve the overall performance with respect to the classical joint DF. The advantages over SDF remain disputable. However, this approach seems difficult to implement from the practical point of view. The reason lies in the fact that the relay does not decode individually each source message, and it can not use the CRC included in source messages to perform joint selective PNC. Soft relaying can remove this problem: the relay can directly derive the soft information on the network-coded message to construct the MSE estimate. The latter, if combined with the ML decoding at the destination under MSE estimate [124], seems to be a promising solution. However, in future works, one may try to circumscribe the configurations where soft PNC could outperform the SDF approach in the context of half-duplex MARC with semi-orthogonal transmission protocol. Finally, it is interesting to develop a cooperative strategy and a proper code design, which superimpose the SDF and Soft PNC, or more generally, SDF and CoF.

- We have shown through theoretical analyses and practical designs that partially or totally exploiting interference is almost always beneficial with respect to the orthogonal transmission protocol. However, the choice between semi-orthogonal and full non-orthogonal transmission protocol in either MARC or MAMRC depends on the configuration and remains an open issue. The goal would be the identification of the scenarios in which each protocol can significantly outperform the other one, and dynamically adapt the appropriate code design.

Appendix A

MAC outage performance at high SNR

We want to prove that, in the large SNR regime, and for the special case of one receive antenna, the outage probability of an M-user slow fading MAC (with Gaussian signaling) behaves as the one of an orthogonal MAC. Here, we refer to as outage probability of an M users' MAC, the probability that at least one user out of M is in outage. The M users are transmitting at the same rate R b./c.u., and the received instantaneous SNR of user i, $i \in \{1, \ldots, M\}$, is $|h_i|^2 P/N_0$, where h_i are independent channel fading coefficients following the pdf $\mathcal{CN}(0,1)$. The outage probability of the considered MAC is defined as

$$p_{out}^{\text{MAC}} = \Pr\left\{\log\left(1 + \frac{P\sum_{i\in S}|h_i|^2}{N_0}\right) < |S|R, \text{ for at least one } S \subseteq \{1,\ldots,M\}\right\}. \quad \text{(A.1)}$$

where $|S|$ is the cardinality of the set S. Under independent Rayleigh fading, $h = \sum_{i\in S}|h_i|^2$, is a sum of $|S|$ i.i.d exponential random variables with parameter 1 and is distributed as

$$f(h) = \frac{1}{(|S|-1)!}h^{|S|-1}e^{-h} \ , \quad h \geq 0. \quad \text{(A.2)}$$

For a fixed R and very high $\gamma = P/N_0$, $\Pr\{h < \frac{2^{|S|R}-1}{\gamma}\}$ is always inferior to that of the case $|S| = 1$. Thus, at very high γ, the dominating events for p_{out}^{MAC} are for $|S| = 1$, which

corresponds to an orthogonal MAC outage event. Thus,

$$\begin{aligned} p_{out}^{\mathrm{MAC}} &\simeq \Pr\left\{\log\left(1+\frac{P|h_i|^2}{N_0}\right) < R, \text{ for at least one } i \in \{1,\cdots,M\}\right\} \\ &= M\Pr\left\{|h_1|^2 < \frac{2^R-1}{\gamma}\right\}, \end{aligned} \tag{A.3}$$

where the equality in (A.3) follows from the fact that the exponential random variables $|h_i|^2$, $i \in \{1,\cdots,M\}$, are independent and have the same Cumulative Distribution Function (CDF). Since, $h = |h_1|^2$ is distributed as $f(h) = e^{-h}$ for $h \geq 0$, it yields

$$p_{out}^{\mathrm{MAC}} \simeq M\left(1-\exp\left(\frac{-(2^R-1)}{\gamma}\right)\right) \tag{A.4}$$

which can be approximated at high SNR as

$$p_{out}^{\mathrm{MAC}} \simeq M\frac{2^R-1}{\gamma}. \tag{A.5}$$

It confirms that the MAC outage probability at high SNR decays as $1/\gamma$ similarly to the case of orthogonal MAC or single-user interference free channels. As a results, the probability of having n users ($1 \leq n \leq M$) in outage decays as γ^{-n}.

Appendix B

Mutual information calculation for different types of input distribution

We consider an M-user slow fading MAC with N_D receive antennas at the destination. Let define the independent input random variables $x_i \sim p(x_i)$, $i \in \{1, \cdots, M\}$ and the associated independent output random vector $\mathbf{y}$, whose channel transition conditional pdf is $p(\mathbf{y} \mid x_1, \cdots, x_M, \mathbf{H}) = \mathcal{CN}\left(\sum_{i=1}^{M} \sqrt{P_i}\mathbf{h}_i x_i, N_0 \mathbf{I}_{N_D}\right)$ with $\mathbf{H} = \left[\begin{array}{ccc} \mathbf{h}_1 & \cdots & \mathbf{h}_M \end{array}\right]$. Here, $\mathbf{h}_i$ are independent channel fading coefficients following the pdf $\mathcal{CN}(\mathbf{0}_{N_D}, \mathbf{I}_{N_D})$, and P_i is the average received energy per dimension and per antenna at the destination from each user. It follows that the mutual information $I(x_1, \cdots, x_M; \mathbf{y})$ is perfectly defined by the pdfs $p(x_1), \cdots, p(x_M)$ and the aforementioned channel transition probability. Let $S = \left\{s_1, s_2, \cdots, s_{|S|}\right\} \subseteq \{1, \cdots, M\}$, and $\mathbf{x}_S$ and $\mathbf{x}_{\bar{S}}$ denote respectively $\{x_{s_i}\}_{s_i \in S}$ and $\{x_{\bar{s}_i}\}_{\bar{s}_i \in \bar{S}}$. In the following, we derive the mutual informations $I(\mathbf{x}_S; \mathbf{y} | \mathbf{x}_{\bar{S}})$ and $I(\mathbf{x}_S; \mathbf{y})$ for two different types of input distribution: Gaussian i.i.d. inputs and discrete i.i.d. inputs.

B.1 Gaussian i.i.d. inputs

In this case, the mutual information is given by

$$I(\mathbf{x}_S; \mathbf{y} | \mathbf{x}_{\bar{S}}) = \log \det \left(\mathbf{I}_{N_D} + \frac{1}{N_0} \mathbf{H}_s \mathbf{K}_s \mathbf{H}_s^{\dagger}\right) \tag{B.1}$$

where $\mathbf{H}_s = \begin{bmatrix} \mathbf{h}_{s_1} & \mathbf{h}_{s_2} & \cdots & \mathbf{h}_{s_{|S|}} \end{bmatrix}$, and $\mathbf{K}_s = \text{diag}\left(P_{s_1}, \cdots, P_{s_{|S|}}\right)$, and

$$I(\mathbf{x}_S; \mathbf{y}) = \log\det\left(\mathbf{I}_{N_D} + \mathbf{H}_s \mathbf{K}_s \mathbf{H}_s^\dagger \mathbf{V}_{\bar{s}}^{-1}\right) \tag{B.2}$$

where

$$\mathbf{V}_{\bar{s}} = N_0 \mathbf{I}_{N_D} + \mathbf{H}_{\bar{s}} \mathbf{K}_{\bar{s}} \mathbf{H}_{\bar{s}}^\dagger \tag{B.3}$$

for $\mathbf{H}_{\bar{s}} = \begin{bmatrix} \mathbf{h}_{\bar{s}_1} & \mathbf{h}_{\bar{s}_2} & \cdots & \mathbf{h}_{\bar{s}_{|\bar{S}|}} \end{bmatrix}$, and $\mathbf{K}_{\bar{s}} = \text{diag}\left(P_{\bar{s}_1}, \cdots, P_{\bar{s}_{|\bar{S}|}}\right)$.

B.2 Discrete i.i.d. inputs

In this case, discrete channel inputs x_i are chosen from the constellations $\mathscr{X}_i$ of order 2^{q_i}. We assume uniform input distributions. Thus, $p(x_i) = 2^{-q_i}$. The mutual information is derived numerically [145] as

$$\begin{aligned}
I(\mathbf{x}_S; \mathbf{y}|\mathbf{x}_{\bar{S}}) &= H(\mathbf{x}_S) - H(\mathbf{x}_S|\mathbf{y}, \mathbf{x}_{\bar{S}}) \\
&= \sum_{i \in S} q_i + \mathbb{E}\left[\log_2 p(\mathbf{x}_S|\mathbf{y}, \mathbf{x}_{\bar{S}})\right] \\
&= \sum_{i \in S} q_i + \mathbb{E}\left[\log_2 \frac{p(\mathbf{y}|\mathbf{x}_S, \mathbf{x}_{\bar{S}}) p(\mathbf{x}_S, \mathbf{x}_{\bar{S}})}{\sum_{\tilde{x}_{s_1} \in \mathscr{X}_{s_1}} \cdots \sum_{\tilde{x}_{s_{|S|}} \in \mathscr{X}_{s_{|S|}}} p(\mathbf{y}|\tilde{\mathbf{x}}_S, \mathbf{x}_{\bar{S}}) p(\tilde{\mathbf{x}}_S, \mathbf{x}_{\bar{S}})}\right] \\
&= \sum_{i \in S} q_i - \mathbb{E}\left[\log_2 \frac{\sum_{\tilde{x}_{s_1} \in \mathscr{X}_{s_1}} \cdots \sum_{\tilde{x}_{s_{|S|}} \in \mathscr{X}_{s_{|S|}}} p(\mathbf{y}|\tilde{\mathbf{x}}_S, \mathbf{x}_{\bar{S}})}{p(\mathbf{y}|\mathbf{x}_S, \mathbf{x}_{\bar{S}})}\right]
\end{aligned} \tag{B.4}$$

where the expectation is with respect to $p(\mathbf{x}_S, \mathbf{x}_{\bar{S}}, \mathbf{y}) = 2^{-\sum_{i=1}^{M} q_i} p(\mathbf{y}|\mathbf{x}_1, \cdots, \mathbf{x}_M)$. Similarly, we have

$$\begin{aligned}
I(\mathbf{x}_S; \mathbf{y}) &= H(\mathbf{x}_S) - H(\mathbf{x}_S|\mathbf{y}) \\
&= \sum_{i \in S} q_i + \mathbb{E}\left[\log_2 p(\mathbf{x}_S|\mathbf{y})\right] \\
&= \sum_{i \in S} q_i + \mathbb{E}\left[\log_2 \frac{\sum_{\tilde{x}_{\bar{s}_1} \in \mathscr{X}_{\bar{s}_1}} \cdots \sum_{\tilde{x}_{\bar{s}_{|\bar{S}|}} \in \mathscr{X}_{\bar{s}_{|\bar{S}|}}} p(\mathbf{y}|\mathbf{x}_S, \tilde{\mathbf{x}}_{\bar{S}}) p(\mathbf{x}_S, \tilde{\mathbf{x}}_{\bar{S}})}{\sum_{\tilde{x}_1 \in \mathscr{X}_1} \cdots \sum_{\tilde{x}_M \in \mathscr{X}_M} p(\mathbf{y}|\tilde{\mathbf{x}}_1, \cdots, \tilde{\mathbf{x}}_M) p(\tilde{\mathbf{x}}_1, \cdots, \tilde{\mathbf{x}}_M)}\right] \\
&= \sum_{i \in S} q_i - \mathbb{E}\left[\log_2 \frac{\sum_{\tilde{x}_1 \in \mathscr{X}_1} \cdots \sum_{\tilde{x}_M \in \mathscr{X}_M} p(\mathbf{y}|\tilde{\mathbf{x}}_1, \cdots, \tilde{\mathbf{x}}_M)}{\sum_{\tilde{x}_{\bar{s}_1} \in \mathscr{X}_{\bar{s}_1}} \cdots \sum_{\tilde{x}_{\bar{s}_{|\bar{S}|}} \in \mathscr{X}_{\bar{s}_{|\bar{S}|}}} p(\mathbf{y}|\mathbf{x}_S, \tilde{\mathbf{x}}_{\bar{S}})}\right]
\end{aligned} \tag{B.5}$$

where the expectation is with respect to

$$p(\mathbf{x}_S, \mathbf{y}) = 2^{-\sum_{i \in S} q_i} p(\mathbf{y}|\mathbf{x}_S) = 2^{-\sum_{i=1}^{M} q_i} \sum_{\tilde{\mathbf{x}}_{\bar{S}}} p(\mathbf{y}|\mathbf{x}_S, \tilde{\mathbf{x}}_{\bar{S}}).$$

Bibliography

[1] R. Graham, D. Knuth, and O. Patashnik, "Concrete mathematics," *Reading, MA: Addison-Wesley*, 1989.

[2] E. V. der Meulen, "Transmission of information in a t-terminal discrete memoryless channel," Ph.D. dissertation, Department of Statistics, University of California, Berkeley, 1968.

[3] A. Sendonaris, E. Erkip, and B. Aazhang, "User cooperation diversity, part I: System description," *IEEE Trans. Commun.*, vol. 51, no. 11, pp. 1927–1938, Nov. 2003.

[4] ——, "User cooperation diversity, part II: Implementation aspects and performance analysis," *IEEE Trans. Commun.*, vol. 51, no. 11, pp. 1939–1948, Nov. 2003.

[5] T. Cover and A. E. Gamal, "Capacity theorems for the relay channel," *IEEE Trans. Inf. Theory*, vol. 25, no. 5, pp. 572–584, Sep. 1979.

[6] A. Wyner, "On source coding with side information at the decoder," *IEEE Trans. Inf. Theory*, vol. 21, no. 3, pp. 294–300, May 1975.

[7] A. Wyner and J. Ziv, "The rate-distortion function for source coding with side information at the decoder," *IEEE Trans. Inf. Theory*, vol. 22, no. 1, pp. 1–10, Jan. 1976.

[8] G. Kramer, M. Gastpar, and P. Gupta, "Cooperative strategies and capacity theorems for relay networks," *IEEE Trans. Inf. Theory*, vol. 51, no. 9, pp. 3027–3063, Sep. 2005.

[9] R. Nabar, H. Bolcskei, and F. Kneubohler, "Fading relay channels: performance limits and space-time signal design," *IEEE J. Sel. Areas Commun.*, vol. 22, no. 6, pp. 1099–1109, Aug. 2004.

[10] A. Host-Madsen and J. Zhang, "Capacity bounds and power allocation for wireless relay channels," *IEEE Trans. Inf. Theory*, vol. 51, no. 6, pp. 2020–2040, Jun. 2005.

[11] A. E. Gamal and S. Zahedi, "Capacity of a class of relay channels with orthogonal components," *IEEE Trans. Inf. Theory*, vol. 51, no. 5, pp. 1815–1817, May 2005.

[12] Y. Liang and V. Veeravalli, "Gaussian orthogonal relay channels: optimal resource allocation and capacity," *IEEE Trans. Inf. Theory*, vol. 51, no. 9, pp. 3284–3289, Sep. 2005.

[13] A. E. Gamal, M. Mohseni, and S. Zahedi, "Bounds on capacity and minimum energy-per-bit for awgn relay channels," *IEEE Trans. Inf. Theory*, vol. 52, no. 4, pp. 1545–1561, Apr. 2006.

[14] M. Khojastepour, "Distributed cooperative communications in wireless networks," Ph.D. dissertation, Rice University, 2004.

[15] M. Gastpar and M. Vetterli, "On the capacity of large gaussian relay networks," *IEEE Trans. Inf. Theory*, vol. 51, no. 3, pp. 765–779, Mar. 2005.

[16] A. Dana and B. Hassibi, "On the power efficiency of sensory and ad-hoc wireless networks," *IEEE Trans. Inf. Theory*, vol. 52, no. 7, pp. 2890–2914, Jul. 2006.

[17] A. del Coso, "Achievable rates for gaussian channels with multiple relays," Ph.D. dissertation, Universitat Politecnica de Catalunya, Spain, 2008.

[18] J. Laneman, "Cooperative diversity in wireless networks: Algorithms and architectures," Ph.D. dissertation, MIT, 2002.

[19] J. Laneman and G. Wornell, "Distributed space-time coded protocols for exploiting cooperative diversity in wireless networks," *IEEE Trans. Inf. Theory*, vol. 49, no. 10, pp. 2415–2425, Oct. 2003.

[20] J. Laneman, D. Tse, and G. Wornell, "Cooperative diversity in wireless networks: Efficient protocols and outage behaviour," *IEEE Trans. Inf. Theory*, vol. 50, no. 12, pp. 3062–3080, Dec. 2004.

[21] T. E. Hunter and A. Nosratinia, "Cooperative diversity through coding," in *Proc. IEEE ISIT'02*, Lausanne, Switzerland, Jul. 2002, p. 220.

[22] A. Nosratinia, T. E. Hunter, and A. Hedayat, "Cooperative communication in wireless networks," *IEEE Communication Magazine*, vol. 42, no. 10, pp. 74–80, Oct. 2004.

[23] T. E. Hunter and A. Nosratinia, "Diversity through coded cooperation," *IEEE Trans. Wireless Commun.*, vol. 5, no. 2, pp. 283–289, Feb. 2006.

[24] M. Janani, A. Hedayat, T. Hunter, and A. Nosratinia, "Coded cooperation in wireless communications: Space-time transmission and iterative decoding," *IEEE Trans. Signal Process.*, vol. 52, no. 2, pp. 362–371, Feb. 2004.

[25] G. Kramer, "Distributed and layered codes for relaying," in *Asilomar Conference on Signals, Systems and Computers*, Oct. 2005.

[26] H. Chong, M. Motani, and H. Garg, "New coding strategies for the relay channel," in *Proc. IEEE ISIT'05*, Adelaide, Australia, Sep. 2005, pp. 1086–1090.

[27] G. Kramer and A. J. van Wijngaarden, "On the white gaussian multiple access relay channel," in *Proc. IEEE ISIT'00*, Sorrento, Italy, Jun. 2000.

[28] L. Sankaranarayanan, G. Kramer, and N. Mandayam, "Capacity theorems for the multiple-access relay channel," in *Proc. Annual Allerton Conference on Communication, Control and Computing*, Monticello, IL, Sep. 2004.

[29] ——, "Hierarchical sensor networks: capacity bounds and cooperative strategies using the multiple-access relay channel model," in *Proc. SECON'04*, Oct. 2004, pp. 191–199.

[30] D. Chen, K. Azarian, and J. Laneman, "A case for amplify-forward relaying in the block-fading multiaccess channel," *IEEE Trans. Inf. Theory*, vol. 54, no. 8, pp. 3728–3733, Aug. 2008.

[31] Y. Liang and V. Veeravalli, "Cooperative relay broadcast channels," in *Proc. International Conference on Wireless Networks, Communications and Mobile Computing'05*, Jun. 2005, pp. 1449–1454.

[32] ——, "Cooperative relay broadcast channels," *IEEE Trans. Inf. Theory*, vol. 53, no. 3, pp. 900–928, Mar. 2007.

[33] A. Reznik, S. Kulkarni, and S. Verdu, "Broadcast-relay channel: capacity region bounds," in *Proc. IEEE ISIT'10*, Adelaide, Australia, Sep. 2005.

[34] Y. Liang and V. Veeravalli, "The impact of relaying on the capacity of broadcast channels," in *Proc. IEEE ISIT'04*, Chicago, IL, Jun. 2004.

[35] Y. Liang and G. Kramer, "Rate regions for relay broadcast channels," *IEEE Trans. Inf. Theory*, vol. 53, no. 10, pp. 3517–3535, Oct. 2007.

[36] S. I. Bross, "On the discrete memoryless partially cooperative relay broadcast channel and the broadcast channel with cooperative decoders," *IEEE Trans. Inf. Theory*, vol. 55, no. 5, pp. 2161–2182, May 2009.

[37] S. Jafar, K. Gomadam, and C. Huang, "Duality and rate optimization for multiple access and broadcast channels with amplify-and-forward relays," *IEEE Trans. Inf. Theory*, vol. 53, no. 10, pp. 3350–3370, Oct. 2007.

[38] Y. Wu, P. A. Chou, and S. Y. Kung, "Information exchange in wireless networks with network coding and physical-layer broadcast," in *Proc. 39th Annual Conference on Information Sciences and Systems (CISS)*, Baltimore, MD, USA, Mar. 2005.

[39] B. Rankov and A. Wittneben, "Achievable rate regions for the two way relay channel," in *Proc. IEEE ISIT'06*, Seattle, Washington, Jul. 2006.

[40] L. Xie, "Network coding and random binning for multi-user channels," in *Proc. Canadian Workshop on Information Theory'07*, Jun. 2007, pp. 85–88.

[41] Y. Song and N. Devroye, "List decoding for nested lattices and applications to relay channels," in *Proc. Annual Allerton Conf.'10*, Sep. 2010.

[42] B. Nazer and M. Gastpar, "Lattice coding increases multicast rates for gaussian multiple-access networks," in *Proc. Annual Allerton Conf.'07*, Seattle, Washington, Sep. 2007, pp. 1089–1096.

[43] K. Narayanan, M. P. Wilson, and A. Sprintson, "Joint physical layer coding and network coding for bi-directional relaying," in *Proc. Annual Allerton Conf.'07*, Sep. 2007.

[44] B. Rankov and A. Wittneben, "Spectral efficient protocols for half-duplex relay channels," *IEEE J. Sel. Areas Commun.*, vol. 25, no. 2, pp. 379–389, Feb. 2007.

[45] T. Oechtering, C. Schnurr, I. Bjelakovic, and H. Boche, "Achievable rate region of a two-phase bidirectional relay channel," in *Proc. 41st Conference on Information Sciences and Systems (CISS)'07*, Mar. 2007.

[46] C. Schnurr, T. J. Oechtering, and S. Stanczak, "Achievable rates for the restricted half-duplex two-way relay channel," in *Proc. 41st Asilomar Conf. on Signals, Systems and Computers'07*, Nov. 2007, pp. 1468–1472.

[47] S. J. Kim, N. Devroye, P. Mitran, and V. Tarokh, "Achievable rate regions and performance comparison of half-duplex bi-directional relaying protocols," *IEEE Trans. Inf. Theory*, vol. 57, no. 10, pp. 6405–6418, Oct. 2011.

[48] M. P. Wilson, K. Narayanan, H. Pfister, and A. Sprintson, "Joint physical layer coding and network coding for bi-directional relaying," *IEEE Trans. Inf. Theory*, vol. 56, no. 11, pp. 5641–5654, Nov. 2010.

[49] T. J. Oechtering, C. Schnurr, I. Bjelakovic, and H. Boche, "Broadcast capacity region of two-phase bidirectional relaying," *IEEE Trans. Inf. Theory*, vol. 54, no. 1, pp. 454–458, Jan. 2008.

[50] P. Larsson, N. Johansson, and K.-E. Sunell, "Coded bi-directional relaying," in *Proc. IEEE VTC Spring'06*, Melbourne, Australia, May 2006.

[51] S. J. Kim, P. Mitran, and V. Tarokh, "Performance bounds for bidirectional coded cooperation protocols," *IEEE Trans. Inf. Theory*, vol. 54, no. 11, pp. 5235–5241, Nov. 2008.

[52] P. Popovski and H. Yomo, "Physical network coding in two-way wireless relay channels," in *Proc. IEEE ICC'07*, Glasgow, Scotland, Jun. 2007, pp. 707–712.

[53] R. Ahlswede, N. Cai, S.-Y. R. Li, and R. W. Yeung, "Network information flow," *IEEE Trans. Inf. Theory*, vol. 46, pp. 1204–1216, Jul. 2000.

[54] S.-Y. R. Li, R. W. Yeung, and N. Cai, "Linear network coding," *IEEE Trans. Inf. Theory*, vol. 49, no. 2, pp. 371–381, May 2003.

[55] R. Koetter and M. Medard, "An algebraic approach to network coding," *IEEE/ACM Transactions on Networking*, vol. 11, no. 5, pp. 782–795, Oct. 2003.

[56] S. Jaggi, P. Sanders, P. Chou, M. Effros, S. Egner, K. Jain, and L. Tolhuizen, "Polynomial time algorithms for multicast network code construction," *IEEE Trans. Inf. Theory*, vol. 51, no. 6, pp. 1973–1982, Jun. 2005.

[57] T. Ho, R. Koetter, M. Medard, D. Karger, and M. Effros, "The benefits of coding over routing in a randomized setting," in *Proc. IEEE ISIT'03*, Yokohama, Japan, Jul. 2003, p. 442.

[58] T. Ho, M. Medard, R. Koetter, D. Karger, M. Effros, J. Shi, and B. Leong, "A random linear network coding approach to multicast," *IEEE Trans. Inf. Theory*, vol. 52, no. 10, Oct. 2006.

[59] T. Ho, M. Medard, M. Effros, and R. Koetter, "Network coding for correlated sources," in *Proc. 38th Annual Conference on Information Sciences and Systems (CISS)'04*, Princeton, NJ, Mar. 2004.

[60] J. Barros and S. Servetto, "Network information flow with correlated sources," *IEEE Trans. Inf. Theory*, vol. 52, no. 1, pp. 155–170, Jan. 2006.

[61] D. Lun, M. Medard, and M. Effros, "On coding for reliable communications over packet networks," in *Proc. Annual Allerton Conference on Communication, Control and Computing'04*, Monticello, IL.

[62] D. Lun, M. Medard, and R. Koetter, "Efficient operation of wireless packet networks using network coding," in *Proc. International Workshop on Convergent Technologies (IWCT)'05*, Jun. 2005.

[63] X. Zhang, G. Neglia, J. Kurose, and D. Towsley, "On the benefits of random linear coding for unicast applications in disruption tolerant networks," in *Proc. IEEE NETCOD'06*, Boston, Massachusetts, Apr. 2006.

[64] S. Katti, D. Katabi, W. Hu, H. Rahul, and M. Medard, "The importance of being opportunistic: Practical network coding for wireless environments," in *Proc. 43rd Allerton Conference'05*, Sep. 2005.

[65] S. Katti, H. Rahul, W. Hu, D. Katabi, M. Medard, and J. Crowcroft, "Xors in the air: Practical wireless network coding," in *Proc. SIGCOMM'06*, Pisa, Italy, Sep. 2006.

[66] Z. Guo, B. Wang, and J.-H. Cui, "Efficient error recovery using network coding in underwater sensor networks," in *Proc. 6th international IFIP-TC6 conference on Networking'07*, Atlanta, Georgia, USA, May 2007, pp. 227–238.

[67] M. Effros, M. Medard, T. Ho, S. Ray, D. Karger, R. Koetter, and b. Hassibi, "Linear network codes: A unified framework for source, channel, and network coding," in *Proc. DIMACS Works. on Network Information Theory*, 2003.

[68] J. D. Ser, P. Crespo, B. Khalaj, and J. Gutierrez-Gutierrez, "On combining distributed joint source-channel-network coding and turbo equalization in multiple access relay networks," in *Proc. IEEE International Conf. on Wireless and Mobile Computing, Networking and Communications (WiMOB)'07*, Oct. 2007.

[69] F. Luus and B. Maharaj, "Joint source-channel-network coding for bidirectional wireless relays," in *Proc. IEEE ICASSP'11*, Prague, Czech Republic, May 2011.

[70] S. Feizi and M. Medard, "A power efficient sensing/communication scheme: joint source-channel-network coding by using compressive sensing," in *Proc. Allerton Conference on Communication, Control and Computing*, 2011.

[71] C. Hausl, F. Schreckenbach, I. Oikonomidis, and G. Bauch, "Iterative network and channel coding on a tanner graph," in *Proc. Annual Allerton Conference on Communication, Control and Computing*, Monticello, IL, Sep. 2005.

[72] C. Hausl and P. Dupraz, "Joint network-channel coding for the multiple access relay channel," in *Proc. 3rd Annual IEEE Communications Society on Sensor and Ad Hoc Communications and Networks*, vol. 3, Sep. 2006, pp. 817–822.

[73] C. Hausl and J. Hagenauer, "Iterative network and channel decoding for the two-way relay channel," in *Proc. IEEE ICC'06*, vol. 4, Istanbul, Turkey, Jun. 2006, pp. 1568–1573.

[74] C. Hausl, "Improved rate-compatible joint network-channel code for the two-way relay channel," in *Proc. Joint Conference on Communications and Coding (JCCC)'06*, Solden, Austria, Mar. 2006.

[75] Z. Zhang and S. L. P. Lam, "Physical layer network coding," in *Proc. ACM MOBICOM'06*, Sep. 2006.

[76] A. Sendonaris, E. Erkip, and B. Aazhang, "Increasing uplink capacity via user cooperation diversity," in *Proc. IEEE ISIT'98*, Aug. 1998, p. 156.

[77] L. Xiao, T. Fuja, J. Kliewer, and D. Costello, "Cooperative diversity based on code superposition," in *Proc. IEEE ISIT'06*, Seattle, Washington, Jul. 2006, pp. 2456–2460.

[78] ——, "A network coding approach to cooperative diversity," *IEEE Trans. Inf. Theory*, vol. 53, no. 10, pp. 3714–3722, Oct. 2007.

[79] ——, "Algebraic superposition of ldgm codes for cooperative diversity," in *Proc. IEEE ISIT'07*, Nice, France, Jun. 2007.

[80] C. Hausl and D. Capirone, "Turbo code design for H-ARQ with cross-packet channel coding," in *Proc. ISTC'10*, Brest, France, Sep. 2010, pp. 112–116.

[81] Y. Chen, S. Kishore, and J. Li, "Wireless diversity through network coding," in *Proc. IEEE WCNC'06*, vol. 3, Monticello, IL, Apr. 2006, pp. 1681–1686.

[82] D. Duyck, D. Capirone, M. Moeneclaey, and J. Boutros, "Analysis and construction of full-diversity joint network-LDPC codes for cooperative communications," *EURASIP Journal on Wireless Communications and Networking*, vol. 2010, pp. 1–16, 2010.

[83] S. Yang and R. Koetter, "Network coding over a noisy relay: A belief propagation approach," in *Proc. IEEE ISIT'07*, Nice, France, Jun. 2007.

[84] G. Zeitler, R. Koetter, G. Bauch, and J. Widmer, "Design of network coding functions in multihop relay networks," in *Proc. 5th International Symposium on Turbo Codes and Related Topics*, Lausanne, Switzerland, Sep. 2008.

[85] ——, "On quantizer design for soft values in the multiple access relay channel," in *Proc. IEEE ICC'09*, Lausanne, Switzerland, Sep. 2009.

[86] R. Pyndiah, F. Guilloud, and K. Amis, "Multiple source cooperative coding using turbo product codes with a noisy relay," in *Proc. ISTC'10*, Brest, France, Sep. 2010, pp. 98–102.

[87] J. Li, M. Azmi, R. Malaney, and J. Yuan, "Design of network-coding based multi-edge type ldpc codes for a multi-source relaying system," in *Proc. ISTC'10*, Brest, France, Sep. 2010, pp. 414–418.

[88] X. Bao and J. Li, "Adaptive network coded cooperation (ancc) for wireless relay networks: matching code-on-graph with network-on-graph," *IEEE Trans. Wireless Commun.*, vol. 7, no. 2, pp. 574–583, Feb. 2008.

[89] K. Pang, Z. Lin, Y. Li, and B. Vucetic, "Joint network-channel code design for real wireless relay networks," in *Proc. ISTC'10*, Sep. 2010.

[90] R. Zhang and L. Hanzo, "Multiple source cooperation: from code division multiplexing to variable-rate network coding," *IEEE Trans. Veh. Technol.*, vol. 60, no. 3, pp. 1005–1015, Mar. 2011.

[91] M. Xiao and T. Aulin, "Optimal decoding and performance analysis of a noisy channel network with network coding," *IEEE Trans. Commun.*, vol. 57, no. 5, pp. 1402–1412, May 2009.

[92] M. Xiao and M. Skoglund, "Design of network codes for multiple-user multiple-relay wireless networks," in *Proc. IEEE ISIT'09*, Seoul, Korea, Jun. 2009.

[93] ——, "Multiple-user cooperative communications based on linear network coding," *IEEE Trans. Commun.*, vol. 58, no. 12, pp. 3345–3351, Dec. 2010.

[94] J. Rebelatto, B. Uchoa-Filho, Y. Li, and B. Vucetic, "Generalized distributed network coding based on nonbinary linear block codes for multi-user cooperative communications," in *Proc. IEEE ISIT'10*, Austin, TX, Jun. 2010.

[95] Z. Guo, J. Huang, B. Wang, S. Zhou, J.-H. Cui, and P. Willett, "A practical joint network-channel coding scheme for reliable communication in wireless networks," *to appear in IEEE Trans. Wireless Commun.*

[96] T. Wang and G. Giannakis, "Complex field network coding for multiuser cooperative communications," *IEEE J. Sel. Areas Commun.*, vol. 26, no. 3, pp. 561–571, Apr. 2008.

[97] G. Zeitler, R. Koetter, G. Bauch, and J. Widmer, "An adaptive compress-and-forward scheme for the orthogonal multiple-access relay channel," in *Proc. IEEE PIMRC'09*, Tokyo, Japan, Sep. 2009.

[98] P. Popovski and H. Yomo, "Bidirectional amplification of throughput in a wireless multi-hop network," in *Proc. IEEE VTCSpring'06*, Melbourne, Australia, May 2006, pp. 588–593.

[99] S. Katti, S. Gollakota, and D. Katabi, "Embracing wireless interference: analog network coding," in *Proc. ACM SIGCOMM'07*, Kyoto, Japan, Aug. 2007.

[100] B. Nazer and M. Gastpar, "Computing over multi-access channels with connections to wireless network coding," in *Proc. IEEE ISIT'06*, Seattle, Washington, Jul. 2006, pp. 1354–1358.

[101] P. Popovski and H. Yomo, "The anti-packets can increase the achievable throughput of a wireless multihop network," in *Proc. IEEE ICC'06*, Istanbul, Turkey, Jun. 2006, pp. 11–15.

[102] B. Nazer and M. Gastpar, "Compute-and-forward: Harnessing interference through structured codes," *IEEE Trans. Inf. Theory*, vol. 57, no. 10, pp. 6463–6486, Oct. 2011.

[103] T. Koike-Akino, P. Popovski, , and V. Tarokh, "Optimized constellations for two-way wireless relaying with physical network coding," *IEEE J. Sel. Areas Commun.*, vol. 27, no. 5, pp. 773–787, Jun. 2009.

[104] Z. Zhang and S. Liew, "Channel coding and decoding in a relay system operated with physical-layer network coding," *IEEE J. Sel. Areas Commun.*, vol. 27, no. 5, pp. 788–796, Jun. 2009.

[105] D. Wubben and Y. Lang, "Generalized joint channel coding and physical network coding for two-way relay systems," in *Proc. IEEE VTC Spring'10*, Taipei, Taiwan, May 2010.

[106] D. To and J. Choi, "Convolutional codes in two-way relay networks with physical-layer network coding," *IEEE Trans. Wireless Commun.*, vol. 9, no. 9, pp. 2724–2729, Sep. 2010.

[107] S. Liew, S. Zhang, and L. Lu, "Physical-layer network coding: tutorial, survey, and beyond," *to appear in Elsevier Physical Communication Journal, 2012.*

[108] S. Zhang, S. C. Liew, H. Wang, and X. Lin, "Capacity of two-way relay channel," in *Proc. 4th International Conference on Access Networks'09*, Nov. 2009.

[109] W. Nam, S. Chung, and Y. Lee, "Capacity of the gaussian two-way relay channel to within 1/2 bit," *IEEE Trans. Inf. Theory*, vol. 56, no. 11, pp. 5488–5495, Nov. 2010.

[110] U. Bhat and T. M. Duman, "Decoding strategies for physical-layer network coding over frequency selective channels," in *Proc. IEEE WCNC'12*, Paris, France, Apr. 2012.

[111] U. Bhat, "Practical coding schemes for multi-user communications," Ph.D. dissertation, Arizona State University, 2011.

[112] J. Hu and T. Duman, "Low density parity check codes over wireless relay channels," *IEEE Trans. Commun.*, vol. 6, no. 9, pp. 3384–3394, Sep. 2007.

[113] Z. Zhang and T. Duman, "Capacity approaching turbo coding for half-duplex relaying," *IEEE Trans. Commun.*, vol. 55, no. 10, pp. 1895–1906, Oct. 2007.

[114] ——, "Capacity approaching turbo coding and iterative decoding for relay channels," *IEEE Trans. Commun.*, vol. 53, no. 11, pp. 1895–1905, Nov. 2005.

[115] G. Kramer, P. Gupta, and M. Gastpar, "Information-theoretic multi-hopping for relay networks," in *International Zurich Seminar on Communications*, ETH Zurich, Switzerland, Feb. 2004.

[116] H. Sneessens and L. Vandendorpe, "Soft decode and forward improves cooperative communications," in *Proc. IEEE 3G'05*, London, UK, Nov. 2005.

[117] K. S. Gomadam and S. A. Jafar, "Optimal relay functionality for snr maximization in memoryless relay networks," *IEEE J. Sel. Areas Commun.*, vol. 25, pp. 390–401, Feb. 2007.

[118] J. W. Craig, "A new, simple, and exact result for calculating the probability of error for two-dimensional signal constellations," in *Proc. IEEE MILCOM'91*, Oct. 1991, pp. 571–575.

[119] E. Malkamaki and H. Leib, "Coded diversity on block-fading channel," *IEEE Trans. Inf. Theory*, vol. 45, no. 2, pp. 771–781, Mar. 1999.

[120] M. K. Simon and M. S. Alouini, "Digital communication over fading channels: A unified approach to performance analysis," *New York: Wiley*.

[121] S. Benedetto and G. Montorsi, "Design of parallel concatenated convolutional codes," *IEEE Trans. Commun.*, vol. 44, no. 5, pp. 591–600, May 1996.

[122] H. Jin and R. J. McEliece, "Coding theorems for turbo code ensembles," *IEEE Trans. Inf. Theory*, vol. 48, no. 6, pp. 1451–1461, Jun. 2002.

[123] A. G. i Amat and I. Land, "Bounds of the probability of error for decode-and-forward relaying with two sources," in *Proc. ISTC'10*, Sep. 2010.

[124] P. Weitkemper and G. Dietl, "Maximum likelihood receiver for mmse relaying," in *Proc. IEEE ICC'11*, Kyoto, Japan, Jun. 2011.

[125] A. Hatefi, R. Visoz, and A. Berthet, "Joint channel-network coding for the semi-orthogonal multiple access relay channel," in *Proc. IEEE VTC-Fall'10*, Ottawa, Canada, Sep. 2010.

[126] D. H. Woldegebreal and H. Karl, "Multiple-access relay channel with network coding and non-ideal source-relay channels," in *Proc. 4th International Symposium on Wireless Communication Systems*, Trondheim, Norway, Oct. 2007.

[127] D. Tse and P. Viswanath, "Fundamentals of wireless communication," *Cambridge University Press*, 2005.

[128] G. Caire, G. Taricco, and E. Biglieri, "Bit-interleaved coded modulation," *IEEE Trans. Inf. Theory*, vol. 44, no. 3, pp. 927–946, May 1998.

[129] J. Hagenauer, "The turbo principle: Tutorial introduction and state of the art," in *Proc. 1st International Symposium on Turbo Codes*, Brest, France, Sep. 1997, pp. 1–12.

[130] D. Raphaeli and Y. Zarai, "Combined turbo equalization and turbo decoding," *IEEE Commun. Lett.*, vol. 2, pp. 107–109, Apr. 1998.

[131] A. Hatefi, R. Visoz, and A. Berthet, "Full diversity distributed coding for the multiple access half-duplex relay channel," in *Proc. IEEE Netcod'11*, Beijing, China, Jul. 2011.

[132] J. Hagenauer, E. Offer, and L. Papke, "Iterative decoding of binary block and convolutional codes," *IEEE Trans. Inf. Theory*, vol. 42, no. 2, pp. 429–445, Sep. 1996.

[133] S. ten Brink, "Convergence behavior of iteratively decoded parallel concatenated codes," *IEEE Trans. Commun.*, vol. 49, pp. 1727–1737, Oct. 2001.

[134] L. Bahl, J. Cocke, F. Jelinek, and R. Raviv, "Optimal decoding of linear codes for minimizing symbol error rate," *IEEE Trans. Inf. Theory*, vol. 20, pp. 284–286, Mar. 1974.

[135] A. Hatefi, R. Visoz, and A. Berthet, "Joint channel-network turbo coding for the non-orthogonal multiple access relay channel," in *Proc. IEEE PIMRC'10*, Istanbul, Turkey, Sep. 2010.

[136] ——, "Near outage limit joint network coding and decoding for the semi-orthogonal multiple-access relay channel," in *Proc. IEEE Netcod'12*, Boston, MA, USA, Jul. 2012.

[137] A. Lapidoth and P. Narayan, "Reliable communication under channel uncertainty," *IEEE Trans. Inf. Theory*, vol. 44, no. 6, pp. 2148–2177, Oct. 1998.

[138] A. Hatefi, R. Visoz, and A. Berthet, "Network coding," *Wiley-ISTE*, Apr. 2012, Chapter 7.

[139] E. Biglieri and M. Lops, "Multiuser detection in a dynamic environment. part i: User identification and data detection," *IEEE Trans. Inf. Theory*, vol. 53, no. 9, pp. 3158–3170, Sep. 2007.

[140] A. Hatefi, R. Visoz, and A. Berthet, "Joint network-channel distributed coding for the multiple access full-duplex relay channel," in *Proc. IEEE ICUMT'10*, Moscow, Russia, Oct. 2010.

[141] ——, "Near outage limit joint network coding and decoding for the non-orthogonal multiple-access relay channel," in *Proc. IEEE PIMRC'12*, Sydney, Australia, Sep. 2012.

[142] S. Benedetto, R. Garello, and G. Montorsi, "A search for good convolutional codes to be used in the construction of turbo codes," *IEEE Trans. Commun.*, vol. 46, no. 9, pp. 1101–1105, Sep. 1998.

[143] F. R. Kschischang, B. J. Frey, and H.-A. Loeliger, "Factor graphs and the sum-product algorithm," *IEEE Trans. Inf. Theory*, vol. 47, no. 2, pp. 498–519, Feb. 2001.

[144] A. Hatefi, R. Visoz, and A. Berthet, "Relaying functions for the multiple access relay channel," in *Proc. ISTC'10*, Brest, France, Sep. 2010, pp. 364–368.

[145] G. Ungerboeck, "Channel coding with multilevel/phase signals," *IEEE Trans. Inf. Theory*, vol. 28, pp. 55–67, Jul. 1982.